2008

APPLICABILITY OF TRADITIONAL DESIGN PROCEDURES TO MODULAR STEEL BUILDINGS

Charles-Darwin Annan
Western University

APPLICABILITY OF TRADITIONAL DESIGN PROCEDURES TO MODULAR STEEL BUILDINGS

(Spine title: Behaviour and Design of Modular Steel Buildings)

(Thesis format: Integrated-Article)

By

Charles-Darwin Annan

Department of Civil and Environmental Engineering

Graduate Program in Engineering Science

A thesis submitted in partial fulfilment
of the Requirements for the degree of
Doctor of Philosophy

School of Graduate and Postdoctoral Studies

The University of Western Ontario

London, Ontario, Canada

December, 2008

THE UNIVERSITY OF WESTERN ONTARIO
SCHOOL OF GRADUATE AND POSTDOCTORAL STUDIES

CERTIFICATE OF EXAMINATION

Supervisors

Dr. Youssef M.A.

Dr. El Naggar H.E.

Examiners

Dr. Miller C.

Dr. Galsworthy, J.

Dr. Asokanthan, S. F.

Dr. Sparling, B.

The thesis by

Charles-Darwin Annan

entitled:

Applicability of Traditional Design Procedures to Modular Steel Buildings

is accepted in partial fulfilment of the
Requirements for the degree of
Doctor of Philosophy

Date_____

Chair of the Thesis Examination Board

Abstract

Modular Steel Buildings (MSBs) have unconventional detailing requirements, compared to traditional onsite steel buildings. This may affect their design and performance. Currently, traditional design procedures are followed in their design. This thesis evaluates the performance of MSBs under gravity and seismic loads. It documents for the first time a detailed description of this unique steel building system and its detailing requirements and provides the first analytical experimental investigation that aims at improving its design methodology.

The effect of directly welded stringer-to-beam connections used in MSBs on behaviour and design of MSBs floors is investigated using the finite element method. The results obtained revealed that this unique connection type affects the design of the floor stringers and welded connections but has little effect on the floor beams. Empirical relations and a simplified model were developed to predict the forces and moments likely to develop in MSB floor stringers.

Nonlinear seismic performance and characteristics of braced frames of a typical MSB were studied using cyclic tests, nonlinear static pushover analysis, and incremental dynamic analyses. These studies consist of (i) an experimental investigation of the hysteretic behaviour of a scaled one-bay one-storey MSB braced frame; (ii) the strength and ductility design of braced frames of a typical MSB dormitory; (iii) the development of analytical models of selected braced frames of MSBs accounting for their unique detailing requirements and the hysteresis of steel bracing members; (iv) a study of the effect of design philosophy on the nonlinear behaviour of MSB braced frames using

pushover analyses; (v) the evaluation of structural overstrength and displacement ductility of the braced frames using pushover analyses; and (vi) the assessment of seismic inelastic drift and ductility demands and capacities of the braced frames using an incremental dynamic analysis. It is concluded that while the MSB frame configuration may not significantly affect certain design and behavioural characteristics, in some others its unique detailing requirements need to be considered during design to eliminate undesirable seismic response.

KEYWORDS: Modular steel buildings, floor system, directly welded stringer-to-beam connections, braced frames, cyclic test, nonlinear static pushover analysis, incremental dynamic analysis, inelastic behaviour and characteristics.

Co-Authorship

This doctoral thesis has been carefully prepared according to the regulations for an integrated-article format thesis stipulated by the Faculty of Graduate and Postdoctoral Studies at the University of Western Ontario and has been co-authored as follows:

Chapter 2: Effect of Directly Welded Stringer-To-Beam Connections on the Analysis and Design of Modular Steel Building Floors

All the design and analytical modeling works were conducted by C. D. Annan under the supervision of Dr. M. A. Youssef. The finite element analysis was carried out by C. D. Annan under the supervision of Dr. M. A. Youssef. Drafts of Chapter 2 were prepared by C. D. Annan and reviewed by Dr. M. A. Youssef and Dr. H. E. El Naggar. A paper co-authored by C. D. Annan, M. A. Youssef and H. E. El Naggar has been accepted for publication in the Advances in Structural Engineering Journal.

Chapter 3: Experimental Evaluation of the Seismic Performance of Modular Steel Braced Frames

All the preparation for testing and testing set-up was undertaken by C. D. Annan under the supervision of Dr. M. A. Youssef. Analytical prediction was conducted by C. D. Annan under the supervision of Dr. M. A. Youssef. Testing was undertaken by C. D. Annan under the supervision of Dr. M. A. Youssef. Drafts of Chapter 3 were prepared by C. D. Annan and reviewed by Dr. M. A. Youssef and Dr. H. E. El Naggar. A paper co-authored by C. D. Annan, M. A. Youssef and H. E. El Naggar is currently under review by the Engineering Structures Journal.

Chapter 4: Seismic Overstrength in Braced Frames of Modular Steel Buildings

All the design and analytical modeling works were conducted by C. D. Annan under the supervision of Dr. M. A. Youssef. Nonlinear static analysis was carried out by C. D. Annan under the supervision of Dr. M. A. Youssef. Drafts of Chapter 4 were prepared by C. D. Annan and reviewed by Dr. M. A. Youssef and Dr. H. E. El Naggar. A paper co-authored by C. D. Annan, M. A. Youssef and H. E. El Naggar has been published in the Journal of Earthquake Engineering, Volume 13 Issue 1, 2009.

Chapter 5: Seismic Vulnerability Assessment of Modular Steel Buildings

All the design and analytical modeling works were conducted by C. D. Annan under the supervision of Dr. M. A. Youssef. Incremental dynamic analysis was carried out by C. D. Annan under the supervision of Dr. M. A. Youssef. Drafts of Chapter 5 were prepared by C. D. Annan and reviewed by Dr. M. A. Youssef and Dr. H. E. El Naggar. A paper co-authored by C. D. Annan, M. A. Youssef and H. E. El Naggar is currently under review by the Journal of Earthquake Engineering.

Dedication

Through you and in you, I have known and experienced love. I dedicate this to you!

And to my late Dad and my sweet mum, this has always been your dream and prayers!

Acknowledgements

Writing could be a difficult creative task. But here there is, a considerable satisfaction at seeing the realisation of hours of effort take shape. Thanks and praise be to God who has shown me new mercies morning by morning!

A debt of gratitude is owed to all the individuals and organisations who generously gave their time, funds and ideas to this work. Special recognition is given to Dr. Maged Youssef, my thesis advisor for his apt and efficient guidance, and Dr. Hesham El Naggar, my co-advisor for his invaluable comments and directions. I am also very grateful to Miss Yvonne Abena Nyinaku for her demonstration of true and loving friendship, spending days and nights with me while running hundreds of analyses on multiple computers. The research was conducted with funding from the Natural Sciences and Engineering Research Council of Canada and The University of Western Ontario. Knowledge of the system under study was obtained at Murray Engineering, P.C., NY.

I would like to thank our wonderful administrative and technical staff, Connie, Debbie, Stephanie, Cindy, Melodie and Wilbert, who always made me feel very special in the Department and cheerfully helped me whenever I needed one. I would also want to express my gratitude to all my good friends, the Amegashies, the Oppongs, the Atta-Konadus, the Alloteys, the Lampteys, Muluken, and to all my smart and wonderful friends and colleagues I have shared office with. You were like a family to me.

Finally, to my beautiful and patient wife, Agnes, and lovely children, Carl, Bradley, and Naa, and to the rest of my family, words cannot just describe how valuable your love, encouragement, prayers, and patience have been to my completion of this work. It simply will not have been possible without you. God richly bless you all.

TABLE OF CONTENTS

	Page
Certificate of Examination	ii
Abstract	iii
Co-Authorship	v
Dedication	vii
Acknowledgements	viii
Table of Contents	ix
List of Tables	xiii
List of Figures	xiv
List of Appendices	xix
List of Abbreviations	xx
List of Symbols	xxii

CHAPTER ONE: INTRODUCTION AND SCOPE OF THESIS

1.1	General	1
1.2	Background Literature	3
1.2.1	Structural Floor System	3
1.2.2	Lateral Load Resisting System	4
1.2.3	NBCC Provisions for Seismic Design	9
1.2.6	Structural Modeling and Analysis	10
1.3	Modular Steel Building Technique	12
1.4	Aim and Objectives of Thesis	14
1.5	Scope of Thesis	15
1.5.1	Effect of Directly Welded Stringer-To-Beam Connections on the Analysis and Design of Modular Steel Building Floors	15
1.5.2	Experimental Evaluation of the Seismic Performance of Modular Steel Braced Frames	16
1.5.3	Structural Overstrength in Braced Frames of Modular Steel Buildings	17
1.5.4	Seismic Vulnerability Assessment of Modular Steel Buildings	17

1.6 References 19

CHAPTER TWO: EFFECT OF DIRECTLY WELDED STRINGER-TO-BEAM CONNECTIONS ON THE ANALYSIS AND DESIGN OF MODULAR STEEL BUILDING FLOORS

2.1 Introduction 23
2.2 Modular Steel Buildings 26
2.3 Floor Stringer-to-Beam Connections 30
2.4 Design of Modular Floor Grid Structure 32
2.5 Finite Element (FE) Model 33
2.6 Parametric Studies 35
2.7 Finite Element Results and Discussions 36
2.7.1 Floor Stringers 37
2.7.2 Floor Beams 41
2.7.3 Stringer-to-Beam Welded Connections 42
2.8 Proposed Analytical Model 44
2.9 Design Methodology for Modular Floor Framing 49
2.10 Summary and Conclusions 50
2.11 References 52

CHAPTER THREE: EXPERIMENTAL EVALUATION OF THE SEISMIC PERFORMANCE OF MODULAR STEEL BRACED FRAMES

3.1 Introduction 54
3.2 Selection of Specimen Configuration and Design 58
3.3 Experimental Setup 63
3.4 Experimental Program 66
3.4.1 Material Properties 66
3.4.2 Pushover Analysis 66
3.4.3 Testing Protocol 70

3.5 Experimental Results 72
3.5.1 Overall Hysteretic Behaviour 72
3.5.2 Strength and Stiffness Characteristics 76
3.5.3 Energy Dissipation Characteristics 80
3.5.4 Force Distribution Pattern 84
3.5.5 Analytical Prediction of MSB Behaviour 90
3.6 Summary and Conclusions 92
3.7 References 95

CHAPTER FOUR: SEISMIC OVERSTRENGTH IN BRACED FRAMES OF MODULAR STEEL BUILDINGS

4.1 Introduction 98
4.2 Modular Steel Building (MSB) System 103
4.3 Design of Modular Steel Braced Frames 108
4.4 Analysis of MSB Braced Frames 116
4.5 Results and Discussions 121
4.5.1 Inelastic Response of MSB Braced frames 121
4.5.2 Overstrength for MSB Braced frames 132
4.5.3 Ductility of MSB Braced frames 138
4.6 Conclusions 139
4.7 References 142

CHAPTER FIVE: SEISMIC VULNERABILITY ASSESSMENT OF MODULAR STEEL BUILDINGS

5.1 Introduction 146
5.2 Selection and Design of MSB System 151
5.3 Analytical Model of MSB Braced Frames 155
5.4 Selection of Ground Motion Records and Analysis Characteristics 157
5.5 Evaluation of Seismic Inelastic Response Characteristics 162
5.5.1 Eigenvalue Analysis 162
5.5.2 Results of Incremental Dynamic Analysis 163

5.5.3 Inelastic Distribution along Height of MSB Braced Frame 175
5.5.4 Structural Drift Demand and Capacity of MSB Braced frame 185
5.5.5 Ductility Demand Assessment 188
5.6 Conclusions 192
5.7 References 195

CHAPTER SIX: CONCLUSIONS AND RECOMMENDATIONS

6.1 Review and Conclusions 199
6.1.1 Effect of Directly Welded Stringer-To-Beam Connections on the Analysis and Design of Modular Steel Building Floors 201
6.1.2 Experimental Evaluation of the Seismic Performance of Modular Steel Braced Frames 201
6.1.3 Seismic Overstrength in Braced Frames of Modular Steel Buildings 202
6.1.4 Seismic Vulnerability Assessment of Modular Steel Buildings 203
6.2 Major Research Contributions 204
6.3 Recommendations for Further Studies 206

APPENDIX I Sample SAP2000 Data File for Model of Modular Steel Floor Grid Structure 208
APPENDIX II Sample Data Used in Multiple Regression Analysis 225
APPENDIX III Stress-Strain Relationships from Standard Coupon Material Tests 226
VITA 229

LIST OF TABLES

		Page
Table 2.1:	Comparison of FE results with Design Forces and Moments For Stringer Beams	39
Table 2.2:	Comparison of FE results with Design Bending Moments at Sections of Floor Beam	42
Table 3.1:	Ductility Levels Reached by Specimens at Different Cycles	72
Table 3.2	Force Distribution Ratios in Members of Braced Specimens	88
Table 4.1:	Member Sections from Strength and Ductility Designs of MSB Braced Frames	112
Table 4.2:	Modified F_y Values for Compression Brace Members of MSB Braced Frames	120
Table 4.3:	Overstrength Factor and Structural Ductility of MSB Braced Frames	134
Table 5.1:	Selected Earthquake Ground Motion Records	160
Table 5.2:	Dynamic Characteristics of Selected MSB Braced Frames	163
Table 5.3:	16%, 50%, and 84% Fractile Capacities in terms of Intensity Measure, $S_a(T_1,5\%)$	187
Table 5.4:	16%, 50%, and 84% Fractile Capacities in terms of Maximum Drift, θ_{max}	188
Table 5.5:	Ductility Capacity based on NBCC Drift Limit and Collapse Prevention Median Capacities in $S_a(T_1,5\%)$	189

LIST OF FIGURES

		Page
Figure 1.1:	A Typical Hysteresis of Steel Brace Member under Cyclic Load	6
Figure 1.2:	A Model Hysteresis of Steel Brace Member	7
Figure 2.1:	A Typical Floor/Ceiling Framing and Details of a Multi-Storey Modular Steel Building	28
Figure 2.2:	A Section of a Typical Modular Floor Assembly	29
Figure 2.3:	Layout of Modular Floor Framing Adopted for FE Study	33
Figure 2.4:	Finite Element Mesh	35
Figure 2.5:	Variation of FE-to-Design Midspan Moment Ratio with Beam-to-Stringer Web Thickness Ratio for Different Beam-to-Stringer Depth Ratios	40
Figure 2.6:	Variation of the Ratio of FE Hogging Moment to Design Midspan Moment with Beam-to-Stringer Web Thickness Ratios	40
Figure 2.7:	Variation of FE-to-Design Midspan Moment Ratio with Beam-to-Stringer Web Thickness Ratio for Different Weld Lengths	44
Figure 2.8:	Schematic of the Proposed Analytical Model	46
Figure 3.1:	A Typical Plan and Sections of a Modular Steel Building	58
Figure 3.2:	Four-storey Braced Frames for Design of Test Specimens (a) MSB Frame (b) Regular Frame	60
Figure 3.3:	Dimensions of Test Specimens (a) MSB Frame (b) Regular Frame	60
Figure 3.4:	Photos of Specimens Member and Connection Details (a) MSB Frame (b) Beam-to-column Connection in Regular Frame (c) Brace Intersection	62
Figure 3.5:	Overall View of Test Setup	65
Figure 3.6:	Schematic of Experiment Setup	65
Figure 3.7:	Model of Vertical Connection of Units of MSB Specimen	68
Figure 3.8:	Pushover Curves for (a) MSB Braced Specimen (b) Regular Braced Specimen	69
Figure 3.9:	Loading History for MSB Braced Specimen (a) Elastic Cycles (b) Inelastic Cycles	71

Figure 3.10: Loading History for Regular Braced Specimen (a) Elastic Cycles (b) Inelastic Cycles 71
Figure 3.11: Base Shear versus Drift Response (a) MSB Specimen (b) Regular Braced Specimen 74
Figure 3.12: (a) Column Bending Deformation in MSB Braced Specimen (b) Brace Out-of-Plane Deformation in Regular Braced Specimen 75
Figure 3.13: Variations of Lateral Stiffness with (a) Peak Drift (b) Maximum Ductility 78
Figure 3.14: Base Shear versus Drift Relationship for Regular Braced Specimen at 3.05% Drift 79
Figure 3.15: Energy Dissipation per Cycle versus (a) Peak Drift (b) Maximum Ductility 82
Figure 3.16: Comparison of Normalised Cumulative Energy Dissipation for Specimens 83
Figure 3.17: Strain Evolution in a Brace Member Section at Load Step 2 (a) Regular Specimen (b) MSB Specimen 85
Figure 3.18: Strain Evolution in a Brace Member Section at Load Step 4 (a) Regular Specimen (b) MSB Specimen 86
Figure 3.19: Force Distribution in Members of (a) MSB Specimen (b) Regular Braced Specimen 87
Figure 3.20 Comparison of Experimental and Analytical Load-Displacement Curves of MSB Braced Specimen 92
Figure 4.1: A Typical Structural Response Envelope 101
Figure 4.2: Typical Details for a Multi-storey MSB 105
Figure 4.3: A Four-storey Modular Steel Braced Frame (a) Floor Plan (b) Elevation (centerline 1 or 7) 107
Figure 4.4: Cumulative Brace Loads for Determining Column Actions in a Four-storey MSB 114
Figure 4.5: Free Body Diagrams of Beam Forces to Support Redistributed Brace Loads 115

Figure 4.6:	Model of Vertical Connections of Units of MSB Braced Frame in Pushover Analysis	118
Figure 4.7:	Sequence of Yielding/Buckling of the Six-storey MSB Braced Frame (Brace induced column actions by SRSS accumulation approach)	122
Figure 4.8:	Sequence of Yielding/Buckling of the Four-storey MSB Braced Frame (Brace induced column actions by SRSS accumulation approach)	123
Figure 4.9:	Sequence of Yielding/Buckling of the Two-storey MSB Braced Frame (Brace induced column actions by SRSS accumulation approach)	124
Figure 4.10:	Sequence of Yielding/Buckling of the Four-storey MSB Braced Frame (Brace induced column actions by DS accumulation approach)	129
Figure 4.11:	Sequence of Yielding/Buckling of the Six-storey MSB Braced Frame (Brace induced column actions by DS accumulation approach)	130
Figure 4.12:	Horizontal Capacity Curves of the Selected MSB Braced Frame (Brace induced column actions by SRSS accumulation approach) (a) six-storey (b) four-storey (c) two-storey	136
Figure 4.13:	Horizontal Capacity Curve of the MSB Braced Frame (Brace induced column actions by DS accumulation approach) (a) six-storey (b) four-storey	137
Figure 5.1:	Plan and Sections of a Typical MSB	149
Figure 5.2:	Four-storey Modular Steel Braced Frame (a) Floor Plan (b) Elevation	152
Figure 5.3:	Model of Vertical Connection of Modular Units of MSB Braced Frame in Dynamic Analysis	157
Figure 5.4:	5% Damped Acceleration Response Spectra for Selected Ground Motions	161

Figure 5.5: IDA Curves of 'first mode' Spectra Acceleration, $S_a(T_1,5\%)$, plotted against Maximum Inter-storey Drift Ratio, θ_{max}, for (a) Six-storey (b) Four-storey (c) Two-storey MSB Braced Frame 166

Figure 5.6: IDA Curves of 'first mode' Spectra Acceleration, $S_a(T_1,5\%)$, plotted against Peak Roof Drift Ratio, θ_{roof}, for (a) Six-storey (b) Four-storey (c) Two-storey MSB Braced Frame 167

Figure 5.7: IDA Curves of Peak Ground Acceleration, PGA, plotted against Maximum Inter-storey Drift Ratio, θ_{max}, for (a) Six-storey (b) Four-storey (c) Two-storey MSB Braced Frame 168

Figure 5.8: IDA Curves of Peak Ground Acceleration, PGA, plotted against Peak Roof Drift Ratio, θ_{roof}, for (a) Six-storey (b) Four-storey (c) Two-storey MSB Braced Frame 169

Figure 5.9: Summary of IDA Curves of the Six-storey MSB Braced Frame Into 16^{th}, 50^{th}, and 84^{th} Fractiles with (a) Maximum Inter-storey Drift Ratio (b) Peak Roof Drift Ratio 172

Figure 5.10: Summary of IDA Curves of the Four-storey MSB Braced Frame Into 16^{th}, 50^{th}, and 84^{th} Fractiles with (a) Maximum Inter-storey Drift Ratio (b) Peak Roof Drift Ratio 173

Figure 5.11: Summary of IDA Curves of the Two-storey MSB Braced Frame Into 16^{th}, 50^{th}, and 84^{th} Fractiles with (a) Maximum Inter-storey Drift Ratio (b) Peak Roof Drift Ratio 174

Figure 5.12: Heightwise Distribution of Peak Inter-storey Drift Ratio for Six-storey MSB (a) $S_a(T_1,5\%) = 0.2g$ (b) $S_a(T_1,5\%) = 1.7g$ (c) $S_a(T_1,5\%) = 2.0g$ 177

Figure 5.13: Heightwise Distribution of Peak Inter-storey Drift Ratio for Four-storey MSB (a) $S_a(T_1,5\%) = 0.3g$ (b) $S_a(T_1,5\%) = 2.0g$ (c) $S_a(T_1,5\%) = 3.0g$ 178

Figure 5.14: Heightwise Distribution of Peak Inter-storey Drift Ratio for Two-storey MSB (a) $S_a(T_1,5\%) = 0.4g$ (b) $S_a(T_1,5\%) = 2.5g$ (c) $S_a(T_1,5\%) = 4.0g$ 178

Figure 5.15: Peak Inter-storey Drift along Height of Six-storey MSB Frame under Selected Ground Motion Records at Different Intensity Levels (a) $S_a(T_1,5\%) = 0.2g$ (b) $S_a(T_1,5\%) = 1.4g$ (c) $S_a(T_1,5\%) = 2.0g$ 181

Figure 5.16: Peak Inter-storey Drift along Height of Four-storey MSB Frame under Selected Ground Motion Records at Different Intensity Levels (a) $S_a(T_1,5\%) = 0.3g$ (b) $S_a(T_1,5\%) = 2.0g$ (c) $S_a(T_1,5\%) = 3.0g$ 182

Figure 5.17: Peak Inter-storey Drift along Height of Two-storey MSB Frame under Selected Ground Motion Records at Different Intensity Levels (a) $S_a(T_1,5\%) = 0.4g$ (b) $S_a(T_1,5\%) = 3.0g$ (c) $S_a(T_1,5\%) = 5.0g$ 183

Figure 5.18: Median Peak Inter-storey Drift Ratios for all Storey Levels at Different Ground Motion Intensities representing Elastic and Post-elastic Response (a) Six-storey (b) Four-storey (c) Two-storey MSB Braced Frames 184

Figure 5.19: IDA Curves of 5% Damped Spectral Acceleration, $S_a(T_1,5\%)$, Plotted against Ductility for (a) Six-storey (b) Four-storey (c) Two-storey MSB Braced Frames 190

Figure 5.20: Summary of Ductility Demand IDA Curves into 16^{th}, 50^{th}, and 84^{th} Fractiles for (a) Six-storey (b) Four-storey (c) Two-storey MSB Braced Frames 191

LIST OF APPENDICES

		Page
APPENDIX I	Sample SAP2000 Data File for Model of Modular Steel Floor Grid Structure	208
APPENDIX II	Sample Data Used in Multiple Regression Analysis	225
APPENDIX III	Stress-Strain Relationships from Standard Coupon Material Tests	226

LIST OF ABBREVIATIONS

AISC	American Institute of Steel Construction
ASCE	American Society of Civil Engineers
ASTM	American Society for Testing and Materials
ATC	Applied Technology Council
CB	Ceiling Beam
CBF	Concentrically Braced Frame
CISC	Canadian Institute of Steel Construction
CS	Ceiling Stringer
CSA	Canadian Standards Association
CSI	Computers and Structures, Inc.
DL	Dead Load
DP	Demand Parameter
DS	Direct Summation
FB	Floor Beam
FE	Finite Element
FEMA	Federal Emergency Management Agency
FS	Floor Stringer
HC	Horizontal Connection
HSS	Hollow Structural Section
IBC	International Building Code
IDA	Incremental Dynamic Analysis
IM	Intensity Measure
LL	Live Load
LVDT	Linear Variable Differential Transformer
MBABC	Modular Building Association of British Columbia
MBI	Modular Building Institute
MSB	Modular Steel Building
NRCC	National Research Council Canada
NBCC	National Building Code of Canada
PEER	Pacific Earthquake Engineering Research

PGA	Peak Ground Acceleration
SCI	Steel Construction Institute
SDOF	Single Degree Of Freedom
SEAOC	Structural Engineers Association of California
SRSS	Square Root of the Sum of Squares
VC	Vertical Connection
W	Wide Flange Section

LIST OF SYMBOLS

Chapter One

P	Applied load
δ	Deformation
P_y	Yield capacity
δ_y	Deformation at yield
C_r	Buckling strength of compressive brace member
V	Design base shear
$S_a(T_a)$	Spectral response acceleration at fundamental mode period of structure
T_a	Fundamental mode period of structure
M_v	Higher mode effect factor
I_E	Importance factor of structure
W	Total weight of structure
R_d	Ductility-related force modification factor
R_o	Overstrength-related force modification factor
E	Modulus of elasticity
G	Shear modulus
A	Cross-sectional area
I	Moment of inertia
h_n	Height of framed structure

Chapter Two

[k]	Stiffness matrix
{u}	Vector of nodal displacement
{r}	Vector of applied loads
t_w^b	Web thickness of floor beam
t_w^s	Web thickness of floor stringer
d_b	Depth of floor beam
d_s	Depth of floor stringer
L_s	Span of floor stringer

L_w	Length of weld
w	Uniformly distributed load
L	Length of beam
M_{FE}	Bending moment at midspan of stringer from FE analysis
M_a	Bending moment at a section of floor beam from FE analysis
M_d	Design bending moment
M_h	Design hogging moment
M_n	Hogging moment from FE analysis
N_{FE}	Axial force from FE analysis
N_d	Design axial force
W	Total load
$f_{bending}$	Bending stress magnitude in weld
f_{normal}	Normal stress magnitude in weld
f_{shear}	Shear stress magnitude in weld
B	Effective width of floor beam web
F	Axial tension force
I_b	Moment of inertia of the effective web of floor beam
I_s	Moment of inertia of floor stringer
h	Depth from centerline of stringer to centerline of top flange of floor beam
r	Coefficient of determination

Chapter Three

w/t	Width-to-thickness ratio
K	Effective length factor
L	Length of bracing member
r	Radius of gyration
F_y	Nominal yield strength of steel
P	Applied lateral force
P_y	Analytical yield force
Δ_y	Actual yield displacement
V_y	Actual yield base shear

Chapter Four

R	Seismic behaviour factor
R_o	Overstrength related force modification factor
R_d	Ductility related force modification factor
R_{yield}	Behaviour factor due to difference in material yield strength
R_{size}	Behaviour factor due to difference in member size
R_{mech}	Behaviour factor due to redistribution of internal forces
R_{phi}	Behaviour factor due to difference between nominal and factored resistance
R_{sh}	Behaviour factor due to material strain hardening behaviour
V_y	Maximum yield strength
V_d	Design base shear
Δ_y	Displacement corresponding to idealized yield strength
Δ_u	Maximum structural displacement
F_y	Specified yield strength
λ	Slenderness coefficient
k	Effective length factor
l	Unsupported length
r	Radius of gyration
b/t	width-to-thickness ratio of brace member
A_g	Gross area of member cross-section

Chapter Five

$S_a(T)$	Spectral acceleration at the fundamental mode period of structure
$S_a(T_1,5\%)$	5% damped spectral acceleration at the fundamental mode period of structure
θ_{max}	Maximum peak inter-storey drift ratio
θ_{roof}	Peak roof drift ratio
g	Acceleration due to gravity
h	Storey height

CHAPTER ONE

INTRODUCTION AND SCOPE OF THESIS

1.1 General

For the efficient design of steel structures, it is imperative that the designer understands how structures are assembled and how they sustain and transmit loads. The designer must also know the applicable design philosophies and processes, including selecting proper connectors and connections. The constitution of the limit state design specification especially requires a sound understanding of the entire structural behaviour since the different limit states of failure must be identified as an integral part of the design process. Building codes and recommendations for design, such as the National Building Code of Canada (NBCC, 2005) and the CSA standard S16.1-01 (CSA, 2001), are generally based on results of extensive research and practical experience.

The performance of a building structural system under loading depends primarily on its configuration and member proportions. The structural configuration encompasses structural members/elements and connections, arranged so that the entire assembly remains stable and without appreciable change in form while meeting the prescribed performance criteria. Modular Steel Buildings (MSBs) are fast evolving as an effective alternative to traditional on-site steel construction. The rational for the use of the modular technique is largely speed of construction, while combining the design flexibility of traditional methods with the quality of controlled manufacturing. However, knowledge and documentation of their behaviour and past performance are limited, if at all existent.

Given the typical application of such buildings in two-to-six storey schools, dormitories, hotels, apartments, hostels, etc., damage due to improper design or unexpected loading poses a significant risk to life and property.

MSBs are characterized by unconventional detailing requirements, compared to traditional onsite steel buildings. This may affect their design and performance under loading conditions. Currently, traditional design procedures are followed as there is no research investigation into their structural design and performance specifications. Generally speaking, structural collapse may be caused by gravity or lateral loads. Gravity loads are supported by a floor system which, in MSBs is typically designed as a grid structure consisting of floor beams and stringers directly welded together. The floor framing are joined to a ceiling framing through columns. Lateral stability of a modular unit is achieved either by developing moment resisting frames of the beams, stringers and columns or by adding diagonal braces. The separately finished modular units are connected both horizontally and vertically on-site in a non-traditional manner. For MSB in seismic regions, its structure may also be detailed for ductile response in the event of an earthquake. Analytical and experimental studies of the behaviour and response characteristics under gravity and seismic loads are necessary to properly design new modular steel buildings.

1.2 Background Literature

The following sub-sections review selected topics related to the design, analysis, and behaviour of regular steel building structures. This is intended to provide an introduction of traditional steel building systems / configurations and the relevant design procedures. This is expected to enhance understanding of the detailing requirements of MSBs as outlined in the following chapters.

1.2.1 Structural Floor System

Building floor systems are designed and built primarily to resist and transfer dead and live loads to columns and walls. The system must also satisfy deflection and vibration limits. The floor lies within a single plane; however, loading and displacements occur out of plane. The floor panels themselves may be subjected to lateral loads and must exhibit suffcient in-plane diaphragm strength and stiffness to transfer these lateral loads. Different steel floor systems have been used in regular buildings. Examples are the stub-girder system (Colaco, 1972), the girder-slab floor system (Naccarato, 1999; Cross, 2003), and the composite steel joist system (Lembeck, 1965; Atkinson and Cran, 1972; Azmi, 1972; Curry, 1988; Leon and Curry, 1987; Brattland and Kennedy, 1992; ASCE, 1996; Samuelson, 2002).

Connections in steel floor systems join elements (i.e. beam webs and flanges) using connecting elements (i.e. plates, angles, gusset) and connectors (i.e. welds, bolts). They have to transmit member end forces (axial forces, shear forces, bending moments, and torsion moments). These steel connections can be simple shear, fully-restrained, or

partially-restrained, depending on the degree of restraint provided. Simple shear are the most commonly used connection type and they are idealized as providing no rotational restraints. Simple shear connections in regular steel floor systems often involve the use of clip angles, which are generally shop-welded to the web of the supported beam and site bolted to the web of the supporting beam.

In reality, connections often behave in a nonlinear manner. The distribution of internal forces and stresses depends on the relative deformations of the component parts and the connectors themselves. Several research attempts have been made to study these behaviours and to predict their response under load (Douty and McGuire, 1963, Kennedy, 1969; Kishi and Chen, 1986; Roeder and Dailey, 1989; Carter, 1999). Computer programs such as ANSYS have been developed and used in connection behaviour studies (Krishnamurthy, 1978). In traditional design, approximate methodologies using simple formulas based on simplifying assumptions are often used. The use of these formulas, however, requires a sound understanding of the basis and limitations of the theories and methods of analysis used in the development of these formulas. The ductile behaviour of structural steel is essential to connections, as plastic yielding may relieve stress concentrations and prevent premature failure.

1.2.2 Lateral Load Resisting System

Concentrically braced frames (CBFs) have long been known to be efficient as a lateral force resisting system with relatively good lateral drift performance. CBFs are traditionally modeled as pin-ended structures (i.e. simple beam to column connections)

with continuity only at the columns of multi-storey frames. The lateral stiffness and strength are provided by diagonal braces that are attached concentrically to the beam-to-column connection by means of gusset plates. Current strength design practice for CBFs typically uses elastic analyses, where the behaviour follows that of a vertical truss system. Many design codes (AISC, 2002; NBCC, 2005; ASCE, 2005; IBC, 2006) treat the various configurations of CBFs as one system in terms of specified design characteristics, but with some recognition of issues specific to certain configurations.

There have been concerns about non-ductile modes of behaviour of CBFs when subjected to large ductility demands. Such behaviour modes include connection and member fracture. The absence of alternative load paths may lead to severe consequences in the event of a failure of one of the components. In addition, buckling of compression diagonal braces may lead to a rapid loss of strength and rigidity without sufficient force redistribution (Jain and Goel, 1978; Goel, 1992). High ductility demand on beams may also result from the unbalanced tension and compression strengths (AISC, 2002).

There have been several studies of the behaviour of brace members subjected to cyclic loading (Wakabayashi et al., 1977; Jain et al., 1980; Popov and Black, 1981; Lee, 1987; Tremblay, 2002). The individual brace members have been found to possess a limited ductile capacity and their hysteretic behaviour is asymmetric between tension and compression. A sample hysteresis response for a rectangular hollow section brace component is shown in Figure 1.1. This indicates a plot of applied load (P) versus deformation (δ), normalised respectively by the yield capacity (P_y) and deformation at yield (δ_y). In the first cycle, the brace is subjected to tension and then reversed to

compression until buckling occurs. Consequently, the compressive resistance decreases due to plastic hinge formation near the mid-length region of the brace. Subsequent cycles of loading result in further degradation of its compressive strength. In tension, the brace reaches its yield strength and it develops some strain hardening.

Nonlinear element models have been proposed to predict the observed brace behaviours (Jain and Goel, 1978; Lee, 1987; Remennikov and Walpole, 1997). An example of such models which simulates the buckling behaviour of a bracing member is shown in Figure 1.2. According to this model, the buckling strength of the compressive brace member, C_r, reduces significantly after the first cycle of loading and then becomes almost steady after a few cycles.

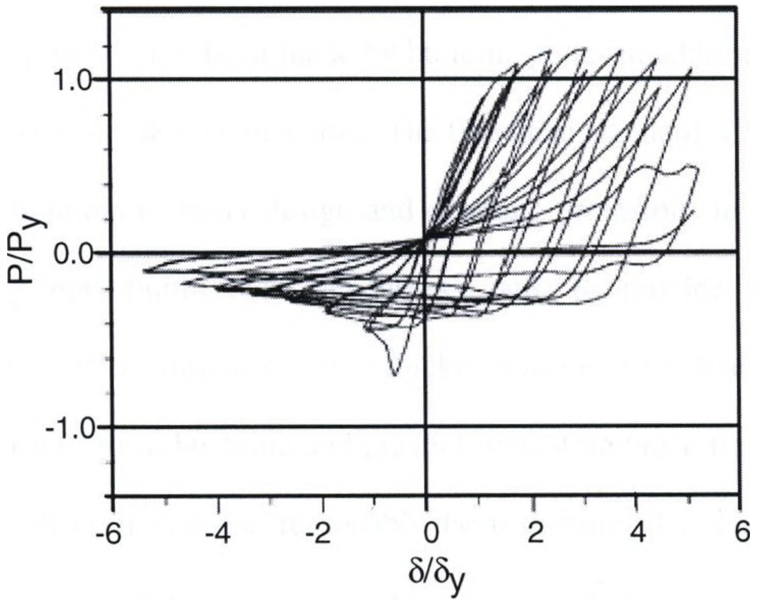

Figure 1.1: A Typical Hysteresis of Steel Brace Member under Cyclic Load (Tremblay 2002)

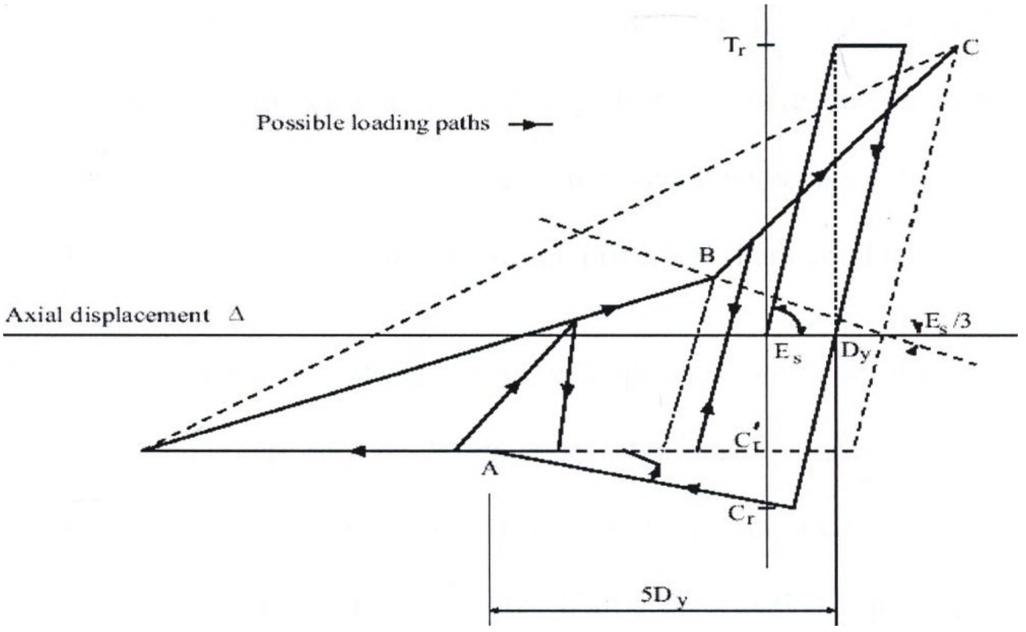

Figure 1.2: Hysteresis Model for Steel Brace Member (Jain and Goel, 1978)

Significant progress has been made by building codes in addressing unfavourable yield modes of braces and their connections. The Canadian standard, CSA-S16-01 (CSA, 2001), specifies minimum capacity design and detailing provisions in Clause 27. These include specifying maximum brace slenderness ratio to provide sufficient energy dissipation capacity, and maximum width-to-thickness ratio for the brace cross-section to delay the occurrence of local buckling and prevent premature brace fracture. In addition, the post-buckling phenomenon has reasonably been captured by applying a buckling reduction factor to the compressive strength of bracing members.

The NBCC (2005) classifies CBFs into moderately ductile, limited ductility and ordinary (or conventional) construction, with ductility related seismic force modification

factors of 3.0, 2.0 and 1.5 respectively. Clearly, the limits are more restrictive when higher inelastic demand is expected or when the frame has reduced energy dissipation capacity as in the case of tension-only bracing. For the more ductile systems, it is required not only to ensure ductile response of individual elements of the seismic force resisting system but also to apply capacity design principles (Park and Paulay, 1975).

The concept of capacity design plays an important role in seismic performance and design. In contemporary seismic design codes, significant inelastic deformations are accommodated under severe earthquakes. Capacity design allows the designer to take advantage of regions or zones of considerable plastic deformation capacity. Once these regions are identified and detailed, other regions in the frame are treated as responding elastically. The designer therefore has control over the failure mechanism of the frame and can dictate where inelastic deformation should and should not occur.

For concentrically braced frames, inelastic deformation in the bracing members is the main source of dissipating seismic energy. These brace members are therefore designed to be capable of sustaining significant inelastic deformation in either compression or tension without significant loss of strength and stiffness. They are detailed to ensure that they go through the expected inelastic demand without premature failure. For other members and components (i.e. beams, columns and connections), they should possess sufficient capacity to resist the maximum forces that might develop in them as a result of yielding and buckling of bracing members. These frame members and components are therefore designed to support maximum induced forces due to yielding and buckling braces.

1.2.3 NBCC Provisions for Seismic Design

The National Building Code of Canada (NBCC, 2005) recognises dynamic analysis as a reliable method for realistic assessment of seismic design forces. NBCC also permits the use of the equivalent static load method for building structures with specified height and regularity restrictions. Seismic hazard in this method is represented by the uniform hazard spectra values corresponding to a 2% in 50 year probability of exceedance. The design base shear, V, is given by:

$$V = \frac{S(T_a)M_v I_E W}{R_o R_d} \geq \frac{S(2.0)M_v I_E W}{R_o R_d} \tag{1.1}$$

where $S(T_a)$ is the design spectral response acceleration at the fundamental mode period of the building, T_a; M_v is a factor that accounts for higher mode effects; I_E is an importance factor of the structure; W is the dead load plus 25% of the design snow load; R_d is a ductility related force modification factor; and R_o is an overstrength-related force modification factor. The stated lower limit stems from uncertainty associated with the spectral acceleration values for periods greater than 2.0 (Humar and Mahgoub, 2003). The code also limits the design base shear for structures with $R_d \geq 1.5$ by:

$$V \leq \frac{2}{3}\frac{S(0.2)I_E W}{R_o R_d} \tag{1.2}$$

This maximum limit is due to observations of limited damage of short-period structures in past earthquakes (Humar and Mahgoub, 2003). The fundamental mode period, T_a, may

be obtained from empirical expression given by Saatcioglu and Humar (2003). For steel braced frames, $T_a = 0.05(h_n)^{3/4}$, where h_n is the height of the framed structure. Alternatively, analytical methods may be used to estimate the period. The design base shears are distributed over the height of the building as explained in the NBCC (2005).

1.2.4 Structural Modeling and Analysis

Generally speaking, a model that represents the essential characteristics of all basic elements is intrinsic to understanding the response of the structure. Elastic rigidities of steel structures can readily be computed on the basis of elastic material properties. Once the sectional geometry is established, member properties are computed analytically. The flexural rigidity EI, shear rigidity GA, and axial rigidity AE can be determined from cross-sectional properties, A and I (where A is the cross-sectional area and I is the moment of inertia), and material moduli, E and G (where E is the modulus of elasticity and G is the shear modulus).

Inelastic behaviour leads to analysis techniques that may require a substantially higher level of sophistication. Any nonlinear analysis procedure generally requires modeling of the complete load-deformation (or moment- curvature) characteristics to failure of each component of the structure. Thus, the stiffness, strength, and post-yield behaviour of all elements in the lateral load path are captured explicitly in the model. The selection and simulation of correct boundary conditions that represent supports and connections is critical in structural modeling and analysis. The use of a two-dimensional model is generally sufficient if torsional effects are deemed to be insignificant or

accounted for elsewhere. When a building with rigid diaphragms is torsionally irregular, or if the behaviour of the members in one plane substantially influences the behaviour in another plane, a three-dimensional model may be more useful.

Structural analysis may be classified as static or dynamic depending on the nature of load the structure is subjected to. When inertial effects are significant, dynamic analysis is required. It may also be classified as linear or nonlinear depending on the assumed behaviour of the structure's material. Thus, structural analysis could follow a linear static, linear dynamic, nonlinear static or nonlinear dynamic procedure. Choice of the analysis type to use depends on the importance and nature of results sought. Linear static and linear dynamic analyses are often used in seismic design. But for extensive evaluation, nonlinear dynamic procedure is preferred.

The distribution and use of lateral load obtained from the NBCC (2005) equivalent static load approach is based on linear static analysis procedure. Response spectrum analysis represents a linear dynamic procedure and has been found to be reasonably accurate for building design (Gupta, 1990). The widely used pushover analysis represents the nonlinear static procedure. The concept, accuracy and applicability have been explained extensively by Lawson et al. (1994), Krawinkler and Seneviratna (1998) and Kim and D'Amore (1999). This analysis type may provide, among other information, estimates of strength and deformation demands on structural elements, response mechanisms and the identification of weak links in the lateral load path. Nonlinear dynamic analysis is a time history analysis that accounts for nonlinear stiffness and strength characteristics of the structural elements. This procedure is the most

sophisticated and time consuming but it yields accurate strength and deformation demands for each structural component if it is conducted properly and with care.

1.3 Modular Steel Building Technique

Over the years, there has been an ever-growing demand by the building industry for speedy, flexible, and cost-effective products. This demand has resulted in the scrutiny of traditional on-site building construction processes. The modular steel building technique is fast evolving as an effective alternative. The technique is widely used in North America, Japan, and in parts of Europe. It involves the design of steel buildings to be built and finished at one location (often in a manufacturing environment) and be transported to and used at another. The volumetric concept of the modular technique may be similar to temporary or relocatable buildings but differs greatly in terms of quality, structural design and general performance criteria. On site, the finished modular units are connected horizontally and vertically in a multi-storey building.

Modular steel buildings are commonly used in one to six storey apartments, hotels, offices, student housing, single family developments, and in other similar buildings where repetitive units are required. The main advantages of this building system is faster time to occupancy, which is due to factors such as simultaneous construction of modular units with site excavation and foundation works, and reduced vulnerability to adverse weather conditions that may slow or stop traditional building construction. Consistent and high quality may also be achieved under a controlled manufacturing environment. The modular design also favours expandability, which may

lead to reduced disruption to operational activities in an existing or neighbouring facilities. Clearly, economy of scale of production is an important factor that has to be considered in the case of non-repetitive building structures. Some examples of modular steel framed buildings are the four-storey SUNY Purchase College dormitory in New York (Murray Engineering, P.C., 2000), and the 131 living units Geneva hotel in New York (Deluxe Building Systems, 2005).

The technique of modular steel building construction leads to detailing requirements that are different from traditional on-site steel buildings. For example, frame members (i.e. floor beams and stringers, and columns) of the modular building system are typically connected by direct welding. Chapters two through to five provide a detailed description of the structural detailing requirements of the modular steel building, highlighting its features that distinguish it from the traditional counterpart.

1.4 Aim and Objectives of Thesis

The primary aim of this thesis is to assess the relevance of contemporary traditional design procedures to the design of Modular Steel Buildings. This was achieved by pursuing the following objectives:

1. To document in a descriptive manner the concept, processes, application and unique detailing requirements of modular steel buildings;
2. To understand the effect of direct welding between the webs of MSB floor beams and stringers on the behaviour and design of modular steel building floors under gravity loads;
3. To investigate experimentally the seismic behaviour of braced frames of modular steel buildings in order to assess the strength, stiffness, inelastic deformation and energy dissipation characteristics of the system;
4. To develop and validate an analytical model capable of simulating the seismic behaviour of MSBs;
5. To analytically investigate and evaluate inelastic behaviour and response characteristics of typical braced frames of modular steel buildings under monotonic lateral loading; and
6. To understand the seismic behaviour of typical braced frames of modular steel buildings and to assess their seismic inelastic demands and capacities under earthquake ground motions.

1.5 Scope of Thesis

The thesis has been prepared in the 'integrated-article' format. In the present chapter, a review of current knowledge in structural steel behaviour and earthquake-resistant design has been provided. Then, the aim and objectives of the study were outlined. The following four chapters address the stated objectives, which are expounded below. The thesis concludes in chapter six by briefly reviewing the main issues and findings in previous chapters, and assessing how far the research has achieved its objectives. An outline of the significant contributions made in this research is also provided in this chapter, and ends with recommendations for future studies.

1.5.1 Effect of Directly Welded Stringer-To-Beam Connections on the Analysis and Design of Modular Steel Building Floors

In Chapter Two, the development of the concept and application of modular design and construction are explained in detail and a summary of commonly used modular steel construction details is provided. This is expected to increase awareness of this unique system among structural engineers and allow researchers to study its critical elements. The chapter then focuses on a typical MSB floor system, which is achieved by welding the webs of the floor stringers directly to the webs of the floor beams. A typical modular steel floor grid structure is designed, as in current practice, using conventional methods. The selected floor is modelled using the finite element method and analysed under the effect of dead and live service loads. The finite element analysis allowed an

assessment of the effect of direct welding between stringers and floor beams on the analysis and design of the floor beams, floor stringers, and welded connections. A simplified analytical model is proposed to capture the floor behaviour. The finite element analysis results were used to develop regression functions to describe the model. In practice, the proposed model can predict the actual forces and moments leading to a reliable design of modular steel building floors. A step-by-step design methodology has been provided for easy application of the developed model.

1.5.2 Experimental Evaluation of the Seismic Performance of Modular Steel Braced Frames

The seismic performance of a framed structure depends on the frame configuration, including its connections. Chapter Three evaluates the hysteretic characteristics of modular steel braced frames under reversed cyclic loading. The design and construction of the modular braced test specimen accounted for its specific detailing requirements. A regular concentrically braced frame with similar physical characteristics (clear height and member proportions) was also tested for comparison. Both test specimens consisted of a one-bay, one-storey X-braced system with tubular brace cross-section. This chapter describes the behaviour characteristics, and provides a detailed comparison of the two systems in order to assess the strength, stiffness, inelastic force and deformation, and energy dissipation characteristics of the modular system. An analytical model capable of capturing the effect of the system's unique detailing requirements is proposed and validated using the test results.

1.5.3 Seismic Overstrength in Braced Frames of Modular Steel Buildings

The seismic behaviour factor, R, is a critical parameter in contemporary seismic design. In Chapter Four, typical braced frames of Modular Steel Buildings were designed for strength and ductility using Canadian standards. Conventional capacity design procedure was adopted in the design. Analytical models of the frames, validated in the previous chapter, were developed. Nonlinear static pushover analyses were conducted to study the inelastic behaviour of these frames. Structural overstrength resulting from redistribution of internal forces in the inelastic range, design assumptions, and strain hardening behaviour of steel, and displacement ductility were evaluated and their relationships with some key response parameters were assessed. Behavioural characteristics observed from this study were subsequently used in rationalising the dynamic analysis conducted in chapter five.

1.5.4 Seismic Vulnerability Assessment of Modular Steel Buildings

Contemporary seismic design is based on dissipating earthquake energy through significant inelastic deformations. In Chapter Five, an attempt is made at developing an understanding of the inelastic seismic behaviour of braced frames of modular steel buildings and assessing their seismic demands and capacities. Nonlinear incremental dynamic analysis is performed on 2-, 4- and 6-storey MSB braced frames, designed for moderate ductility according to current Canadian standards. Two-dimensional models that represent the important behavioural aspects of different elements and components of MSB braced frames, including their unique detailing requirements, are developed. The

dynamic behaviour of the modeled frames under an ensemble of 20 ground motions, each scaled to several intensity levels, is investigated. Maximum inter-storey drift and peak global roof drift were adopted as critical response parameters for the evaluation of structural drift and ductility demands and capacities.

1.6 References

AISC [2002] *Seismic provisions for structural steel buildings,* ANSI/AISC 341-02, American Institute of Steel Construction, Chicago

ASCE [1996] "Proposed specification and commentary for composite joists and composite trusses," *Journal of Structural Enginnering* (April), 350-358.

ASCE [2005] *ASCE/SEI 7-05: Minimum design loads for buildings and other structures*, Standard Committee, American Society of Civil Engineers, Virginia, USA.

Atkinson, A. H. and Cran, J. A. [1972] "The design and economics of composite open-web steel joists," *Canadian Structural Engineering Conference.*

Azmi, M. H. [1972] *Composite open-web trusses with metal cellular floor*, A Master of Engineering Thesis, McMaster University, Hamilton, Ontario.

Brattland, A. and Kennedy, D. J. L. [1992] "Flexural tests of two full-scale composite trusses," *Canadian Journal of Civil Engineering*, 19 (2), 279-295.

Carter, C. J. [1999] "Stiffening of wide-flange columns at moment connections: wind and seismic applications," *Steel Design Guide Series*, 13, AISC, Chicago, IL.

Collaco, J. P. [1972] "A stub-girder system for high-rise buildings," *AISC Engineering Journal*, 89-95.

Cross, J. [2003] "Coordinated construction," *Modern Steel Construction* (July).

CSA [2001] *Limit state design of steel structures, Standard CSA-S16-01*, Canadian Standards Association, Rexdale, Ontario.

Curry, J. H. [1988] *Full-scale tests on two long-span composite open-web steel joists*, Masters Thesis, University of Minnesota, MN.

Deluxe Building Systems, Inc. [2005] www.deluxehomes.com. Accessed on November 20, 2008

Douty, R. J. and McGuire, W. [1963] "Research on bolted moment connections – A progress report," *Proceedings of National Engineering Conference*, AISC, 48-55.

Goel, S. C. [1992] "Cyclic post-buckling behaviour of steel bracing members," In: *Stability and ductility of steel structures under cyclic loading*, CRC Press, 75-84.

Gupta, A. K. [1990] *Response spectrum method in seismic analysis and design of structures,* Blackwell Scientific Publications, Boston, Massachusetts.

Humar, J. and Mahgoub, M.A. [2003] "Determination of seismic design forces by equivalent static load method," *Canadian Journal of Civil Engineering*, 30, 287-307.

IBC [2006] *International Building Code*, International Code Council, ICC, USA.

Jain, A. K. and Goel, S. C. [1978] *Hysteresis model for steel members subjected to cyclic buckling or cyclic end moments an buckling – User's guide for DRAIN-2D: EL9 and EL10*, Department of Civil Engineering, University of Michigan, Ann Arbour, MI.

Jain, A. K., Goel, S. C. and Hanson, R. D. [1980] "Hysteretic cycles of axially loaded steel members," *Journal of Structural Division, ASCE*, 106 (8), 1777-1795.

Kennedy, D. J. L. [1969] "Moment-rotation characteristics of shear connections," Engineering Journal, AISC, Chicago, 6 (4), 105-115.

Kim, S. and D'Amore, E. [1999] "Push-over analysis procedure in earthquake engineering," *Earthquake Spectra*, 15 (3), 417-434.

Kishi, N. and Chen, W. F. [1986] "Data base of steel beam-to-column connections," *CE-STR-86-26, Purdue University*, School of Engineering, West Lafayette, IN.

Krawinkler, H. and Seneviratna, G. D. P. K. [1998] "Pros and cons of a pushover analysis of seismic performance evaluation," *Engineering Structures*, 20 (4-6), 452-464.

Krishnamurthy, N. [1978] "A fresh look at bolted end-plate behaviour and design," *Engineering Journal*, AISC, 25 (2), 39-49.

Lawson, R. S., Vance, V., and Krawinkler, H. [1994] "Nonlinear static push-over analysis – why, when, an how?," *Proceedings of the 5th US National Conference on Earthquake Engineering*, Chicago, 1, 283-292.

Lee, S. [1987] *Seismic behaviour of hollow and concrete-filled square tubular bracing members*, Deapartment of Civil Engineering, University of Michigan, Ann Arbor, MI.

Lembeck, H. G. [1965] *Composite design of open-web steel joists*, Masters Thesis, Washington University, St Louis, MO.

Leon, R. T. and Curry, J. [1987] "Behaviour of long-span composite joists," *ASCE Structures Congress proceedings*, Florida, 390-403.

Murray Engineering, P.C. [2000] *SUNY Purchase College Dormitory Construction Drawings*, Materials obtained by personal communication with Mr. Robert J. Murray, P.E., Principal, Murray Engineering, P.C.

Naccarato, P. A. [1999] "New alternative to flat plate construction," *Modern Steel Construction*.

NBCC [2005] *National Building Code of Canada*, Institute for Research in Construction, National Research Council of Canada, Ottawa, Ontario, Canada.

Park, R., and Paulay, T. [1975] *Reinforced concrete structures*, John Wiley & Sons, New York.

Popov, E. P. and Black, R. G. [1981] "Steel struts under severe cyclic loadings," *Journal of Structural Engineering*, 107 (9), 1857-1881.

Remennikov, A. and Walpole, W. [1997] "Analytical prediction of seismic behaviour for concentrically-braced steel systems," *Earthquake Engineering and Structural Dynamics*, 26, 859-874.

Roeder, C. W. and Dailey, R. W. [1989] "The results of experiments on seated beam connections," Engineering Journal, AISC, Chicago, 26 (3), 90-95.

Saatcioglu, S. and Humar, J. [2003] "Dynamic analysis of buildings for earthquake-resistant design," *Canadian Journal of Civil Engineering*, 30, 338-359.

Samuelson, D. [2002] "Composite steel joists," *AISC Engineering Journal* (3rd quarter), 111-120.

Tremblay, R. [2002] "Inelastic seismic response of steel bracing members," *Journal of Constructional Steel Research*, 58, 665-701.

Wakabayashi, M., Nakamura, T., and Yoshida, N. [1977] "Experimental studies on the elastic-plastic behaviour of braced frames under repeated horizontal loading," *Bulletin of Disaster Prevention Research Institute*, Kyoto Univ., 27 (251), 121-154.

CHAPTER TWO

EFFECT OF DIRECTLY WELDED STRINGER-TO-BEAM CONNECTIONS ON THE ANALYSIS AND DESIGN OF MODULAR STEEL BUILDING FLOORS*

2.1 Introduction

The modular construction technique is fast evolving as an effective alternative to traditional on-site building. The technique is widely used in North America, Japan, and in parts of Europe. It involves the design of structures to be built and finished at one location and transported to and used at another. The main advantage of the modular construction technique is the combination of the speed of construction with the quality of controlled manufacturing.

In the building industry, the concept of modular design refers to factory construction of pre-engineered building units, delivered to site and assembled as large volumetric components. The volumetric concept may be similar to temporary or relocatable buildings but differs greatly in terms of quality, structural design and general performance criteria. The collection of discrete modular units usually forms a self-supporting structure in its own right. The modular units are often fully fitted, complete with floors, lighting, plumbing, heating, etc. before they are delivered to site for installation.

* Annan, C.D.,Youssef, M.A., and El Naggar, M.H. "Effect of directly welded stringer-to-beam connections on the analysis and design of modular steel building floors," *Advances in Structural Engineering*, accepted in October 2008.

The application of modular construction is found mainly in general building construction, particularly apartment buildings, schools, hotels, student housing, hospitals, offices, single family developments, correctional facilities, and other buildings where units are repetitive. Rapid construction and installation has been the major driving force behind the modular building industry. For example, it has been suggested that on-site construction times in hotels and fast-food restaurants could be reduced by over 60% with the adoption of modular construction (Lawson et al., 1999). Such a huge potential savings in time and costs may be due to such factors as allowing simultaneous site preparation and modular units' construction, and reduced vulnerability to adverse weather conditions that may slow down or stop traditional construction. Other related benefits include the avoidance of disruption and loss of operation during extension works in existing or neighboring facilities such as hotels, and also the achievement of high quality control under off-site manufacturing conditions, including pre-installation checks. Clearly, however, economy of scale of production is an important factor that has to be considered against these benefits; it may be more expensive than traditional methods to use a modular design for irregular buildings or non-repetitive units.

Light steel framing has been widely used in modular construction. The Steel Construction Institute (SCI) of the United Kingdom conducted performance specification studies for modular construction using this material (Lawson et al., 1999). The limitations of the use of light steel framing are evident in its range of applications. For frequently used building structures, higher strength and durable steel members, such as hot-rolled I-sections, are more useful and efficient. The use of such sections in modular building construction is what has been referred to, in this thesis, as Modular Steel Buildings

(MSBs). An example of such a building is the four-storey modular steel building for SUNY Purchase College Dormitory in New York (Murray Engineering, P.C., 2000).

To the best of the author's knowledge, this is the first technical documentation explaining how high strength and durable steel sections are being used by MSBs manufacturers. It is expected that this would provide other researchers and structural engineers an opportunity to study the critical elements of MSBs. Another objective of this chapter is to study the effect of direct welding between the webs of MSB floor stringers and floor beams on the analysis and design of the floor system.

The following sections provide a description of typical MSB details, including the floor stringer-to-beam connections, making comparisons with conventional steel buildings. A typical MSB floor-system was designed using the Canadian steel design code (CSA, 2001). The system was modeled and analysed using the finite element (FE) method. A parametric study was conducted based on some geometric parameters likely to affect the response of the floor framing in order to further investigate its behaviour. The results of the FE analysis were used to reassess the capacities of the various components of the floor system. A simplified analytical model is proposed in this chapter to simulate the floor behaviour in order to predict the forces and moments in members of the modular floor system. This is expected to lead to an optimum and reliable design of the various components of the floor system. A step-by-step design methodology has also been provided for ease of design application

2.2 Modular Steel Buildings

High strength steel sections are used in the construction of durable and frequently used MSB structures. They have been typically used for one-to-six storey schools, hotels, apartments, and student housing. The modules are assembled in a manufacturing environment which ensures a consistently high quality standard and speed of construction to occupancy. Each module consists of a floor and a ceiling grid system separated by a number of columns. The floor system is typically composed of two floor beams, a number of floor stringers, and a metal deck floor with concrete topping. Similarly, the ceiling framing includes two ceiling beams and a number of ceiling stringers.

Figure 2.1 shows typical floor/ceiling steel framing of a multi-storey MSB. It consists of six modules, labeled M#1 to M#6. The floor beams (FB) and ceiling beams (CB) are oriented along the building width and the floor stringers (FS) and ceiling stringers (CS) in each module are along the building length. Horizontal and vertical connections for the separately finished modules are made onsite. A typical horizontal connection (HC) is shown in section A-A of Figure 2.1. This section consists of four modular units; two upper and two lower units. The horizontal connection is shown between the upper units, which involves the field bolting of clip angles which are shop-welded to the floor beams. Section B-B of Figure 2.1 depicts a typical vertical connection (VC). The section shows the base plates of the upper module column field-welded to the cap plates of the lower module column.

Lateral stability of MSBs is achieved either by developing moment resisting frames using the floor beams, ceiling beams, floor stringers, ceiling stringers and

columns within each module or by adding diagonal braces as shown by the dashed lines in the floor plan of Figure 2.1. Lateral loads are resisted in the shorter direction by the external braced frame of modules M#1 and M#6 and in the longitudinal direction by the external braced frame of modules M#2 and M#5.

Within each floor, lateral loads are transferred to the braced frame system through the horizontal connections (HC). The total lateral load is then transferred through the vertical connections (VC) to the foundation. The combined behaviour of the composite floor in each unit and the horizontal module connections between units is designed to be sufficiently rigid in order to transfer lateral loads between the floors to the lateral load resisting systems. The lateral response and characteristics of typical braced frames of MSBs are investigated in chapters three, four, and five of this thesis.

Figure 2.2 shows further details of the modular steel floor assembly. This consists of a section through a typical floor arrangement. The second floor assembly depicts floor arrangements for two modules on the second storey located side-by-side and ceiling arrangements for two modules on the first storey. The assembly also shows sections of steel deck (usually welded to the flange of the floor beam), concrete floor and the ceiling finishes. The first floor assembly (bottom section) depicts floor arrangements of two side-by-side modules on the first storey and their connection to the concrete footing.

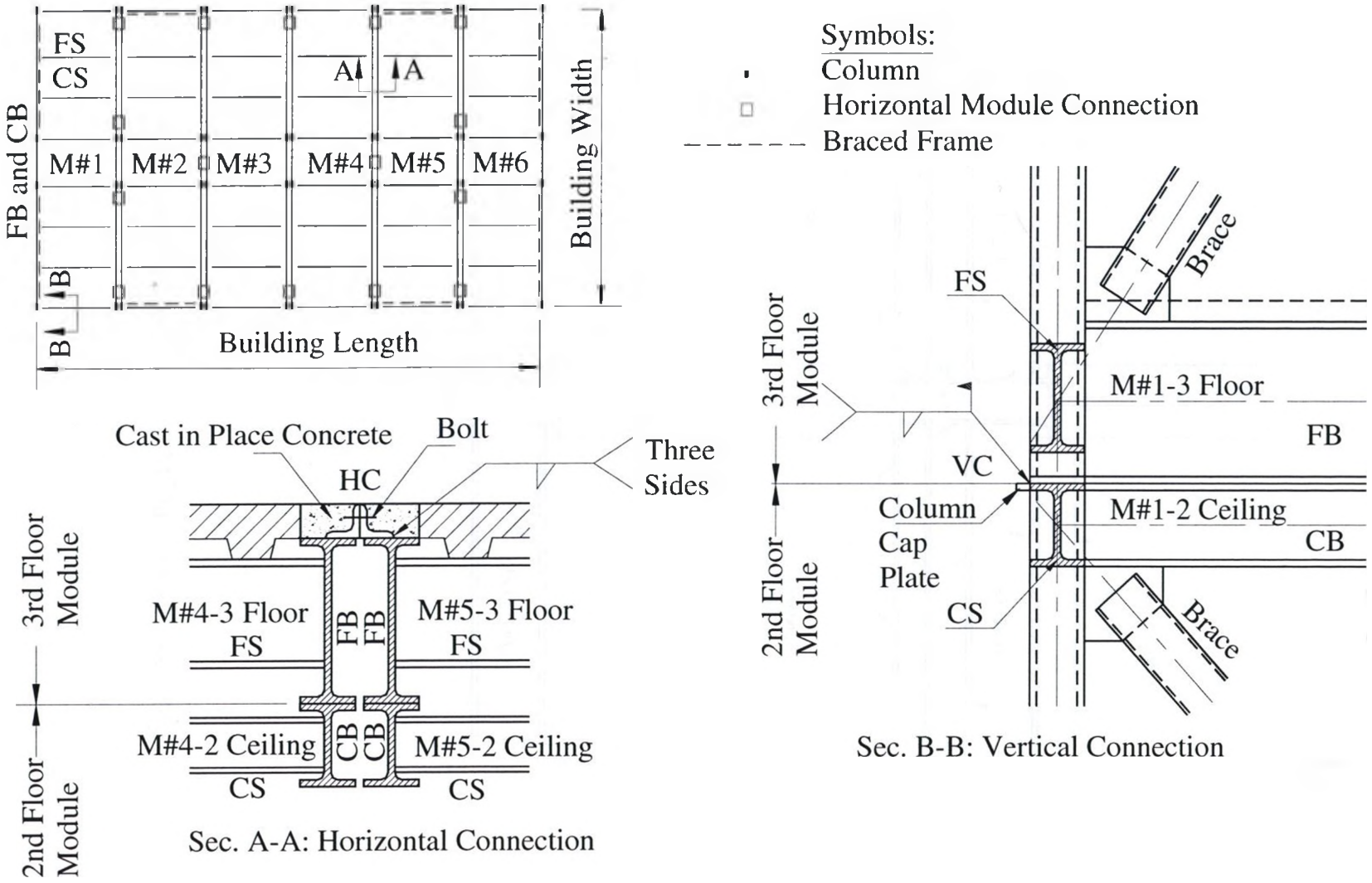

Figure 2.1: A Typical Floor Plan and Sections of a Multi-Storey Modular Steel Building

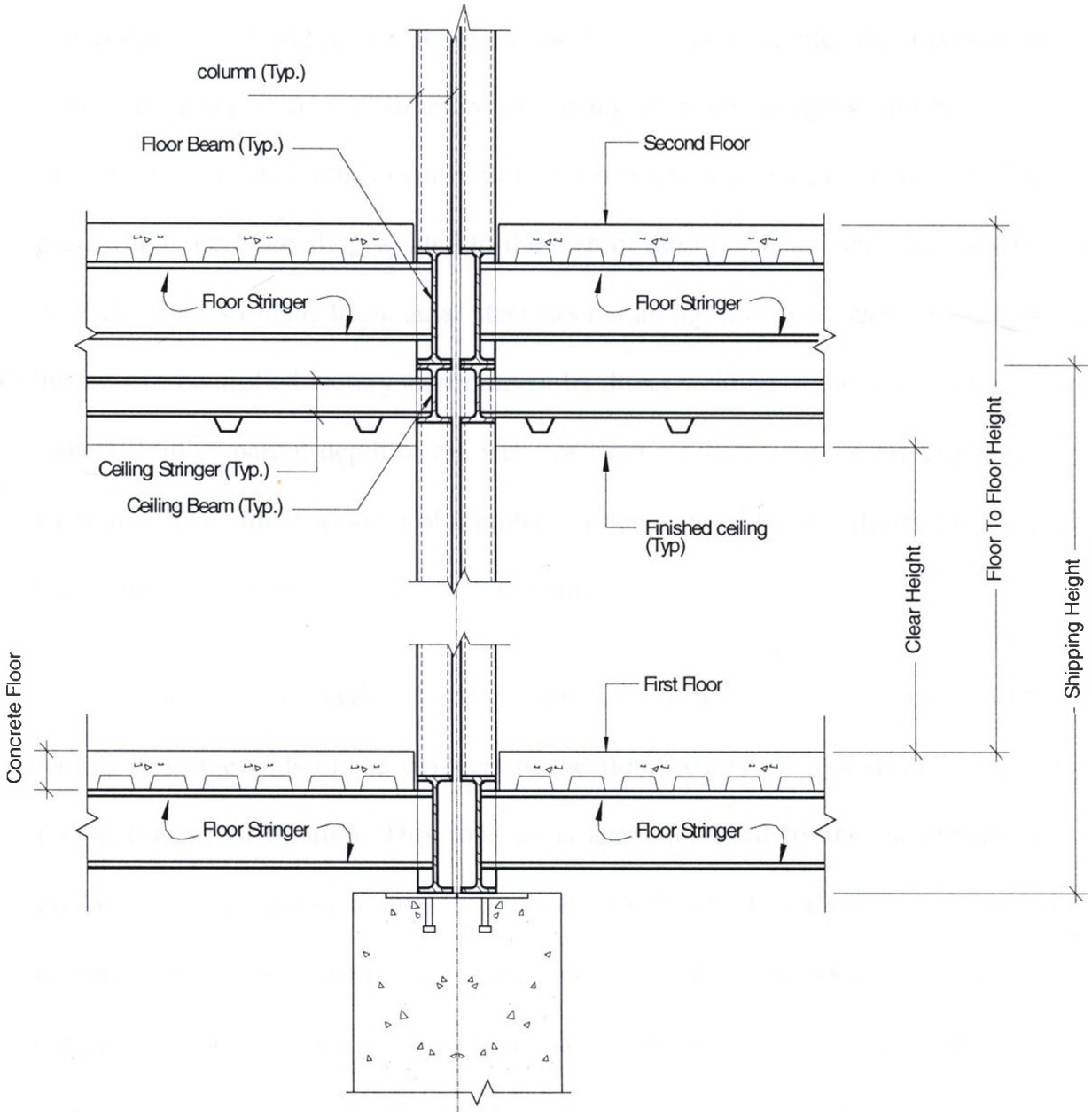

Figure 2.2: A Section Through a Typical Modular Floor Assembly

2.3 Floor Stringer-to-Beam Connections

Significant differences exist between the methods of MSB construction and conventional steel building construction. In MSBs, for example, the floor-system is typically designed as a grid structure consisting of floor stringers and beams. Floor stringer-to-beam connections in conventional construction are usually achieved using clip angles, which are often shop welded to the web of the floor beam and site bolted to the web of the floor stringer. In modular steel floor framing, however, such connections are achieved in a controlled factory environment by direct welding of the webs of the joining members. Full or partial depth of the webs of floor stringers may be directly welded to floor beams. This direct welding of members is necessitated by the lifting, handling, and transportation requirements of the modular units.

The use of clip angles in conventional construction results in the transfer of reactions from the ends of the stringers to the floor beams through shear action, while allowing for partial rotation. This rotation is accommodated by the movement of clip angles within the clearance around the bolts and by the elastic and inelastic deformations occurring in the bolts, clip angles, and stringer beams. This enables redistribution of any negative moment that might develop at these connections. To analyse this type of connection, material nonlinearities for the clip angles, bolts, and stringer beam need to be considered. Also, the contact behaviour between the bolts, the clip angles, and the floor beams must be modelled. Lipson (1968) made an experimental study to evaluate the static behaviour of single web angle connections. It was reported that these connections exhibited nonlinear moment-rotation behaviour at early stages of loading, which is

expected to allow redistribution of beam moments. Al-Emrani and Kliger (2003) conducted a finite element analysis to study the behaviour of double angle stringer-to-floor beam connections in riveted railway bridges. The stringers were modeled using shell elements and solid elements were used to model the angles and the rivets in the connection. The contact between the back-face of the leg of the connection angle and the web of the floor beam was modeled using linear quadratic rigid elements. The Coulomb-friction model was used to characterize the interface conditions at all the contact surfaces. They concluded that a connection moment might develop in these connections, which would make such connections vulnerable to fatigue damage.

In the case of the directly welded connections commonly used in MSB floor systems, the behaviour is different. The weld is known to have much higher stiffness than a bolted clip angle connection. Thus, it would allow for only limited deformations before exhibiting a brittle failure mode (Faella et al., 2000). Rotation in these connections would occur only as a result of a plastic hinge forming at the ends of the stringers when the negative moment exceeds the yielding moment. It is expected, however, in such directly welded floor stringer-to-beam MSB connections that the positive midspan moment will be much higher than the negative end moments. Hence, redistribution of end moments will not occur and such hogging moments need to be accounted for in design should they develop. This, combined with the fact that welds have very limited deformation capacity, means that a linear elastic finite element analysis is adequate for evaluating the effect of hogging moments likely to develop as a result of the direct welding in MSB floor systems.

2.4 Design of Modular Floor Grid Structure

A four-storey modular steel dormitory is examined in this study. Each floor is made up of six identical modules consisting of bedrooms and a corridor. The modular steel floor-system adopted for the study is designed as a grid structure consisting of floor stringers and beams. The floor framing consists of two floor beams supporting eleven floor stringers as shown in Figure 2.3. Each floor stringer has a span of 3600 mm and the total length of each floor beam is 16500 mm. The stringers are labeled as SB1 to SB6, with the module symmetric about SB6.

The dead load (DL) is composed of the weights of the concrete floor (100 mm thick), an all round metal curtain wall system and insulation, steel deck and the self weights of the members. A superimposed load of 1.4 kN/m^2 is assumed to account for finishes and other installations. The live loads (LL) used for the design are 1.9 kN/m^2 for the bedrooms and 4.8 kN/m^2 for the corridor as given by the National Building Code of Canada (NBCC, 2005). The floor beams and stringers are designed using traditional methods. The stringers are designed as simply supported beams and the floor beams are designed as continuous beams. The resulting steel sections are W200X21 (W8X14 imperial designation) for the floor stringers and W310X39 (W12X26 imperial designation) for the floor beams. The nominal yield strength of the steel sections is 350MPa (50 ksi imperial designation).

In the design of the directly welded connections between beams and stringers, designers of MSBs typically specify a minimum weld length of 80% of the depth of floor stringer web. Designers often check this weld length against the shear transferred from

the stringer to the beam, assuming no restraint to rotation at the ends of the stringer. This weld length was checked for the selected floor system and was found to be adequate with a high safety factor.

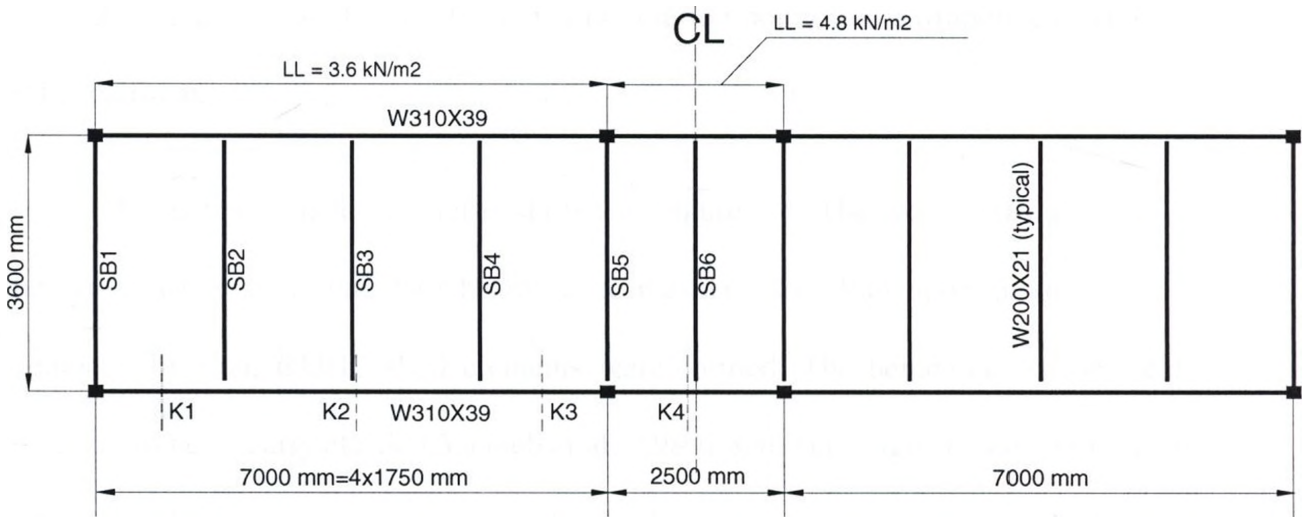

Figure 2.3: Layout of Modular Floor Framing adopted for FE Study

2.5 Finite Element (FE) Model

The level of complexity of finite element models of structural elements and connections generally depends on the method of structural analysis that is adopted, the structure geometry and, more importantly, the type of results required. In this study, a 3D FE model was adopted. The floor itself lies within a single plane; however, loading and displacements occur out of plane.

The model was developed using the nonlinear finite element computer program, SAP2000 (CSI, 2000). In this program, the principle of minimum potential energy is used and the system of equations to be solved is represented by $[k]\{u\} = \{r\}$, where $[k]$ is the stiffness matrix, $\{u\}$ is the vector of nodal displacement, and $\{r\}$ is the vector of applied loads. Stresses and internal forces and moments, in an element local coordinate system, are evaluated at the two-by-two Gaussian integration points and extrapolated to the joints of the element.

A schematic of the model is shown in Figure 2.4. The webs and flanges of both the floor stringers and the floor beams were meshed using four-node quadrilateral shell elements. In total, 63,012 shell elements were formed. The behaviour of the welds is expected to be linearly elastic (Astaneh et al., 1989) with very high stiffness (Doerk et al., 2003). For this reason, nodal points at the weld locations in the webs of the stringers and the beams were constrained to have the same deformations. The remaining contact points between the stringers and the floor beams were modelled using compressive rigid links with zero tensile stiffness.

Column restraints were simulated along an array of nodes located at centerline of column locations under the bottom flanges of beams. The effect of the concrete slab and its restraint to the steel grid structure was simulated by assuming full lateral restraint to the top flanges of the floor beams. The loading on the steel framing was applied as uniform pressure on the frame members. The number of shell elements was chosen after conducting trial analyses using different sizes of shell elements. The selected sizes of shell elements used in the analysis were found to give sufficiently accurate results when

compared with a finer mesh. Appendix I shows a sample SAP2000 data file coded to develop the model.

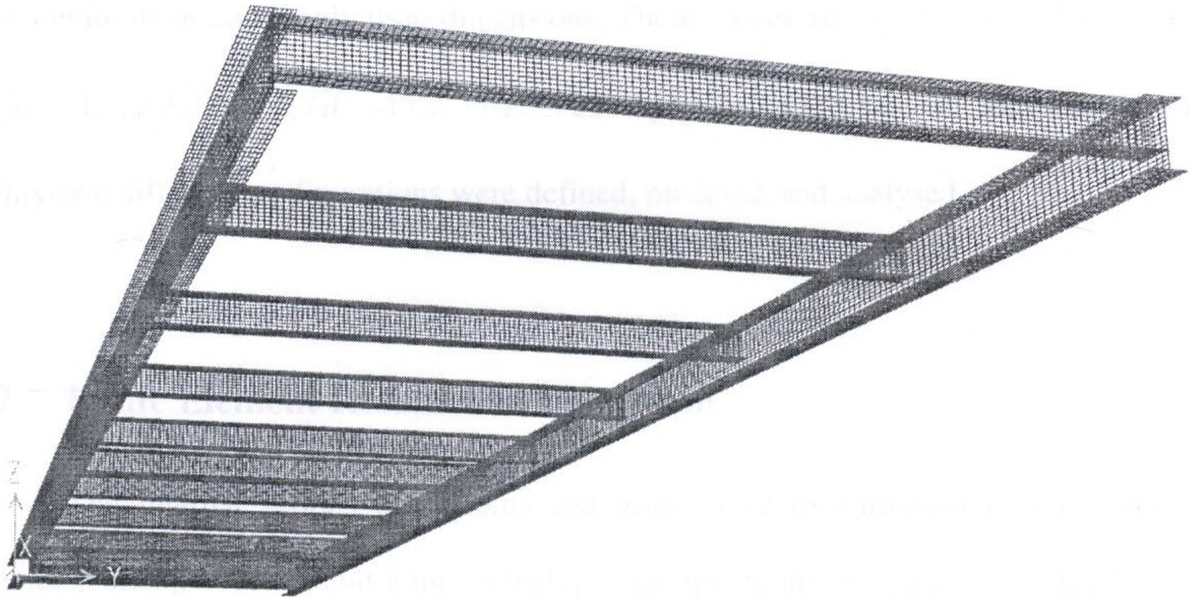

Figure 2.4: Finite Element Mesh

2.6 Parametric Studies

The floor grid structure designed in section 2.4 was analysed using FE analysis. Additionally, a parametric study was performed to further investigate the effect of varying the geometric properties of the components of the modular floor structure. The parameters considered were the ratio of the beam web thickness to the stringer web thickness (t_w^b / t_w^s), the floor beam-to-stringer depth ratio (d_b / d_s), the length-to-depth ratio of the floor stringer (L_s / d_s), and the ratio of the weld length to the depth of the

floor stringer (L_w / d_s). All other properties, dimensions and unit weights were kept constant. The selection of the parameters was based on an understanding of elementary mechanics principles regarding their influence on the response of the floor grid structure. Three typical values for each of the selected parameters were defined based on practical considerations of commonly used dimensions. These values are: $t_w^b / t_w^s = 1.16, 2.32, 3.48$; $d_b / d_s = 1.5, 2.3, 3.0$; $L_s / d_s = 17.7, 35.4, 53.2$; $L_w / d_s = 0.4, 0.8, 1.0$. In all, a total of eighty-one different configurations were defined, modeled, and analysed.

2.7 Finite Element Results and Discussion

The internal actions that beams and joints have to withstand depend on the rotational stiffness of the end joints, which in turn affects the resistance provided by the beams and joints. A simply supported beam of length, L, subjected to a uniformly distributed load, w, is traditionally designed to have a flexural resistance of $wL^2/8$ at the midspan. In this case, it is assumed that there is no restraint to rotation at the joints and the end moment is assumed to be zero. Considering the case of a fixed-end restraint, the maximum bending moment develops at the supports and can be evaluated as $wL^2/12$. This moment is fully transferred to a supporting member and thus no relative rotation exists in the connection. These assumptions simplify much the structural design and analysis. In reality, however, most connections are neither perfect hinges nor fully rigid and thus will lead to different patterns of moment distribution. For nominally pin-jointed frames, the actual joint or rotational stiffness allows to optimize the distribution of bending moments in beams, thus leading to optimal weight and moment distribution. In

nominally rigid frames, the actual joint deformability adversely influences the sensitivity of the frame to second order effects (Faella et al., 2000). In the following sections, the finite element (FE) results for a typical floor of the MSB are summarised and discussed.

2.7.1 Floor Stringers

Table 2.1 shows a comparison between the design forces and moments and results of the FE analysis for various floor stringers of the configuration shown in Figure 2.3 ($t_w^b / t_w^s = 1.16$, $d_b/d_s = 1.5$, $L_s / d_s = 17.7$, $L_w / d_s = 0.8$). The FE model is validated, as shown in Table 2.1, by the agreement of the sum of negative end moments and positive midspan moments to requirements of elementary structural mechanics. For this configuration, it is noted that the bending moments at the midspan of the floor stringer obtained from the FE analysis (M_{FE}) are about 90% of the design midspan moments (M_d). This percentage is not significantly affected by the variation in the magnitudes of the applied load on the various floor stringers. In other words, floor stringer SB6 produced almost the same percentage of M_{FE}/M_d as floor stringer SB5, which was subjected to 70% more imposed loading. The percentage of M_{FE}/M_d is, however, significantly affected by the ratio of the beam web thickness (t_w^b) to the stringer web thickness (t_w^s) and the beam-to-stringer depth ratio (d_b/d_s), as revealed by the results of the parametric study described below.

Figure 2.5 shows the variation of the midspan moment for the floor stringer with changes in some geometric properties of the floor grid structure. The midspan moment

obtained from the FE analysis decreases with an increase in the ratio of the beam web thickness to the stringer web thickness (t_w^b / t_w^s). As the thickness of the web of the supporting beam increases relative to that of the stringer, the joint becomes more rigid and its capacity to restrain rotation is enhanced. However, as the depth of the supporting beam increases in relation to that of the supported stringer, the joint capacity to restrain rotation is reduced. The rigidity of the connection partially restrains the rotation of the stringers. Consequently, hogging (negative) moments are developed at their ends. As shown in Table 2.1, the hogging moments at the ends of the stringers, M_h, was about 10% of the design midspan moment of a simply supported beam, M_d. The results of the parametric study revealed that this negative end moment is significantly increased with an increase in the ratio of the beam web thickness to the stringer web thickness, t_w^b / t_w^s, and decreased with an increase in the beam-to-stringer depth ratio, d_b / d_s (Figure 2.6).

In addition to the observed negative end moments that are not taken account of in a typical MSB floor design, tensile forces are developed in the stringers and opposing compressive forces are developed in the concrete slab. The horizontal restraint provided by the slab to the top flange of the floor beams caused this axial force to develop. The magnitude of this axial (tensile) force developed in the stringers (N_{FE}) was as high as 39.5% of the total load (W) supported by the stringers, as shown in Table 2.1. The compressive force is transmitted from the flange of the floor beam to the slab by bearing of the flange on the concrete slab.

Table 2.1. Comparison of FE Results with Design Forces and Moments for Stringers

Configuration Considered $d_b/d_s=1.5 \quad t_w^b/t_w^s=1.16 \quad L_s/d_s=17.7 \quad L_w/d_s=0.8$	**FLOOR STRINGERS**					
	SB1	**SB2**	**SB3**	**SB4**	**SB5**	**SB6**
Mid-Span Moment (Design) M_d, (kNm)	22.28	22.03	22.03	22.03	30.8	18.26
Mid-Span Moment (FE) M_{FE}, (kNm)	20.2	20.09	20.14	20.05	27.75	16.54
M_{FE} as a percentage of M_d (%)	**90.66**	**91.19**	**91.42**	**91**	**90.1**	**90.58**
Hogging Moment at end of span (Design) M_h, (kNm)	0	0	0	0	0	0
Hogging Moment at end of span (FE) M_n, (kNm)	2.08	1.94	1.89	1.98	3.05	1.72
M_n as a percentage of M_d (%)	**9.34**	**8.81**	**8.58**	**9**	**9.9**	**9.42**
Axial Force (Design) N_d, (kN)	0	0	0	0	0	0
Axial Tensile Force (FE) N_{FE}, (kN)	15.16	18.55	19.08	18.14	21.79	13.84
Total Load on Beams excl. self wt. W (kN)	48.74	48.2	48.2	48.2	67.68	39.82
N_{FE} as a percentage of W (%)	**31.1**	**38.49**	**39.59**	**37.63**	**32.2**	**34.76**

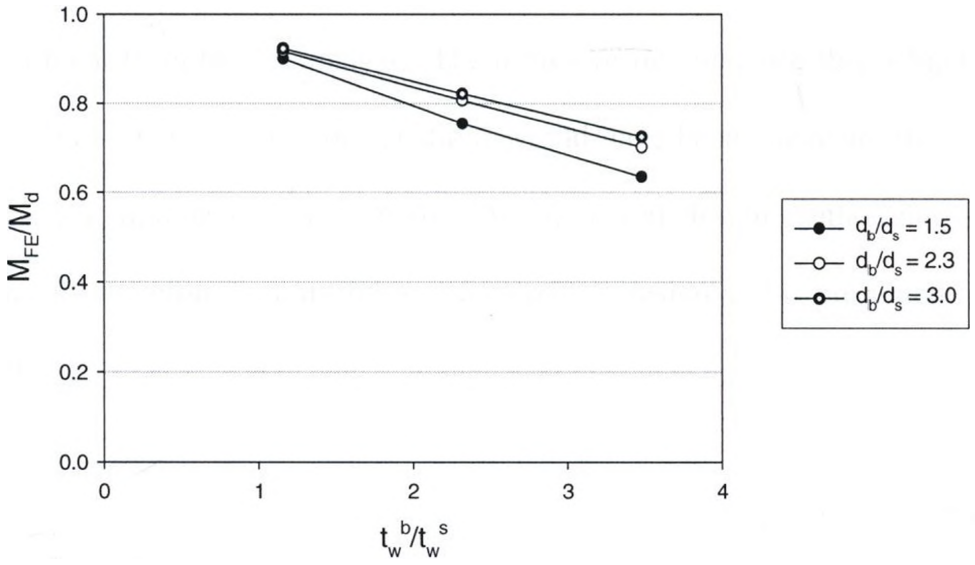

Figure 2.5: Variation of FE-to-Design Midspan Moment Ratio with Beam-to-Stringer Web Thickness Ratio for different Beam-to-Stringer Depth Ratios

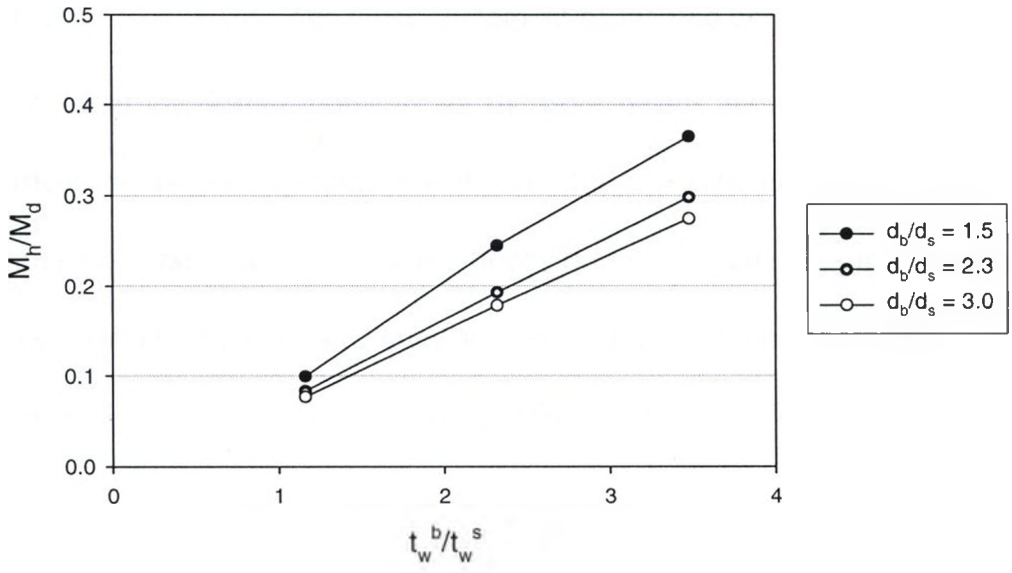

Figure 2.6: Variation of the ratio of FE Hogging Moments to Design Mid-Span Moment with Beam-to-Stringer Web Thickness Ratio

The stringers were redesigned to take account of the axial force and the reduced midspan moment from the FE analysis. The design results revealed that a lighter section (W200X15 or W8X10 imperial designation) would have been adequate, thus leading to more efficiency, lightness, and economy. An improved design methodology for floor stringers would therefore be a useful tool for optimal design and is presented in sections 2.8 and 2.9.

2.7.2 Floor Beams

For the floor beams, the bending moments obtained from the FE analysis closely matched that of the design moments at the selected sections. Table 2.2 shows a comparison between FE results and design bending moments at the specified sections of the floor beam, indicated in Figure 2.3 for the configuration $t_w^b / t_w^s = 1.16$, $d_b / d_s = 1.5$, $L_s / d_s = 17.7$, $L_w / d_s = 0.8$. The close agreement of the two corresponding sets of values demonstrates that the design moments for the floor beams are accurate and do not need any modification. To some extent, this observation also validates the FE model since it agrees with elementary mechanics of the floor grid system. The hogging moments at the ends of the stringers, however, resulted in some torsional moments in the floor beams, but these were found to have an insignificant effect on the floor analysed.

Table 2.2. Comparison of FE Results with Design Bending Moments at Sections of Floor Beam

Configuration Considered $d_b/d_s=1.5 \quad t_w^b/t_w^s=1.16 \quad L_s/d_s=17.7 \quad L_w/d_s=0.8$	Sections of Main Beam, measured from point A (mm)			
	900 (K1)	**3550 (K2)**	**6100 (K3)**	**8100 (K4)**
Bending Moment at section (Design) M_d, (kNm)	44.83	91.57	-21.93	71
Bending Moment at section (FE) M_a, (kNm)	44.44	91.34	-21.34	69.22
M_a as a percentage of M_d (%)	**99.13**	**99.75**	**97.3**	**97.49**

2.7.3 Stringer-to-Floor Beam Welded Connections

Floor stringer-to-beam welded connections are typically designed to resist only shear forces. The FE analysis revealed, however, that these welded connections do experience bending stresses due to the hogging moments developed at the ends of the stringers. In addition, these connections are subjected to the effect of axial tensile forces. The capacity of the weld was reassessed because of this combination of axial and shear forces, and moments. The loads at weld joints were derived from the stress results of the FE analysis. The total stress magnitude (total weld load) was evaluated using classical weld stress analysis (Weaver, 1999), defined as:

$$f_{weld} = \sqrt{\left(\left|f_{bending}\right| + \left|f_{normal}\right|\right)^2 + \left(f_{shear}\right)^2} \qquad \text{..... (2.1)}$$

The results showed a significant increase in the weld stresses. The percentage increase in the total weld load from the design assumption (shear only) to the actual case (shear, bending and normal force) was as much as 226% for a specified configuration, $t_w^b / t_w^s = 1.16$, $d_b / d_s = 1.5$, $L_s / d_s = 17.7$, $L_w / d_s = 0.8$. This suggests that the actual behaviour of a directly welded modular steel floor framing connection may have a significant effect on the design of the connections and on the bahaviour of the steel floor framing. Nevertheless, within the range of parameters studied, it was observed that the weld length commonly provided in current practice (about 80% of the depth of stringer web) was adequate.

It was found that weld length greatly affects the results of the FE analysis. Figure 2.7 shows the effect of two weld lengths, $L_w / d_s = 0.4$ and $L_w / d_s = 0.8$, adopted in the FE analysis on the midspan bending moments of a floor stringer (labeled SB5 in Figure 2.3). If the length of the weld was halved for the case of $d_b / d_s = 1.5$, $L_s / d_s = 17.7$, $t_w^b / t_w^s = 3.48$, the bending moments at the midspan of the stringer obtained from the FE analysis (M_{FE}) increased from 63% to about 80% of M_d. In other words, the decreased stiffness at the connection resulting from a reduction in weld length shifts the negative bending moment from the ends of the stringer to a positive moment at its midspan.

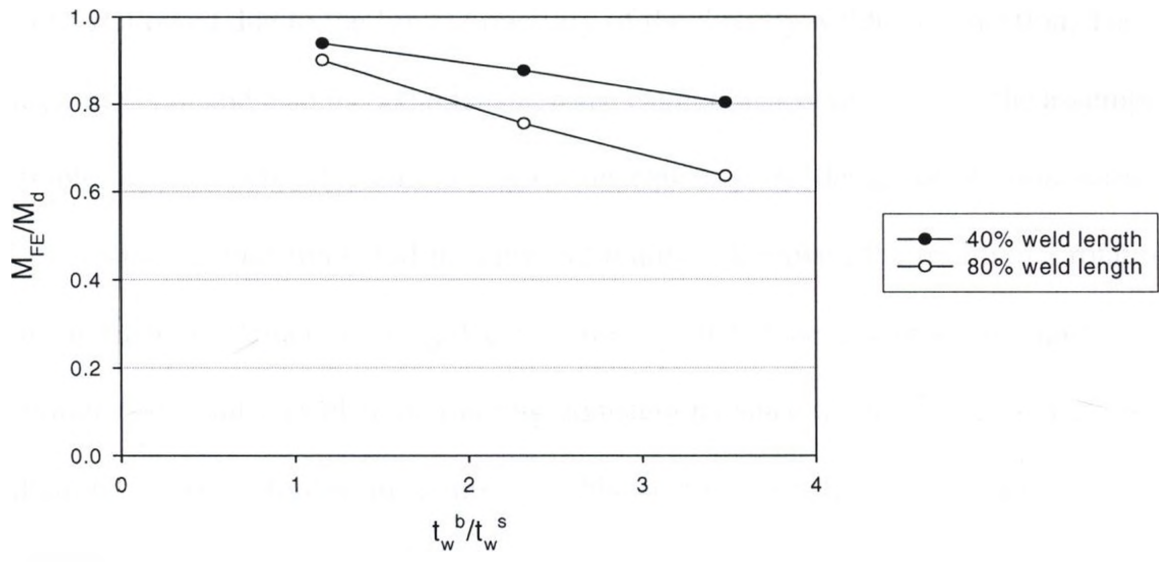

Figure 2.7: Variation of FE-to-Design Midspan Moment Ratio with Beam-to-Stringer Web Thickness Ratio for different Weld Lengths

2.8 Proposed Analytical Model

Extensive research has been conducted in order to predict the behaviour of steel joints (e.g. Lipson, 1968; Thompson et al., 1970; Marley, 1982; Mazzolani and Piluso, 1992; Chen and Toma, 1994). Major efforts have focused on the response of steel joints acting predominantly in bending. Moment-rotation curves have been developed for many types of connection and have been recommended for use in design (e.g. Thompson et al., 1970; Goverdan, 1983; Kishi and Chen, 1986; Chen and Toma, 1994; Faella et al., 2000). Computer programs (e.g. JMRC, developed by Faella et al., 2000) have also been developed for use in predicting joint moment rotation curves.

From the FE results, it is apparent that the assumption of simple supports in the typical design of floor stringers in MSBs is deficient. Redistribution of bending moments cannot be allowed due to the limited ductility of the directly welded connection. The end rotation moment and also the axial tensile force cannot be accounted for if the assumption of simple support were adopted in design. Consequently, the design of the floor stringers and the welded connections will ill represent reality. Moreover, the traditional rotational spring used to represent semi-rigid connections will not be adequate in capturing the bahaviour of modular steel floor framing connections since a spring does not allow the prediction of axial forces in joints. In this section, a simplified analytical model consistent with the actual bahaviour of modular steel floor framing is proposed.

Figure 2.8 shows a schematic of the proposed analytical model (hereafter referred to as the "*B*" model). Members *ab* and *cd* represent the web of the supporting floor beams at the ends of a floor stringer, whose centreline is represented by *bc*. w is the load supported by the floor stringer and F is the horizontal reaction provided by the slab restraint to the top flange of the floor beam and it is equal to the axial tensile force developed in the stringer.

The proposed model frame is statically indeterminate (i.e. it cannot be analysed based on only geometry, but requires component stiffnesses) and will require the stiffness of the web of floor beams in order to analyse it. The floor beam webs are continuous and so will require a definition of an effective width, *B*.

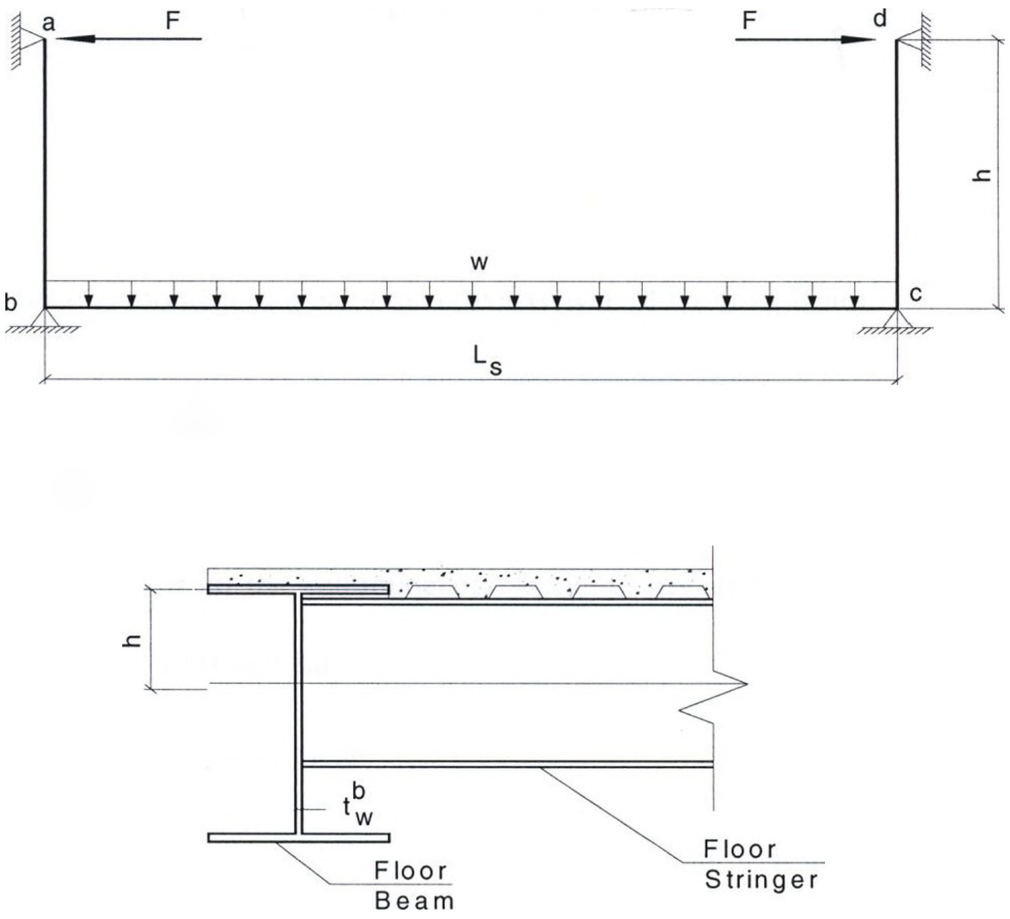

Figure 2.8. Schematic of Proposed Analytical Model

Using principles of elementary statics and the slope deflection method, the following relationship between the effective width of the floor beam web, *B*, the axial tensile force developed in the floor stringer as a result of the floor slab restraint, F, the distributed load supported by the stringer, w, and geometric characteristics of the floor stringer and beam can be derived.

$$\Rightarrow B = \frac{12 I_b}{\left(t_w^b\right)^3} = \frac{96 I_s \mathrm{h}^2 \mathrm{F}}{\left(\mathrm{w} L_s^{\ 3} - 12 L_s \mathrm{hF}\right)\left(t_w^b\right)^3} \qquad \text{..... (2.2)}$$

where,

I_b,: Second moment of area of the effective web of the floor beam.

I_s: Second moment of area of the floor stringer

w: Uniform load supported by the floor stringer.

h: the depth from the centreline of the floor stringer to the centreline of the top flange of the floor beam

L_s: Span of the floor stringer

The results of the parametric study were analysed and the effective width, B, was determined using Equation 2.2, for each of the eighty-one (81) floor framing configuration defined. A multiple regression analysis was conducted to investigate the relationship between the effective width, B, and the other parameters. In this regression model, the dependent variable is the dimensionless parameter B/t_w^b (the ratio of the effective width of beam web to the beam web thickness), and the predictor variables are the stringer length-to-depth ratio (L_s/d_s), the ratio of the weld length to the depth of the floor stringer (L_w/d_s), the ratio of the beam web thickness to the stringer web thickness (t_w^b/t_w^s), and the floor beam-to-stringer depth ratio (d_b/d_s). Recognizing that the relationships between B/t_w^b and the individual independent variables are exponential,

two regression functions, exponential and linear 'logarithmic', were fitted for the combined parameters, using the principle of least squares. The resulting regression functions were obtained as:

$$\ln\left(\frac{B}{t_w^b}\right) = -0.03\left(\frac{L_s}{d_s}\right) + 1.34\left(\frac{L_w}{d_s}\right) - 1.66\left(\frac{t_w^b}{t_w^s}\right) + 0.46\left(\frac{d_b}{d_s}\right) + 6.97 \qquad \text{... (2.3)}$$

for the exponential function, and

$$\ln\left(\frac{B}{t_w^b}\right) = -1.07\ln\left(\frac{L_s}{d_s}\right) + 0.78\ln\left(\frac{L_w}{d_s}\right) - 3.48\ln\left(\frac{t_w^b}{t_w^s}\right) + 1.04\ln\left(\frac{d_b}{d_s}\right) + 9.74 \qquad \text{.... (2.4)}$$

for the linear 'logarithmic' function.

For both functions, the coefficient of determination, r^2, was greater than 96.5%, which indicates a strong relationship among the independent parameters and the effective width of beam web, *B*. The F-statistic was used to determine whether such a high r^2 value occurred by chance. The F-observed statistic (382), for the exponential function, was substantially greater than the F-critical value (2.53) indicating an extremely small probability (2.754E-36) that the high F value occurred by chance. For the linear "logarithmic" function, the F-observed statistic was 594 and the probability that it occurred by chance was 7.525E-41. Thus, it can be suggested that the each of the regression equations above is useful in predicting the magnitude of the effective width of

floor beam web, B. Appendix II contains a sample data from which the regression functions were developed. The following section is a proposed design methodology for an efficient application of the proposed analytical model for designing MSB floor grid structure.

2.9 Design Methodology for MSB Floor Grid Structure

The design forces and moments in the floor beams match the results of the FE analysis and hence no modification in the design methodology for floor beams is required. In other words, the traditional design procedure is adequate for floor beam design. However, for the design of floor stringers and the welded connections, the following is an outline of a proposed design methodology based on the above proposed analytical model:

Step 1. The configuration of the modular floor framing is selected and preliminary sizing of framing components is performed based on traditional methods.

Step 2. The dimensionless parameters L_s/d_s, L_w/d_s, t_w^b/t_w^s, and d_b/d_s are determined from the preliminary dimensions.

Step 3. The dimensionless parameter B/t_w^b is evaluated from either Equation 2.3 or Equation 2.4. The two equations are expected to yield similar values as suggested by the regression analysis.

Step 4. The second moment of area for the effective floor beam web, I_b, is evaluated and used to analyse the proposed analytical model shown in Figure 2.8.

Step 5. The axial force and the bending moments developed in the floor stringer is determined by using principles of elementary statics and the slope deflection equation 2.2.

Step 6. Based on the forces and bending moments obtained from step 5, the floor stringers are redesigned.

Step 7. Steps 2 to 6 are repeated until sections obtained from the revised design are consistent with the initial preliminary design sections.

Step 8. With the actual forces and moments developed in the stringer obtained, the welded connection between the stringers and the floor beams is designed for the combined shear and axial forces, and bending moment.

2.10 Summary and Conclusion

MSBs are fast becoming an effective alternative to conventional on-site constructed steel buildings. The concept and detailing of these unique buildings have been described in this chapter. This is expected to provide other researchers with knowledge of the modular steel building system for them to study its critical elements.

The chapter also describes an investigation into the most commonly used connection detail in modular floor grid systems, which involves the direct welding of floor stringers to floor beams. The structural behaviour of this connection detail has been

studied using the FE method. The effect of this behaviour on the analysis and design of floor beams and stringers, as well as the direct welded connection was also studied. Results of the FE analysis reveal that consideration of the actual behaviour of the directly welded connections in modular floor framing leads to distributions of forces and moments in members and connections that are different from those occurring in conventional steel buildings.

Axial forces are developed in the floor stringers and hogging moments develop at the ends of these stringers. These are not predicted by the conventional assumptions adopted in current design practice by designers of MSBs. Moreover, traditional rotational springs used commonly to represent semi-rigidity of connections fail to predict axial forces. These forces and bending moments, which are not taken into account, will lead to inadequate design of the floor stringers and the welded connection of the floor structure. Results of the parametric study further highlighted the significance of these forces and bending moments. The study has also demonstrated that the welds must have the capacity to transfer significant bending moment and axial force, in addition to the vertical shear force from the floor stringer to the supporting beams.

The study proposed a simplified practical analytical model, which predicts more realistic forces and moments and leads to a reliable prediction of the structural response of a modular steel floor framing. The results of the parametric study were used to develop regression functions to describe the proposed analytical model. A step-by-step design methodology has been developed for easy and practical application of the proposed model in design.

2.11 References

Al-Emrani, M. and Kliger, R. [2003] "FE analysis of stringer-to-floor-beam connections in riveted railway bridges," *Journal of Constructional Steel Research*, 59, 803-818.

Astaneh, A., Nader, M. N., and Malik, L. [1989] "Cyclic behaviour of double angle connections," *ASCE Journal of Structural Engineering*, 115 (5), 1101-1118.

Chen, W. F. and Toma, S. [1994] *Advanced analysis of steel frames: theory, software and applications,* New Directions in Civil Engineering, CRC Press, Boca Raton, Florida.

CSA [2001] *Handbook of Steel Construction, 7th Edition*, Canadian Institute of Steel Construction, Willowdale, Ontario, Canada.

CSI, Computers and Structures, Inc [2000] *SAP2000 Nonlinear computer program,* Berkeley, USA.

Doerk, O., Fricke, W., and Weissenborn, C. [2003] "Comparison of different methods for structural stresses at welded joints," *International Journal of Fatigue*, 25, 359-369.

Faella, C., Piluso, V. and Rizzano, G. [2000] *Structural steel semi-rigid connections: theory, design and software,* New Directions in Civil Engineering, CRC Press, Boca Raton, Florida.

Goverdan, A. V. [1983] *A collection of experimental moment-rotation curves and evaluation of prediction equations for semi-rigid connections*, Vanderdilt University, Nashville, Tennesse.

Kishi, N. and Chen, W. F. [1986] "Steel connection data bank program," *Structural Engineering Report, No. CE-STR-86-18*, School of Civil Engineering, Purdue University, West Lafayette, Indiana.

Lawson, R. M., Grubb, P. J., Prewer, J. and Trebilcock, P. J. [1999] *Modular construction using light steel framing: An Architect's Guide,* The Steel Construction Institute Publication SCI-P272, UK.

Lipson, S. L. [1968] "Single-angle and single-plate beam framing connections," *Canadian Structural Engineering Conference*, Toronto, Ontario, 141-162.

Marley, M. J. and Gerstle, K. H. [1982] "Analysis and tests of flexible-connected steel frames," *Engineering Structures*, 8 (2), 107-118.

Mazzolani, F. M. and Piluso, V. [1992] "Evaluation of the rotation capacity of steel beams and beam-columns," *1st COST C1 Workshop*, Strasbourg, 28-30 October.

Murray Engineering, P.C. [2000] *SUNY Purchase College Dormitory Construction Drawings*, Materials obtained by personal communication with Mr. Robert J. Murray, P.E., Principal, Murray Engineering, P.C.

NBCC [2005] *National Building Code of Canada*, Institute for Research in Construction, National Research Council of Canada, Ottawa, Ontario, Canada.

Thompson, L. E., Mckee, R. J. and Visintainer, D. A. [1970] *An investigation of rotation characteristic of web shear framed connections using A-36 and A-441 steel*, Department of Civil Engineering, University of Missouri-Rolla, MO.

Weaver, M. A. [1999] "Determination of weld loads and throat requirements using finite element analysis with shell element models – A comparison with classical analysis," *Welding Journal Research Supplement, 78 (4),* (April 1999).

CHAPTER THREE

EXPERIMENTAL EVALUATION OF THE SEISMIC PERFORMANCE OF MODULAR STEEL BRACED FRAMES[‡]

3.1 Introduction

In spite of the increasing use of concentrically braced frames as an earthquake-load resisting system, there has been a growing concern related to their ultimate deformation capacity because of observed damages in past earthquakes. For example, concentrically braced frames were damaged during the 1985 Mexico earthquake (Osteraas and Krawinkler, 1989), 1994 Northridge earthquake (Tremblay et al., 1995), and 1995 Hyogo-ken Nanbu earthquake (Tremblay et al., 1996). The main source of energy dissipation in these frames is through inelastic deformation of bracing members. Seismic response of such frames is therefore dominated by the inelastic behaviour of the bracing members.

Bracing members in braced frames of regular buildings are expected to buckle in compression and yield in tension when subjected to reversed cyclic loading. Plastic hinges often form after brace buckling. This may cause permanent plastic deformations and deterioration of the resistance in the braces. To promote ductile response, brace connections are designed to tolerate large rotations associated with brace buckling. They must also support the full tensile and compressive capacity of the brace during cyclic

[‡] Annan, C.D., Youssef, M.A., and El Naggar, M.H. "Experimental evaluation of the seismic performance of modular steel braced frames," *Engineering Structures*, under review.

inelastic deformation demands. This implies that the connection cannot buckle or fracture prior to the development of the full resistance and ductility of the brace.

Several studies have revealed the complexity of the hysteretic behaviour of steel braced frames (Jain et al. 1978; Ikeda and Mahin, 1984; Tremblay, 2002; Tremblay et al., 2003). This is due to significant degradation of strength and stiffness of braces in compression after a few post-buckling cycles. These studies further revealed that the main parameters that control this behaviour are the width-to-thickness (w/t) ratio and the effective slenderness ratio (KL/r), where K is the effective length factor, L is the length of bracing member, and r is the radius of gyration. These observations have caused considerable revision to design requirements of earthquake resistant steel braced frame structures (CSA, 2001; AISC, 2002). These design codes now specify maximum design limits on KL/r and w/t to provide sufficient energy dissipation capacity and resistance to local buckling, respectively. In addition, the post-buckling phenomenon has been reasonably captured by applying a buckling reduction factor to the compressive strength of bracing members.

The complete hysteretic response of any framed structure, however, depends to a large extent on the overall frame configuration including its connection type. Modular Steel Buildings (MSBs) are being used increasingly for one to six storey schools, apartments, dormitories, hotels and in similar buildings where repetitive units are required. The lateral resistance of this unique building type is often achieved by adding diagonal braces. The characteristics and unique detailing requirements of MSBs have

been described extensively in Annan et al. (2005, 2007, 2008, and 2009) and also included in Chapters Two and Four.

In MSBs, modular units made of high strength and durable steel sections are built and finished under a controlled manufacturing environment and are transported to the building site and connected horizontally and vertically. Lateral loading on each floor is transferred through the horizontal connections (HC) to the modular braced frame and then through the vertical connections (VC) to the foundation. Figure 3.1 shows a typical plan and sections of a modular steel building. The following features specifically distinguish the MSB braced frame from a regular steel braced frame: (1) the existence of ceiling beams (CB) and ceiling stringers (CS) in the MSB frame system may result in natural periods and mode shapes different from those of conventional systems; (2) the floor beams (FB) may be set directly above the ceiling beams (CB) without mechanical connections except at column locations, and this may result in structural contact interaction between these beam members; (3) the brace members in a typical modular steel frame do not intersect at a single working point which may lead to high seismic demands on the vertical connection (VC) of different units/modules; (4) the horizontal connection (HC) of separately finished modules, shown in section A-A, is achieved by field-bolting of clip angles which are shop-welded to the floor beams; (5) the vertical connection (VC), shown in section B-B, typically involves partial welding of the columns of a lower and an upper modules which may lead to independent upper and lower rotations at the same joint. Column continuity is known to contribute effectively in preventing soft-storey response in multi-storey structures (Tremblay 2000). Discontinuity of columns coupled with a possible high seismic demand on the vertical connection of

different modules may result in a concentration of inelasticity in one storey over the height of the frame.

Currently, conventional design methods are followed in the seismic design of MSBs. There have been no previous studies to predict their behaviour. Consequently, there are no specific guidelines to help engineers correctly assess their stiffness, strength, ductility, and cumulative hysteretic energy dissipation capacity. This chapter introduces the first experimental investigation of the behaviour of MSB braced frames under repeated cyclic loading. The study takes into account their specimen detailing requirements. The following is a description of the selection of specimen configuration and its design, experimental set-up, testing protocol, and results of the cyclic testing of a MSB braced specimen and a regular braced specimen. Experimental results are also compared to numerical predictions to validate the proposed modeling technique.

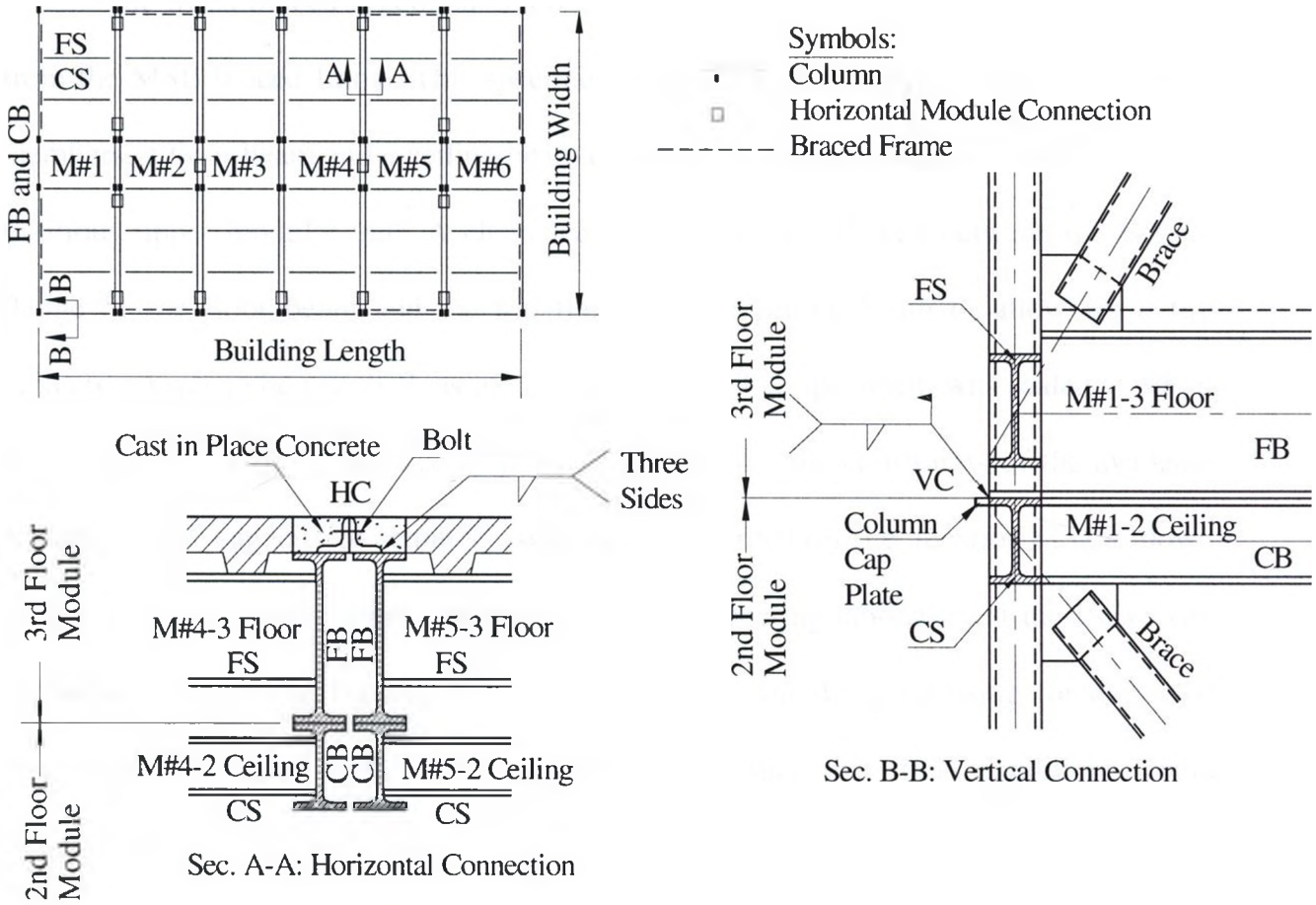

Figure 3.1. A Typical Plan and Sections of a Modular Steel Building

3.2 Selection of Specimen Configuration and Design

The experimental program involved testing two specimens: one MSB braced frame and one regular braced frame. A four-storey MSB braced frame and a four-storey regular braced frame of similar physical characteristics (i.e. same clear height, width and member proportions), shown in Figure 3.2, were selected and designed. The design was in accordance to the requirements of the Canadian standard CSA-S16.1 (CSA, 2001) and the National Building Code of Canada (NBCC, 2005).

The MSB braced specimen is a one-storey, one-bay cross-braced panel extracted from the MSB braced frame. This specimen consists of two columns, two cross bracing members, a floor beam and a ceiling beam of a lower modular unit, and a floor beam of a fictitious upper modular unit. A clearance of 40 mm was allowed between the bottom flange of the floor beam and the top flange of the ceiling beam to allow for a fire protective layer to be installed, as in current practice. The specimen was scaled at 3/8 of the full-scale size to be as large as possible considering the constraints of the available equipment (i.e. capacity of actuator) and supporting structures (i.e. location of hold-down bolts for the supporting frame) in the structural engineering laboratory at the University of Western Ontario in Canada. The MSB specimen was designed using forces scaled from those developed in the full-scale panel design such that stress conditions would remain similar in the two panels.

The regular braced specimen is a one-storey, one-bay cross-braced frame and was scaled to have similar physical characteristics as the MSB specimen for effective comparison (i.e. same clear height, width and member proportions). This specimen consists of two columns, two cross bracing members, and top and bottom floor beams connected to the columns.

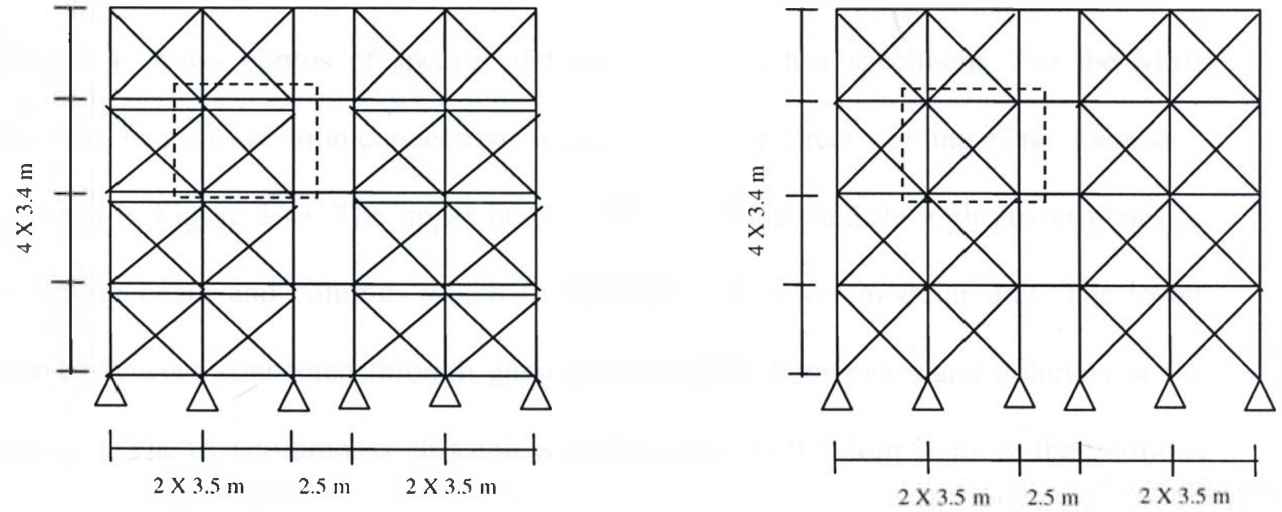

(a) (b)

Figure 3.2. Four-storey Braced Frames for Design of Test Specimens (a) MSB Frame (b) Regular Frame

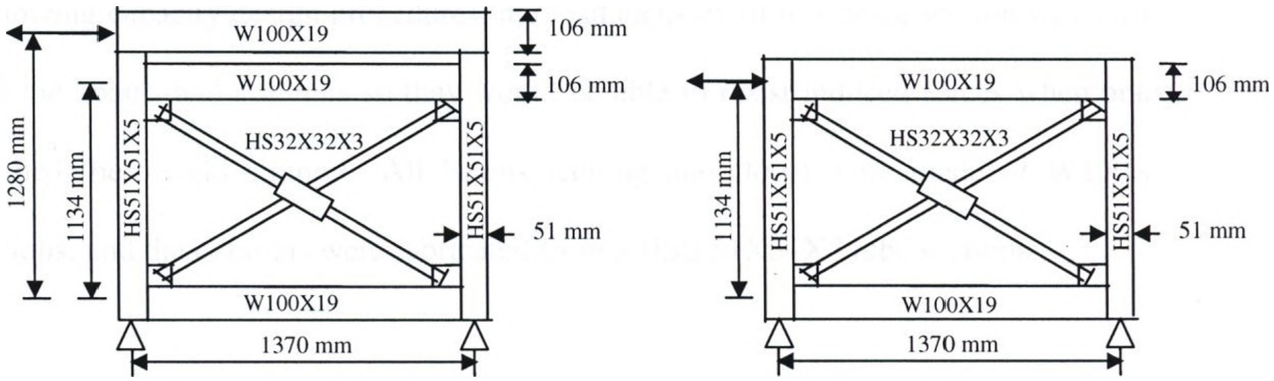

(a) (b)

Figure 3.3. Dimensions of Test Specimens (a) MSB Frame (b) Regular Braced Frame

The dimensions and sections of the two frame specimens are shown in Figure 3.3. Detailing of the specimens was done in accordance with current professional practice. Figure 3.4 shows photos of specific details in the two test specimens. For the MSB specimen, beam-to-column connections were achieved by direct welding of the members, as shown in Figure 3.4a. The upper brace ends were connected through gusset plates to the ceiling beam and columns which form part of the lower modular unit. The lower brace ends were connected through gusset plates to the floor beam and columns of the same unit. The two columns of this unit were connected to the floor beam of the fictitious upper unit by welding column cap plates to the lower flange of the beam, as shown in Figure 3.4a. This welding was achieved only at the three exterior faces/sides, at each end of the specimen, which were accessible. In the regular braced specimen, beam-to-column connections were achieved by welding a plate to both the beam and column allowing for partial rotation between adjoining members, as shown in Figure 3.4b.

The design yielded a HSS 32X32X3 hollow tube sections for the brace members. Following capacity design procedures, the load capacity of this brace section was used to size the beams and columns so they would be able to resist induced forces when braces reached their yield strength. All beams (ceiling and floor) were made of W100X19 sections, and the columns were fabricated from a HSS 51X51X5 tube sections.

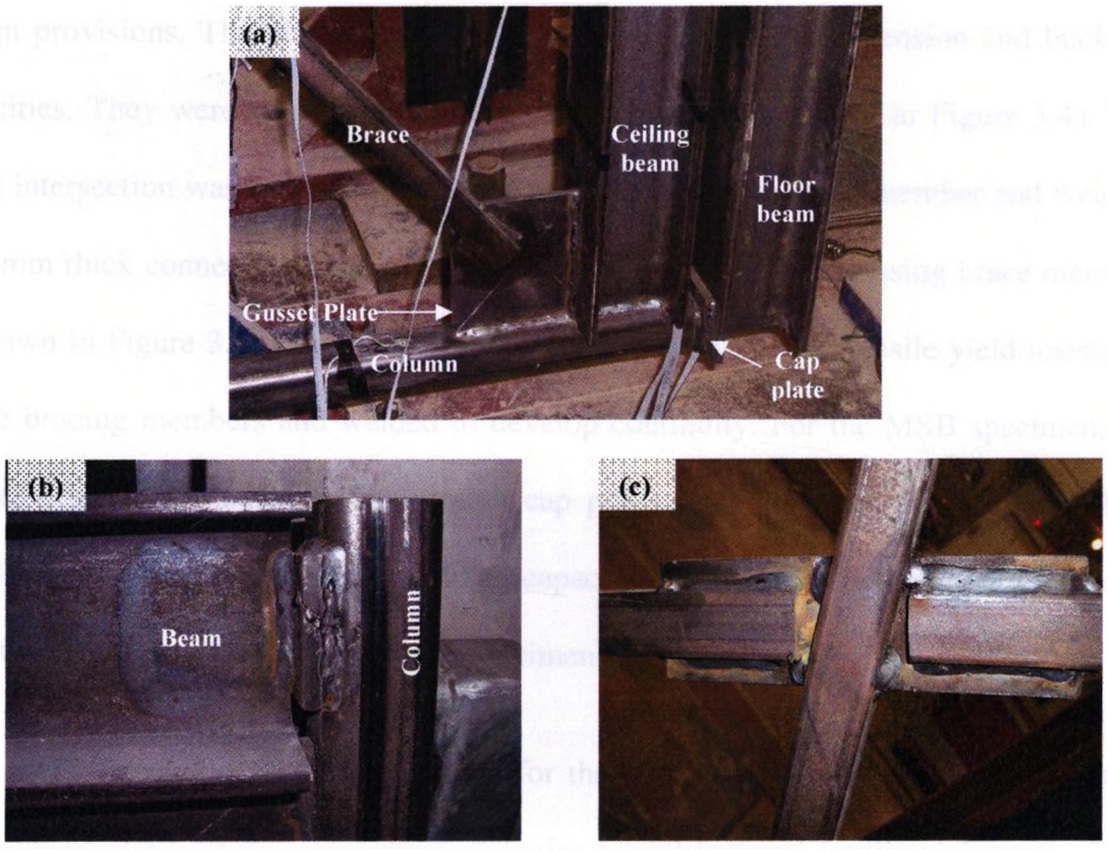

Figure 3.4. Photos of Specimens Member and Connection Details (a) MSB Frame (b) Beam-to-column Connection in Regular Frame (c) Brace Intersection

The brace end connections were designed to remain elastic at all times so they would be at least as strong as the bracing member. This design maximised the energy dissipation capacity of the specimens. Single gusset plates of 8 mm thickness were selected for the brace end connections to the beams and columns. The tube brace members were slotted at each end and fillet welded to the gusset plates, as shown in Figure 3.4a. The gusset plates were designed with a free length of twice the gusset plate thickness to allow for rotation of the brace ends as recommended in the AISC (2002)

design provisions. The plates were designed to possess sufficient tension and buckling capacities. They were welded to the beams and columns, as shown in Figure 3.4a. The brace intersection was achieved by cutting a slot through one brace member and welding a 10 mm thick connecting plate to this member and to the other crossing brace member, as shown in Figure 3.4c. The plate was designed to carry the full tensile yield resistance of the bracing members and welded to develop continuity. For the MSB specimen, the welded connections between the column cap plates and the lower flange of the floor beam was designed based on the yielding capacity of bracing members, assuming equal distribution of forces at the ends of the specimen.

The selected boundary conditions for the specimens simulated those of the full-scale panels. Two 19 mm diameter bolts, with a total factored tensile resistance of 236 kN and separated by 152 mm on center, were used to connect each column base plate to the reaction frame. Prying action was accounted for in the design of these base plates. This provided the basis for selecting a 20 mm thick plate. Typical 5 mm circumferential fillet welds were used to connect the columns to the base and cap plates.

3.3 Experimental Setup

The test setup was chosen to adequately simulate all important field and boundary conditions. The specimens were mounted as shown in the photos of Figure 3.5. Figure 3.6 shows a schematic representation of the setup. The specimens were rotated at an angle of 90 degrees, making their columns align horizontally and the beams vertically. The load actuator, with a maximum load capacity of 250 kN, was thus mounted in a vertical position to provide the "lateral" cyclic loading to the test specimens at the level of

"upper" floor beams. The specimens were connected to the actuator by means of a 25.4 mm thick plate welded to one end of top floor beam and bolted to a plate-tube welded assembly which is attached to the load actuator by a pin. They were braced, as shown in Figure 3.5, to prevent out-of-plane movement or twisting of specimens during loading. The specimens were connected to the reaction frame by bolting of base plates of the two tube columns. The effect of gravity loading on stability of restoring force characteristics of the test specimens was not simulated as it was considered to have no detrimental effect on the performance of the specimens. Moreover, the gravity loading was considered not to follow a well established pattern that is applicable to all possible configurations.

The drift behaviour of the test specimens was studied to allow an assessment of their ductility. The applied load and specimen drift were monitored at the top floor beam levels by the actuator. A total of 50 strain gauges and 7 LVDTs were installed at several locations on members of each specimen to measure strains and deformations. These readings were used to study the distribution of forces in the various members and at different sections of the specimens. Out-of-plane deformations of brace members were measured with LVDTs that were installed at ¼, ½, and ¾ times the distance between the free length regions of the gusset plates (shown as a, b, c, d, and e in Figure 3.6). Four strain gauges were attached at each selected section to measure bi-axial bending stress and longitudinal stress For the brace members, the strain gauges were installed at a number of locations (shown as a, b, c, d, and e in Figure 3.6) along their longitudinal directions. All the instrumentations were plugged into a computerized data logger. The data logger was set up to take measurements at an average rate of 2 to 3 readings per second.

Figure 3.5. Overall View of Test Setup

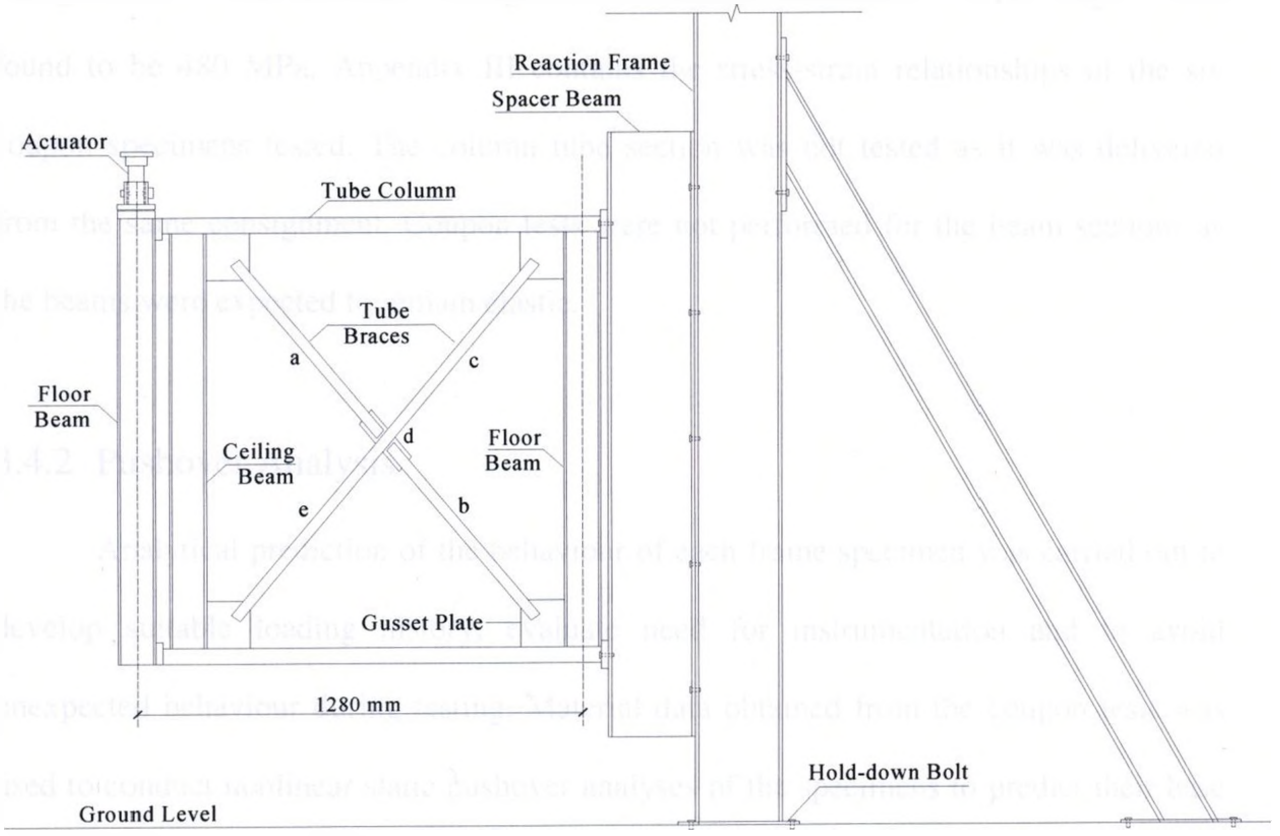

Figure 3.6. Schematic Representation of Test Setup

3.4 Experimental Program

The experimental program involved material testing, analytical predictions, and testing protocols.

3.4.1 Material Properties

Before the testing of the specimens, material testing was conducted to determine the basic monotonic steel stress-strain properties. The test procedure followed the ASTM standard test methods (ASTM, 2002). Standard coupon tests were conducted on six specimens of the bracing material to obtain an average yield stress of the tube brace section. There was no definite yield plateau for each of the specimens tested. The yield strength, F_y, was thus calculated using the 0.2% strain offset method. The average F_y was found to be 480 MPa. Appendix III contains the stress-strain relationships of the six coupon specimens tested. The column tube section was not tested as it was delivered from the same consignment. Coupon tests were not performed for the beam sections as the beams were expected to remain elastic.

3.4.2 Pushover Analysis

Analytical prediction of the behaviour of each frame specimen was carried out to develop suitable loading history, evaluate need for instrumentation and to avoid unexpected behaviour during testing. Material data obtained from the coupon tests was used to conduct nonlinear static pushover analyses of the specimens to predict their base shear-top displacement behaviour.

Two-dimensional models were developed based on centerline dimensions of the specimens. A bilinear material model for steel was employed, with a kinematic strain hardening parameter of 2%. Inelastic beam-column frame element, which employs a cubic shape function (Izzuddin, 1991), was used to represent the behaviour of all frame members. This element type accounts for both geometric and material non-linearities. The element formulation is based on the fibre modeling approach that models the spread of material inelasticity along the member length and across the section area to allow for accurate estimation of structural damage distribution. In such elements, the sectional stress-strain state is obtained through the integration of the nonlinear uniaxial stress-strain response of the individual fibres in which the section has been subdivided. For the frame members, 200 section fibres were employed. The element response (curvatures and stress/strain peak values) was assembled from contributions at two gauss points, where the cross sections are discretised into a number of monitoring points.

A joint element with uncoupled axial, shear and moment actions was utilised to simulate the assumed pin-jointed behaviour at the ends of bracing members. All beam-column joints in the MSB specimen model were assumed rigid to represent the directly welded connection between these members.

Figure 3.7 shows a schematic representation of a proposed analytical model of vertical connection between columns of a lower unit and the top floor beam (or columns) of an upper unit in the MSB specimen. The model utilises a number of beam-column elements, rigid links, and a link element. Rigid end blocks (shown by thick dark lines J1-J2, J3-J4, J5-J4, and J6-J4) were provided at each end of frame members to capture the

rigidity of connection regions. The short column segment between the bottom flange of the floor beam and top flange of the ceiling beam was represented by a vertical beam-column element, M1, whose height represents the clearance between the two beams. A link element was defined to connect the column top ends to the bottom flange of the floor beam at J2, such that an independent upper and lower module rotation would develop at this joint.

The characteristic reduction in strength of a brace member after buckling was incorporated in the model by assuming an elasto-plastic brace behaviour for the compression brace with the yield force taken as the residual strength after buckling (Rahgozar and Humar, 1998; FEMA, 2000; CSA, 2001).

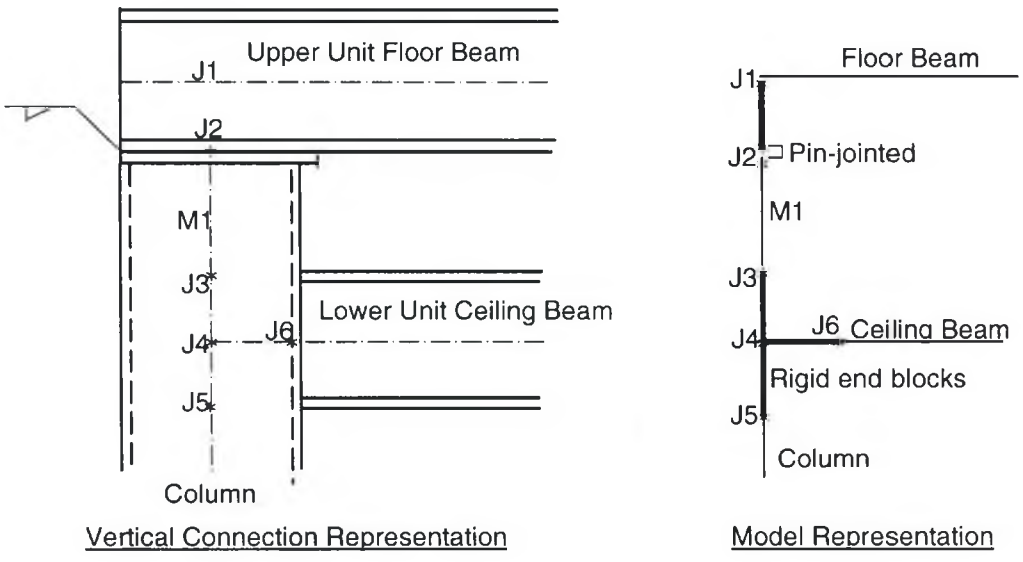

Figure 3.7. Model Representation of Vertical Connection of Units of MSB Specimen

The analytical models of the test specimens were subjected to response control nonlinear pushover analyses. The magnitude of lateral forces, with a distribution pattern along specimens' height similar to the actual test loading, was gradually increased up to a deformation similar to the expected maximum actuator movement. A total of 250 incremental steps to the target displacement were applied.

Figure 3.8 shows the base shear versus specimen displacement curves. The analytical yield strength, P_y, were estimated as 97.5 kN and 82.5 kN for the MSB and regular braced specimens, respectively. The yield strength was estimated by idealising the actual structural response curve by a bilinearly elasto-plastic curve such that the two curves yield the same total energy dissipation up to the point of ultimate deformation. The stiffnesses corresponding to the elastic portion of response were estimated as 17.2 kN/mm and 19.1 kN/mm for the MSB and regular braced specimens, respectively.

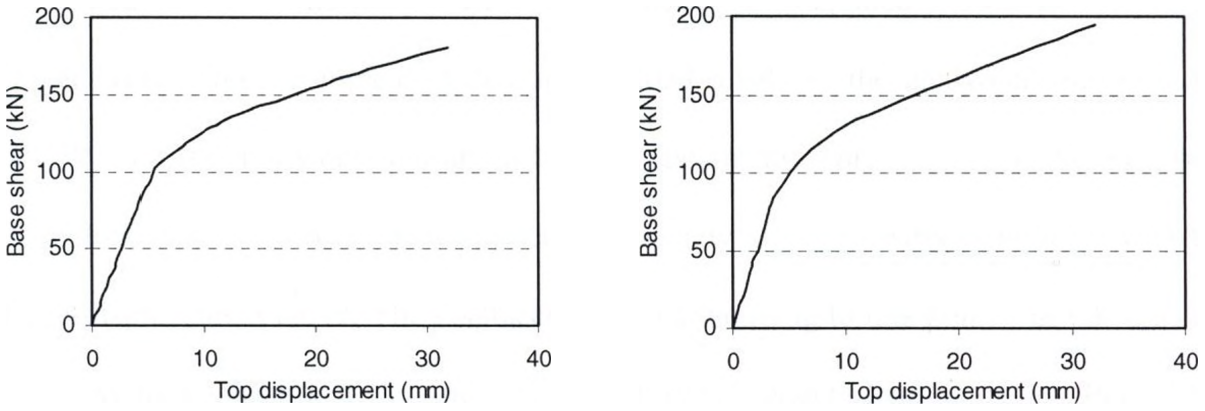

(a) (b)

Figure 3.8. Pushover Curves for (a) MSB Braced Specimen (b) Regular Braced Specimen

3.4.3 Testing Protocol

Testing of the frame specimens followed the Applied Technology Council's ATC-24 (ATC, 1992) single specimen testing program. The test specimens were subjected to symmetric reversed-cyclic loading histories to characterize their performance. Loading imposed by the actuator was done at a sufficiently slow rate (an average of 3.5 – 4.0 kN/sec in the elastic load cycles and 1.8 – 2.2 mm/sec in the inelastic load cycles) to prevent the development of any dynamic effects. In both loading and unloading branches of an excursion, loading was applied continuously without intermittent stops in order to reduce any strain rate effects. The yield values of specimen forces from the analytical study were used to initially control the test. Beyond the elastic range, the experimentally obtained values of the yield displacements were used as test control parameters.

Figures 3.9 and 3.10 summarise the loading histories for both elastic (force-controlled) and inelastic (displacement-controlled) cycles applied to the two specimens, respectively. Three complete cycles at two load levels in the analytical elastic range ($0.33P_y$ and $0.67P_y$) were first applied to the specimens. Three cycles at the analytical yield load level, P_y, were then applied, noting any sign of visible nonlinearity in the force-displacement curve. The displacement corresponding to this point was taken as the actual yield displacement, Δ_y, and used to control subsequent loading cycles. Full cycles (3 or 2) at a constant peak deformation increment equal to twice the yield displacement were applied until significant strength deterioration was observed or the maximum actuator movement or capacity was reached. In the case of the latter, the specimen was

cycled at the maximum peak deformation until severe deterioration was evident. Table 3.1 shows the ductility levels reached for the test specimens.

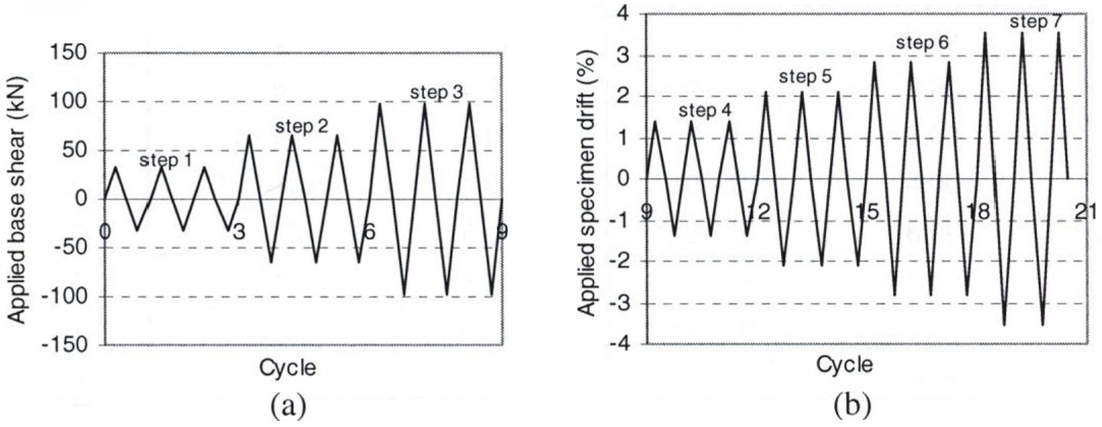

Figure 3.9. Loading History for MSB Braced Specimen (a) Elastic Cycles (b) Inelastic Cycles

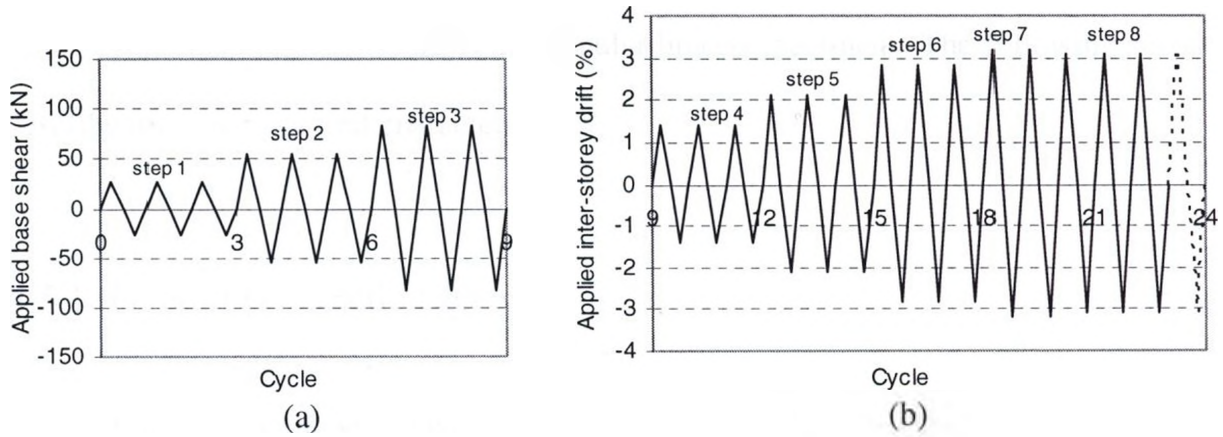

Figure 3.10. Loading History for Regular Braced Specimen (a) Elastic Cycles (b) Inelastic Cycles

Table 3.1. Ductility Levels reached by Specimens at Different Cycles

Step	MSB braced specimen		Regular braced specimen	
	Cycle number	Normalised peak deformation (Δ/Δy)	Cycle number	Normalised peak deformation (Δ/Δy)
1	1 - 3	0.49	1 - 3	0.48
2	4 - 6	0.97	4 - 6	0.95
3	7 - 9	2.00	7 - 9	2.00
4	10 - 12	4.00	10 - 12	4.00
5	13 - 15	6.00	13 - 15	6.00
6	16 - 18	8.00	16 - 18	8.00
7	19 - 20.5	10.00	19 - 20	9.00
8			21 - 40	8.75

3.5 Experimental Results

The experimental results reveal some similarities as well as significant differences in the cyclic response of the MSB and regular braced specimens. The following sections describe these behavioural characteristics.

3.5.1 Overall Hysteretic Behaviour

Figure 3.11 shows the base shear versus peak drift hysteresis obtained for the two specimens. Both test specimens showed ductile behaviour and are stable up to large drift levels, although some degree of pinching is apparent in the hysteretic loops, especially for the regular specimen. Clearly, both specimens exhibited almost linear elastic response

upon applying the first two load steps (i.e. six cycles of loading) in spite of possible existence of initial imperfections. The initial stiffnesses were evaluated as 14.3 kN/mm and 15.5 kN/mm for the MSB and regular braced specimens, respectively. Within the third load step, significant nonlinearity was observed mid-way in the load-displacement curve for each specimen. The movements in the actuator corresponding to this point were found to be about 4.5 mm and 3.8 mm for the MSB and regular braced specimens, respectively. These displacements correspond to a 0.35% and 0.34% drift, respectively. Strain guage data obtained from the various members indicated that, in the regular braced specimen, buckling of compression brace resulted in the first significant sign of nonlinear behavior, while in the MSB specimen, flexural response due to column yielding caused initial nonlinearity.

The MSB specimen was tested successfully to a 3.5% drift, corresponding to ten times the yield displacement, Δ_y, and a base shear of 225 kN. This level of loading resulted in a significant bending deformation in the column segment between the bottom flange of the upper floor beam and the top flange of the ceiling beam, as shown in Figure 3.12a. The test was terminated at this high ductility level. Prior to the end of the test, a maximum out-of-plane deformation of 2.2% of the brace length was measured at the mid-section of a lower half side of a brace member (labeled "b" in Figure 3.6). The ratio of the maximum attained base shear to the yield base shear was evaluated as 3.5.

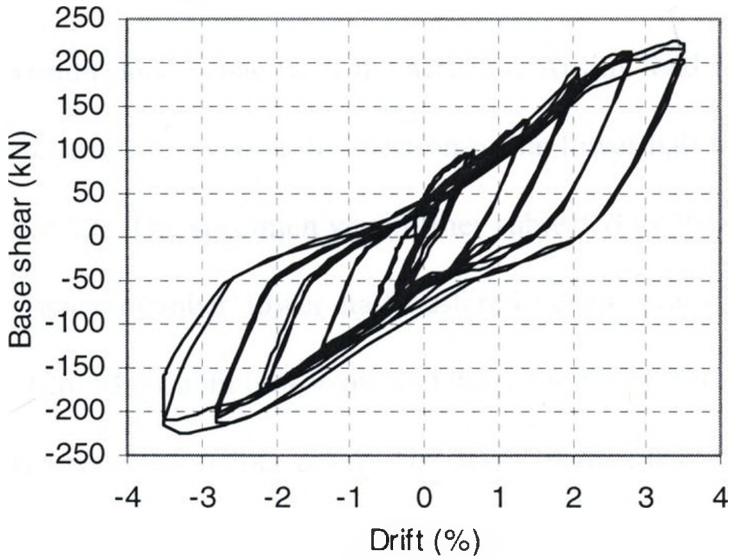

(a)

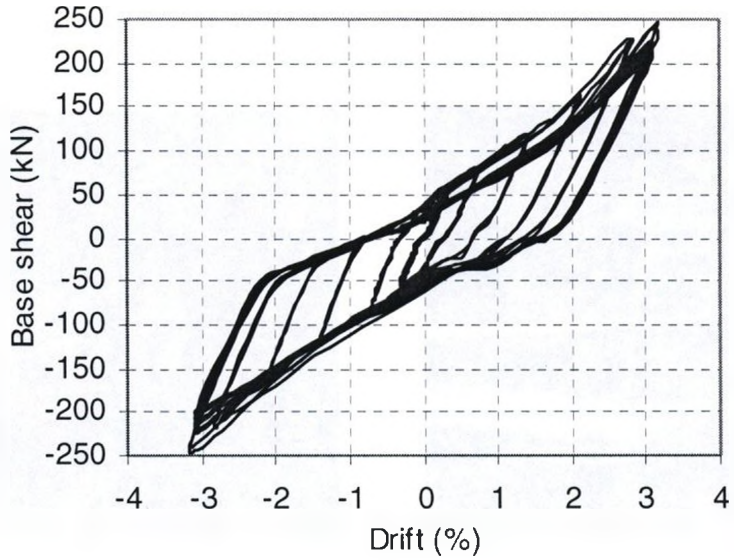

(b)

Figure 3.11. Base Shear versus Drift Hysteretic Response (a) MSB Brace Specimen (b) Regular Braced Specimen

The regular braced specimen was successfully tested to 3.1% drift at displacement ductility of 9. The maximum base shear at this drift level was found to be 245 kN, which was about the maximum load capacity of the actuator. At this load step, significant out-of-plane deformation was observed at mid-section of the lower half of the brace member labeled "b" in Figure 3.6. The specimen was further subjected to 20 cycles at 3.05% drift during which the brace member lower half suffered severe out-of-plane buckling, as shown in Figure 3.12b. Maximum out-of-plane deformation of 4.0% of the total length of brace member was measured at this point. The level of ductility reached was deemed sufficient to terminate the test. The ratio of the maximum attained base shear to the yield base shear was evaluated as 4.2.

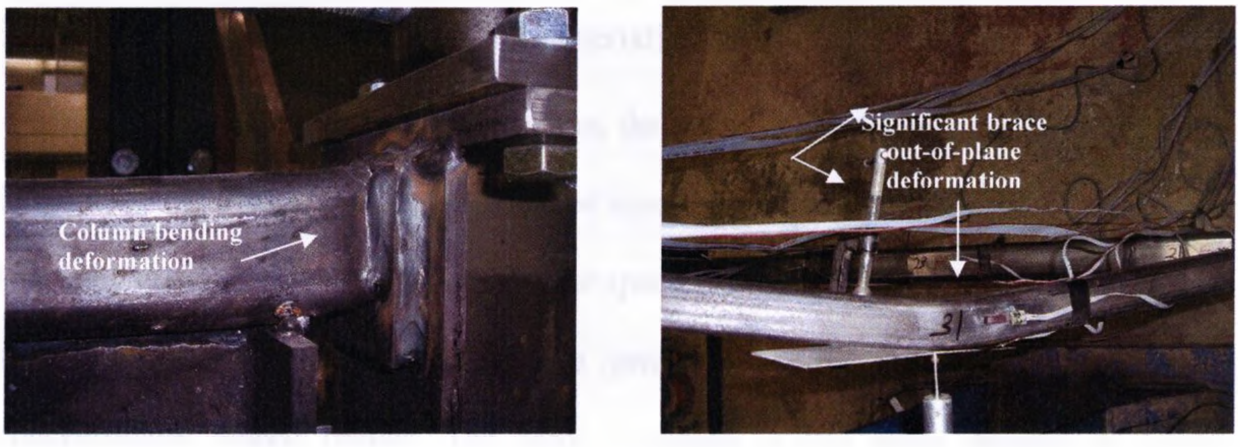

(a) (b)

Figure 3.12. (a) Column Bending Deformation in MSB Braced Specimen (b) Brace Out-of-Plane Deformation in Regular Braced Specimen

Strain gauges installed on the floor and ceiling beams showed that these members remained elastic throughout the different loading phases of the specimens as anticipated from the design. A maximum strain of 0.84% (8400 micro strain) was reached at the mid-section of the lower half of a tube brace member of the MSB specimen at 3.5% drift level. At the upper end section of the same brace member, maximum strain of 0.23% (2300 micro strain) was recorded at this stage of loading. At 2.8% drift, maximum strain of 0.33% was recorded at the mid-section of the lower half side of the brace member. For the regular braced specimen, strain of 0.35% was reached at the mid-section of the lower half side of a brace member at 2.8% drift. At 3.1% drift, maximum strain of 0.73% was recorded at the same section. Upon a number of repeated cycling at load step 8, brace members in this specimen reached maximum strain of 2.9% before the test was terminated.

3.5.2 Strength and Stiffness Characteristics of Specimens

As indicated in the previous section, the regular braced specimen showed greater initial lateral stiffness than the MSB braced specimen (i.e. initial lateral stiffness of MSB specimen was about 93% that of the regular specimen). This is because the regular braced specimen has greater lateral resistance provided by the truss action typical of concentrically braced frames. The MSB specimen in this range derived its lateral resistance from a combination of the brace action and some moment resisting action due to direct welding of members and moment connection between the column and the bottom flange of the upper floor beam.

The hystereses for the two specimens are fairly symmetrical in both the elastic and inelastic cycles. Both specimens showed stable behaviour (small strength and stiffness degradation) in almost every step of repeated loading. Figure 3.13 shows the change in lateral stiffness with specimen peak drift and with maximum ductility. Within the elastic response range, the lateral stiffness was evaluated as the slope of the base shear versus displacement relationships. Beyond this range, it was estimated as the slope of the line joining the peaks of positive and negative drifts in each remaining load step.

Up to a ductility level of 2, the MSB braced specimen provided less lateral stiffness than the regular braced specimen. Both specimens, however, showed a sharp drop in lateral stiffness after the first sign of brace buckling in the regular braced specimen and column flexural yielding in the MSB braced specimen. Between ductilities of 2 and 6, there was no significant difference in lateral stiffness between the two specimens. Beyond ductility of 6, the regular braced specimen again showed superior lateral stiffness, almost remaining constant up to a ductility of 9. The overall reductions in lateral stiffness from start of loading up to ductility of 6 were 46% and 45% for the MSB specimen and regular braced specimen, respectively.

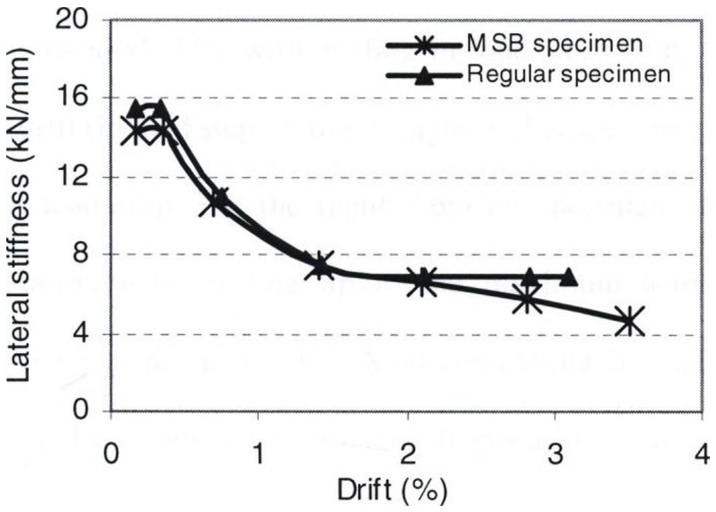

(a)

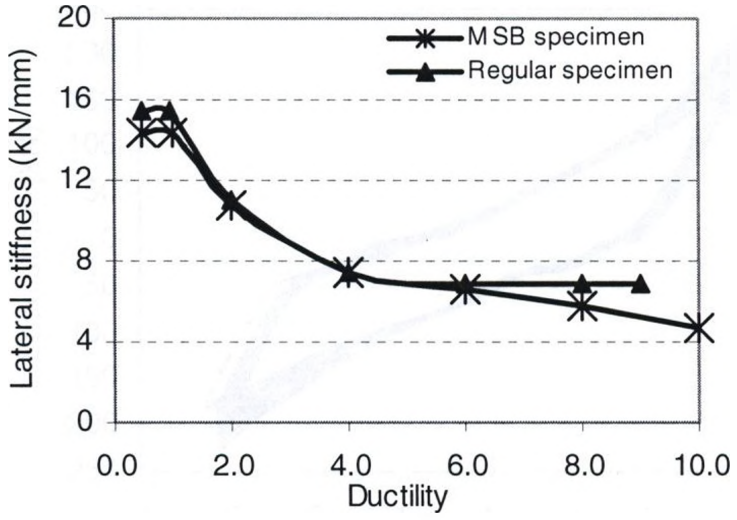

(b)

Figure 3.13. Variations of Lateral Stiffness with (a) Peak Drift (b) Maximum Ductility

Within a specified load step, there was no significant degradation in stiffness with cycling in both specimens (Figure 3.11). However, the strength of the MSB braced specimen deteriorated slightly with cycling in load steps 5, 6, and 7 as drift exceeded 2.1%. At 3.5% drift (in load step 7), the strength of this specimen dropped by about 9% at the end of that load step. For the regular braced specimen, there was no significant strength degradation with cycling up to the maximum actuator load capacity (i.e. corresponding to 3.1% specimen drift). After completing 20 load cycles of this specimen at 3.05% drift (in load step 8), its strength dropped by about 18% before the test was terminated. Figure 3.14 shows the base shear-drift response for only this final load step.

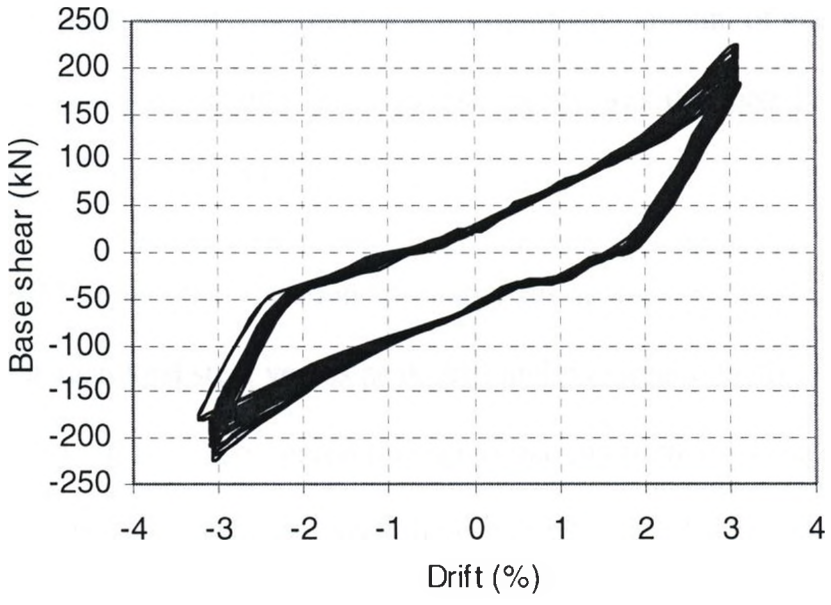

Figure 3.14. Base Shear versus Drift Relationship for Regular Braced Specimen at 3.05% Drift

3.5.3 Energy Dissipation Characteristics of Specimens

Seismic performance of a framed structure can be measured by its energy dissipation characteristics. Energy dissipation is represented by the experimentally obtained hysteretic area, which is evaluated as the area enclosed by the base shear-deformation diagram. The cumulative hysteretic energy dissipation is a useful measure of the seismic efficiency of a structural system. In this study, both the energy dissipation per cycle, using the first complete cycle in each load step, and the cumulative energy dissipation were presented and used in assessing individual performances and comparing the relative effectiveness of the test specimens. The cumulative dissipated hysteretic energy was normalized at each cycle by the product of specimen yield base shear and yield displacement, $V_y\Delta_y$, to eliminate the effect of varying yield loads and displacements. For both specimens, there was no significant amount of energy dissipation within the elastic range of loading. Appreciable energy was dissipated after the elastic cycles, and increased in the following cycles.

Figure 3.15 shows the variation in energy dissipation per cycle, using the first complete cycle at each load step, versus peak drift and maximum ductility reached during that same load cycle. It can be observed that up to maximum displacement ductility of 2, both the MSB and the regular braced specimens exhibited similar energy dissipation per cycle. Beyond this ductility level, the MSB specimen showed superior energy dissipation per cycle in each of the load steps until end of the test. At the maximum ductility of 4, for example, the energy dissipated per cycle by the regular braced specimen was about 77% that by the MSB specimen. For the regular braced specimen, there was no significant

deterioration of dissipated energy with cycling in load step 8 (i.e. at 3.05% drift) before the end of the test. Energy dissipated in the first cycle of this load step reduced by only about 1.5% at the end of the 18^{th} cycle of that same load step.

Figure 3.16 shows the variation of normalized cumulative energy dissipation with cumulative number of cycles and maximum displacement ductility of the test specimens. Clearly, both specimens dissipated similar amount of normalized cumulative energies. The majority of dissipated energy in the MSB braced specimen was the result of a combination of bending deformation in the tube column segment between the top flange of the ceiling beam and the bottom flange of the floor beam, and tension yielding and inelastic buckling of the bracing members. For the regular braced specimen, energy was mainly dissipated through tension yielding and inelastic buckling of the HSS bracing members.

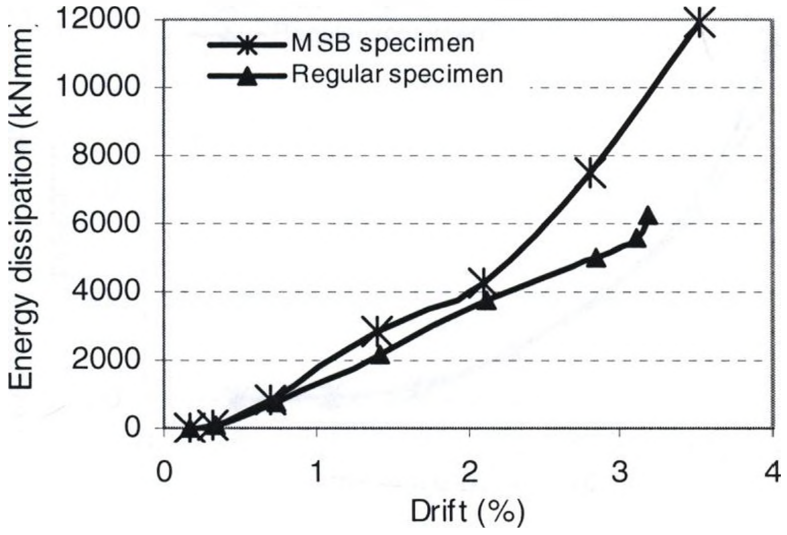

(a)

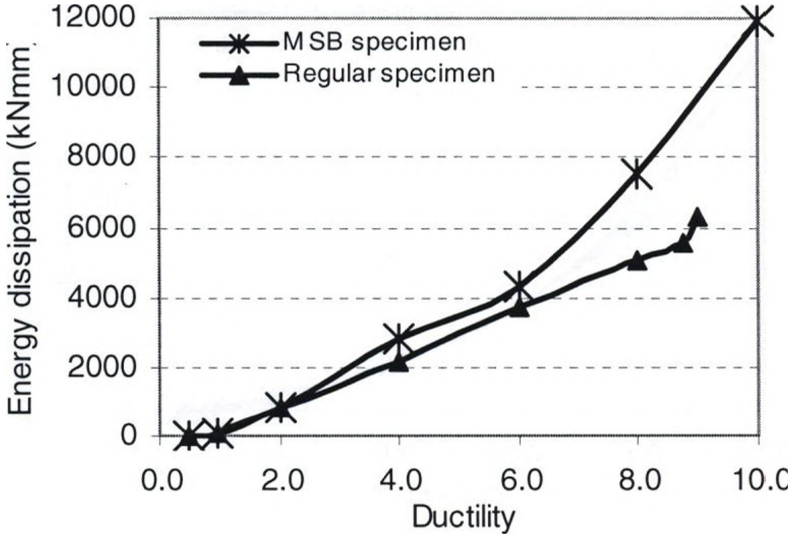

(b)

Figure 3.15. Energy Dissipation per Cycle versus (a) Peak Drift (b) Maximum Ductility

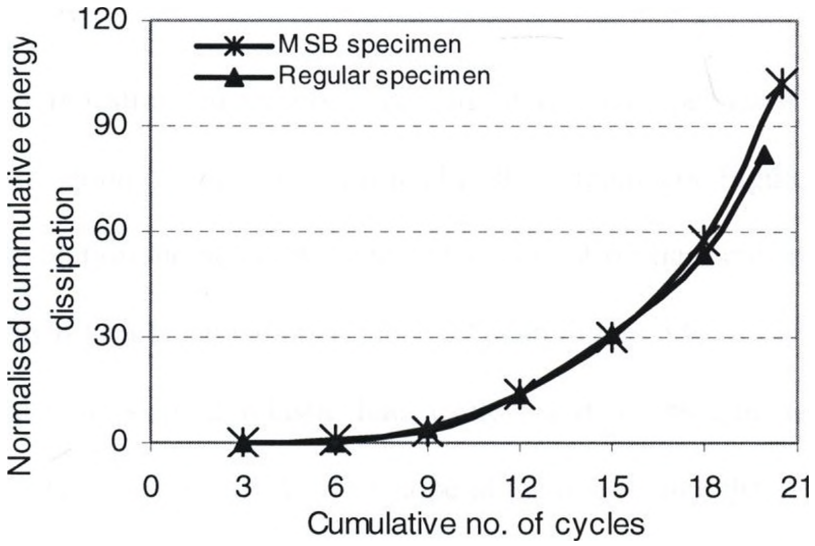

(a)

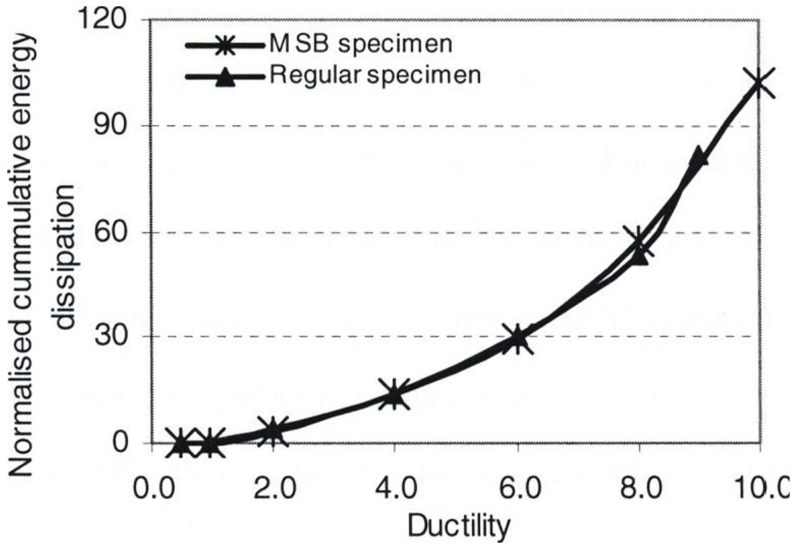

(b)

Figure 3.16. Comparison of Normalized Cumulative Energy Dissipation for Specimens (a) against Cumulative Number of Cycles (b) against Ductility

3.5.4 Force Distribution Pattern

The measured strain in member sections of the test specimens can be closely linked to the distribution of applied lateral load in these members. Figures 3.17 and 3.18 show the strain evolution measured at a selected section of similar brace members (a mid-section of upper half of a brace member, labeled "e" in Figure 3.6) of the specimens with cyclic loading at load steps 2 (elastic load cycles) and 4 (inelastic load cycles with maximum ductility of 4), respectively. The slope of the line joining the peaks of the strain distribution curves is used here as indicative of the distribution of applied shear force at a specified deformation level in the two specimens. This is used to obtain a rough estimate of the force distribution pattern in the selected brace member of the two specimens.

In the elastic load cycle (i.e. step 2), the slopes of the peak-to-peak lines from the two specimens were found to be similar, indicating that the distribution of the applied lateral load within the selected brace member section is of similar pattern. The difference in configuration of the test specimens appears not to have any effect on this force distribution. In the inelastic load cycle (i.e. load step 4), the MSB braced specimen appear to yield greater slope than the regular braced specimen (9.1 micro strain per kN compared to 8.7 micro strain per kN). This implies that, the brace member of the MSB specimen at the selected brace section experienced greater strain than that of the regular specimen under the same load level. In other words, to achieve the same level of strain (deformation) in the member section selected, a greater amount of shear needs to be applied to the regular specimen than the MSB specimen.

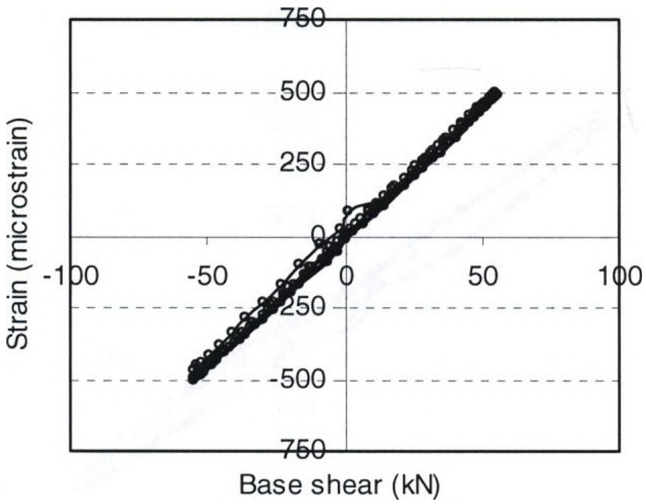

(a)

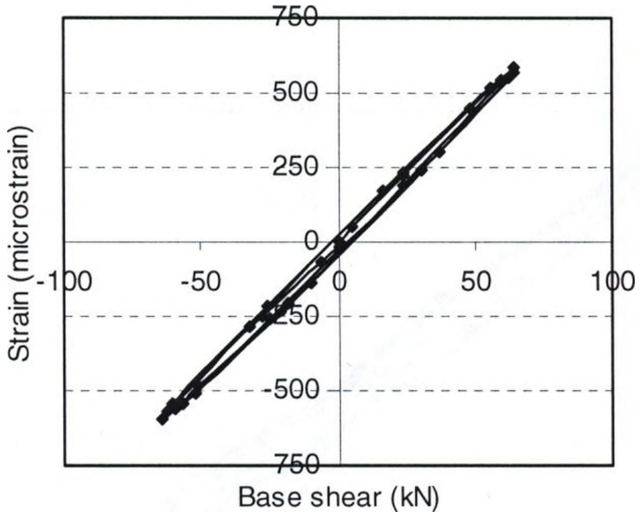

(b)

Figure 3.17. Strain Evolution in a Brace Member Section at Load Step 2 (a) Regular Specimen (b) MSB Specimen

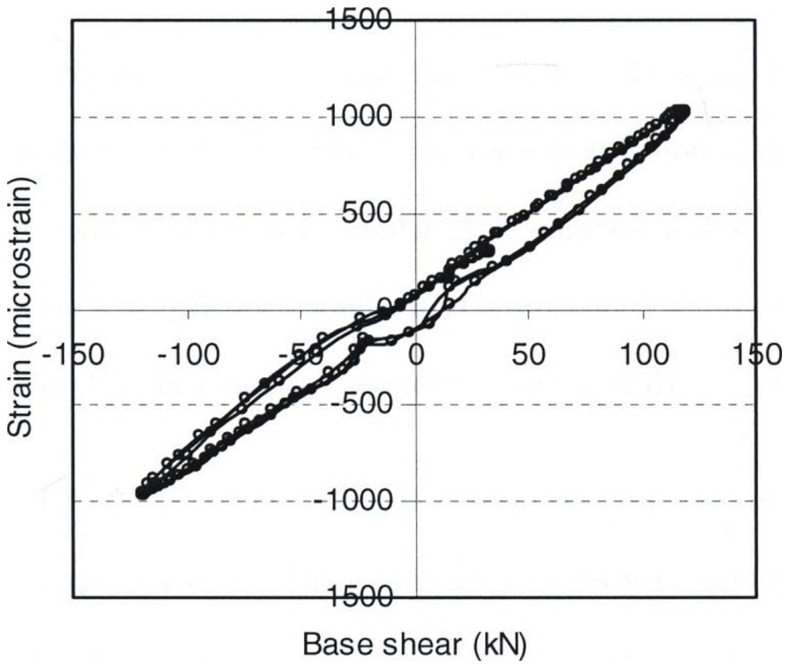

(a)

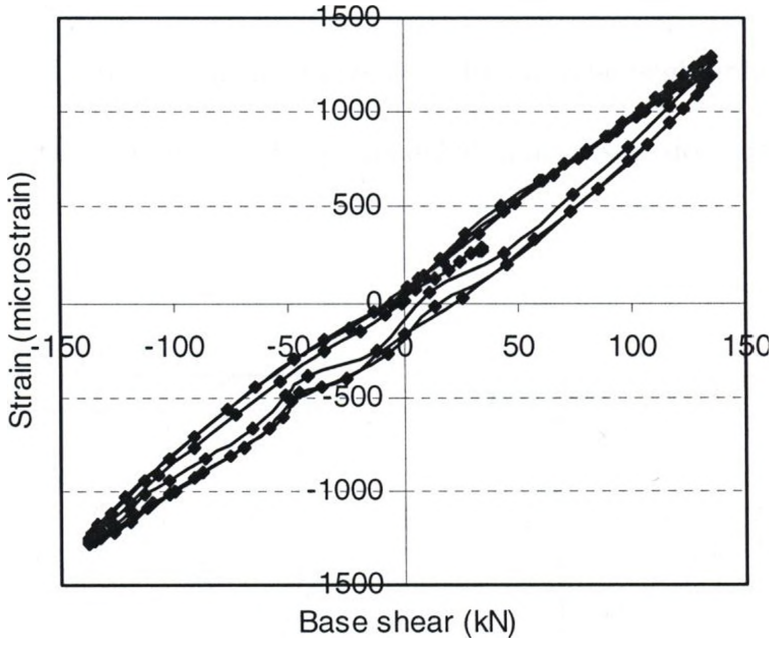

(b)

Figure 3.18. Strain Evolution in a Brace Member Section at Load Step 4 (a) Regular Specimen (b) MSB Specimen

Strain guage readings at several sections of the various members of the specimens were extracted at a number of load levels belonging to both elastic and inelastic ranges of response and in both directions of loading. The force distribution in the two specimens was compared for same load levels in similar cycle numbers within similar load steps. Also, the comparison was made for a similar load level applied at different load steps and for a similar load level applied in opposite directions of the MSB specimen.

Figure 3.19 can be used to explain the force distribution pattern in both the MSB and regular braced specimens. Buckling of brace sections was identified by observing high discrepancies in the magnitude of forces, and the magnitude of moments evaluated for these sections in-plane and out-of-plane. Table 3.2 provides the ratios of calculated normal forces in members of the test specimens to the applied lateral load, P. Negative signs in this table represent a reverse of force sense from that shown in Figure 3.19. The calculated moments in the various members were found to be negligible compared to the normal forces, and have therefore not been included in the discussions below.

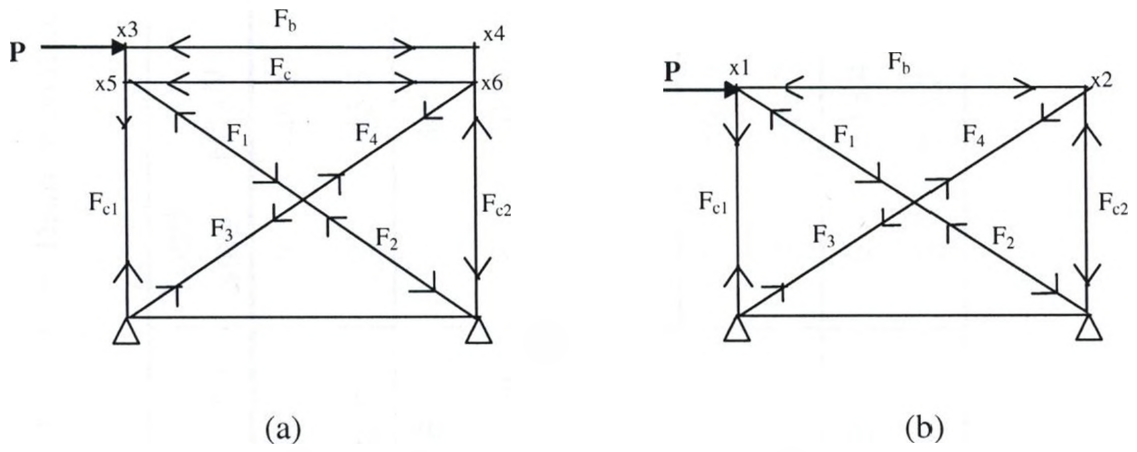

Figure 3.19. Force Distribution in Members of (a) MSB Specimen (b) Regular Specimen

Table 3.2. Force Distribution Ratios in Members of Braced Specimens

Specimen	Load step	P (kN)	F_1	F_2	F_3	F_4	F_{c1}	F_{c2}	F_b	F_c
MSB	2	-45.1	-0.65	-0.64	-0.65	-0.65	-0.45	-0.45	-0.36	-0.14
Regular	2	-45.3	-0.66	-0.66	-0.63	-0.63	-0.43	-0.40	-0.49	
MSB	2	40.8	0.65	0.64	0.64	0.64	0.46	0.45	0.35	0.15
Regular	2	40.5	0.67	0.66	0.64	0.64	0.44	0.42	0.49	
MSB	3	82.5	0.59	0.58	0.71	0.71	0.42	0.50	0.36	0.19
Regular	3	81.8	0.61	0.60	0.69	0.69	0.40	0.45	0.54	
MSB	5	-193.7	-0.76	-0.75	-0.52	-0.53	-0.53	-0.38	-0.37	-0.05
MSB	6	-193.7	-0.78	-0.76	-0.50	-0.51	-0.54	-0.37	-0.36	-0.04
MSB	6	-213.4	-0.78	-0.75	-0.49	-0.51	-0.55	-0.37	-0.36	-0.04
MSB	6	213.3	0.48	0.43	0.80	0.78	0.35	0.56	0.36	0.27

At load levels within the elastic response range (load step 2), there is only a small difference in magnitude of distributed loads in the columns and braces between the two specimens. However, the overall mechanisms of load transfer vary due to difference in configuration. For the regular braced specimen (Figure 3.19b), similar force levels are transmitted through joints x1 and x2, with a difference of only about 2% of the applied lateral force. The top floor beam thus carries almost half of the applied force along its longitudinal plane. Consequently, the columns and braces develop the induced forces. This force distribution pattern is due to the near truss action exhibited by the frame. For the MSB specimen, unequal forces are transmitted through joints x3 and x4. This is due to the welding detail at the vertical module connection. There is partial welding between the columns and the top floor beam, which leaves interior sides of the joints without weld. Thus, in the direction of loading, the leading joint allows some rotation to occur. The trailing joint, on the other hand, develops some moments. The ceiling beam aids redistribution of these unbalanced forces by developing a normal force with the same sense of direction as the floor beam. Joints x5 and x6 thus transmit an equal amount of force, and consequently the brace members and column members develop equal amount of forces between themselves.

In the inelastic range of response of the regular specimen (load steps 3, 5, 6), buckling of compression brace member section results in the reduction of distributed force through the end joint of this brace member and an increase in the force through the end joint of the tension brace. This results in an unequal force distribution in bracing members, and also in column members as shown in Table 3.2. For the MSB specimen, joints x3 and x4 experience different degrees of transmitted force as explained above.

Once buckling of the compression brace occurs, the ceiling beam member helps in redistributing these forces allowing greater force levels through the end joint of the tension brace. If the direction of loading is reversed, a similar behaviour is observed in the opposite direction. At high lateral loads, however, the transmission of compression forces across brace intersection in the non-continuous brace member is significantly affected by buckling and this complicates the overall transfer mechanism.

3.5.5 Analytical Prediction of MSB Specimen Behaviour

The behaviour of the MSB test specimen was predicted analytically using a two-dimensional model. A basic two-dimensional centerline model of the frame specimen was used with floor and ceiling beams, columns and braces extending from centerline to centerline. A bilinear material model for steel was employed, using the experimentally obtained material properties. An inelastic steel beam-column frame element was used to represent column members. A one component beam element was used for all beam representations. The inelastic behaviour of both the beam and the beam-column elements follows the concept of the Giberson one-component model (Sharpe, 1974), which has a plastic hinge possible at one or both ends of the elastic central length of the member. The Remennikov Steel Brace member hysteresis (Remmennikov and Walpole, 1997) was used to represent brace members. This hysteresis model represents the out-of-plane buckling of the steel brace member but essentially captures the inelastic behaviour under alternate axial tension and compression. The member only permits this hysteresis in the axial component; it is generally assumed to be bilinear in flexure.

All beam-column joints in the MSB specimen model were assumed rigid to represent the directly welded connection between these members. Rigid end blocks were provided at each end of the frame members to capture the rigidity of connection regions. A truss action of the bracing members was activated by allowing both ends to be pinned internally to the joints. This was to simulate the assumed pin-ended behaviour of bracing members. The proposed analytical model of the vertical connection of modular units, between columns of a lower unit and the top floor beam (or columns) of an upper unit, described in section 3.4.2 above was adopted in this prediction analysis. The developed analytical model of the MSB specimen was subjected to a cyclic displacement history similar to that used in the experimental investigation.

Figure 3.20 shows a comparison between the experimentally and theoretically obtained load-displacement curves of the MSB braced specimen. It can be observed that the theoretical model provided a fairly good prediction up to 2.8% drift, beyond which it experienced numerical instability. Prior to termination of the analysis, bracing members experienced repeated inelastic deformations in cyclic tension beyond yield and compression into the post-buckling range. The columns, including column segments between the bottom flange of the floor beam and top flange of the ceiling beam, also experienced repeated cycles of bending deformation before the end of the analysis.

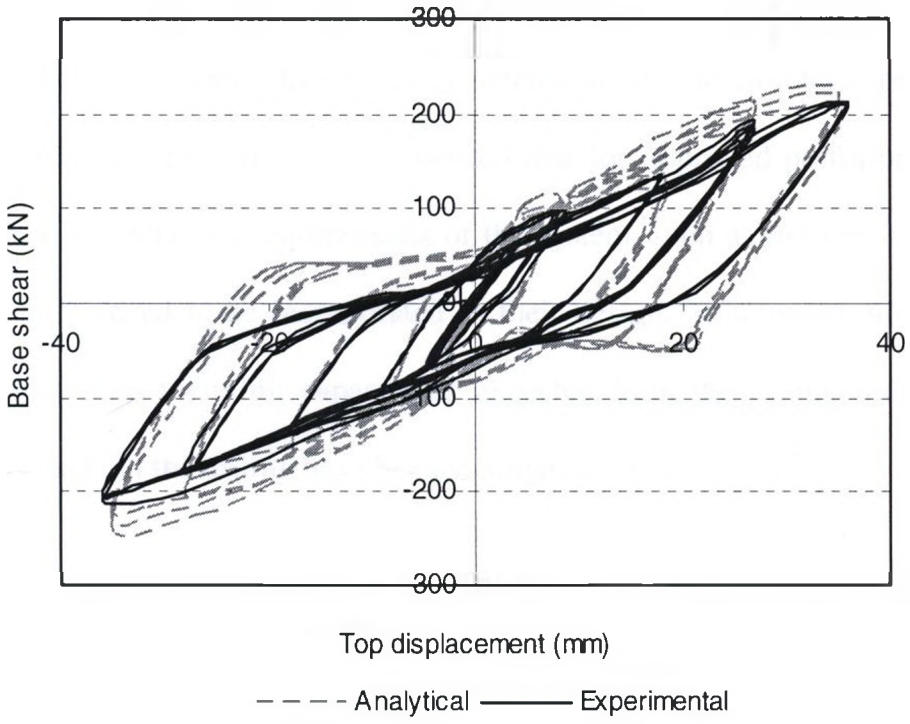

Figure 3.20. Comparison of Experimental and Analytical Load-Displacement Curves of MSB Braced Specimen

3.6 Summary and Conclusions

In this chapter, the hysteretic characteristics of modular steel building (MSB) braced frame under repeated cyclic loading has been evaluated. The stiffness, ductility, cumulative hysteretic energy dissipation capacity, and force distribution pattern were assessed. The behaviour of the MSB specimen was predicted analytically to validate a proposed modeling technique. The design and construction of the test specimen accounted for the building's specific detailing requirements. A regular concentrically

braced frame with similar physical characteristics, such as the clear height and member proportions, was also tested to compare behaviour. The results of the tests indicate some similarities as well as some differences in behaviour of the two test specimens. The differences in behaviour particularly suggested that for improved performance of MSB braced frames, the detailing requirements of the system, such as the vertical connection of separate units, need to be incorporated in their design. This would allow the frame members to develop their full capacity as expected from the design philosophy. The observations made in the testing have been summarised below.

1. Both the MSB and regular braced specimens showed stable and ductile behaviour up to very high drift levels. The MSB specimen reached a ductility of 10 at 3.5% drift and the regular specimen reached a ductility of 9 at 3.1% drift at a load level equal to the load capacity of the actuator. The regular specimen further sustained 20 more cycle at 3.05% drift before the test was terminated.
2. The hystereses of both specimens were fairly symmetrical with some degree of pinching, especially in the regular specimen. For this specimen, the first sign of nonlinearity occurred as a result of buckling in a brace member while in the MSB specimen, flexural response due to column yielding caused the initial nonlinearity.
3. The regular braced specimen was found to be slightly superior in terms of stiffness at low ductility (below 2) and at high ductility (above 6). Between these ductilities, both frame specimens showed similar stiffness levels. For both specimens, initial stiffness degraded by about 45% at a ductility level of 6.
4. Within each load step in the regular braced specimen, there was no significant strength and stiffness degradation with cycling. The MSB specimen also showed

no significant stiffness degradation but only slight reduction (less than 10% at 3.5% drift) in strength with cycling beyond a 2.1% drift.

5. For the MSB specimen, the test was terminated after a high level of ductility was reached. In this stage of loading, severe bending deformation was observed for the column segment between the top flange of the ceiling beam and the bottom flange of the floor beam. The brace members in this specimen did not suffer severe deformation. For the regular braced specimen, the test was terminated after several inelastic cycles at sufficiently high ductility level. Prior to this point, a lower half side of a brace member experienced severe out-of plane buckling at its mid-section.
6. Both specimens dissipated significant and similar amount of cumulative energies. Both specimens also exhibited similar energy dissipation per cycle up to ductility of 2. Beyond this ductility level, the MSB specimen appeared to show superior energy dissipation per cycle in each of the load steps until failure.
7. Significantly different force distribution patterns were observed in the two test specimens. At the same load level corresponding to the same number of cycles in a similar load step, the load transfer mechanism in the MSB specimen produced force distribution that are different from the regular braced specimen because of the presence of the ceiling beam and the unique vertical connection of separate modules.
8. The proposed analytical modeling technique is capable of predicting the seismic behaviour of MSB braced frames up to high drift levels beyond traditional design requirements.

3.7 References

AISC [2002] *Seismic provisions for structural steel buildings*, American Institute of Steel Construction, Chicago, IL.

Annan, C.D., Youssef, M.A. and El-Naggar, M.H. [2005] "Analytical investigation of semi-rigid floor beams connection in modular steel structures," *33rd Annual general conference of the Canadian Society for Civil Engineering,* Toronto, Canada, GC-352.

Annan, C. D., Youssef, M. A. and El-Naggar, M. H. [2007] "Seismic performance of modular steel braced frames," *Proc. of the Ninth Canadian Conference on Earthquake Engineering*, Ottawa, Ontario, Canada.

Annan, C.D., Youssef, M.A. and El-Naggar, M.H. [2008] "Effect of directly welded stringer-to-beam connections on the analysis and design of modular steel building floors," *Advances in Structural Engineering,* Accepted in October 2008.

Annan, C. D., Youssef, M. A. and El-Naggar, M. H. [2009] "Seismic overstrength in braced frames of Modular Steel Buildings," *Journal of Earthquake Engineering*, 13(1), 1-21.

ASTM [2002] *Standard test methods and definitions for mechanical testing of steel products*, American Society for Testing and Materials, Philadelphia, PA.

ATC [1992] *ATC-24/Guidelines for cyclic seismic testing of components of steel structures*, Applied Technology Council, Redwood City, California.

CSA [2001] *Handbook of Steel Construction, 7th Edition*, Canadian Institute of Steel Construction, Willowdale, Ontario, Canada.

Ikeda, K., and Mahin, S.A. [1984] "A refined physical theory model for predicting the seismic behaviour of braced steel frames," *Report no. UCB/EERC-84/12*, Berkeley, CA.

Izzuddin, B.A. [1991] "Nonlinear dynamic analysis of framed structures'" *PhD Thesis, Imperial College*, University of London, London, UK.

Jain, A.K. and Goel, S.C. [1978] *Hysteresis models for steel members subjected to cyclic buckling or cyclic end moments and buckling – User's guide for DRAIN-2D: EL9 and EL10*, Report UMEE 78R6, Department of Civil Eng., Univ. of Michigan, Ann Arbour, MI, USA.

NBCC [2005] *National Building Code of Canada*, Institute for Research in Construction, National Research Council of Canada, Ottawa, Ontario, Canada.

Osteraas, J. and Krawinkler, H. [1989] "The Mexico earthquake of September 19, 1985 – behaviour of steel buildings," *Earthquake Spectra*, 5 (1), 51-88.

Remennikov, A. and Walpole, W. [1997] "Analytical prediction of seismic behaviour for concentrically-braced steel systems," *Earthquake Engineering and Structural Dynamics* 26, 859-874.

Sharpe, R. D. [1974] *The seismic response of inelastic structures*, Ph.D Thesis, Department of Civil Engineering, University of Cantebury.

Tremblay, R., Timler, P. Bruneau, M., and Filiatrault, A. [1995] "Performance of steel structures during the January 17, 1994 Northridge earthquake," *Canadian Journal of Civil Engineering,* 22 (2), 338-60.

Tremblay, R., Bruneau, M. Nakashima, M., Prion, H. G. L., Filiatrault, A., and DeVall, R. [1996] "Seismic design of steel buildings: Lessons from the 1995 Hyogo-ken Nanbu earthquake," *Canadian Journal of Civil Engineering,* 23 (3), 727-56.

Tremblay, R. [2000] "Influence of brace slenderness on the seismic response of concentrically braced steel frames," *Proc. STESSA 2000 Conference*, Montreal, Canada, pp. 527-534.

Tremblay, R. [2002] "Inelastic seismic response of steel bracing members," *Journal of Constructional Steel Research*, 58, 665-701.

Tremblay, R., Archambault, M.H., and Filiatrault, A. [2003] "Seismic response of concentrically braced steel frames made with rectangular hollow bracing members," *Journal of Structural Engineering*, ASCE, 129 (12), 1626-36.

CHAPTER FOUR

SEISMIC OVERSTRENGTH IN BRACED FRAMES OF MODULAR STEEL BUILDINGS[§]

4.1 Introduction

Contemporary seismic design of building structures involves reducing the forces obtained from an idealised elastic response spectrum by a ductility related force reduction factor R_d. The magnitude of such reduction primarily depends on the ability of the structure to undergo inelastic deformation without collapse. Furthermore, it is observed that structures usually possess a considerable amount of reserve strength. This extra strength is known to be one of the key characteristics which influence the seismic response of building structures. Many modern seismic design codes therefore permit further reduction of the design forces to account for the dependable portion of this reserve strength.

The 2005 edition of the National Building Code of Canada (NBCC, 2005) and the New Zealand Earthquake Load Standard (NZS4203, 1992) explicitly recognise this reserve strength by providing an overstrength related modification factor, R_o. Other codes such as the ASCE standard 7-05 (ASCE, 2005), the International Building Code (IBC, 2006), and the Australian Earthquake Standard (AS1170.4, 1993) use a composite reduction factor to account for both overstrength and ductility. Many sources of overstrength can be easily identified but not all can be readily quantified. Sources that

[§] Annan, C.D., Youssef, M.A., and El Naggar, M.H. "Seismic overstrength in braced frames of modular steel buildings." Journal of Earthquake Engineering, Vol. 13, Issue 1, pp. 1-21.

have been reviewed by Uang (1991), Mitchell and Paultre (1994), Rahgozar and Humar (1998), Bruneau et al. (1998) and Mitchell et al. (2003) include: material effects caused by higher yield stress compared with the nominal value, R_{yield}; the effect of using discrete member sizes and practical considerations that require the provision of larger sections than required for some elements, R_{size}; strain hardening behaviour in steel, R_{sh}; redistribution of internal forces in the inelastic range, R_{mech}; difference between nominal and factored resistances, R_{phi}; as well as code requirements for considering multiple loading combinations and the contributions of non-structural elements.

Many experimental studies have been conducted to assess lateral overstrength of different structural systems (Bertero et al., 1984; Uang and Bertero, 1986; Whitaker et al., 1989; Osteraas and Krawinkler, 1989). Analytical procedures (Rahgozar and Humar, 1998; Elnashai and Mwafy, 2002; Balendra and Huang, 2003; Kim and Choi, 2005) have also been used extensively to estimate structural overstrength from capacity curves of different structural systems. Nonlinear static pushover analysis has been a reliable tool employed to produce these curves (Rahgozar and Humar, 1998; Kim and Choi, 2005). Based on results from pushover analyses of 2 to 30 storey concentrically braced frames designed using the same lateral load, Rahgozer and Humar (1998) observed that for concentrically steel braced frame structures, the main parameter that controls the reserve strength is the slenderness ratio of the bracing members. They also observed that the structural overstrength is almost independent of the height of the frame and the effect of building sway. The average observed reserve strength ratio for these frames, accounting for only internal force redistribution, R_{mech}, was about 2.1. The NBCC (2005) recommends an R_o of 1.3 (which includes R_{yield}, R_{size}, R_{sh}, R_{mech}, and R_{phi}) for both

moderately and limited ductility concentrically steel braced frame, regardless of the height of the building and the magnitude of the design earthquake. It is important to note that overstrength factors provided by different codes can only be achieved by applying the design and detailing provisions of the appropriate standard; therefore, for the use of R_o given by the NBCC, design and detailing have to be in conformity with the appropriate Canadian standard (CSA, 2001).

The analytical definition of structural overstrength is reasonably well established. For many structural systems, a dependable source of reserve strength that can be reliably estimated is due to redistribution of internal forces in the inelastic range R_{mech}. Considering a typical structural response envelope in Figure 4.1, showing the relationship between base shear and roof displacement, the structural overstrength accounting for all possible sources can be defined by Equation 4.1:

$$R_O = \frac{V_y}{V_d} \qquad \text{..... (4.1)}$$

where V_y is the load that corresponds to the achievement of the specified failure mode and V_d is the design base shear. For the reserve strength that accounts for only redistribution of internal forces, V_d would represent the load corresponding to the first significant yield. Displacement ductility μ is defined in terms of maximum structural drift (Δ_u) and the displacement corresponding to the idealised yield strength (Δ_y) as

$$\mu = \frac{\Delta_u}{\Delta_y} \qquad \text{..... (4.2)}$$

The actual force reduction factor R_d is a factor which reduces the elastic force demand to the level of the maximum yield strength V_y.

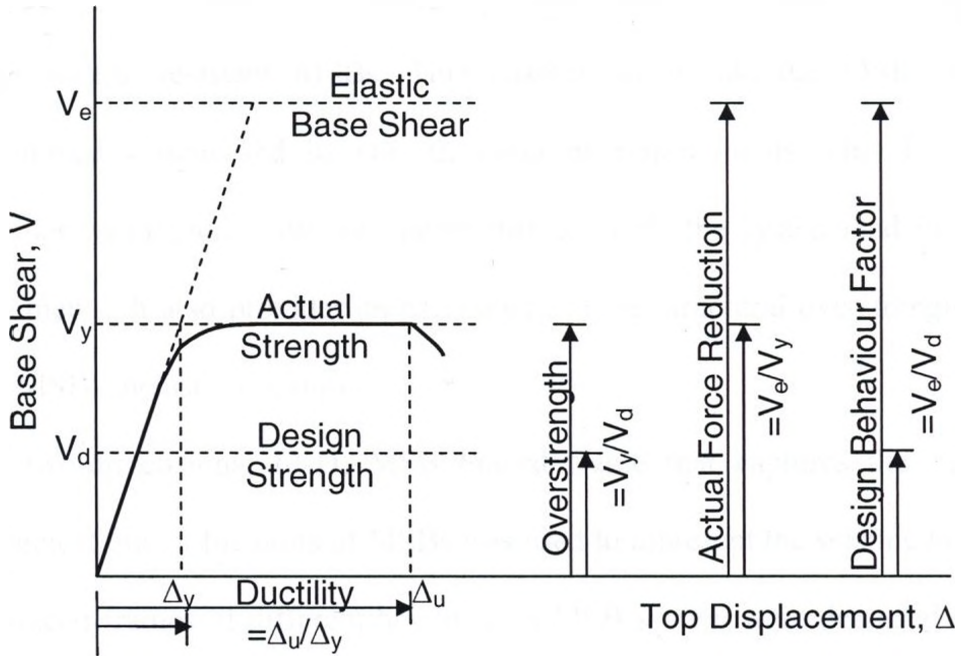

Figure 4.1. Typical Structural Response Envelope

The Modular Steel Building (MSB) is fast evolving as an effective alternative to traditional on-site steel building. The modular technique involves the design of buildings which are built and finished at one location and transported to be used at another. The finished units of a MSB are connected both horizontally and vertically onsite. MSBs

make use of hot-rolled steel sections for enhanced strength and durability. They have been typically used for one-to-six storey schools, apartments, hotels, correctional facilities, and dormitories, with essentially repetitive units. A detailed description of the concept, process, advantages and limitations of this unique steel building technique was presented by Annan et al. (2005) and given in chapters One and Two. Seismic design of this building type is performed using conventional methods, as no seismic performance studies for MSB systems are presently available. This study is part of an extensive research program that aims at providing basis for development and production of next generation seismic-resistant MSBs. This chapter documents the MSB lateral force resisting braced system and its specific detailing requirements. This is expected to provide other researchers with the opportunity to study the system and investigate its critical elements. It also provides an assessment of the structural overstrength in braced frames of MSBs inelastic response.

A two-dimensional (2-D) MSB braced frame that captures the behaviour of vertical connections of the units of MSBs was used to represent the seismic load resisting system. Braced frames of different heights of a MSB system were designed considering moderate ductility in accordance with the Canadian standard (CSA, 2001). The seismic design forces were determined based on the provisions of the NBCC (2005). The frame systems were modelled using the non-linear finite element computer program, SeismoStruct (SeismoSoft, 2003). Special attention was given to the specific detailing requirements of the MSB frame system. Non-linear static pushover analyses were conducted to determine the ultimate lateral load resistance as well as the sequence of yielding/buckling events. Structural overstrength factors were extracted from the

observed response curves and compared with code-specified values and those reported by other researchers for regular steel braced frames (eg. Rahgozar and Humar, 1998; Uang and Bertero, 1986).

4.2 Modular Steel Building (MSB) System

Figure 4.2 shows typical details for a multi-storey MSB. A typical storey of a MSB structural frame consists of a set of columns, a floor framing made up of floor beams (FB) and floor stringers (FS), as well as a ceiling framing made up of ceiling beams (CB) and ceiling stringers (CS). These components are connected together mainly by direct welding of their members. Results of a study on the response of a MSB floor framing system under gravity loading (Annan et al., 2005; Annan et al., 2008) showed that direct welding between floor beams and floor stringers of the MSB floor framing system significantly affected the design of the stringers and the welded connections but had a negligible effect on the design of the floor beams. The horizontal connection (HC) between the units of a MSB involves field bolting of clip angles that are shop-welded to the floor beams (section A-A of Figure 4.2). The vertical connection (VC) consists of field welding of base plates of upper module columns to cap plates of lower module columns (section B-B of Figure 4.2). Only the outer faces of these columns that are accessible during assembling are welded. The floor beams are either set directly above the ceiling beams shown in Figure 4.2 or at a specified clearance to allow for a fire protective layer to be installed. Lateral stability of the entire MSB is achieved by adding diagonal braces as shown in Figure 4.2. Lateral loading on each floor is transferred

through the horizontal connections to the modular braced frame and then through the vertical connections to the foundation.

The braced frame of MSBs is clearly different from regular braced frames and may respond differently in an event of any lateral movement due to earthquakes. In terms of structural configuration, the following specific features distinguish MSBs from conventional steel building construction: 1) the existence of ceiling beams in MSBs is expected to result in natural periods and mode shapes different from those of conventional systems; 2) in a typical modular steel braced frame, brace members do not intersect at a single working point which may lead to high seismic demands on the vertical connections; 3) the vertical module connections typically involve welding one face of the columns of a lower and an upper modules which may lead to independent upper and lower rotations at the same joint; and 4) the connections between floor beams and columns and also ceiling beams and columns are achieved using direct welding, which is unconventional for regular steel buildings.

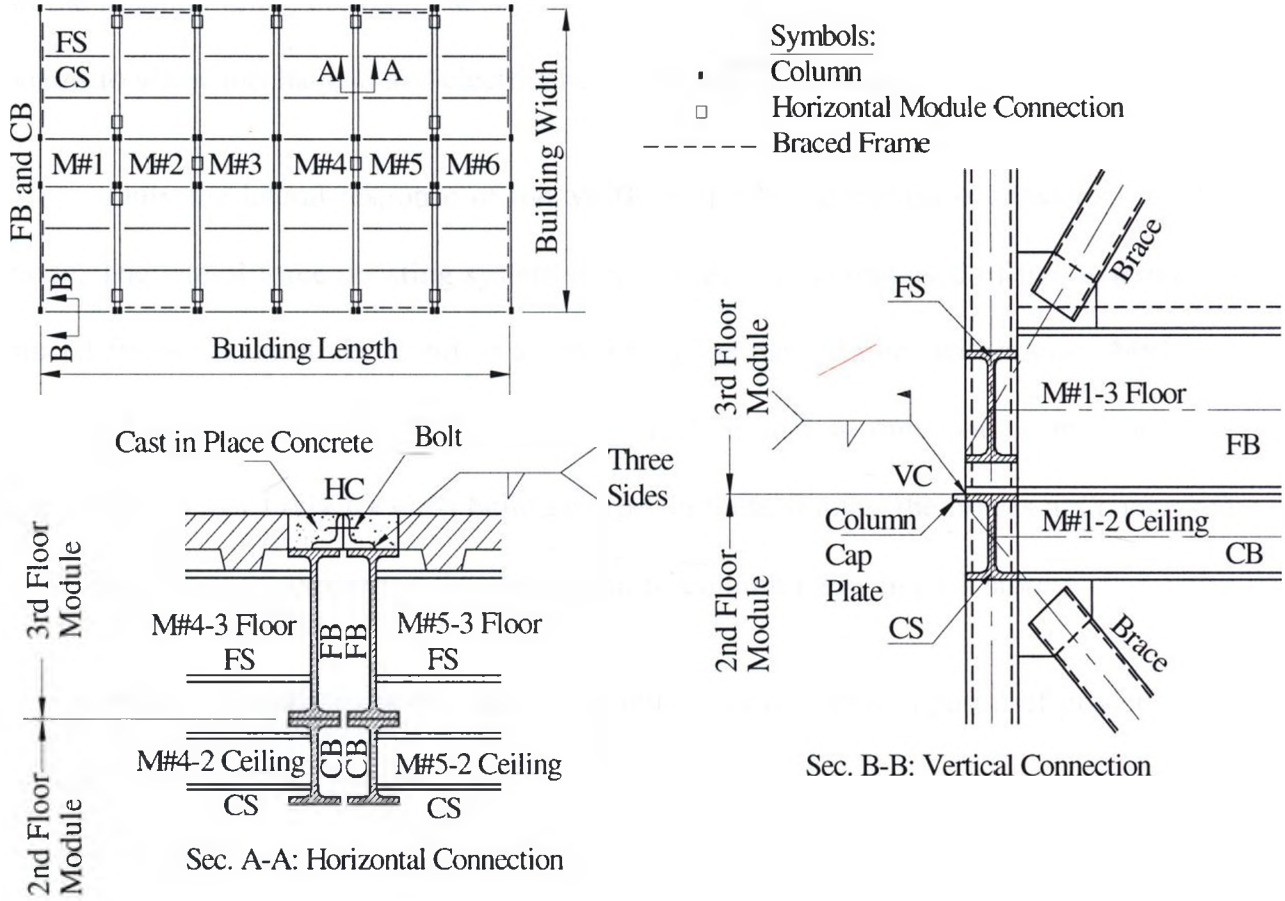

Figure 4.2. Typical Details for a Multi-storey MSB

Three heights of a typical modular steel dormitory are considered in the study: two-storey, four-storey and six-storey structures, with the same overall plan dimensions (Figure 4.3a). These frame types/sizes and plan layout represent typical applications of the MSB system. Each storey is made up of six modules, labelled M#1 to M#6, comprising twelve individual rooms and a corridor. The floor framing of a modular unit is composed of two floor beams, a number of floor stringers and a metal deck with concrete composite floor. Similarly, the ceiling framing includes two ceiling beams and a number of ceiling stringers. The corridor on each floor runs through the middle portion of

all the modular units, between the two interior columns. The corridors are without ceiling beams to allow mechanical and electrical ducts to run along them.

Only the lateral response of the MSBs in the N-S direction is considered in this study. The lateral force resisting system in this direction is composed of two external X-braced frames (centrelines 1 and 7) as shown by the dashed lines within units M#1 and M#6 in Figure 4.3a. These two frames are identical and so only one (centreline 7) is considered in this study for each building type. In these frames, the braces are connected to the floor beam-to-column and ceiling beam-to-column joints in each storey.

Brace connections to the modular framing system are composed of gusset plates welded to the braces. For the vertical connection of units of these frames, welding is achieved only on the outer faces of all the columns on centerlines A, B, C, D, E, and F. Figure 4.3b shows the elevation of the braced frame of the four-storey MSB. A clearance of 150 mm was allowed between floor beams and ceiling beams. For ease of discussions in subsequent sections, all columns located on centerlines A and F will be referred to as outer external columns and columns located on centerlines C and D will be referred to as inner external columns. Columns that are located on centerlines B and E will be referenced as internal columns.

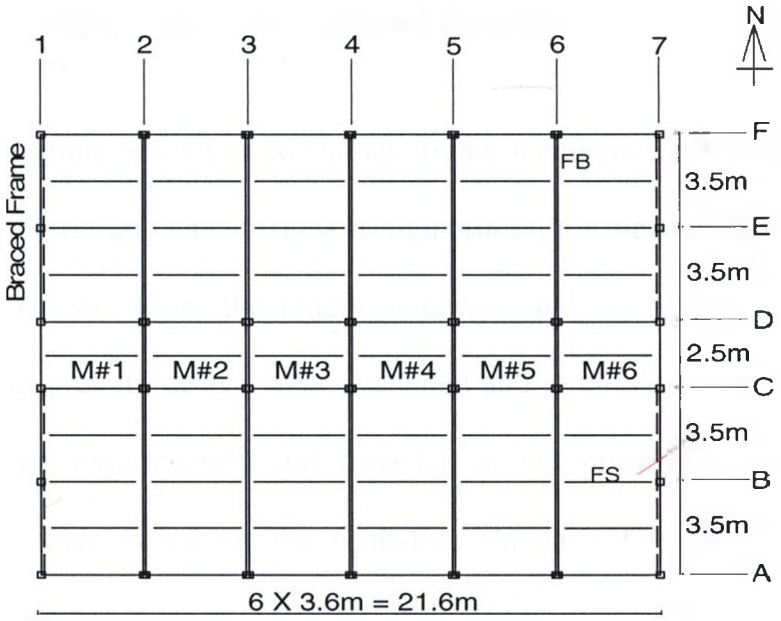

(a) Floor Plan

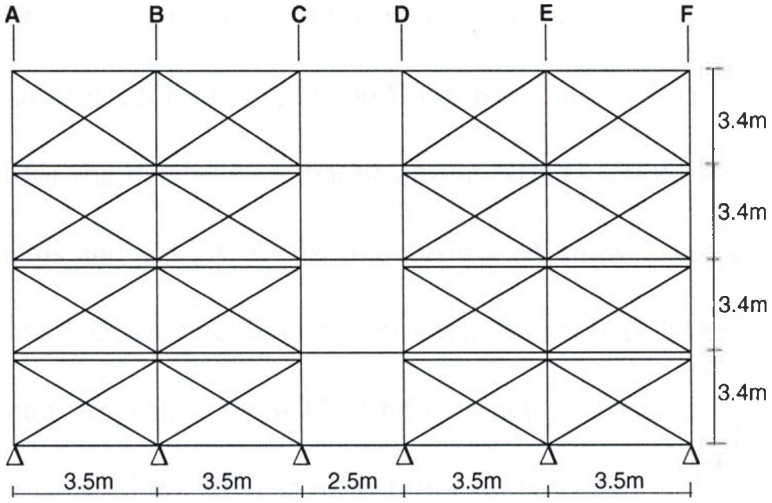

(b) Elevation (centerline 1 or 7)

Figure 4.3. Four-storey Modular Steel Braced Frame

4.3 Design of Modular Steel Braced Frames

When designing MSB braced frames, frame members were initially sized on the basis of traditional strength and stiffness design criteria for the specified imposed gravity and earthquake actions. Then, the braces, columns, and floor and ceiling beams sizes obtained from the strength design were evaluated and modified, as necessary, according to ductility design requirements and capacity design procedures. The strength and ductility designs were based on the Canadian standard, CAN/CSA-S16.1-01 (CSA, 2001).

The dead load (DL) from a typical floor was composed of the weights of the concrete floor, an all round metal curtain wall system and insulation, a steel deck and the self-weight of the frame members. Superimposed dead load of 0.75, 0.32, and 0.7 kN/m^2 were applied to account for additional loads on floor, roof, and ceiling, respectively. The live loads (LL) used for the design were based on the NBCC (2005) and are 1.9 kN/m^2 for the individual rooms and 4.8 kN/m^2 for the corridor. A snow load of 1.0 kN/m^2 was assumed for the roof. The seismic loading on each frame was based on the NBCC Equivalent Static Load Approach (NBCC, 2005), which is based on uniform hazard values corresponding to a 2% in 50-year probability of exceedance. The location of the MSBs was selected as Vancouver in British Columbia, Canada. The buildings were assumed to be founded on a very dense soil (site class C) with an average shear wave velocity range between 360 m/s and 760 m/s. The design base shear values of the frames were calculated assuming moderate ductility with an overstrength factor of 1.3 and

ductility factor of 3.0. The design base shears were distributed over the height of the building as per the NBCC (2005).

CISC Grade 350W steel with a specified yield stress, F_y, of 350MPa was used to design the beams, columns, and brace members. The least weight section required for strength for each frame element was selected. For all brace members and columns, specified sections were limited to square hollow structural sections (HSS), which are used widely for MSB systems. Wide flange sections (W shape) were specified for the floor, ceiling and roof beams as per common practice. Demand/capacity ratios for axial, flexural and shear, based on factored loads and factored resistances, were used as the criterion for the selection of optimal sections. Additionally, selected sections were modified to conform to more practical arrangements. Table 4.1 gives a summary of the resulting sections from the strength design of the MSB braced frames considered in the study.

The bracing members were assumed to belong to class H (hot-formed or stress relieved) of the CAN/CSA-S16.1-01 standard (CSA, 2001). Brace member capacities were calculated based on the same standard. The buckling strength, C_r', of compression brace members is given in this code in terms of the compressive yield strength, C_r, and the slenderness coefficient, λ, by Equation 4.3:

$$C_r' = \frac{C_r}{1+0.35\lambda} \qquad \text{..... (4.3)}$$

The ductility provision by the Canadian standard, CAN/CSA-S16.1-01 (CSA, 2001) for the design of steel braced structures is based on the assumption that columns, beams and brace connections within the structure must be able to resist the resulting induced forces when braces reach their ultimate strength. For that purpose, the ultimate strength of brace members was taken as the nominal resistance. Specific requirements for brace members to ensure ductile behaviour during severe earthquakes are given in Clause 27 of the CAN/CSA-S16.1-01 standard (CSA, 2001) as follows:

1) the slenderness ratio of bracing members, *kl/r*, where k is the effective length factor, l is the unsupported length, and r is the radius of gyration, must be less than or equal to $1900/(F_y)^{1/2}$;

2) the width-to-thickness ratio, b/t, of bracing members must be less than or equal to $330/(F_y)^{1/2}$ for hollow structural sections; and

3) both tension and compression braces must be able to carry a minimum of 30% of shear in the storey.

The effect of the reduction in compressive strength of the brace members due to repeated buckling (Jain and Goel, 1978; Popov and Black, 1981) was accounted for by checking the forces in the bracing members against the reduced brace compressive strength, given by Equation 4.3. In the case where the tension brace in the same bent and at the same level had excess capacity to compensate for this reduction in compressive strength, the reduction factor, $[1/(1+0.35\lambda)]$, was not applied. In other words, if the tension brace in the same level and plane as the compression brace was found to possess sufficient reserve strength, the compression brace member was sized based on the

resistance, C_r and not C_r'. Columns 5 and 6 of Table 4.1 contain a summary of the brace member sections for ductile response of the MSB braced frames.

The column members obtained from the strength design were also reviewed to meet ductility requirements. According to the Canadian standard, CAN/CSA-S16.1-01 (CSA, 2001), columns are to be proportioned to resist the gravity loads together with the forces induced by the brace connection loads. In order to meet this requirement, many engineers design the columns to withstand accumulation of the vertical components of yielding and buckling brace forces in addition to gravity loads. For a multi-storey frame, however, a widely used approach for column design for ductility is based on the assumption that all the bracing members would not reach their capacities simultaneously. Thus, a statistical accumulation of earthquake-induced brace forces using the Square Root of the Sum of the Squares, SRSS, approach (Khatib et al., 1988; Redwood and Channagiri, 1991) is preferred to a direct summation of the vertical components of yielding and buckling brace loads.

Table 4.1. Member Sections from Strength and Ductility Designs of MSB Braced Frame

Number of stories	Frame Member	Storey / Floor #	Strength Design	Ductility Design (column design by SRSS approach)	Ductility Design (column design by DS approach)
2-storey MSB braced frame	Braces	2	HS 89X89X6	HS 89X89X6	
		1	HS 89X89X6	HS 89X89X6	
	Columns	2	HS 89X89X6	HS 127X127X5	
		1	HS 127X127X5	HS 178X178X8	
	Beams	Roof	W100X19	W100X19	
		Floor 2	W100X19	W100X19	
		Floor 1	W100X19	W100X19	
		Ceiling	W100X19	W100X19	
4-storey MSB braced frame	Braces	4	HS 76X76X5	HS 76X76X6	
		3	HS 76X76X5	HS 76X76X6	
		2	HS 89X89X6	HS 89X89X6	
		1	HS 89X89X6	HS 89X89X6	
	Columns	4	HS 76X76X5	HS 102X102X6	HS 102X102X6
		3	HS 178X178X5	HS 178X178X6	HS 178X178X6
		2	HS 178X178X5	HS 203X203X6	HS 203X203X10
		1	HS 178X178X6	HS 203X203X8	HS 254X254X10
	Beams	Roof	W100X19	W100X19	
		Floor 4	W100X19	W100X19	
		Floor 3	W100X19	W100X19	
		Floor 2	W100X19	W100X19	
		Floor 1	W100X19	W100X19	
		Ceiling	W100X19	W100X19	
6-storey MSB braced frame	Braces	6	HS 76X76X5	HS 76X76X5	
		4	HS 102X102X5	HS 102X102X6	
		4	HS 102X102X5	HS 102X102X6	
		3	HS 102X102X5	HS 102X102X6	
		2	HS 102X102X5	HS 102X102X6	
		1	HS 102X102X5	HS 102X102X6	
	Columns	6	HS 89X89X5	HS 102X102X6	HS 102X102X6
		5	HS 127X127X6	HS 178X178X6	HS 178X178X6
		4	HS 178X178X10	HS 178X178X10	HS 203X203X10
		3	HS 203X203X10	HS 203X203X10	HS 305X305X10
		2	HS 254X254X10	HS 254X254X10	HS 305X305X13
		1	HS 305X305X10	HS 305X305X10	HS 305X305X13
	Beams	Roof	W100X19	W100X19	
		Floor 6	W250X33	W250X33	
		Floor 5	W250X33	W250X33	
		Floor 4	W250X33	W250X33	
		Floor 3	W250X33	W250X33	
		Floor 2	W250X33	W250X33	
		Floor 1	W250X33	W250X33	
		Ceiling	W100X19	W100X19	

The SRSS approach has been found to be reasonably conservative for regular braced frames. This approach was considered in the design of columns of the MSB braced frames. In the SRSS approach, the induced force in a column under consideration is taken as equal to the vertical brace components (nominal capacity) at the level of the column, plus the square root of the sum of the squares of all other brace load components at levels above the column under consideration. The resulting loads were combined with specified dead and live loads. Figure 4.4 shows a free body diagram for determining brace induced column actions in the four-storey MSB frame based on the SRSS approach, including a calculation example at the second storey. The column loads that would result from a Direct Summation (DS) approach, where column actions are derived from a direct sum of vertical components of yielding and buckling brace forces are also shown in the figure.

Clearly, this load accumulation approach results in much higher forces for columns located at lower levels of the braced frame. It is to be noted that induced forces are determined for external columns only, as they are likely to be subjected to greater effective brace-induced loads than internal columns. The resulting column section at one level was applied to all other columns on the same level of the frame. Columns 5 and 6 of Table 4.1 contain a summary of the revised column sections in the MSB braced frames obtained from the use of the SRSS accumulation approach, as well as the DS approach. It is observed that there is significant difference in the size of columns located at lower levels of the frame resulting from the two load accumulation approaches; in addition, the variance is greatest for the six-storey MSB braced frame. It is noted that column sections

at all levels of the six-storey MSB frame obtained from the strength design are found to be inadequate for the required ductility when using the DS accumulation approach.

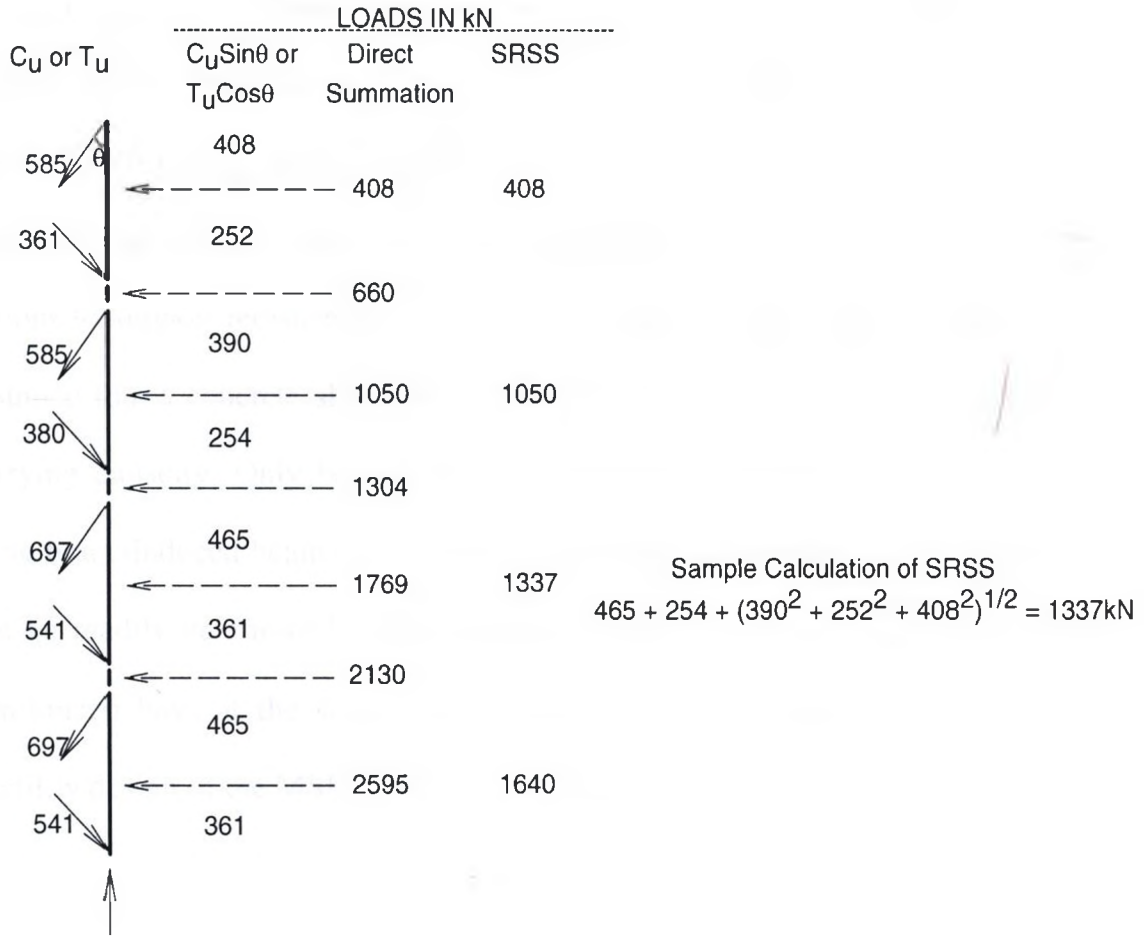

Figure 4.4. Cumulative Brace Loads for Determining Column Actions in Four-storey MSB

In the ductility design of the ceiling, roof and floor beam members, the effect of redistribution of loads due to brace buckling or yielding was considered in designing the beams in braced bays. Beams were thus designed as beam-columns, with the design moment resulting from tributary gravity loads and the axial compression coming from unequal capacity of braces in tension and compression, considering a horizontal equilibrium of brace-induced forces at each beam end. The configuration of the braced frame would clearly play a significant role in determining these axial loads in beams. Figure 4.5 shows free body diagrams for determining floor and ceiling (or roof) beam actions to support redistributed loads, including typical calculation examples. Here, it is assumed that a concrete slab would prevent instability but would not contribute to load carrying capacity. Only beams in braced bays wasconsidered in the determination of these brace-induced beam actions, as this is the only case where such redistributed loads can be readily determined. The resulting section at any level was applied to beams in non-braced bays at the same level. A summary of the beam sections resulting from ductility design of the MSB braced frames is also contained in Table 4.1.

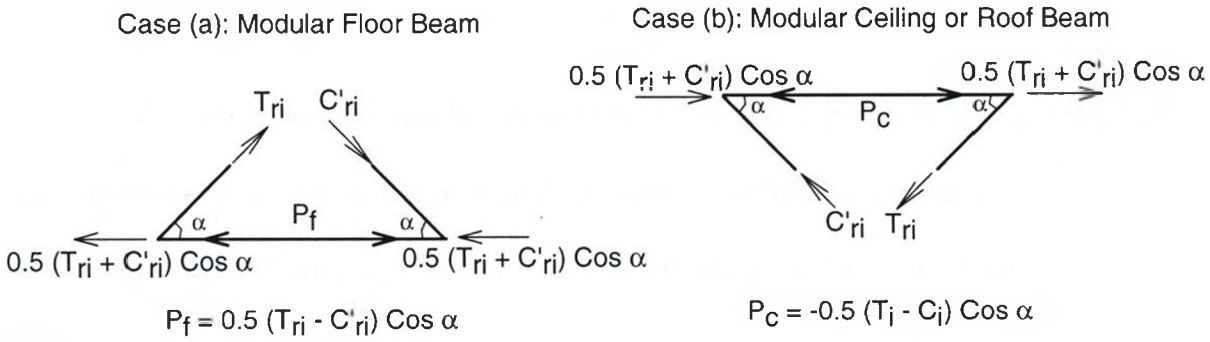

Figure 4.5. Free Body Diagrams of Beam Forces to support Redistributed Brace Loads

The brace end connections were designed to remain elastic at all times so they could be at least as strong as the bracing member in order to maximize the energy dissipation capacity of the frame. These connections were therefore designed to support the full yielding brace resistance, given by the brace nominal tensile strength, $A_g F_y$. The design of the vertical welded connections of units of the MSB was based on traditional elastic method and accounted for the eccentric loading which results from welding only one side (i.e. outside faces) of the connected columns in the MSB frame. The eccentricity of the force would impose bending stresses on the weld. The Canadian standard, CAN/CSA-S16.1-01 (CSA, 2001) was used in the design of these welded connections.

4.4 Analysis of MSB Braced Frames

Assessment of inelastic behaviour of steel structures requires analysis techniques with a substantially higher level of sophistication as compared to linear elastic analysis. Any nonlinear analysis procedure (static or dynamic) generally requires modeling of the complete load-deformation (or moment- curvature) characteristics to failure of each component of the structure.

In this study, the SeismoStruct nonlinear computer program (SeismoSoft, 2003) was employed in the modeling and analysis of the modular steel braced frames. For all the modular braced frames considered, two-dimensional models were developed based on centerline dimensions of the bare frames. This was chosen owing to the limited significance of torsional effects in MSB systems and was deemed sufficient for the

objectives of the study. A bilinear material model for steel was employed, with a kinematic strain hardening parameter of 1%, a yield stress of 350 N/mm^2, and an elastic modulus of 200 kN/mm^2. An inelastic beam-column frame element, which employs a cubic shape function (Izzuddin, 1991), was used to represent all structural frame members. This element type accounts for member geometric and material non-linearities.

The element formulation is based on the fibre modeling approach that models the spread of material inelasticity along the member length and across the section area to allow for accurate estimation of structural damage distribution. In such elements, the sectional stress-strain state is obtained through the integration of the nonlinear uniaxial stress-strain response of the individual fibres in which the section has been subdivided. For the frame members, 200 section fibres were employed based on sensitivity study. The element response (curvatures and stress/strain peak values) is assembled from contributions at two gauss points, where the cross sections can be discretised into a number of monitoring points. A joint element with uncoupled axial, shear and moment actions was utilised to simulate the assumed pin-jointed behaviour at the ends of bracing members. All beam-to-column joints were assumed to be rigid to represent the directly welded connection between these members in the MSB braced frame system.

The analytical model of the vertical connection of different frame units (i.e. different levels/stories of frame) is likely to influence the lateral response of the entire frame, particularly the global ultimate strength. These vertical connections typically involve welding the exterior faces of the column cap and base plates of lower and upper frame units (Figure 4.2), respectively, leading to independent upper and lower rotations at

a common joint. An analytical model that utilises a number of beam-column elements, rigid links, and a joint element was developed and validated in Chapter Three and is shown in Figure 4.6. The frame elements, J1-J2, J2-J3, J2-J4, J5-J6, J6-J7, and J6-J8 were modelled as rigid elastic elements to capture the rigidity at the region of beam-column joints within the tube section columns. The internal element, J4'-J5, had the same geometric and mechanical properties as the column of the lower frame unit, C1. This element represents part of the lower unit column with height equal to the clearance between the bottom flange of floor beam of the upper frame unit and the top flange of ceiling beam of the lower frame unit. A joint link element was defined to connect nodes J4 and J4' to capture the independent rotation likely to develop between column members present at this vertical connection.

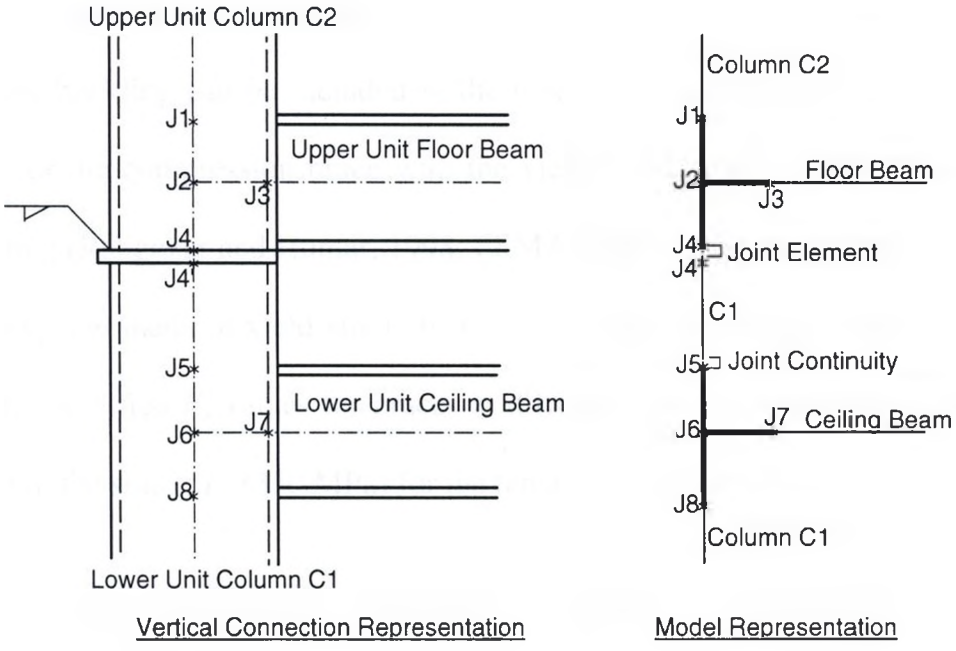

Figure 4.6. Model of Vertical Connection of units of MSB Braced Frame

During a strong earthquake, a brace member in a concentrically braced frame will be subjected to large inelastic deformations in cyclic tension beyond yield and compression into the post-buckling range. The post-elastic compression capacity of the bracing members plays an important role in seismic analysis of such frames. Jain and Goel (1978) conducted an extensive series of experimental work to study the buckling behaviour of a bracing member. They concluded that the buckling strength of the compressive brace members reduces significantly after the first cycle of loading and then becomes almost steady after a few cycles. Modern seismic design standards (e.g. CSA, 2001) and recommendations (e.g. SEAOC, 1999) have reasonably captured this post-buckling phenomenon by applying a buckling reduction factor to the compressive strength of bracing members. In the Canadian standard (CSA, 2001), the reduced compressive strength is captured by Equation 4.3.

In a nonlinear static procedure, i.e. pushover analysis, the reduction in strength of a brace after buckling can be included in the model by assuming an elastoplastic brace behaviour for the compression brace with the yield force taken as the residual strength after buckling (Rahgozar and Humar, 1998; FEMA, 2000). This was adopted in this study by modifying the material yield strength, F_y, of compression brace members. Table 4.2 contains the modified F_y values for braces at different levels of the MSB braced frames considered in the study. F_y (350 MPa) for the tension braces remained unchanged.

The analytical models of the MSB braced frames were subjected to non-linear pushover analyses to estimate their lateral capacity. The gravity loads, lumped at nodal points, were held constant while the magnitude of lateral forces with an assumed

triangular distribution pattern along the building height was gradually increased until the formation of structural mechanism. The analysis was carried out under response control algorithm. For each analysis, a target displacement was defined and was subdivided into 250 for incremental application. Thus the load factor was automatically calculated by the computer program.

Table 4.2. Modified F_y Values for Compression Brace Members of MSB Braced Frames

Number of stories	Storey Braces	Slenderness, λ	$B(\lambda) = (1+\lambda^{2n})^{-1/n}$	$k = B(\lambda)/(1+0.35\lambda)$	kF_y (MPa)
2-storey MSB brace frame	2	0.98	0.75	0.56	195.7
	1	0.94	0.78	0.58	204.7
4-storey MSB brace frame	4	1.16	0.62	0.44	153.9
	3	1.12	0.65	0.47	163.6
	2	0.94	0.78	0.59	204.6
	1	0.94	0.78	0.59	204.6
6-storey MSB brace frame	6	1.13	0.64	0.46	161.0
	5	0.81	0.86	0.67	234.8
	4	0.81	0.86	0.67	234.8
	3	0.81	0.86	0.67	234.8
	2	0.81	0.86	0.67	234.8
	1	0.81	0.86	0.67	234.8

4.5 Results and Discussions

4.5.1 Inelastic Response of MSB Frames

Figures 4.7a, 4.8a and 4.9a show the order and distribution of plasticity in the six, four, and two-storey MSB braced frames in which the SRSS accumulation approach was utilised to derive the brace induced column actions. The filled dots represent plastic hinge formation in the beams and columns. The brace members drawn with bold lines had either buckled or yielded. The numbers associated with the dots and on the brace members describe the sequence of plasticity formation or yielding/buckling, with the number one (1) representing the first member to buckle or yield. It is observed that there was a good distribution of energy dissipation along the height and across the length of the four- and six-storey frames. The two-storey MSB frame tended to concentrate the distribution of plasticity in only one-half of the entire frame width.

The order and distribution of plasticity in braced frames may be affected by the brace sizes, slenderness ratio, frame configuration and analysis type. If the brace sizes are uniform along the height of the frame and the braces have the same slenderness ratio, buckling would most likely occur first in the first storey. The analysis type might also affect the results as in static pushover analysis a lateral force is applied at each storey level while for dynamic analysis this lateral force would be distributed across the floor according to the distribution of masses.

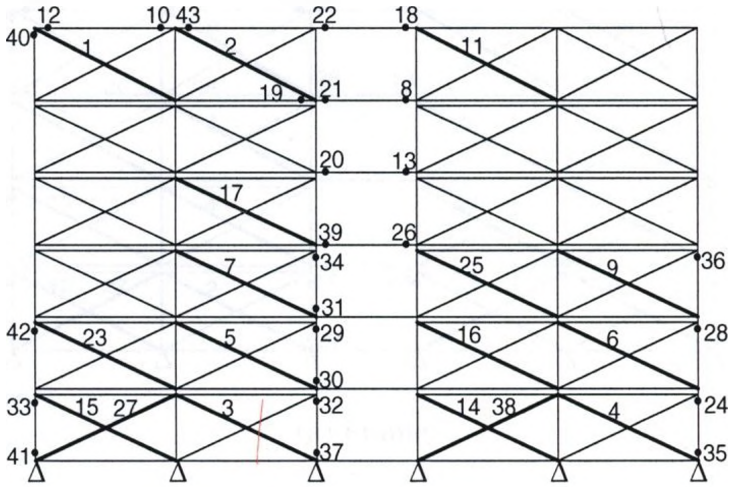

(a) Frame

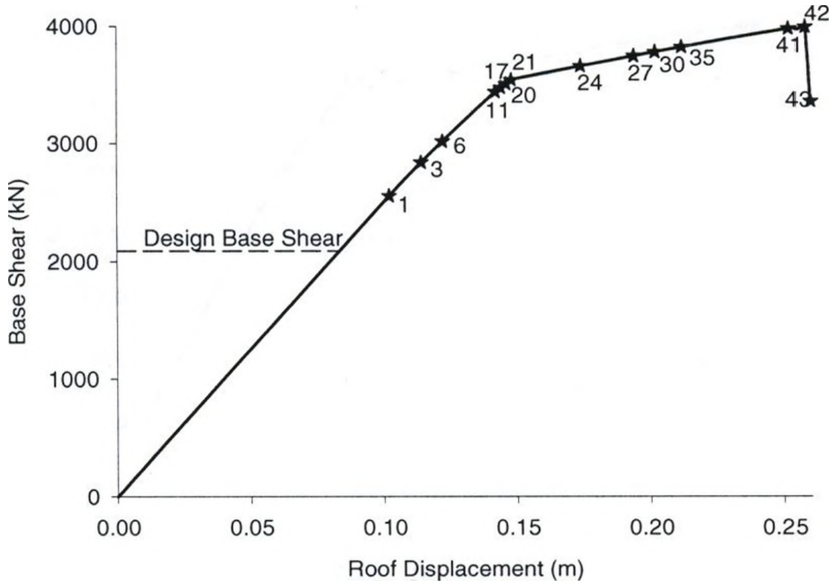

(b) Capacity Curve

Figure 4.7. Sequence of Yielding/Buckling of the Six-storey MSB Braced Frame (Brace induced column actions by SRSS accumulation approach)

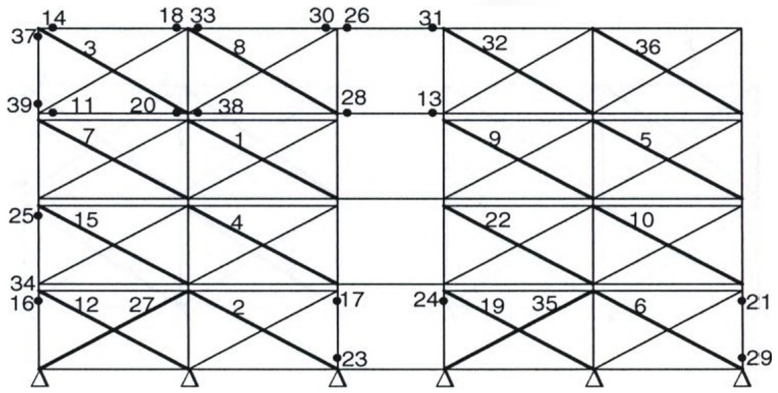

(a) Frame

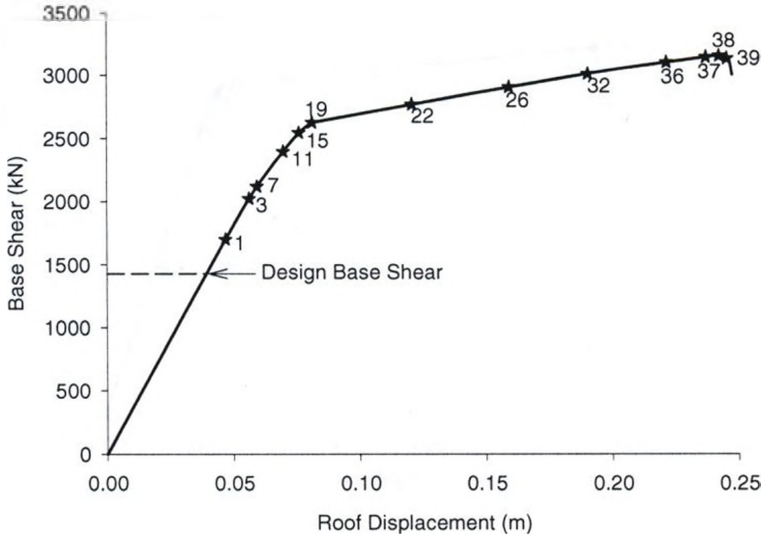

(b) Capacity Curve

Figure 4.8. Sequence of Yielding/Buckling of the Four-storey MSB Braced Frame (Brace induced column actions by SRSS accumulation approach)

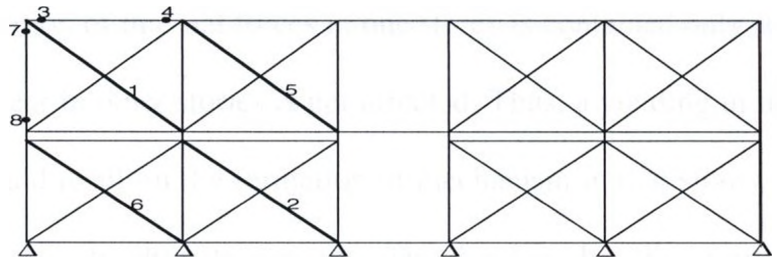

(a) Frame

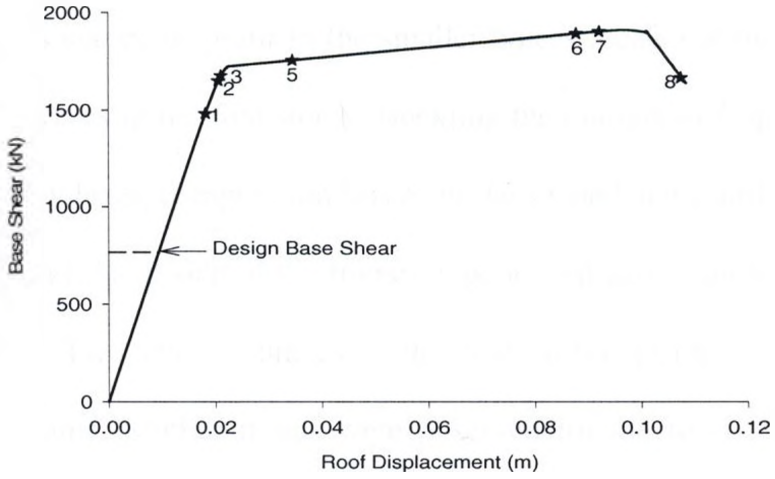

(b) Capacity Curve

Figure 4.9. Sequence of Yielding/Buckling of the Two-storey MSB Braced Frame (Brace induced column actions by SRSS accumulation approach)

In ductile concentrically braced frames of regular buildings, the global ultimate strength is controlled by the formation of structural mechanism in one storey. This is because redistribution of internal forces in one storey is contained only in that storey. The distribution of shear in other stories is not affected. Thus, a yielding in the tension braces in one storey would result in the formation of mechanism in that storey and the structure consequently reaches its ultimate capacity. This implies that the reserve strength of the critical storey is also the global reserve strength of the frame.

In the six-storey MSB braced frame (Figure 4.7), the brace member size was uniform in the first five stories and much smaller in the sixth storey. This was due to the distribution of design lateral forces along the height of the frame. Buckling of compression braces started to occur in the smaller braces located at the sixth storey and then followed by braces in the first storey. Buckling then progressed up the height of the frame. At any storey level, compression braces in the second and fourth braced bays (i.e. counting from the left hand side of the frame) experienced earlier buckling than those in other braced bays. Two tension braces at the first storey yielded before failure was reached for this frame. Similar trends were observed for the four-storey MSB braced frame (Figure 4.8). In this frame, the first two stories have the same brace member size; the top two stories also have the same brace size which is smaller than that of the lower stories. Buckling in compression braces initiated from the lowest level with the smaller brace section (i.e. the third floor in this frame). For the same brace size, buckling progressed up the height of the frame (i.e. from the third to fourth and from the first to second stories). The second braced bay experienced early buckling of its compression braces as in the six-storey frame and two tension braces at the first storey again yielded

before failure was reached. In the two-storey MSB braced frame (Figure 4.9), plasticization was not as well distributed within the frame as it was in the other two frame heights. Failure of this frame was reached before any of the tension braces could yield.

It is observed in Figures 4.7a, 4.8a, and 4.9a that plastic hinges formed in some columns and beams before buckling/yielding of some bracing members, and before failure was reached. For instance, some of the outer and inner external columns located at the lower storey levels of the six- and four-storey MSB braced frames experienced plasticization at an early stage of the inelastic response. In all the frames, plastic hinges formed in the outer external column at the topmost storey level before failure. Some roof and top floor beams of the MSB frames also experienced plasticization early during the inelastic response. These occurred notwithstanding the design philosophy to prevent yielding or buckling of columns and beams before all of the braces. The internal columns were, as expected, not affected by plasticization because of the design simplification that assigned sections resulting from the design of more critical external columns to these internal columns.

The formation of plastic hinges in the columns at lower storey levels was more pronounced in the six-storey MSB braced frame than the four-storey; none were present in the two-storey frame. In the two-storey MSB braced frame, the SRSS approach utilised for capacity design of its columns resulted in the same column actions/sections as the DS approach that sums vertical components of yielding/buckling brace forces directly. This is always true for two-storey braced frames as there is only one storey level above the first storey level; in this case, the DS accumulation approach would always yield same

results as the SRSS accumulation approach. The variance in design loads for lower level columns from the two load accumulation approaches, however, would increase significantly as the number of stories increased from the two-storey configuration. Thus, in the six-storey MSB braced frame, column actions at the first two storey levels were significantly less for the SRSS approach compared to the DS approach.

The above observations tend to raise questions about the appropriateness of the use of the SRSS approach for MSB braced frames, more so as it is evident from the results that all the braces did not yield/buckle simultaneously, thereby validating the main assumption that governs its use. It therefore appears that the unique vertical connection requirements of different units of the MSB seem to impose an additional demand on the columns, especially those at lower levels. The four-storey and six-storey MSB braced frames were redesigned for ductility with brace-induced column actions obtained from the DS accumulation approach. These frames were modeled and analysed by the pushover method. Results of the analyses are shown on Figures 4.10 and 4.11 respectively (i.e. sequence of yielding/buckling and horizontal capacity curves). The distributions of plasticity observed for these frames indicate no formation of plastic hinges in columns located at lower levels of these frames. The sequence of brace buckling/yielding are, however, almost similar to those of the four-storey and six-storey MSB braced frames in which the SRSS accumulation approach was utilised to determine column actions (Figures 4.7a and 4.8a). The use of the SRSS approach for accumulating brace-induced column actions in capacity design, therefore, does not appear to be conservative for MSB braced frames. Rather, the DS approach seems to be yielding the desired response for these frames.

For the hinges formed in some roof and top floor beams and the outer external column of the top storey level, it is probably an indication of some limitation of the analysis method used in this study (i.e. the pushover method). These members are left to carry much greater loads than they are designed for after buckling of some of the brace members located at the top storey level. Once the compression brace member in the first braced bay at this storey level buckles and is no longer able to support further loading, the design lateral load at this level is directly carried by the roof beam in this bay. The outer external column and, consequently, columns and beams making up this braced bay, and in its vicinity, are subjected to load levels that have not been accounted for in their designs, so they begin to fail. In effect, the bracing action for supporting lateral load is lost in this region. This sequence of events is more evident in the two-storey MSB braced frame where the compression brace in the top storey of the first braced bay buckles early. This may also have contributed to the poor distribution of plasticity within this frame.

The order of events, as described above, is evident in both the four-storey and the six-storey MSB braced frames, where column actions are obtained from both the DS load accumulation approach (Figures 4.7 and 4.8) and the SRSS approach (Figures 4.10 and 4.11). This further suggests that the formation of plastic hinges as observed in beams and columns of this frame region is most probably a result of analysis limitations rather than a design deficiency. This situation is likely to be avoided in reality during earthquake with mass distributed over the entire floor.

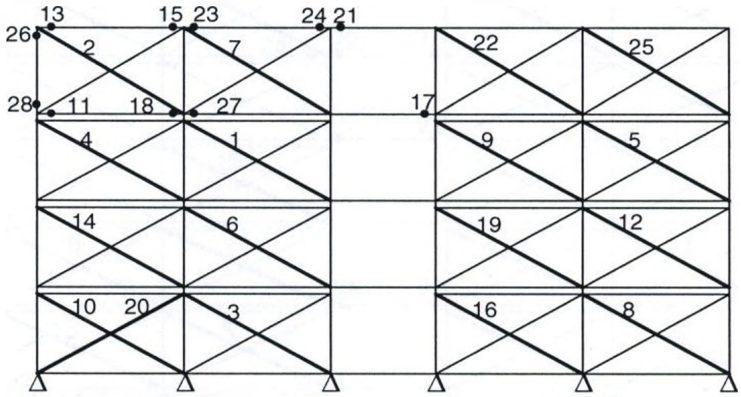

(a) Frame

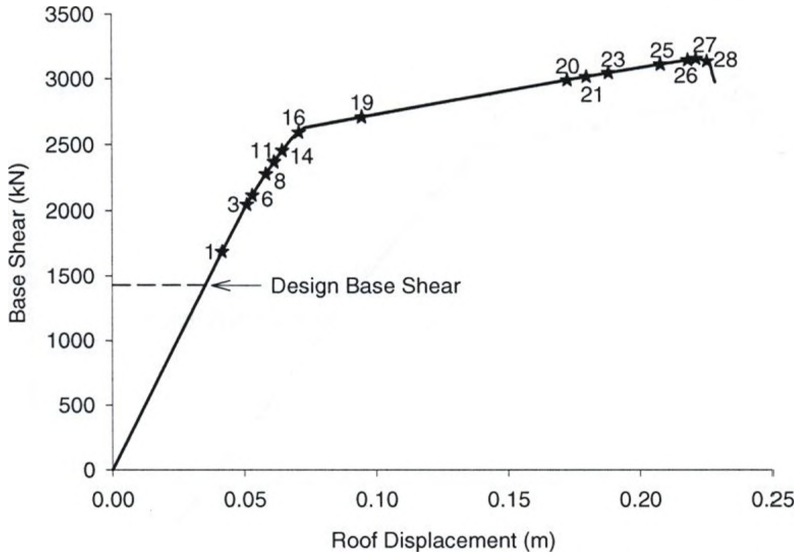

(b) Capacity Curve

Figure 4.10. Sequence of Yielding/Buckling of the Four-storey MSB Braced Frame (Brace induced column actions by DS accumulation approach)

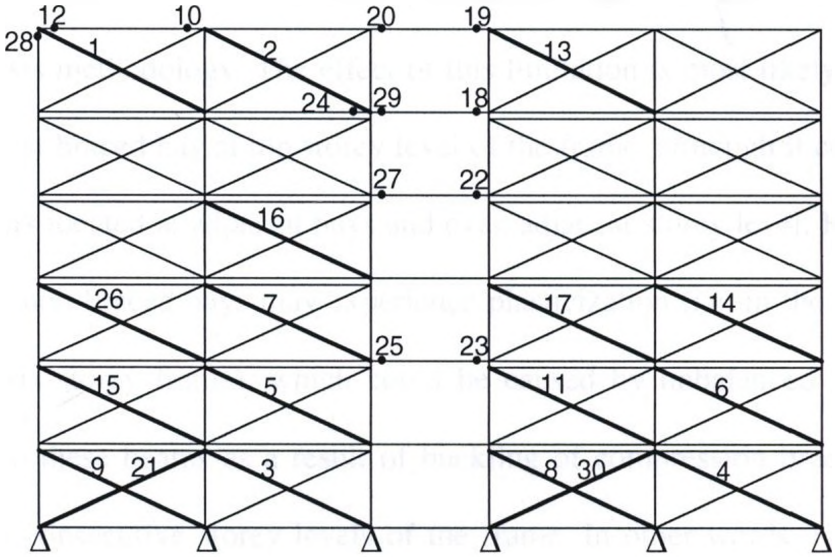

(a) Frame

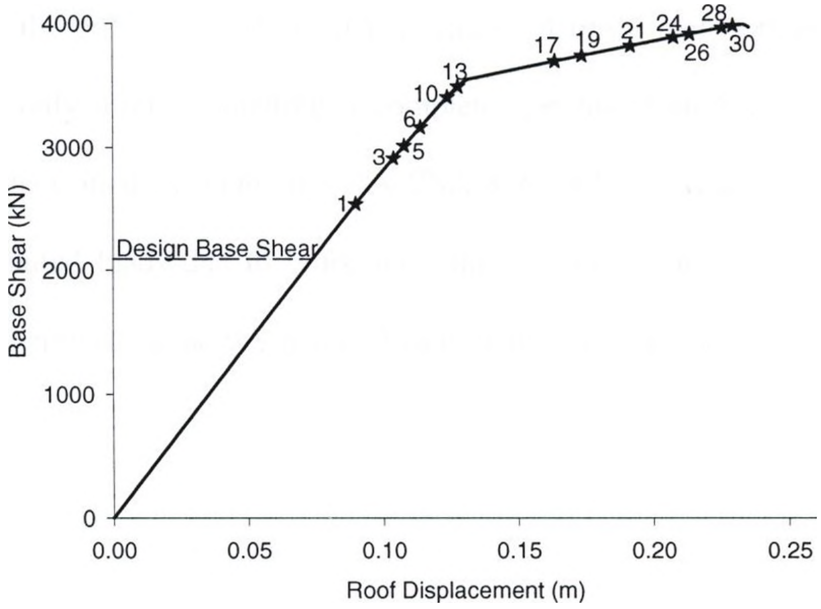

(b) Capacity curve

Figure 4.11. Sequence of Yielding/Buckling of the Six-storey MSB Braced Frame (Brace induced column actions by DS accumulation approach)

The formation of plastic hinges in some of the beams of non-braced bays of the frames may be a result of the load transfer mechanism, described above, which develops from the analysis methodology. The effect of this limitation is most likely present in the region of the first braced bay at top storey level of the frame, although it could be carried over to members located at adjacent bays and even adjacent storey level. However, some other beams in non-braced bays may experience plasticization (i.e. in the region of mid-height of the six-storey frame), which could be caused by unbalanced forces that are transferred onto these beams as a result of buckling of compression braces in different degrees at two consecutive storey levels of the frame. In other words, redistribution of forces to attain equilibrium between two consecutive storey levels after more compression braces buckle in one storey than the other may leave these beams with load magnitudes that have not been accounted for in their designs. This can only be identified and quantified if the order/sequence of plasticization of brace members is known. This will be possible only after conducting a complete non-linear analysis to failure. The requirements of the Canadian standard, CAN/CSA-S16.1-01 (CSA, 2001) to consider the effect of redistributed loads due to brace buckling or yielding in the determination of beam actions is therefore vague when such beam members in non-braced bays are under consideration.

4.5.2 Overstrength for MSB Frames

Primarily, overstrength is a direct consequence of redundancies resulting from member and system/structural configurations and design simplifications. Generally, frame members are designed for critical loading conditions and the resulting sections are applied to other non-critically loaded members in the frame, which may add to the redundancy. Redistribution of internal forces due to redundancy in the braced system is another source of extra strength. Also, some requirements of the design code for ductility may result in some redundancy in the braced system. The main simplification in the design procedure for concentrically braced frames is related to the treatment of buckling and post-buckling behaviour of compression brace members. For tension-compression braced frames, overstrength arises once buckling of the compression braces has occurred and additional force is required to develop yielding in the tension braces. The redistribution of lateral force from a compression brace to a tension brace allows such structures to carry significantly higher lateral force than at compression buckling.

For ductile concentrically braced frames, the overstrength is generally identified as the difference between the strength corresponding to the first buckling of any compression brace and the ultimate lateral strength of the structure. The first brace buckling strength would coincide with the design strength of the structure if internal force redistribution in the inelastic range was the only source of overstrength. Figures 4.7b, 4.8b, 4.9b, 4.10b and 4.11b indicate that, in all of the MSB braced frames considered in the study, the base shear force, V, which corresponds to the first buckling of a compression brace member, is higher than the design base shear. Since nominal material

properties were utilised in this study, the only dependable sources of extra strength were therefore caused by redundancies in the bracing system (i.e. design and system redundancies) and brace member ductility capacities. The overstrength factor (R_o=1.3) provided by the Canadian NBCC standard (NBCC, 2005) accounts also for the difference between actual and nominal material properties. In this code, the overstrength factor accounting for the braced system's ability to mobilise full capacity before collapse (i.e. due to redistribution of internal forces), R_{mech}, is conservatively set to unity in view of the strength degradation of compression braces under reversed cyclic loading (Mitchell et al., 2003). Thus, experimental investigations that yielded overstrength factor of the order of 2.4 – 2.8 for regular six-storey braced steel frame (Uang and Bertero, 1986; Whitaker et al., 1989) as well as an analytical study that estimated overstrength factor due to internal force redistribution in the range of 1.5 to 2.1 for ten-storey X-braced frames under different design earthquake forces (Rahgozar and Humar, 1998) both suggest that the Canadian code's provision is rather conservative.

The capacity envelopes obtained from the pushover analyses were used to estimate the reserve strength ratio. The base shear force versus lateral roof drift for each of the MSB frames (six-, four-, and two-storey) in which the SRSS accumulation approach was used to determine brace-induced column actions are depicted in Figure 4.12. The roof drift is defined as the ratio of the top displacement to the height of the MSB frame. It is observed that, in all these frames, failure was caused by the formation of a collapse mechanism when the frames were no longer able to carry additional loads.

Table 4.3 contains a summary of the calculated overstrength factors, obtained from the ratio of the ultimate load to the design load. The results indicate that lateral forces 90 – 150% greater than those considered during design are necessary to trigger failure of the frames. The overstrength factors for the six-, four-, and two-stories are respectively 1.9, 2.2 and 2.5, indicating that a decrease in height of the MSB resulted in an increase in overstrength. This variation of the reserve strength ratio with the height of the MSB is significant when compared to observations by Rahgozar and Humar (1998) that the height of ductile concentrically braced frames contributes very little or nothing at all to the frame's reserve strength. For example, if the MSB frame was decreased from four-storey to two-storey or from six-storey to four-storey, there was an increase of about 15% in overstrength. This observation is also not accounted for by the 2005 edition of the NBCC, which requires the use of the same overstrength factor irrespective of the height of the steel braced frame being designed.

Table 4.3. Overstrength Factor and Structural Ductility of MSB Braced Frames

Number of Stories	Overstrength Factor, R_0		Structural Ductility, μ	
	SRSS Approach	DS Approach	SRSS Approach	DS Approach
6	1.91	1.91	1.84	1.89
4	2.20	2.20	3.30	3.48
2	2.49		4.62	

Figure 4.13 depicts the base shear force versus lateral roof drift for the four-storey and six-storey MSB braced frames in which the DS accumulation approach was used to determine brace-induced column actions. It is observed from these figures and from Table 4.3 that, for the same frame height, overstrength of MSB resulting from the use of both the DS accumulation approach and the SRSS approach remains unchanged. This further suggests that overstrength in braced frames is more sensitive to the brace sectional properties than it is to the columns' as it results primarily from redistribution of lateral force from compression braces to tension braces. The reserve strength of a critical storey is also the global reserve strength of the frame. It has to be emphasised that the overstrength factors observed for the MSB braced frames above were obtained from the use of nominal material properties and the actual overstrength accounting for other sources identified in section 4.1 may be higher. Thus, the use of R_o given by the Canadian NBCC code (NBCC, 2005) appears to be conservative for the design of MSB braced frames.

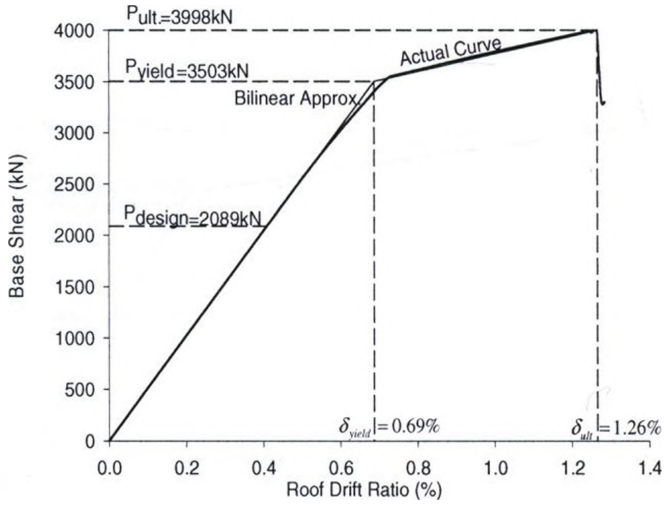

(a) Six-storey

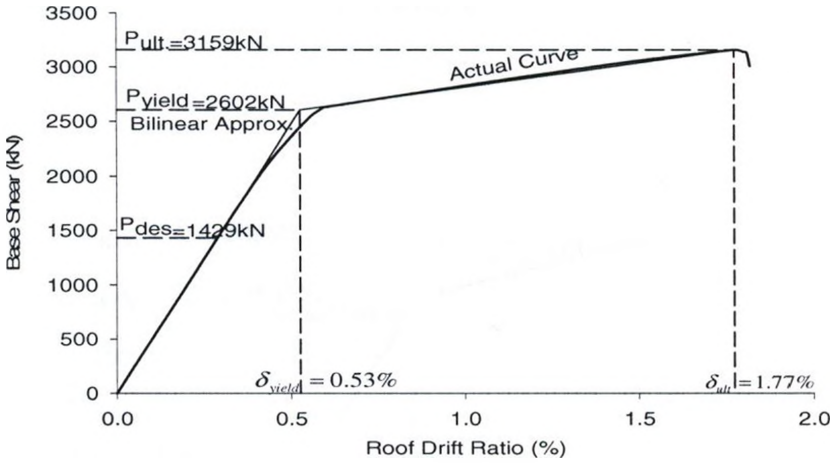

(b) Four-storey

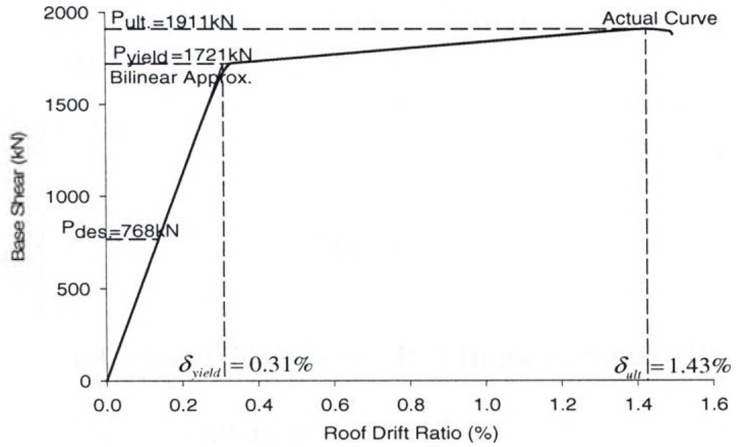

(c) Two-storey

Figure 4.12. Horizontal Capacity Curves of Selected MSB Braced Frames (Brace induced column actions by SRSS accumulation approach)

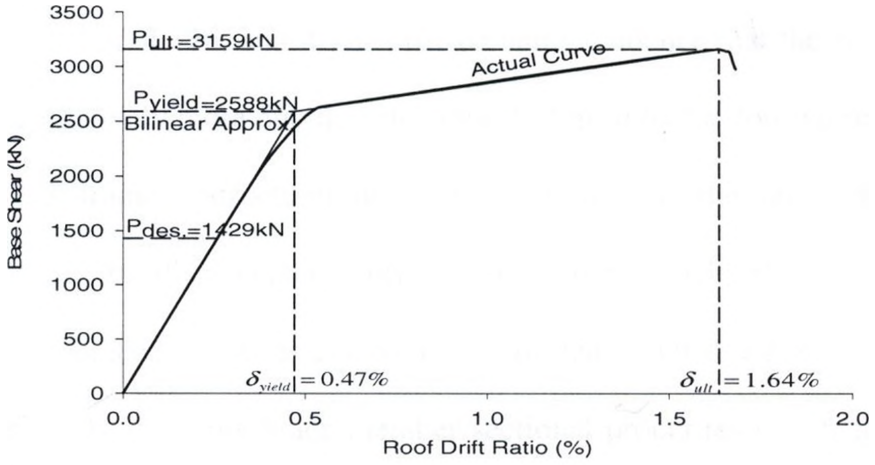

(a) 4-storey

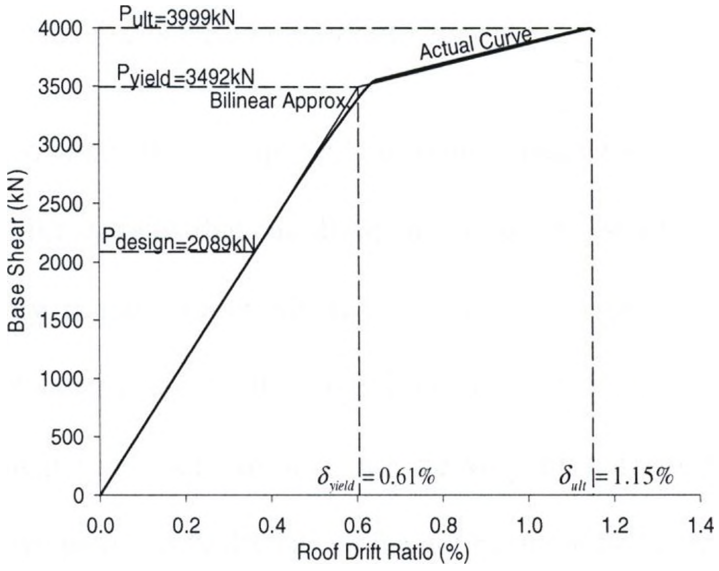

(b) 6-storey

Figure 4.13. Horizontal Capacity Curves of MSB Braced Frames (Brace induced column actions by DS accumulation approach)

4.5.3 Ductility of MSB Frames

Figures 4.12a, 4.12b, and 4.12c provide some evidence that the two-storey MSB frame shows a relatively more ductile behaviour, followed by the four-storey and then the six-storey MSB frames. Structural ductility is defined as the ratio of the ultimate structural drift to the displacement corresponding to the yield strength. Global yield displacement for braced frames is essentially controlled by buckling of bracing members which in turn depends on the brace member sectional properties (i.e. brace slenderness ratio and width-to-thickness ratio, b/t). The yield strength can be obtained by idealising the actual structural response curve by a bilinearly elasto-plastic curve, as shown in Figures 4.12 and 4.13, such that the total energy dissipation up to the point of ultimate deformation before collapse is the same for both curves.

It is known that this simplified response idealization described above is representative only for systems that can dissipate energy in a stable manner, especially in simple single storey frames. For multi-storey buildings, especially those that exhibit significant strength degradation, the definition of the yield deformation is more complicated and analytical methods may not be very reliable in estimating structural ductility. The behaviour of the MSB has so far not been studied extensively to draw any conclusion on its energy dissipation characteristics. Nonetheless, the ductility values given in Table 4.3 for the selected MSB braced frames were obtained by this simplified method for the purpose of assessing the effect of the height of MSB frames on ductility. For the three building frame heights considered in the study, there is a significant

increase in yield displacement with increasing building height as the slenderness of the brace sections decreases.

The maximum structural drift is controlled by the capacity of tension braces as well as the mechanics of internal force redistribution in the inelastic range from compression braces to tension braces. The latter is largely influenced by the behaviour of the entire braced frame, including the boundary or skeleton frame behaviour. The configuration of the MSB braced frame, particularly the vertical connections of different modular units, is more effective on the structural response at higher storey levels and this influences the behaviour of the entire frame. The rate of increase in the global maximum drift with frame height is much less than that of the global yield displacement. Displacement ductility of the frames ranges from 1.8 to 4.6. Ductility also increased slightly, in the range of 3-6%, for the four-storey and six-storey MSB braced frames when brace induced column actions are derived from the DS accumulation approach instead of the SRSS approach.

4.6 Conclusions

MSBs are fast evolving as an alternative to conventional onsite steel buildings but knowledge on their behaviour has been limited. There is also no record on the performance of MSB under lateral loading, and this further limits understanding of its behaviour and response under load. This chapter has highlighted some unique features of the MSB and has assessed the inelastic behaviour of its braced frames designed using

conventional methods. Canadian standards were used in the strength and ductility designs. The SRSS approach, widely used for accumulating brace induced forces in capacity design of columns for regular braced frames, as well as a Direct Summation approach were considered during the ductility design. The MSB braced frames were modeled and nonlinear pushover analyses were performed to study their response mechanism and to obtain their capacity curves. Overstrength factors of the selected MSB braced frame were evaluated. Also, structural ductility for these frames was estimated. The results were compared with code-specified overstrength values as well as experimentally and analytically determined values for regular braced frames.

The results showed that the use of SRSS approach in the determination of brace induced column actions in capacity design is not conservative for MSB braced frames due to the system's unique detailing requirements. The main assumption that governs the use of this approach might hold for this frame type but the specific connection details in the MSB frame seem to impose additional demand on columns located at lower levels of the frame. It is shown that the use of the direct summation (DS) approach in which vertical components of yielding/buckling brace forces are added directly to determine column actions for design may compensate this additional demand.

The analysis results revealed that MSB frames possess considerable overstrength due to the intrinsic redundancies in the frame system. Overstrength factors for the selected frame heights (i.e. two to six-storey MSB braced frames) range from 1.9 to 2.5 compared to 1.3 given by the Canadian code (NBCC, 2005) for regular braced frames. For the same MSB frame height, there was no difference in overstrength obtained from

the use of the SRSS and the DS accumulation approaches to determine brace-induced column actions. The use of the code's value for the design of MSB is, thus, shown to be conservative for the braced frame heights considered in this study.

The results also show significant displacement ductility in the MSB frame system, especially in the two-storey MSB braced frame. Furthermore, overstrength and ductility of MSB frames appear to depend on building height contrary to many seismic design codes prescribing a single value for all buildings with a specific structural system. The reserve strength ratio was found to increase with decrease in the height of the frame and ductility also increased with a reduction in frame height. The increase in ductility may be related to its definition, since the yield displacements appeared to increase with height at a greater rate that the ultimate displacements.

The analysis also revealed that care must be taken in the ductility design of beams in braced frame configuration with non-braced bays. For such beams in non-braced bays, the effect of redistributed loads due to brace buckling or yielding cannot be reliably accounted for in their designs unless the complete failure mechanism of the entire frame including sequence of plasticization is known. This can be possible only after a complete nonlinear analysis to failure is conducted. Assigning these beams with sections obtained from the capacity design of beams in braced bays may appear convenient but may lead to undesirable response of the entire frame since they could be more critical and govern the design of floor beams at any level.

4.7 References

Annan, C.D., Youssef, M.A. and El-Naggar, M.H. [2005] "Analytical investigation of semi-rigid floor beams connection in modular steel structures," *33rd Annual general conference of the Canadian Society for Civil Engineering, GC-352*, Toronto, Canada.

Annan, C.D., Youssef, M.A. and El-Naggar, M.H. [2008] "Effect of directly welded stringer-to-beam connections on the analysis and design of modular steel building floors," *Advances in Structural Engineering,* Accepted in October 2008.

ASCE [2005] "ASCE/SEI 7-05: Minimum design loads for buildings and other structures," *Standard Committee, American Society of Civil Engineers*, Virginia, USA.

Balendra, T. and Huang, X. [2003] "Overstrength and ductility factors for steel frames designed according to BS5950," *Journal of Structural Engineering, ASCE*, 129 (8), 1019-1035.

Bertero, V.V., Aktan, A.E., Charney, F.A. and Sause, R. [1984] "Earthquake simulation tests and associated studies of a 1/5th-scale model of a 7-storey R/C frame-wall test structure," *Report No. UCB/EERC-84/05, Earthquake Engineering Research Center*; Univ. of California, Berkeley, CA, USA.

Bruneau, M., Uang, C.M. and Whittaker, A. [1998] *Ductile design of steel structures,* McGraw-Hill, New York, NY, USA, 381-409.

CSA [2001] *Limit states design of steel structures; Standard CAN/CSAS16.1- 01*, Canadian Standards Association, Rexdale, Ontario, Canada.

Elnashai, A.S. and Mwafy, A.M. [2002] "Overstrength and force reduction factors of multistorey reinforced concrete buildings," *Struct. Design Tall Build.* 11, 329–351.

FEMA [2000] "Pre-standard and Commentary for the seismic rehabilitation of buildings," prepared by the American Society of Civil Engineers for the *Federal Emergency Management Agency*, Washington, D.C, (FEMA Publication No. 356).

IBC [2006] "International Building Code," *International Code Council, ICC*, http://www.iccsafe.org, USA.

Izzuddin, B.A. [1991] "Nonlinear dynamic analysis of framed structures'" *PhD Thesis, Imperial College*, University of London, London, UK.

Jain, A.K. and Goel, S.C. [1978] "Hysteresis models for steel members subjected to cyclic buckling or cyclic end moments and buckling – User's guide for DRAIN-2D: EL9 and EL10," *Report UMEE 78R6*, Department of Civil Engineering, University of Michigan, Ann Arbour, MI, USA.

Khatib, I.F., Mahin, S.A. and Pister, K.S. [1988] "Seismic behaviour of concentrically braced steel frames," *Report UCB/EERC-88/01, Earthquake Engineering Research Center*, University of California. Berkeley, CA, USA.

Kim, J. and Choi, H. [2005] "Response modification factors of chevron-braced frames'" *Engineering Structures*, 27, 285-300.

Mitchell, D. and Paultre, P. [1994] "Ductility and overstrength in seismic design of reinforced concrete structures," *Canadian Journal of Civil Engineering*, 21, 1049-1060.

Mitchell, D., Tremblay, R., Karacabeyli, E., Paultre, P., Saatcioglu, M. and Anderson, D. L. [2003] "Seismic force modification factors for the proposed 2005 edition of the National Building Code of Canada," *Canadian Journal of Civil Engineering*, 30, 308–327.

NBCC [2005] "National Building Code of Canada," *Institute for Research in Construction*, National Research Council of Canada, Ottawa, Ontario, Canada.

NZS4203 [1992] "Code of practice for general structural design and design loadings for buildings," *Standard Association of New Zealand,* Wellington, New Zealand.

Osteraas, J. and Krawinkler, H. [1989] "The Mexico earthquake of September 19, 1985. Behaviour of steel buildings," *Earthquake Spectra*, 5, 51-88.

Popov, E. P. and Black, R. G. [1981] "Steel struts under severe cyclic loadings," *Journal of the Structural Division*, ASCE, 107(ST9), 1857-1881.

Rahgozar, M.A. and Humar, J.L. [1998] "Accounting for overstrength in seismic design of steel structures," *Canadian Journal of Civil Engineering*, 25, 1–15.

Redwood, R. G. and Channagiri, V. S. [1991] "Earthquake resistant design of concentrically braced frames," *Canadian Journal of Civil Engineering*, 18(5), 839-850.

AS1170.4 [1993] "Minimum design loads on structures. 4: earthquake loads," *Standards Association of Australia*, North Sydney, NSW 2059, Australia.

SEAOC [1999] "Recommended lateral force requirements and commentary (SEAOC Blue Book)," *Structural Engineers Association of California, http://www.seaoc.org., Seismology Committee*, Sacramento/ San Francisco/ Los Angeles, USA.

SeismoSoft [2003] "SeismoStruct - A computer program for static and dynamic nonlinear analysis of framed structures," Available from *URL: http://www.seismosoft.com*.

Tremblay, R. [2002] "Inelastic seismic response of steel bracing members," *Journal of Constructional Steel Research*, 58(5–8), 665–701.

Uang, C. M. [1991] "Establishing R (or R_w) and C_d factors for building seismic provisions," *Journal of Structural Engineering,* ASCE, 117, 19–28.

Uang, C.M. and Bertero, V.V. [1986] "Earthquake simulation tests and associated studies of a 0.3-scale model of a 6-storey concentrically braced steel structure," *Report No. UCB/EERC-86/10, Earthquake Engineering Research Center*; Univ. of California, Berkeley, CA, USA.

Whitaker, A.S., Bertero, V.V., Alonso J. and Thompson C. [1989] "Earthquake simulator testing of steel plate added damping and stiffness elements," *Report No. UCB/EERC-89/02*, *Earthquake Engineering Research Centre*, University of California, Berkeley, CA, USA.

CHAPTER FIVE

SEISMIC VULNERABILITY ASSESSMENT OF MODULAR STEEL BUILDINGS[**]

5.1 Introduction

The seismic response of a structural building system depends on several factors including its configuration and dynamic characteristics, and the characteristics of the applied earthquake ground motion. It is imperative to simulate these factors as close to reality as possible in order to correctly predict seismic performance or vulnerability of a given structural system, using experimental and/or analytical techniques. Uncertainties and randomness inherent in many of these factors pose a serious challenge in the analysis procedure, especially when the response is largely inelastic. This requires incorporating these uncertainties in the modeling and analysis of the building frame as well as in the definition of structural demand and capacity. Dynamic inelastic analysis is the preferred choice for assessing the seismic capacity of building structures, since realistic and reliable estimates of both force and deformation demands at various locations of the structural system can be obtained.

Inelastic characteristics such as energy dissipation and strength degradation significantly affect structural vulnerability under seismic loading. For instance, building systems with large energy dissipation capacity are likely to undergo significantly greater inelastic deformations than systems with relatively limited energy dissipation capacity. In modern design codes, building systems are expected to deform well into the inelastic

[**] Annan, C.D., Youssef, M.A., and El Naggar, M.H. "Seismic vulnerability assessment of modular steel buildings," Journal of Earthquake Engineering, under review.

region under severe earthquakes. The forces resulting from the idealised elastic response spectra, representing site seismicity, are reduced by a force modification or response behaviour factor, R. This factor is also used to amplify the calculated elastic drift which provides an assessment of the potential seismic damage. Drift limits are generally based on the storey height of the building frame. The R factor is generally specified for a typical frame configuration and is partly attributed to system's ductility, and partly to the increase in strength beyond design strength as a result of strain hardening of steel, design assumptions, and internal force redistribution in the inelastic range of response. In the National Building Code of Canada (NBCC, 2005), the R factor is the product of the ductility-related force modification factor, R_d, and the overstrength-related force modification factor, R_o. Selecting appropriate values for these factors to estimate the seismic design base shear and to assess the structural drift demand is an essential step in the design process.

Modular steel building (MSB) systems differ significantly from their traditional onsite counterpart in terms of detailing requirements and method of construction. This building system has been typically used for one-to-six storey schools, apartments, hotels, correctional facilities, dormitories and other similar buildings where repetitive units are required. A detailed description of the MSB concept highlighting its advantages, application and unique detailing requirements has been provided in Chapters Two to Four and published by Annan et al. (2005, 2007, 2008a, 2009). The technique involves the design of buildings, which are built and finished at one location and transported to be used at another. The finished units/modules of a MSB are connected both horizontally and vertically on-site. Typical details of the horizontal and vertical connections of

different modular units have been described in Chapter Four and also presented by Annan et al. (2007, 2008b). Lateral stability of the entire MSB is achieved by adding diagonal braces. Currently, there have been no studies on the seismic performance of modular steel building braced systems and their design follows procedures for the design of regular steel braced frame. The conventional braced frame design provisions generally treats the various brace configurations the same.

The inelastic characteristics of the MSB system under severe ground motions may differ significantly from those of regular steel building systems. A typical plan and sections of a MSB is reproduced in Figure 5.1. In terms of structural configuration and detailing requirements, the following specific features distinguish the MSB braced frame from a regular steel braced frame: (1) the existence of ceiling beams in the MSB frame system may result in natural periods and mode shapes different from those of conventional systems; (2) in a typical modular steel frame, brace members do not intersect at a single working point which may lead to high seismic demands on the vertical connections of different units/modules; (3) the vertical connections (VC) typically involve welding one face of the columns of a lower and an upper modules leading to independent upper and lower rotations at the same joint. Column continuity is known to contribute effectively in preventing soft-storey response in multi-storey structures (Tremblay 2000). Discontinuity of columns coupled with a possible high seismic demand on the vertical connection of different modules could render inter-storey drifts critical in the design and performance of modular buildings under earthquake ground motions. Proper design of MSB systems is also essential as the system may inherently possess very limited capacity to redistribute internal forces between stories and

may be prone to early brace fractures leading to large storey drifts and excessive ductility demands during severe earthquakes.

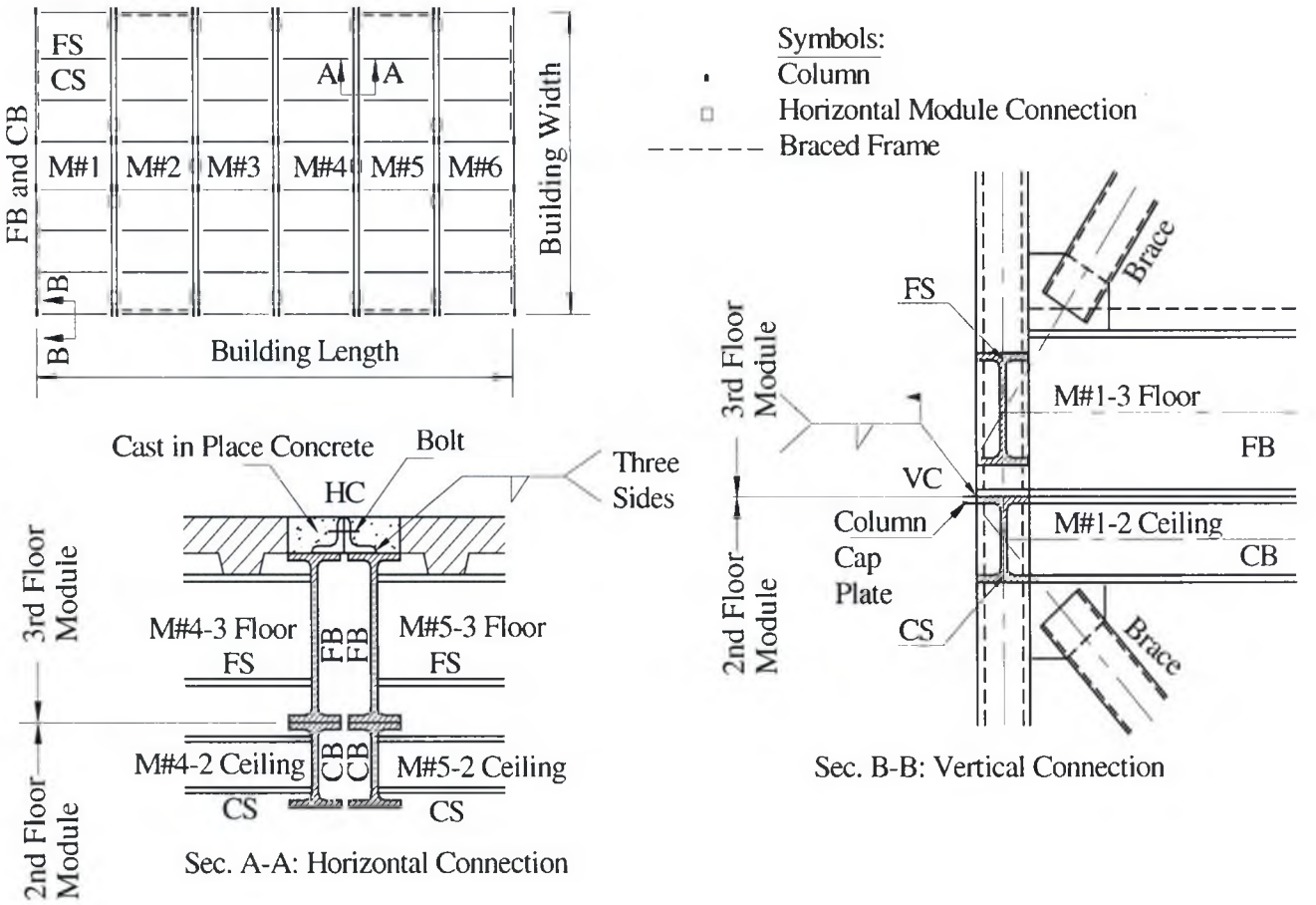

Figure 5.1. Plan and Sections of a Typical MSB

The present study focuses on quantifying seismic inelastic demands and capacities at the structure level for two-, four-, and six-storey MSB braced frames located in Vancouver and designed for moderate ductility according to Canadian standards. The

behaviour and response of these structures were examined by subjecting representative nonlinear analytical models of the frames to an ensemble of 20 earthquake ground motions scaled to different intensity levels. The spectral acceleration at the structure's fundamental mode period was used to scale each record, thus allowing a reduction in record-to-record variability. The corresponding peak ground acceleration (PGA) was also used as a seismic hazard representation for comparison, in order to determine the more consistent intensity measure for the MSB braced frame system.

Results of nonlinear static analysis (pushover analysis) conducted in Chapter Four (which has also been published by Annan et al., 2008a) were used to identify behavioural characteristics of the selected frames that cannot be obtained from time history analysis but are important in understanding and rationalizing the dynamic response. The effect of design philosophy on the nonlinear behaviour of MSB braced frames was studied, which led to the selection of the Direct Summation load accumulation approach for obtaining brace-induced column actions as the preferred method for selecting column member section for use in the time history analyses.

In the present study, the influence of ground motion intensities and number of stories on maximum inter-storey and global drift demands as well as on maximum inelastic force demands were assessed. The heightwise distribution and record-to-record variability of the maximum inter-storey drift demands were also studied. The drift behaviour provided an assessment of the ductility demands and capacity of the selected MSB braced frames.

5.2 Selection and Design of MSB system

The MSB braced frames defined and used for the nonlinear static analysis in Chapter Four were chosen for the nonlinear time history analysis of this study. Figure 5.2 reproduces the typical floor plan of the selected modular buildings and the elevation of the four-storey MSB braced frame. As described in the preceding chapter, each storey is made up of six modules comprising twelve individual dormitory rooms and a corridor. Floor framing of a typical modular unit is composed of two floor beams, eleven floor stringers, and a metal deck with a concrete composite floor. Similarly, the ceiling framing includes two ceiling beams and a number of ceiling stringers. The composite floor within a modular unit was assumed to be rigid in-plane. The corridor on each floor runs through the middle portion of all the modular units, between the two interior columns. The corridors are constructed without ceiling beams to allow mechanical and electrical ducts to run along them.

The lateral response of the buildings in the N-S direction is considered in this study. The lateral force resisting system in this direction is composed of two identical external X-braced frames as shown by the dashed lines within units M#1 and M#6 in Figure 5.2. The combined behaviour of the composite floor of the modules and the horizontal connections between these modules is designed to be sufficiently rigid to transfer lateral loads between the modular floor units and to the braced frames. In these frames, the braces are connected to the floor beam-to-column and ceiling beam-to-column joints in each storey/module. Brace connections to the modular framing system are composed of gusset plates welded to the braces.

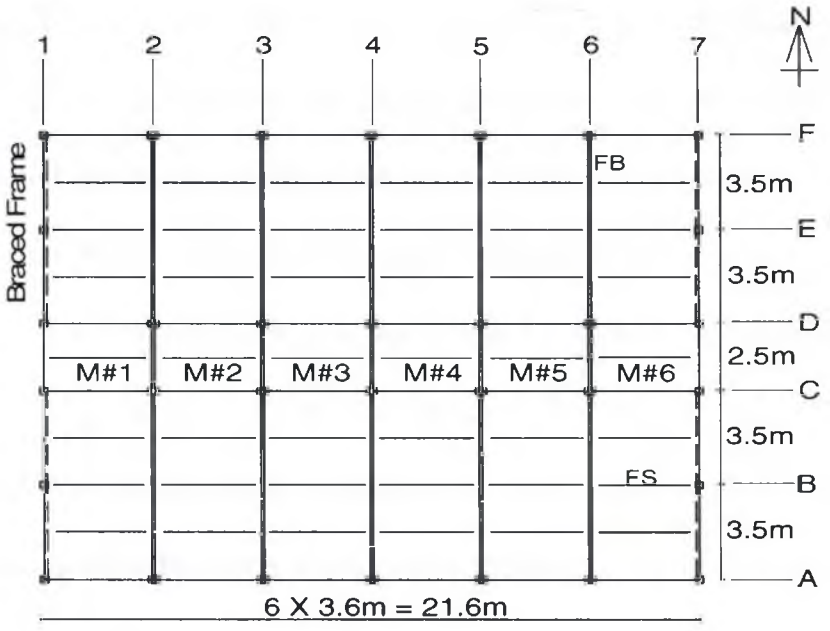

(a)

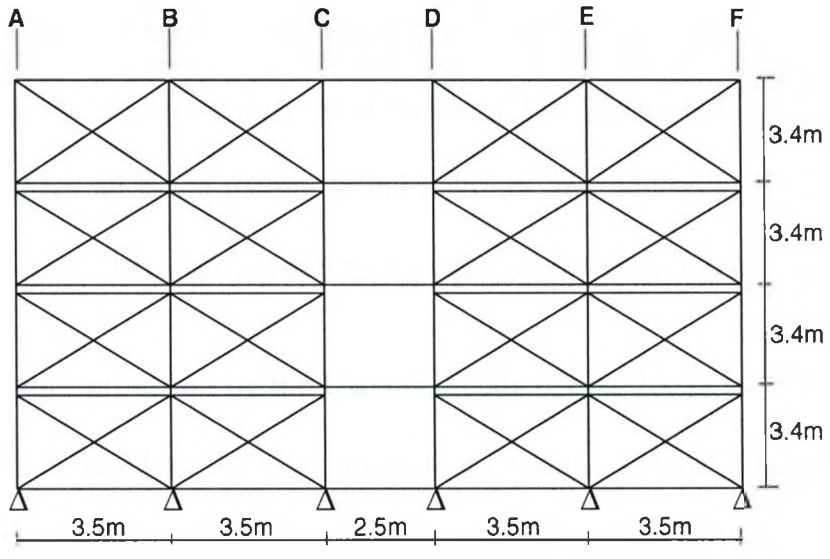

(b)

Figure 5.2. Four-storey Modular Steel Braced Frame (a) Floor plan (b) Elevation (centerline 1 or 7)

The design of the selected MSB system has been described extensively in Chapter Four and summarised below. When designing the MSB braced frame, frame members were initially sized on the basis of traditional strength and stiffness design criteria for the specified imposed gravity and earthquake actions. The section sizes of braces, columns, floor beams, roof beams, and ceiling beams obtained from the strength design were evaluated and modified, as necessary, according to ductility design requirements and capacity design procedures. Both the strength and ductility designs were based on the Canadian standard, CAN/CSA-S16.1-01 (CSA, 2001). The live and seismic loadings used for the design were based on the National Building Code of Canada (NBCC, 2005). The location of the MSBs was selected as Vancouver (Western Canada). The buildings were assumed to be founded on a very dense soil with a shear wave average velocity range between 360 m/s and 760 m/s. The design base shear values of the frames were calculated assuming moderate ductility with an overstrength-related modification factor of 1.3 and a ductility-related modification factor of 3.0. Square hollow structural section (HSS) were used for all brace members and columns and wide flange W shape sections were specified for the floor, ceiling and roof beams, as per common practice.

The ductility provision by the Canadian code (CSA, 2001) for the design of steel braced structures is based on the assumption that columns, beams and brace connections within the structure must be able to resist the resulting induced forces when braces reach their ultimate strength. Floor, ceiling and roof beam members are thus designed as beam-columns, with the design moment resulting from tributary gravity loads and the axial compression coming from unequal capacity of braces in tension and compression, considering the horizontal equilibrium of brace-induced forces at each beam end. The

brace end connections are designed to support the full yielding brace resistance, given by the brace nominal tensile strength, A_gF_y. The design of the vertical welded connections of units of the MSB is based on traditional elastic method and it accounts for the eccentric loading resulting from partial welding of all connected columns. The column members obtained from the strength design were also reviewed to meet ductility requirements. Columns are proportioned to resist the gravity loads together with the forces induced by the brace loads.

The direct summation (DS) and the Square Root of the Sum of the Squares (SRSS) force accumulation approaches (Khatib et al., 1988; Redwood and Channagiri, 1991) have been used to estimate brace induced column actions for design. The use of the SRSS approach is justified by the assumption that in a multi-storey braced frame, all bracing members would not reach their ultimate capacities simultaneously. This assumption has been found to be reasonably conservative for regular braced frames. For MSB braced frames, however, it was observed from the results of the nonlinear static analysis conducted in Chapter Four that the DS approach would yield the desired response. Thus, only column sections resulting from the use of the DS force accumulation approach were utilised in the dynamic time history analysis.

5.3 Analytical Model of MSB Braced Frames

Nonlinear analysis requires modeling of the complete load-deformation (or moment- curvature) characteristics of each component of the structure. Generally, a model that represents the essential characteristics of all basic elements is intrinsic to understanding the response of the structure. In this study, one of the two identical external braced frames in each building was modeled as a two-dimensional frame supporting half the building mass. A basic centerline model of the bare MSB braced frame was used with floor, ceiling and roof beams, columns and braces extending from centerline to centerline. Each floor was assumed to behave as a rigid plate. The mass representation was via lumped mass matrices. The damping exhibited by the structure was modeled using the traditional Rayleigh damping model proportional to the initial stiffness matrix. The commonly used householder QR algorithm was utilised for the eigenvalue analysis to compute the natural frequencies and mode shapes of free vibration.

An elasto-plastic material model for steel was employed with a yield stress of 350 N/mm^2, and an elastic modulus of 200 kN/mm^2. An inelastic steel beam-column frame element was used to represent column members in all modules. A one component beam element was used for all beam representations. These elements account for geometric and material non-linearities. The inelastic behaviour of both the beam and the beam-column elements follows the concept of the Giberson one-component model (Sharpe, 1974), which has a plastic hinge possible at one or both ends of the elastic central length of the member.

During a strong earthquake, a brace member in a concentrically braced frame will be subjected to large inelastic deformations in cyclic tension beyond yield and compression into the post-buckling range. The post-elastic compression is accompanied by significant degradation in compressive resistance after a few cycles of loading (Jain and Goel, 1978). The Remennikov Steel Brace Member Hysteresis (Remmennikov and Walpole, 1997) was used to represent all bracing members. This hysteresis model represents the out-of-plane buckling of the steel brace member but essentially captures the inelastic behaviour under alternate axial tension and compression. The member only permits this hysteresis in the axial component; it is assumed generally to be bi-linear in flexure.

Figure 5.3 shows a schematic representation of the analytical model of vertical connection of modular units. This model was developed and validated in the experimental studies in Chapter Three. Rigid end blocks (shown by bold lines J1-J2, J2-J3, J2-J4, J5-J6, J6-J7, J6-J8) were provided at each end of frame members to capture the rigidity of connection regions. The short column segment between the bottom flange of the floor beam and top flange of the ceiling beam was represented by a vertical inelastic beam-column frame element, M1, whose height represents the clearance between the two beams. This vertical element was pinned internally into a common joint with the upper unit column, J4, such that an independent upper and lower module rotation would develop at this common joint.

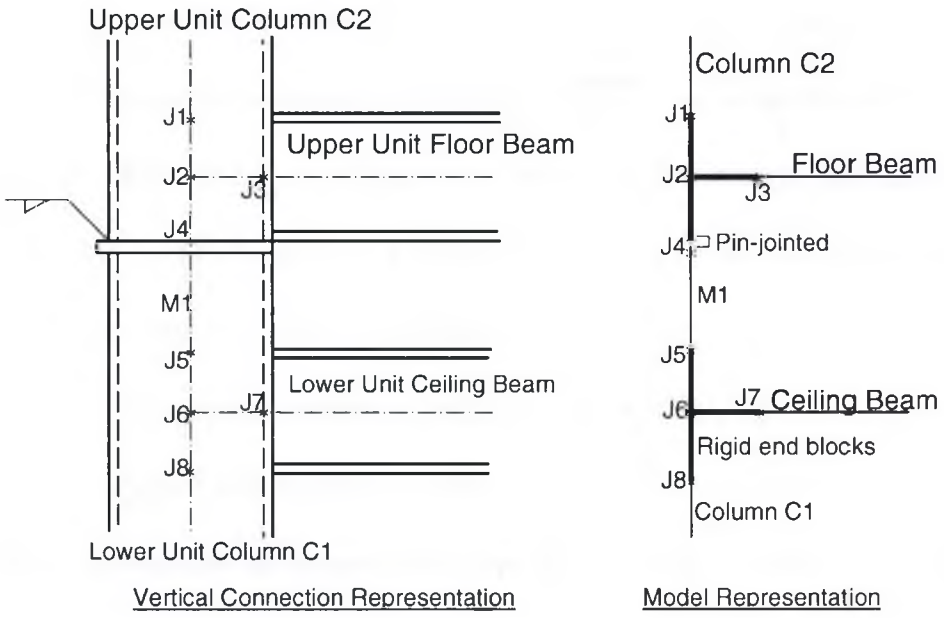

Figure 5.3. Model of Vertical Connection of Modular Units of MSB Braced Frame

5.4 Selection of Ground Motion Records and Analysis Characteristics

Most seismic design codes and recommendations specify seismic hazard in terms of a single intensity measure such as the peak ground acceleration (PGA) or a spectral ordinate at a given period. In the NBCC (2005), the seismic hazard is described by spectral-acceleration values at periods of 0.2, 0.5, 1.0 and 2.0 seconds. Spectral acceleration is a measure of ground motion that takes into account the sustained shaking energy at a specific period. For the selected site of the selected modular buildings, the 2% in 50 year intensities of ground motion (expressed as spectral accelerations, $S_a(T)$, that correspond to fundamental periods of the building frames) were evaluated as 0.96g, 0.85g, and 0.75g for the two-, four-, and six-storey frames respectively.

It is well known that different ground motion records scaled to the same PGA do not induce the same level of response in, and do not cause the same amount of damage to a given structure. This is due to variation in other seismic hazard parameters such as frequency content, event duration and effective number of loading cycles. Hence, the response obtained using one ground motion may not provide sufficient confidence that the structure will yield similar response if subjected to another ground motion record with the same PGA. Shome and Cornell (1999) showed that sufficient accuracy can be obtained in the estimation of seismic demands of mid-rise buildings if ten to twenty ground motion records are considered. FEMA (2000a) recommends selecting a suite of 10 to 20 accelerograms representative of the site and hazard level to achieve the collapse prevention level.

Vamvatsikos and Cornell (2004) compiled and used a scenario earthquake comprising of 20 historical ground motion records from three earthquakes (i.e. 1979 Imperial Valley; 1987 Superstition Hills; and 1989 Loma Prieta) to analyse mid-rise buildings. The records selected belong to a bin of relatively large magnitudes, 6.5 – 6.9, and moderate epicentral distances in the range of 15-32 km. All of the accelerograms were recorded on firm soil and bear no marks of directivity. This study adopted the same ensemble of earthquake ground motion records; they were obtained from the PEER strong motion database and their characteristics are listed in Table 5.1. Figure 5.4 presents the 5% damped acceleration response spectra for the selected ground motion records, together with the uniform hazard spectrum (shown by the dark bold line) given in the NBCC (2005) for the selected site of the MSB considered. The response spectra were developed by the Newmark (1959) numerical integration scheme.

The seismic inelastic demands of the selected building systems were determined using the incremental dynamic analysis (IDA) procedure. IDA was developed by Luco and Cornell (1998) and has been described in detail in Vamvatsikos and Cornell (2002) and Yun et al. (2002). This analysis technique has also been incorporated in a modern seismic design recommendation (FEMA, 2000a). The IDA requires a series of nonlinear response history analyses of a modeled structure for an ensemble of ground motions, each scaled to many intensity levels. Intensity levels are selected to cover the entire range of structural response, from elastic behaviour through yielding to dynamic instability (or until a limit state "failure" occurs). From the results of these multiple analyses, statistics on the variation of demand and capacity with ground motion character can be evaluated to summarise the results.

Estimating seismic demand with sufficient accuracy requires selection of efficient analysis characteristics. Shome et al. (1998) observed that by scaling ground motion records to the target spectral acceleration at the fundamental-mode period of a structure, seismic demands at this intensity can be efficiently estimated. The spectral acceleration at 5% damping, $S_a(T_1, 5\%)$, was primarily used as the intensity measure (IM) in this study. The simple stepping algorithm (Vamvatsikos and Cornell, 2002) was used to scale the ground motion records. Demand distribution with Peak Ground Acceleration, PGA, was also studied in order to compare the dispersion of response parameters, and consequently to assess the most efficient intensity measure parameter for the MSB system within the entire response spectrum.

Table 5.1. Selected Earthquake Ground Motion Records

No.	Event	Year	Record station	Φ[1]	M*[2]	R*[3] (km)	PGA (g)	PGV (m/s)	a/v
1	Imperial Valley	1979	Plaster City	45	6.5	31.7	0.042	0.032	1.31
2	Imperial Valley	1979	Plaster City	135	6.5	31.7	0.057	0.054	1.06
3	Imperial Valley	1979	Westmoreland Fire Sta.	90	6.5	15.1	0.074	0.212	0.35
4	Imperial Valley	1979	Westmoreland Fire Sta.	180	6.5	15.1	0.110	0.219	0.50
5	Imperial Valley	1979	El Centro Array #13	140	6.5	21.9	0.117	0.147	0.80
6	Imperial Valley	1979	El Centro Array #13	230	6.5	21.9	0.139	0.130	1.07
7	Loma Prieta	1989	Agnews State Hospital	90	6.9	28.2	0.159	0.176	0.91
8	Loma Prieta	1989	Coyote Lake Dam	285	6.5	22.3	0.179	0.226	0.79
9	Superstition Hill	1987	Wildlife Liquefaction Array	90	6.7	24.4	0.180	0.299	0.60
10	Superstition Hill	1987	Wildlife Liquefaction Array	360	6.7	24.4	0.200	0.345	0.58
11	Loma Prieta	1989	Sunnyvale Colton Ave	270	6.9	28.8	0.207	0.373	0.56
12	Loma Prieta	1989	Sunnyvale Colton Ave	360	6.9	28.8	0.209	0.360	0.58
13	Loma Prieta	1989	Anderson Dam	270	6.9	21.4	0.244	0.203	1.20
14	Imperial Valley	1979	Chihuahua	282	6.5	28.7	0.254	0.301	0.84
15	Loma Prieta	1989	Hollister Diff. Array	165	6.9	25.8	0.269	0.439	0.61
16	Loma Prieta	1989	Hollister Diff. Array	255	6.9	25.8	0.279	0.356	0.78
17	Imperial Valley	1979	Cucapah	85	6.9	23.6	0.309	0.363	0.85
18	Loma Prieta	1989	WAHO	0	6.9	16.9	0.370	0.272	1.36
19	Loma Prieta	1989	Holister South &Pine	0	6.9	28.8	0.371	0.624	0.59
20	Loma Prieta	1989	WAHO	90	6.9	16.9	0.638	0.379	1.68

[1] Component, [2] Moment Magnitudes, [3] Closest Distances to Fault Rupture

Source: PEER Strong Motion Database, http://peer.berkeley.edu/svbin

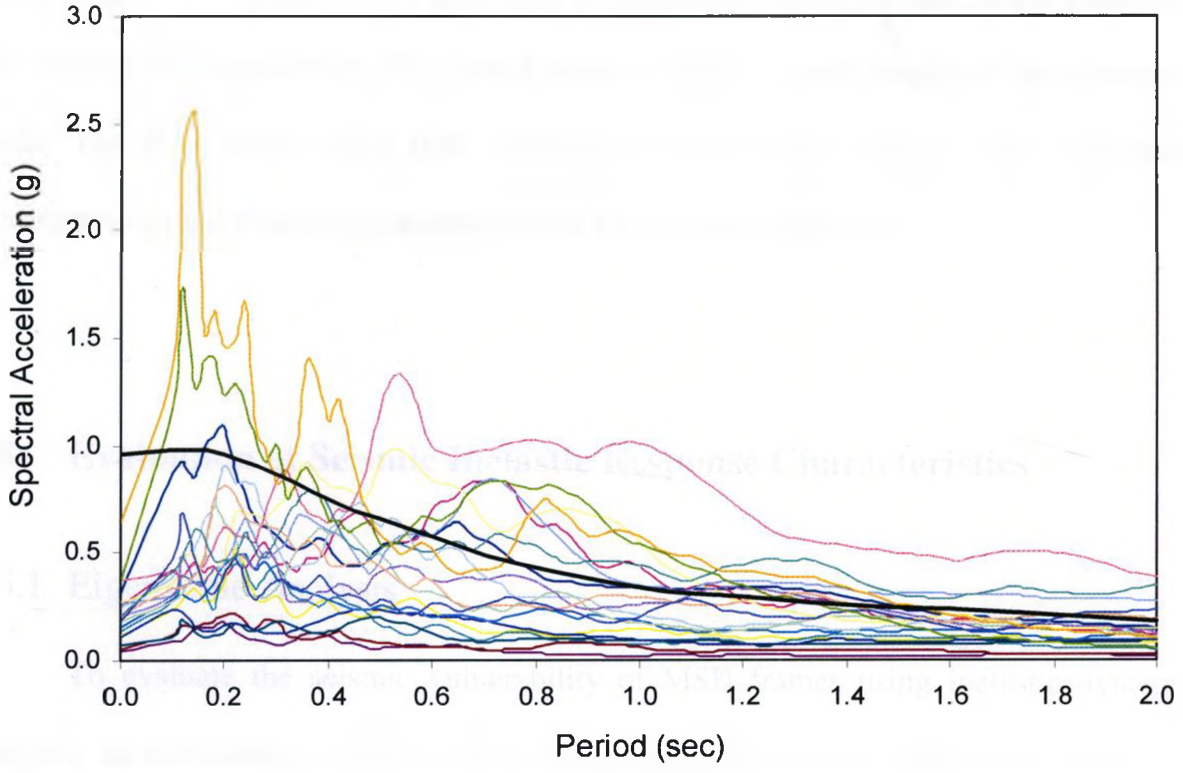

Figure 5.4. 5% Damped Acceleration Response Spectra for Selected Ground Motions

Seismic behaviour can be measured using fracture life, energy dissipation capacity, maximum drift and ductility capacity, etc. Maximum inter-storey drift is often used as a primary damage intensity parameter in the vulnerability assessment of moment resisting frames but have also been used to characterise global dynamic response of ductile concentrically braced frame structures (Sabelli, 2001; Uriz and Mahin, 2004). The maximum (over all stories) peak inter-storey drift ratio (θ_{max}), and peak roof drift ratio (θ_{roof}) were selected as global Demand Parameters (DP) to study the structural response of the modeled frames during the ground motions duration. The inter-storey drift ratio

was computed as the difference in displacements of adjacent stories divided by the inter-storey height, and the peak roof drift ratio was obtained from the ratio of the peak roof drift during the duration of the ground motion to the overall height of the structural frame. The IDA curves were then obtained for each record from a plot of demand parameters against their corresponding intensity measure parameters.

5.5 Evaluation of Seismic Inelastic Response Characteristics

5.5.1 Eigenvalue Analysis

To evaluate the seismic vulnerability of MSB frames using inelastic dynamic analyses, an assessment of their dynamic response characteristics is necessary. Modal or eigenvalue analyses were conducted for the two-, four- and six-storey MSB braced frames to find the frequencies and mode shapes of free vibration. Essentially, the behaviour of these frames was dominated by their first-mode but there was some sensitivity to higher modes. Table 5.2 shows the first and second-mode periods and mass participation factors for the selected frames. It also shows the empirical estimate of design periods based on the NBCC (2005). Shorter empirical design periods would result in the provision of greater base shear capacities to the structures, which is the case for the four- and six-storey MSB frames.

Table 5.2: Dynamic Characteristics of Selected MSB Braced Frames

Dynamic characteristics		MSB Braced frame		
		2-storey	4-storey	6-storey
Period (sec)	NBCC design	0.21	0.35	0.48
	1st mode	0.20	0.42	0.61
	2nd mode	0.08	0.16	0.21
Mass participation factor (%)	1st mode	94	81	77
	2nd mode	5	15	17

5.5.2 Results of Incremental Dynamic Analysis

Results of a total of about 2500 nonlinear time history analyses, conducted on the three nonlinear analytical models of the MSB braced frame for the selected ground motion records, were plotted as IDA curves and are shown in Figures 5.5 to 5.8. In each plot, a structural Demand Parameter (DP) resulting from a scaled ground motion record of a known Intensity Measure (IM) provided a single point. Similar responses which correspond to different values of IM for the same ground motion record provided other points that joined together to produce a spline fit of the IDA curve for that record and the selected frame model. Thus, for the three selected MSB braced frames under the suite of 20 ground motion records, a total of 60 IDA curves were generated for a specified IM versus DP. In Figures 5.5 and 5.6, the ground motion IM was the 5% damped spectral acceleration of the scaled ground motion at the fundamental mode period of the structure, $S_a(T_1, 5\%)$. The engineering DP in these plots were, respectively, the maximum (over all

stories) peak inter-storey drift ratio, θ_{max}, and the peak roof drift ratio, θ_{roof}, all expressed as a percentage. These demand parameters were also plotted against the corresponding PGA of the scaled ground motion records in Figures 5.7 and 5.8, respectively. These IM versus DP combinations used in this study resulted in an overall total of 240 IDA curves.

The variety and dispersion of the responses obtained for different earthquake ground motions and the same frame model, and also for different frame models and the same ground motion, as shown by these curves is remarkable. All curves, however, exhibited a distinct linear elastic behaviour before the first sign of significant nonlinearity occurred. Comparing Figures 5.5 and 5.6 against Figures 5.7 and 5.8 it is observed in the linear elastic response range that, the $S_a(T_1, 5\%)$ is a more consistent intensity measure than the PGA. The elastic 'stiffness' (defined here as the ratio of the intensity measure to the demand parameter in the linear elastic range of response) varies from record to record when the PGA was used as the intensity measure (Figures 5.7 and 5.8). On the other hand, the $S_a(T_1, 5\%)$ provided almost the same elastic 'stiffness' across records. Smaller dispersion of the demand parameter for a given intensity measure implies that an efficient prediction of demand can be made with a smaller sample of records and hence a fewer non-linear time history analyses.

Based on the above observation, it can be inferred that the $S_a(T_1, 5\%)$ is a more suitable intensity measure for the MSB braced frames and will subsequently be adopted as the primary intensity measure in the inelastic demand and capacity assessment of the selected frames. It can also be observed in the linear elastic range of response that, the dispersion across records is smaller in the Two-storey MSB braced frame than the Six-storey frame because the former exhibits more resemblance to a SDOF system by the

dominance of its first mode. The magnitude of the elastic 'stiffness' is dependent on the period of the structure. Based on the plots of $S_a(T_1, 5\%)$ versus θ_{max}, the average elastic 'stiffness' was estimated as 4.0, 1.8, and 1.25 (in units of g over %) for the Two-, Four-, and Six-storey MSB braced frames, respectively. For all the three selected frames, the first significant sign of nonlinearity occurred at θ_{max} of about 0.33%.

In the inelastic range of response, the IDA curves are generally dissimilar, some displaying a softening behaviour with a gradual degradation towards collapse and others displaying a weaving behaviour indicative of excessive 'hardening' and 'softening' of the structure. Generally, these curves indicate a non-monotonic relation between demand parameters and intensity measures as discussed below.

The demand parameter by definition is non-differentiable. It contains absolute values of maximum responses of the time history analyses. These maxima may occur at different time instants. In addition, scaling of the records, as well as the pattern and timing of the ground motion excitation may alter the properties of the structure as it is subjected to different ground motion intensity levels at different times. At a lower intensity, the frame may deform significantly in one direction due to a strong pulse occurring at a later stage of the ground motion record. If the ground motion intensity level of the same record is increased, an earlier pulse may be strong enough to deform the frame in the opposite direction and this may change its dynamic characteristics and behaviour, and may protect the structure from the effects of the later stronger pulse. Inelastic drifts may also occur disproportionately in one lateral direction depending on the characteristics of the excitation and asymmetry between the tensile capacity and buckling resistance of the braces.

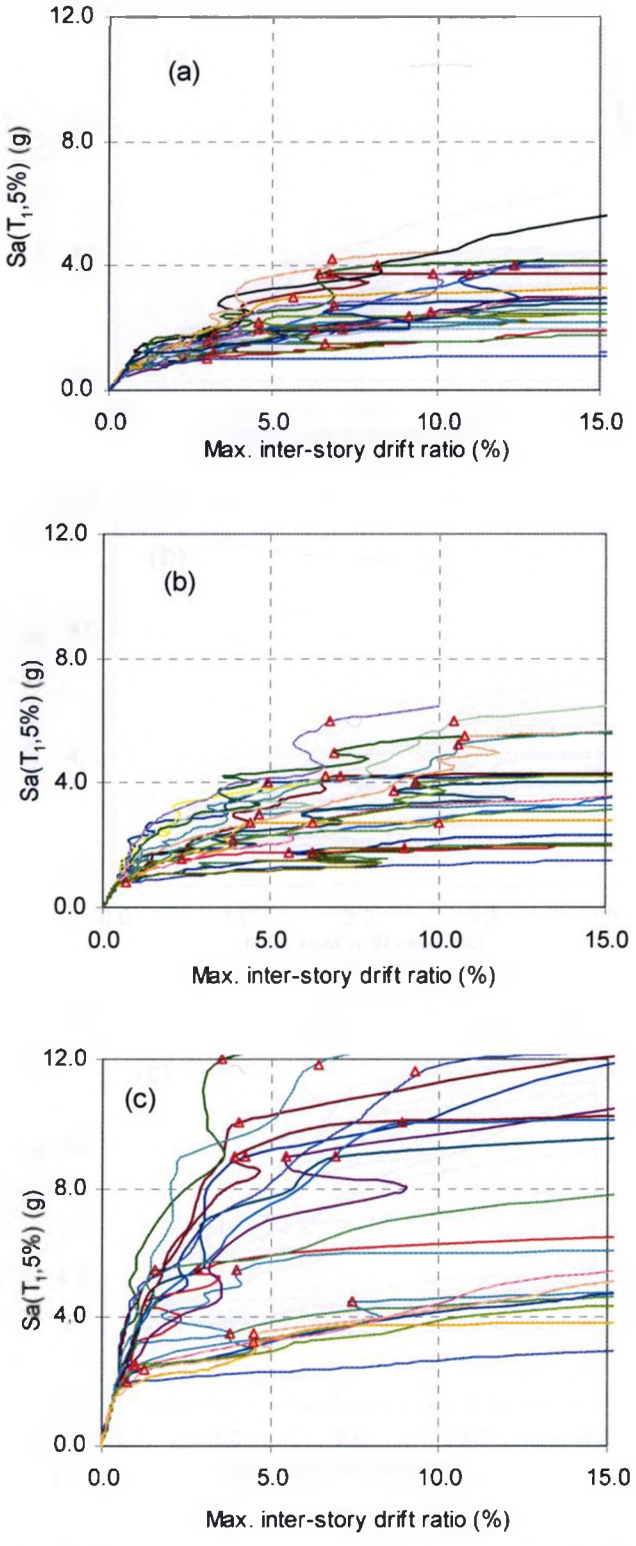

Figure 5.5. IDA Curves of 'first mode' Spectral Acceleration, $S_a(T_1, 5\%)$, plotted against Maximum Inter-storey Drift Ratio, θ_{max}, for (a) Six-storey (b) Four-storey (c) Two-storey MSB Braced Frames.

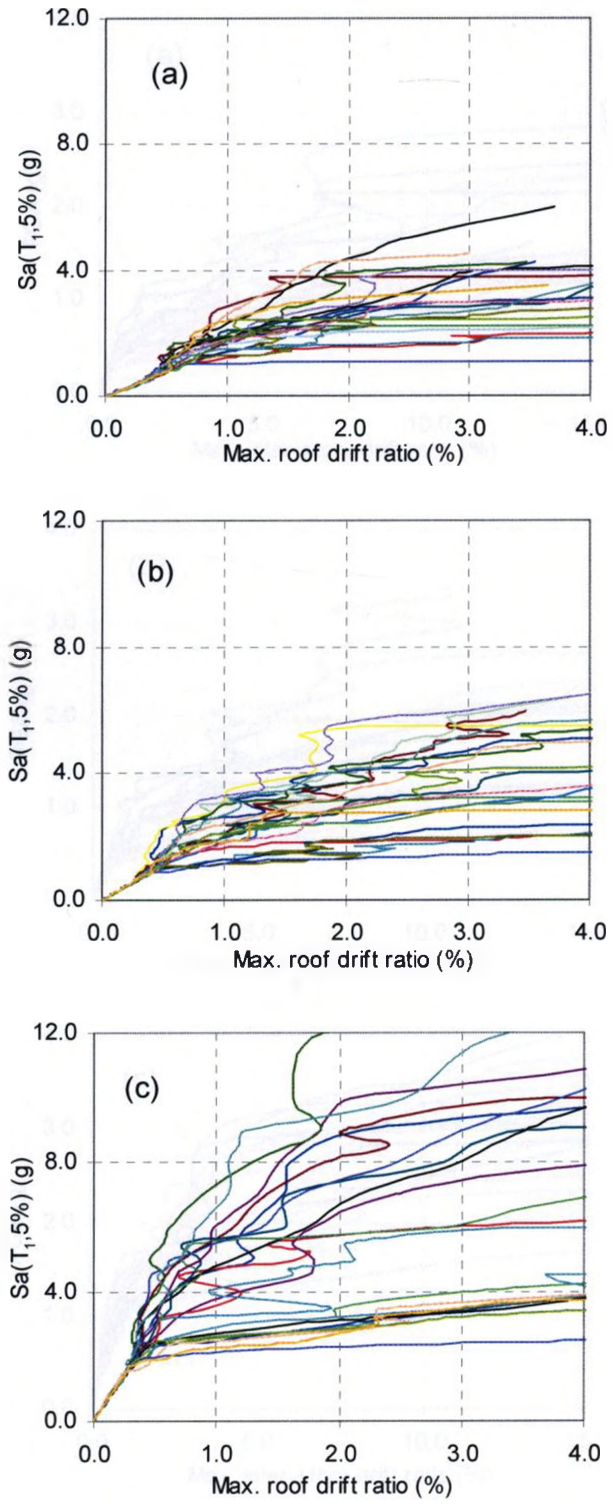

Figure 5.6. IDA Curves of 'first mode' Spectral Acceleration, $S_a(T_1, 5\%)$, plotted against Peak Roof Drift Ratio, θ_{roof}, for (a) Six-storey (b) Four-storey (c) Two-storey MSB Braced Frames.

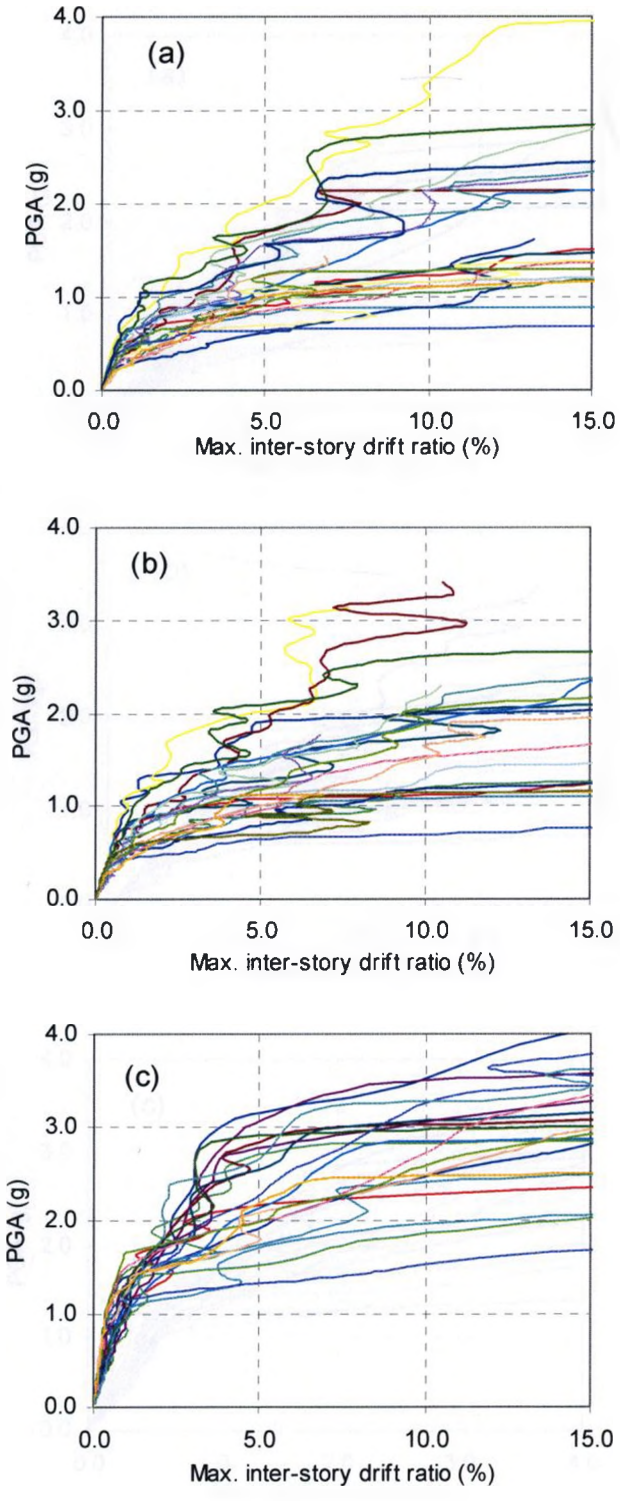

Figure 5.7. IDA Curves of Peak Ground Acceleration, PGA, plotted against Maximum Inter-storey Drift Ratio, θ_{max}, for (a) Six-storey (b) Four-storey (c) two-storey MSB Braced Frames.

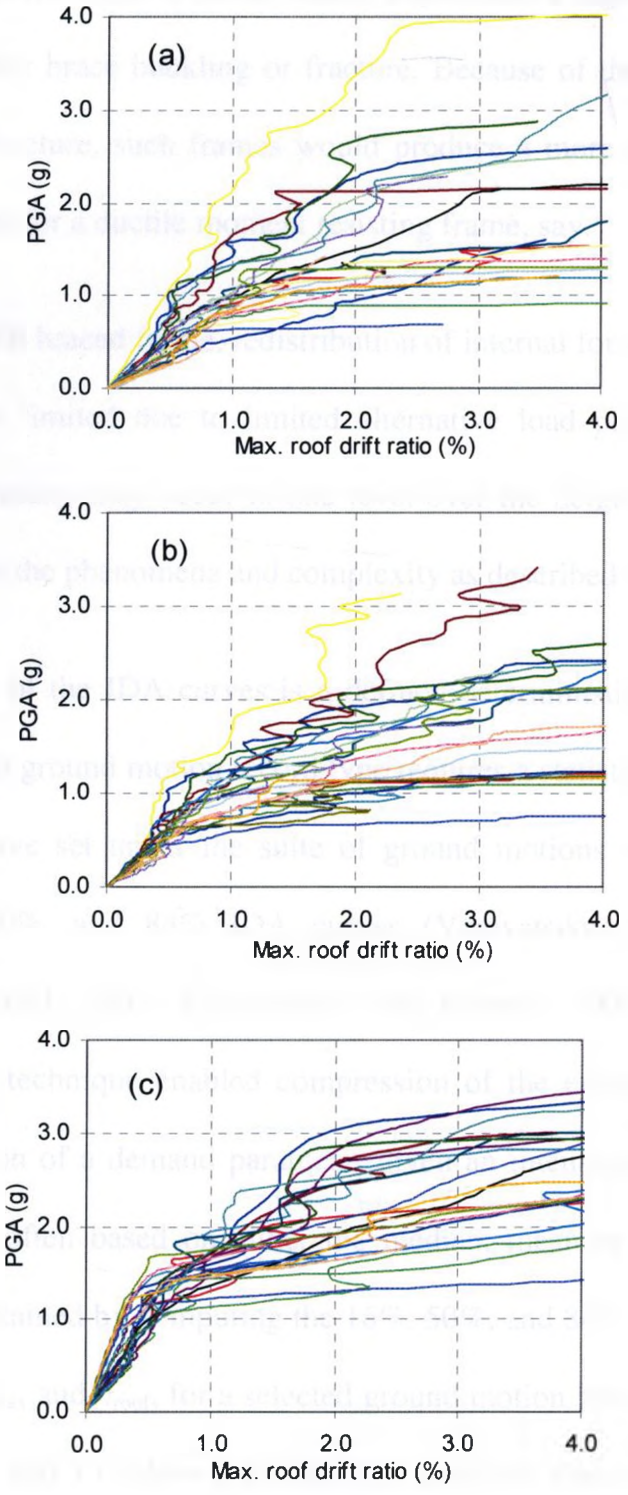

Figure 5.8. IDA Curves of Peak Ground Acceleration, PGA, plotted against Peak Roof Drift Ratio, θ_{roof}, for (a) Six-storey (b) Four-storey (c) Two-storey MSB Braced Frames.

In general, a stiffer braced frame would experience a significant change in its dynamic properties after brace buckling or fracture. Because of the sensitivity of inter-storey drift to brace fracture, such frames would produce a more complex IDA curves than would be expected for a ductile moment resisting frame, say.

Finally, for MSB braced frame, redistribution of internal forces from one storey to another may be more limited due to limited alternative load paths. Consequently, a concentration of inelasticity may occur in one level over the height of the frames. This may further exaggerate the phenomena and complexity as described above.

Although each of the IDA curves is a defined deterministic entity, the inherent random variability with ground motion record type requires a statistical assessment of the demand. The IDA curve set under the suite of ground motions were summarised by defining the 16%, 50%, and 84% IDA curves (Vamvatsikos and Cornell, 2002; Vamvatsikos and Cornell, 2004; Vamvatsikos and Cornell, 2005; Han and Chopra, 2006). This summary technique enabled compression of the enormous IDA data to a probabilistic distribution of a demand parameter given an intensity measure. Moreover, engineering design is often based on either the median, mean or 84^{th} percentile. The fractile curves were obtained by computing the 16%, 50%, and 84% fractile values of the demand parameters, θ_{max} and θ_{roof}, for a selected ground motion intensity measure, $S_a(T_1, 5\%)$. Figures 5.9, 5.10, and 5.11 show the 16%, 50%, and 84% fractile IDA curves for the Six-, Four-, and Two-storey MSB braced frames. Such fractile curves can be combined with a probabilistic seismic hazard analysis to produce mean annual frequencies of exceeding specified limit states.

The fractile IDA curves can also represent seismic demand curves of the selected MSB frames and may be used to assess their performance by comparing with allowable drift demands at any given intensity and probability level. For example, given the design level ground motion intensity of $S_a(T_1, 5\%) = 0.75g$ at the 2% in 50 year probability level for the Six-storey MSB frame, 16% of the records would produce $\theta_{max} \leq 0.62\%$, 50% would produce $\theta_{max} \leq 0.79\%$, and 84% of the records would yield $\theta_{max} \leq 1.15\%$. For the Four-storey MSB frame at its design level intensity of $S_a(T_1, 5\%) = 0.85g$, 16% of the records would produce $\theta_{max} \leq 0.46\%$, 50% of the records would yield $\theta_{max} \leq 0.51\%$, and 84% of the records would yield $\theta_{max} \leq 0.73\%$. For the Two-storey MSB frame at the design level intensity of $S_a(T_1, 5\%) = 0.96g$, 16% of the records would produce $\theta_{max} \leq 0.22\%$, 50% of the records would yield $\theta_{max} \leq 0.23\%$, and 84% of the records would yield $\theta_{max} \leq 0.24\%$.

The above probabilistic drift demand distribution of the Two-storey MSB frame are essentially within its elastic response range. In the NBCC (2005), drift limits are based on the median 2% in 50 year seismic hazard level and are given as 1% for post-disaster buildings, 2% for high importance buildings, and 2.5% for other buildings. Hence, the use of median ground motions for these frames would yield satisfactory performance in any building category.

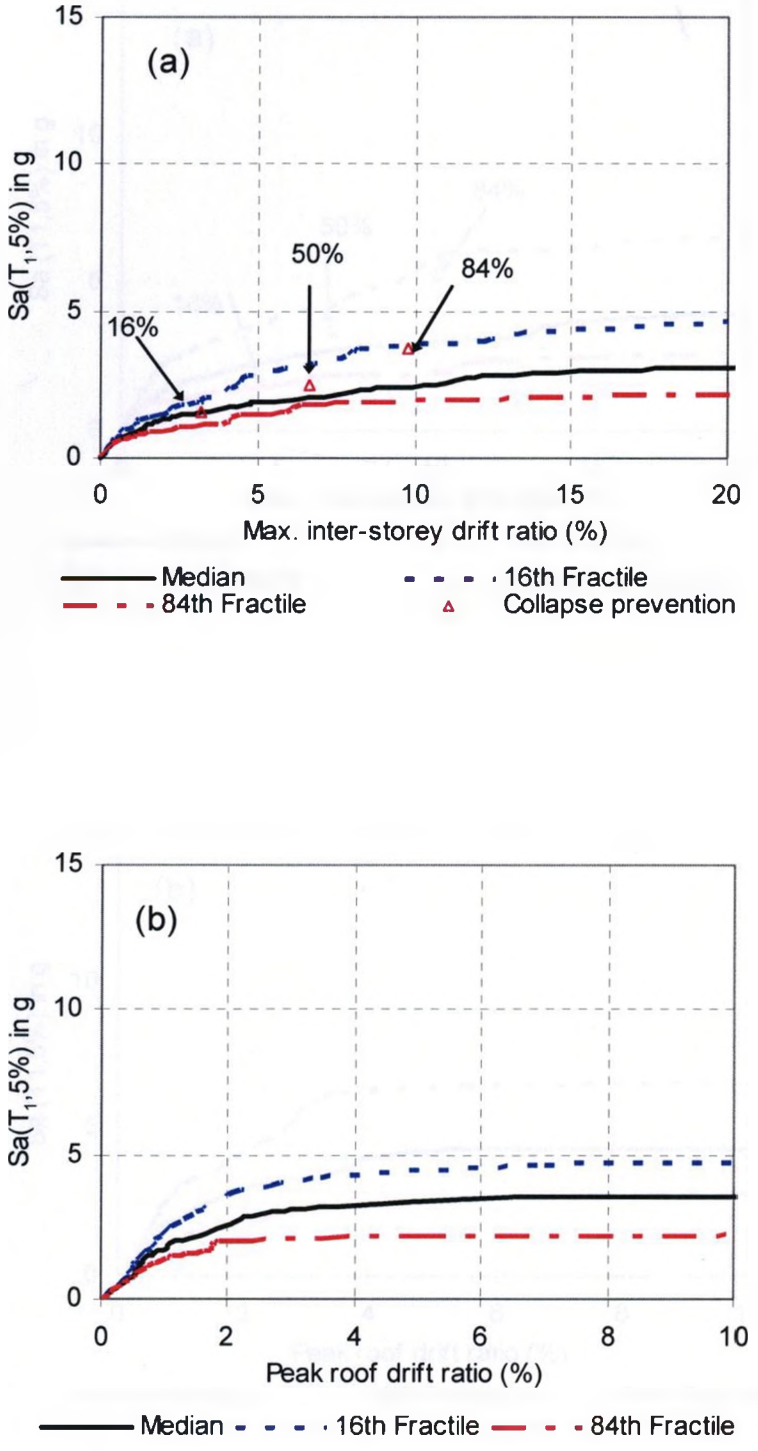

Figure 5.9. Summary of IDA Curves of the Six-storey MSB Frame into16th, 50th, and 84th Fractiles with (a) Maximum Inter-storey Drift Ratio (b) Peak Roof Drift Ratio.

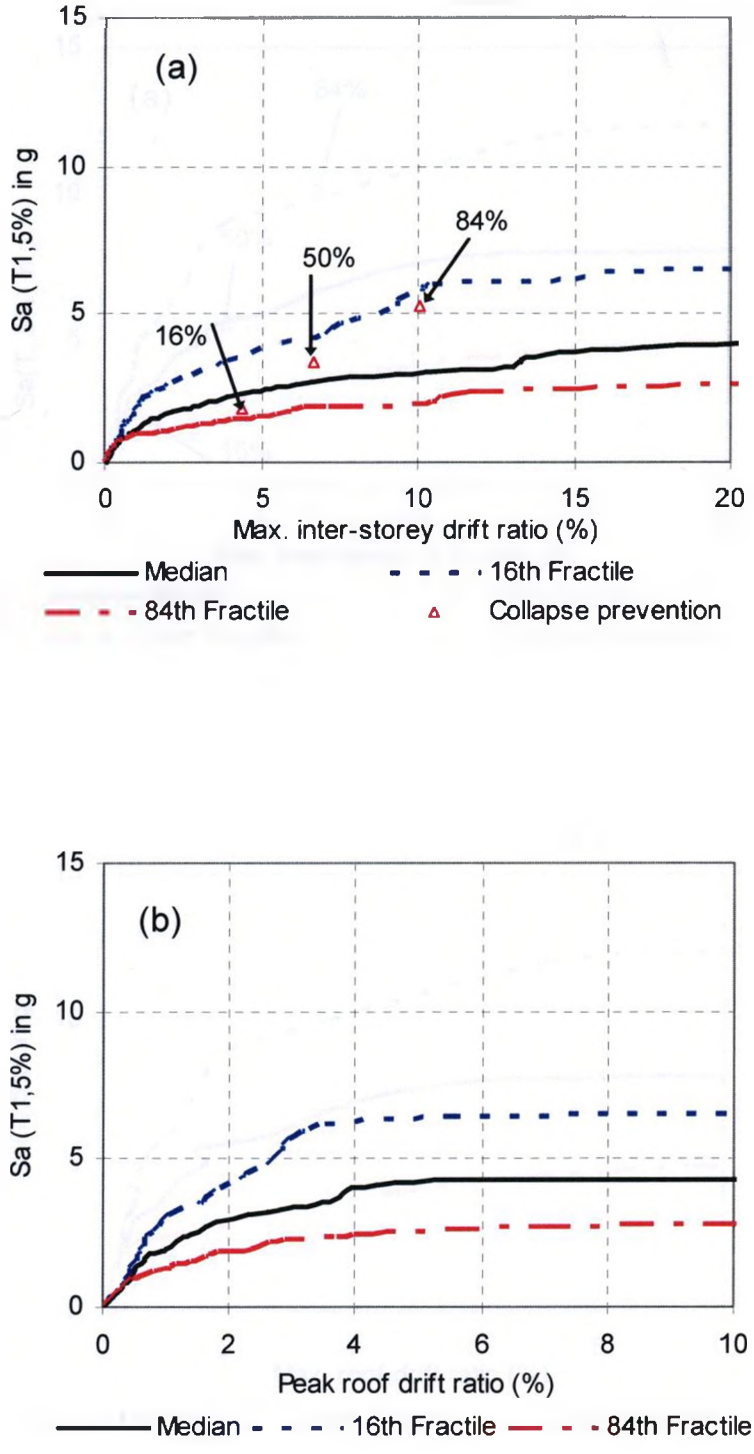

Figure 5.10. Summary of IDA Curves of the Four-storey MSB Frame into16th, 50th, and 84th Fractiles with (a) Maximum Inter-storey Drift Ratio (b) Peak Roof Drift Ratio.

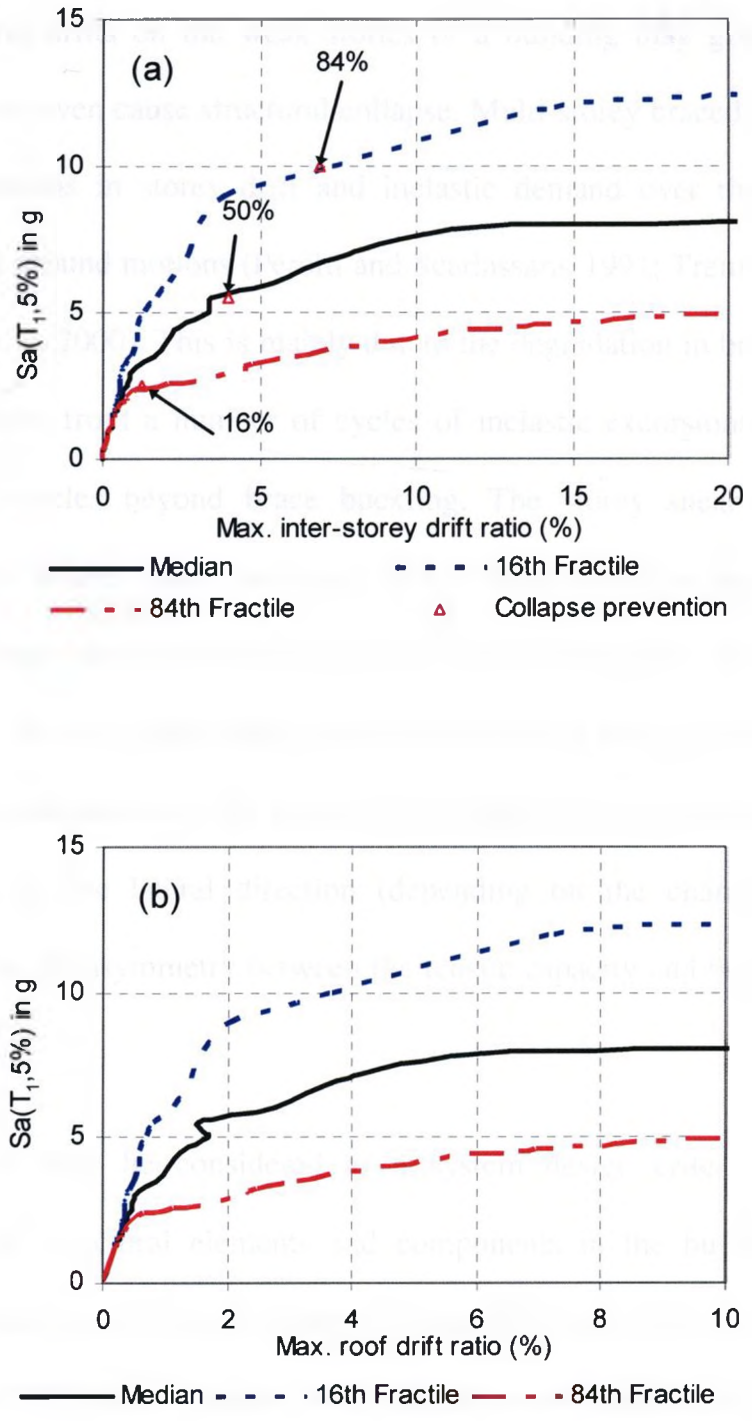

Figure 5.11. Summary of IDA Curves of the Two-storey MSB Frame into16th, 50th, and 84th Fractiles with (a) Maximum Inter-storey Drift Ratio (b) Peak Roof Drift Ratio.

5.5.3 Inelastic Distribution along Height of MSB Frame

Acute lateral drifts on the weak stories of a building may give rise to severe structural damage or even cause structural collapse. Multi-storey braced frames typically exhibit large variations in storey drift and inelastic demand over their height when subjected to strong ground motions (Perotti and Scarlassara, 1991; Tremblay and Robert, 2001; Martinelli et al. 2000). This is mainly due to the degradation in brace compressive resistance that results from a number of cycles of inelastic excursions and successive compression load cycles beyond brace buckling. The storey shear resistance may diminish at levels where brace buckling occurs first, and this may promote the development of larger storey drifts at these floors and consequently the formation of a storey mechanism. Seismic vulnerability may increase when there is limited capacity to redistribute inelastic demand over the height of a building. Inelastic drifts may also occur disproportionately in one lateral direction (depending on the characteristics of the excitation) owing to the asymmetry between the tensile capacity and buckling resistance of the braces.

Lateral drift may be considered as a system design criterion that requires consideration of all structural elements and components in the building system. As mentioned earlier and also shown in Figures 5.1 and 5.2, one of the significant features that distinguish an MSB braced frame from a regular braced frame is the incorporation of ceiling beams in the former. These beams also serve as upper horizontal members for brace end connections in each modular unit. The vertical connections of different modular units is such that columns are not fully continuous over two consecutive vertical

units, with some clearance allowed between ceiling beams of a lower modular unit and floor beams of an upper unit. The behaviour of this configuration and the vertical connections of modular units may result in independent rotation of upper and lower module columns at the same joint. This may influence the definition of inter-storey drift for this frame system and consequently affect its inelastic demands (including P-delta effect) especially after brace fracture. Furthermore, this unique frame detail may present additional limitation on redistribution of internal forces from one modular unit unto another, which may lead to a high concentration of inelasticity in one level over the height of the frames.

In the IDA plots and summaries presented above, inter-storey drift was evaluated as the difference in displacements at floor beam levels of consecutive modular units. This ignores any influence due to the presence of the ceiling beam between these floor beams. From one floor to another, the peak inter-storey drift angle at the lower floor beam level may change (either increase or decrease) at the ceiling beam level during a ground motion event, thus altering the distribution of lateral deformation over the height of the frame.

Figures 5.12, 5.13 and 5.14 examine the inter-storey drift distribution over the height of the selected MSB frames, taking into account the presence of the ceiling beam levels. In these figures, heightwise distributions of peak floor-to-ceiling and peak ceiling-to-floor drifts (accounting for ceiling beam level drifts) in the Six-, Four-, and Two-storey MSB frames for the ground motion recorded at El Centro Array #13 during the 1979 Imperial Valley earthquake (see No. 14 in Table 1) are compared with inter-storey

drifts as defined above at three different intensity levels: $S_a(T_1, 5\%)$ = 0.2g, 1.7g, and 2.0g for the 6-storey frame; $S_a(T_1, 5\%)$ = 0.3g, 2.0g, and 3.0g for the 4-storey frame; $S_a(T_1, 5\%)$ = 0.4g, 2.5g, and 4.0g for the 2-storey MSB frame.

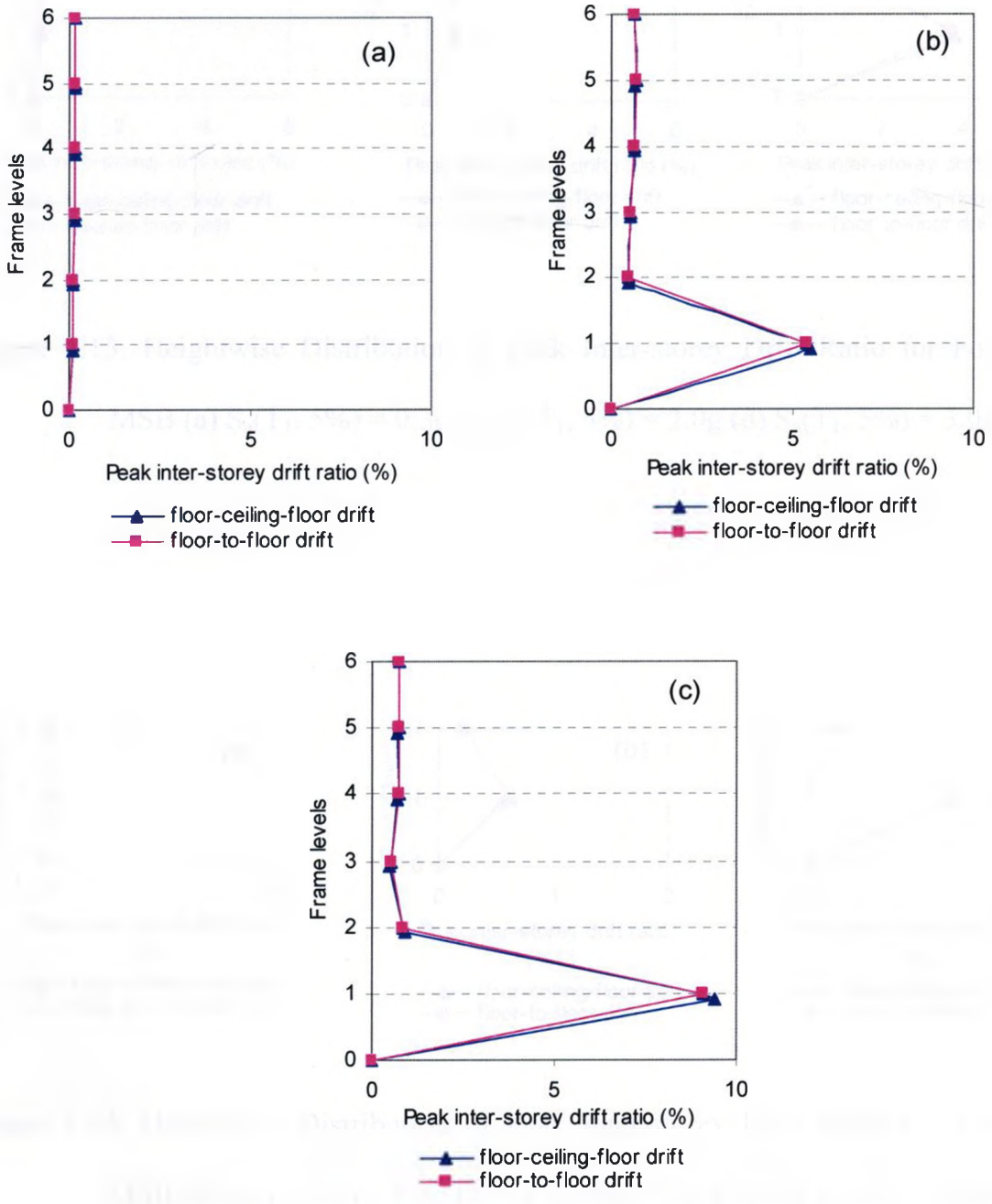

Figure 5.12. Heightwise Distribution of Peak Inter-storey Drift Ratio for Six-storey MSB

(a) $S_a(T_1, 5\%)$ = 0.2g (b) $S_a(T_1, 5\%)$ = 1.7g (c) $S_a(T_1, 5\%)$ = 2.0g

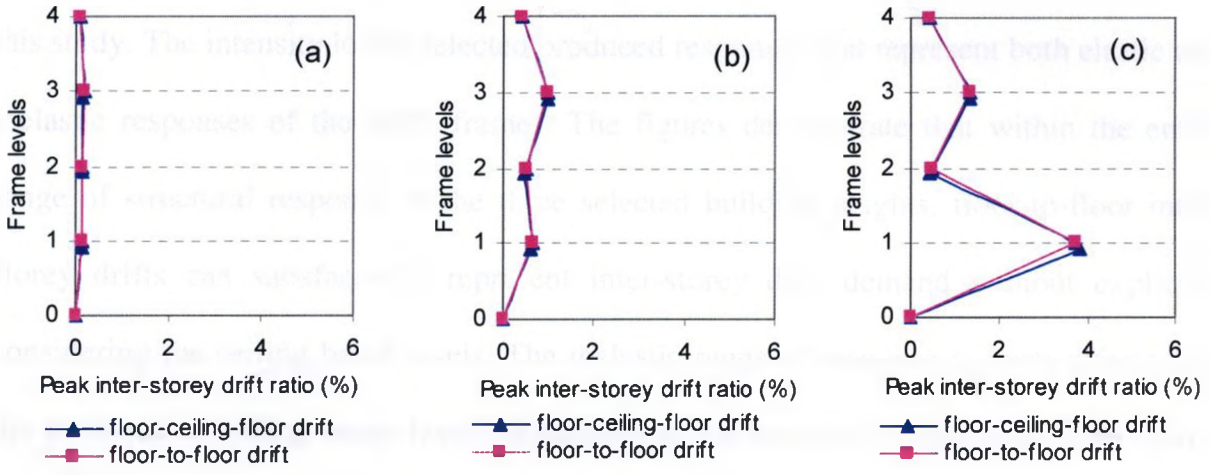

Figure 5.13. Heightwise Distribution of Peak Inter-storey Drift Ratio for Four-storey MSB (a) $S_a(T_1, 5\%) = 0.3g$ (c) $S_a(T_1, 5\%) = 2.0g$ (d) $S_a(T_1, 5\%) = 3.0g$

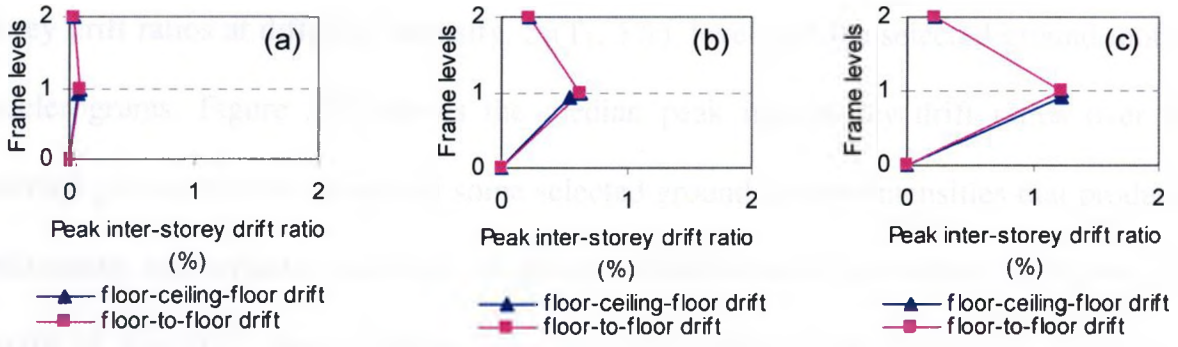

Figure 5.14. Heightwise Distribution of Peak Inter-storey Drift Ratio for Two-storey MSB (a) $S_a(T_1, 5\%) = 0.4g$ (b) $S_a(T_1, 5\%) = 2.5g$ (c) $S_a(T_1, 5\%) = 4.0g$

The behaviour observed above under the selected earthquake record was found to be representative of the response under all the other ground motion records selected for this study. The intensity levels selected produced responses that represent both elastic and inelastic responses of the MSB frames. The figures demonstrate that within the entire range of structural response of the three selected building heights, floor-to-floor inter-storey drifts can satisfactorily represent inter-storey drift demand without explicitly considering the ceiling beam levels. The inelastic range of response is more affected by the presence of ceiling beam levels, especially at the location of maximum inter-storey drift (lower level), but this effect can be neglected. In this range of response, the inter-level drift angle between the ceiling beam and floor beam levels at maximum inter-storey drift regions are slightly lower than that between floor-to-floor beam levels. In the elastic range of response, i.e. at lower ground motion intensities, there is almost no variation in this drift angle.

Figures 5.15, 5.16, and 5.17 display a storey-to-storey profile of the peak inter-storey drift ratios at different intensity, $S_a(T_1, 5\%)$, levels for the selected ground motion accelerograms. Figure 5.18 shows the median peak inter-storey drift ratios over the selected ground motion records at some selected ground motion intensities that produced both elastic and inelastic responses. In general, distribution of inter-storey drift along the height of the MSB braced frames becomes non-uniform with increasing intensity of ground motion, often concentrating at specific storey levels. In the elastic range of response (Figures 5.15a, 5.16a, and 5.17a), the storey level experiencing maximum drift varies from record to record. The upper storey levels are mostly affected in this response range: For the Six-storey MSB braced frame subjected to the selected ground motion

records, the 3rd to 5th storey levels experience maximum inter-storey drifts for different ground motion records; the 3rd storey level is almost solely affected in the Four-storey MSB frame; for the Two-storey, the maximum inter-storey drift occurred in the 1st storey level for all the ground motion records.

Within the post-elastic range of response, distribution of inter-storey drift demand varies from record to record in terms of amplitude but follows a very similar pattern for a specified model MSB braced frame. Also, a similar trend is maintained as the ground motion intensity increases within the inelastic range of response. Clearly, in this response range, there is a very high concentration of inelasticity mainly in the 1st storey level for all the selected frame heights.

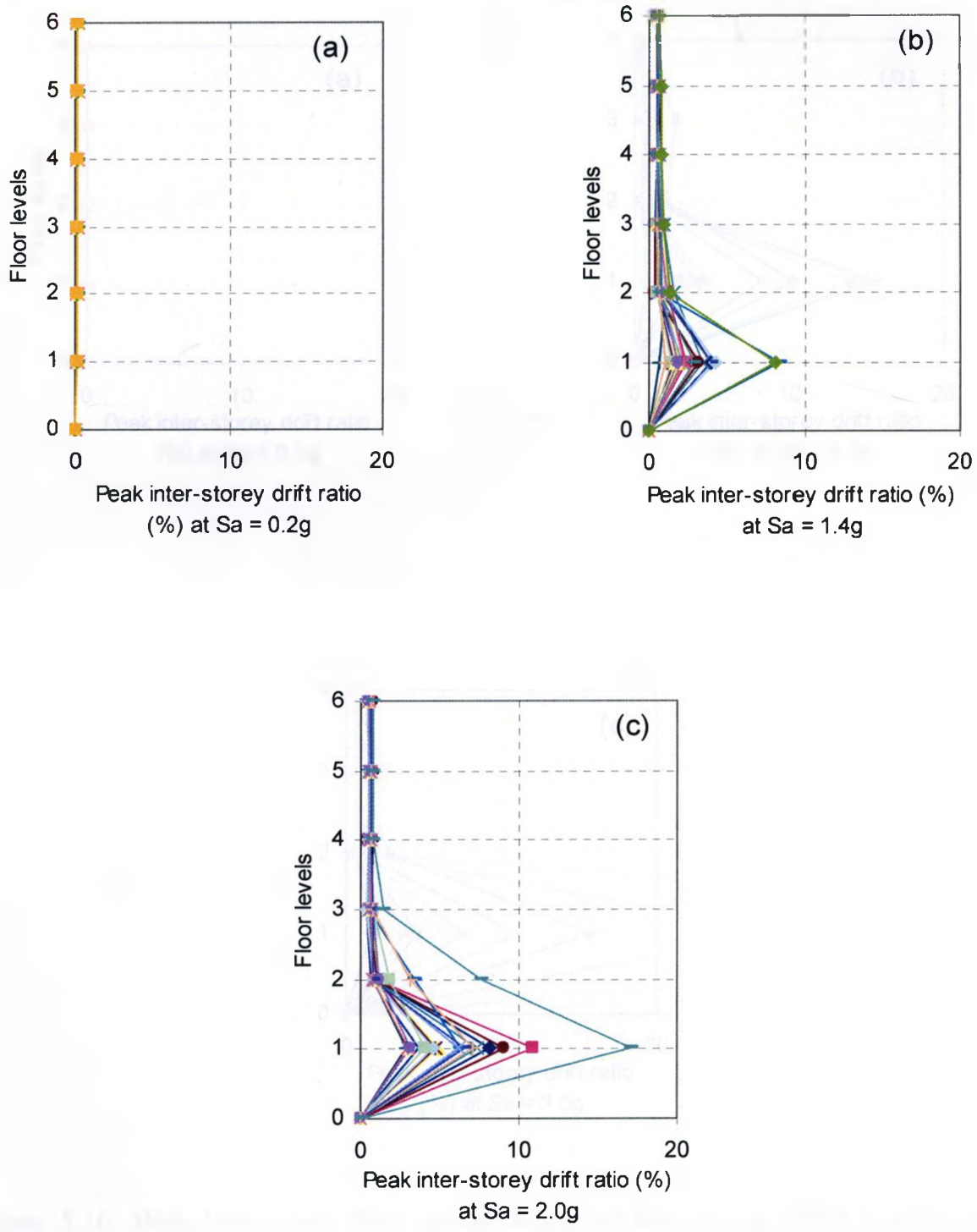

Figure 5.15. Peak Inter-storey Drift along Height of Six-storey MSB Frame under Selected Ground Motion Records at Different Intensity Levels (a) S_a = 0.2g (b) S_a = 1.4g (c) S_a = 2.0g

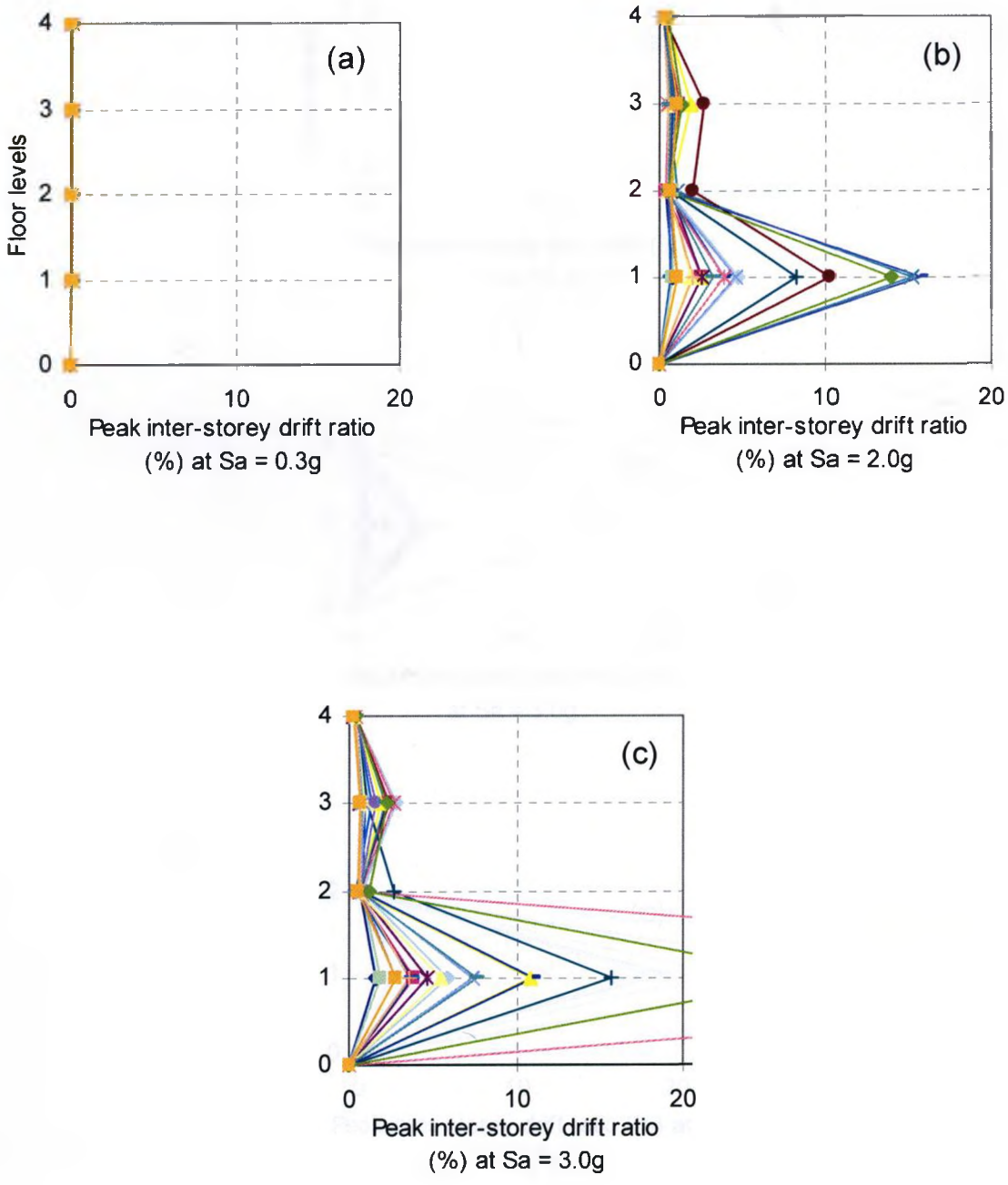

Figure 5.16. Peak Inter-storey Drift along Height of Four-storey MSB Frame under Selected Ground Motion Records at Different Intensity Levels (a) S_a = 0.3g (b) S_a = 2.0g (c) S_a = 3.0g

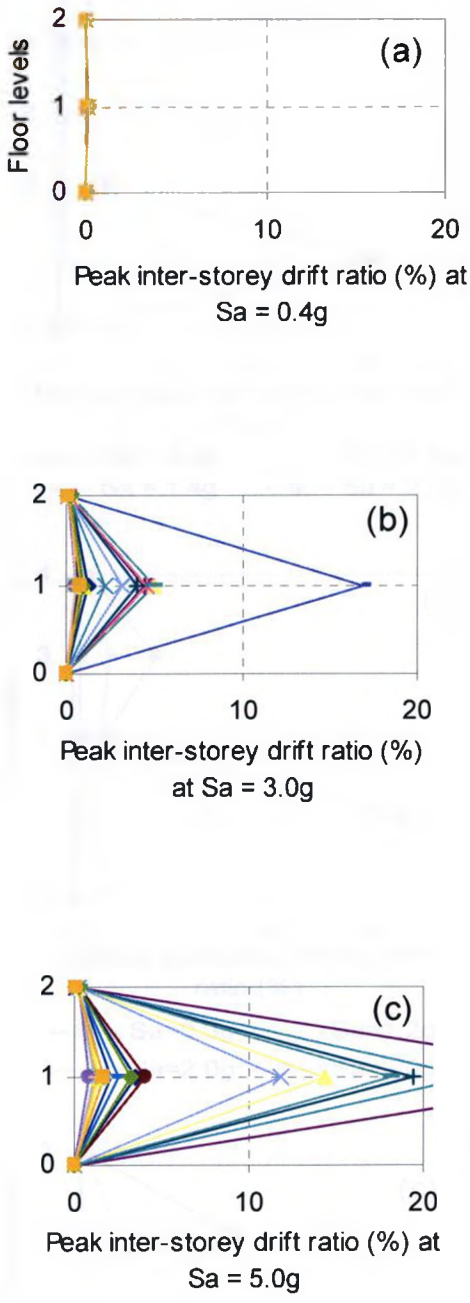

Figure 5.17. Peak Inter-storey Drift along Height of Two-storey MSB Frame under Selected Ground Motion Records at Different Intensity Levels (a) Sa = 0.4g (b) Sa = 3.0g (c) Sa = 5.0g

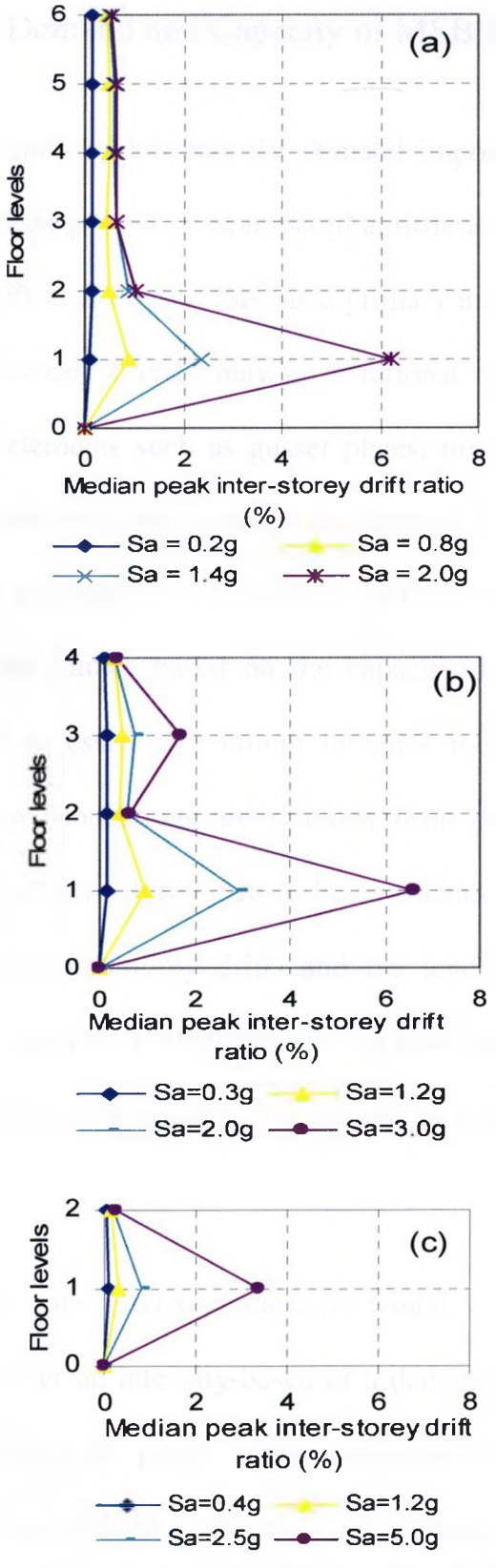

Figure 5.18. Median Peak Inter-storey Drift Ratios for all Storey Levels at Different Ground Motion Intensities representing Elastic and Post-elastic Response (a) Six-storey (b) Four-storey (c) Two-storey MSB Braced Frame

5.5.4 Structural Drift Demand and Capacity of MSB Braced Frame

Each of the IDA curves illustrates the demand imposed on the modeled MSB frame structure by a specified ground motion record at different intensities. The question of whether inter-storey drift ratio can be used as a primary damage parameter to predict global capacity of MSB braced frames may be a rational one. Several local damage events can take place in elements such as gusset plates, bracing members, beams and columns, and in connections including vertical connections of different modular units. However, results from the nonlnear static (pushover) analyses conducted in Chapter Four revealed that designing the frames based on the capacity design philosophy restricts global failure mechanism to essentially failure in brace members alone. Meanwhile, beams, columns and brace connections are shielded from premature inelastic failure. Because of the sensitivity of inter-storey drift to brace fracture (i.e. failure of braces are more evident in maximum inter-storey drift) and the tendency for concentration of inelastic effects within a storey of a MSB system, the peak inter-storey drift can relate well to both global and local storey collapse. Thus, it can be used as a reasonable damage measure.

Clearly, the global system dynamic capacity would vary from record to record. For a single IDA curve, either an intensity-based or a demand-based limit state or even both can be useful in defining the global collapse capacity (Vamvatsikos and Cornell, 2002). In general, the demand-based limit states are known to be useful for defining performance levels other than structural collapse, and the intensity-based limits better assess collapse capacity. In the FEMA (2000a) methodology, structural capacity is

defined at the point when the rate of increase of the maximum inter-storey drift with increasing ground motion intensity exceeds five times that associated with the initial 'elastic' slope (that is, a tangent slope of 20% of elastic slope). Alternatively, it is defined at a prescribed maximum inter-storey drift ratio beyond which the reliability of the analysis is not considered trustworthy (e.g. 10% for collapse prevention of special moment resisting frames). Due to the weaving nature of some of the IDA curves, both the former intensity-based and the latter demand-based limit states may result in more than one capacity point. In such a case, the first capacity point along the IDA curve from the origin is recommended when using the demand-based rule and the final capacity point is recommended for the intensity-based rule (Vamvatsikos and Cornell, 2002). The 20% tangent slope approach is assumed to be indicative of imminent collapse. Therefore, it is adopted in this study to define global capacity of the MSB braced frames under the selected ground motions.

The global capacity of the MSB braced frames under the selected ground motion records representing the collapse prevention limit state defined by FEMA (2000a) are shown by the open triangular shaped markers on the IDA curves in Figure 5.5. Such limit states can also be summarised into their 16th, 50th, and 84th percentile values as shown on the fractile IDA curves in Figures 5.9a, 5.10a, and 5.11a. These points are obtained by determining the capacities individually for each earthquake ground motion record and then estimating their fractile values. Table 5.3 summarises the fractile structural drift capacities in terms of $S_a(T_1,5\%)$ for the selected MSB braced frames. It also shows the standard deviation of the capacities over the selected ground motions based on the assumed lognormal probability distribution (Hamburger et al., 2003). The median

capacities in terms of spectral acceleration associated to the NBCC design drift limit of 2.0% have also been included in this table.

Table 5.3: 16%, 50%, and 84% fractile capacities in terms of intensity measure (IM), $S_a(T_1,5\%)$

MSB frame	Design level intensity, $Sa(T_1)$ in g	Fractile S_a capacity (g) based on collapse prevention level			Standard Dev. of median capacity	S_a capacity (g) based on NBCC drift limit
		16%	50%	84%		
2-storey	0.96	2.50	5.50	10.00	0.61	4.00
4-storey	0.85	1.80	3.30	5.25	0.53	1.75
6-storey	0.75	1.60	2.45	3.75	0.44	1.25

It is observed that the median capacities associated to the collapse prevention limit state are in the range of between 1.4 and 2.0 times the median capacities associated to the NBCC drift limit (and about 3 to 5 times the design intensity levels). Capacity reduction factors have been recommended (FEMA, 2000a) to be applied in the case of ductile moment resisting frames to account for the variability in the computed capacities. Such factors are statistically based and are currently not available for ductile braced frames. The capacities shown in Table 5.3 are those obtained without explicitly accounting for uncertainties and randomness inherent in their prediction. Table 5.4 shows the fractile capacities in terms of θ_{max}, including their standard deviations. The median

capacities are between 1.6 and 2.6 times the NBCC drift limit for the selected MSB frames.

Table 5.4: 16%, 50%, and 84% fractile capacities in terms of maximum drift, θ_{max}

MSB frame	Fractile θ_{max} capacities (%)			Standard Dev. of capacities
	16%	50%	84%	
2-storey	1.2	4.0	6.9	0.76
4-storey	4.4	6.7	10.0	0.63
6-storey	3.2	6.7	9.8	0.43

5.5.5 Ductility Demand Assessment

Ductility represents the capacity of a structure to dissipate energy and plays an important role in the determination of seismic design forces and evaluation of seismic vulnerability. From the incremental dynamic analyses, IDA curves are constructed with ductility as the engineering demand parameter against the 5% damped spectral acceleration at the fundamental-mode period of the structure, $S_a(T_1, 5\%)$. Figure 5.19 shows the ductility demands of the Six-storey, Four-storey and Two-storey MSB braced frame under the selected ground motion records. This global ductility demand is indicative of the overall deformation of the structure and defined as the average value of the storey ductilities. This definition yields reasonable results for moment resisting frames (Reyes-Salazar, 2002) and is adopted in this study. The storey ductility is defined for each storey as the ratio of the maximum inter-storey drift during the ground motion

duration to the maximum inter-storey drift over all stories when plasticization occurs in the structure for the first time. A large variation of ductility demand with frame height and from ground motion record to record is observed.

The ductility demands of the selected frames under the twenty ground motion records are summarised into their 16^{th}, 50^{th}, and 84^{th} fractile curves, as shown in Figure 5.20. Ductility capacities are evaluated based on the $S_a(T_1, 5\%)$ median capacities associated to the NBCC 2.0% drift limit as well as the collapse prevention limit state identified in Section 5.4 above. Table 5.5 consists of the ductility capacities obtained for the selected MSB braced frames. These capacities range from 1.8 to 4.8 and increase with a decrease in frame height.

Table 5.5: Ductility capacity based on NBCC drift limit and collapse prevention limit median capacities in $S_a(T_1,5\%)$

MSB frame	Ductility capacity based on NBCC drift limit median capacity in Sa	Ductility capacity based on collapse prevention level median capacity in Sa
2-storey	2.80	4.80
4-storey	2.40	4.50
6-storey	1.80	3.90

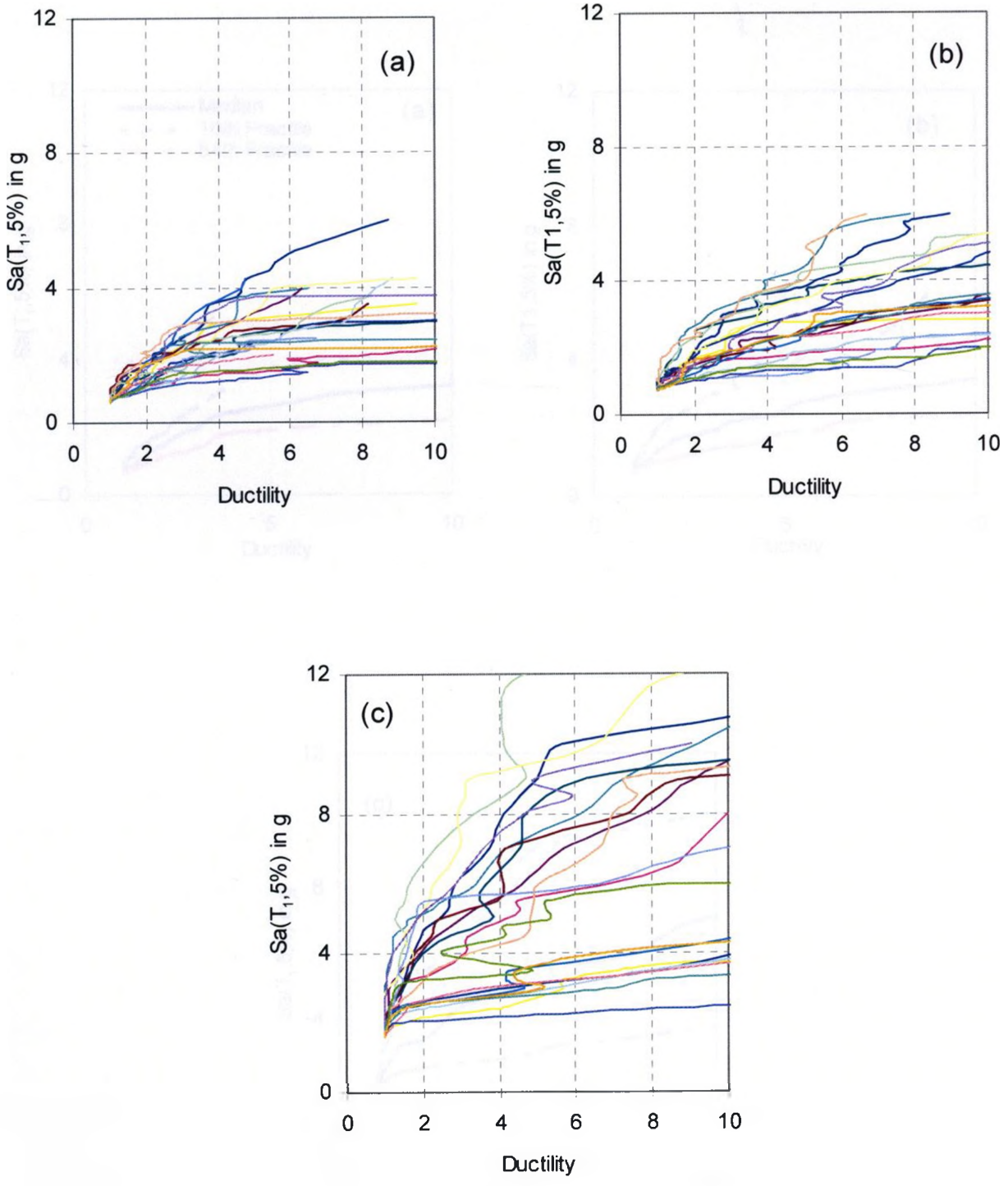

Figure 5.19. IDA Curves of 5% Damped Spectral Acceleration, $S_a(T_1, 5\%)$, plotted against Ductility for (a) Six-storey (b) Four-storey (c) Two-storey MSB Braced Frames.

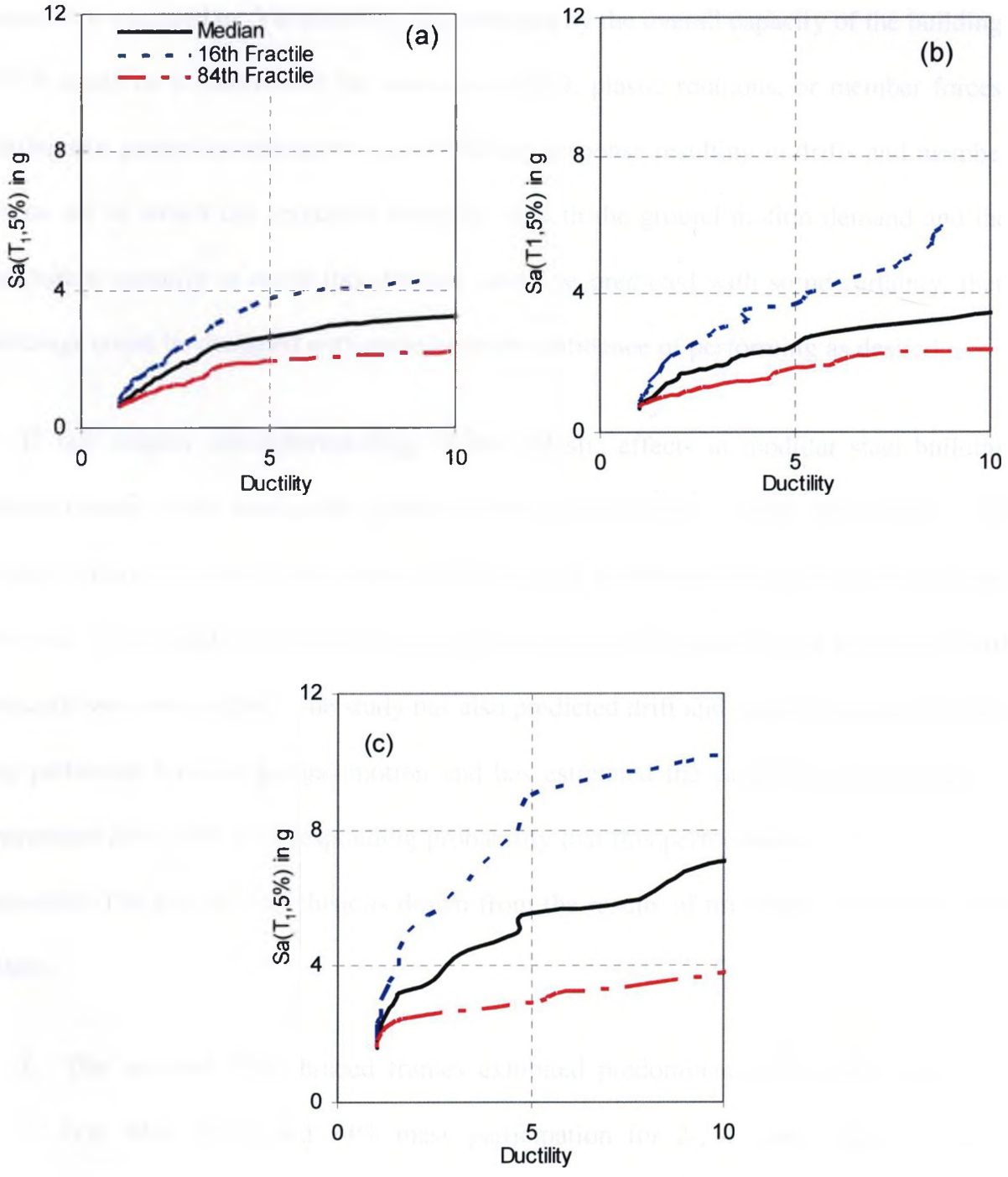

Figure 5.20. Summary of Ductility Demand IDA Curves into 16th, 50th, and 84th Fractiles for (a) Six-storey (b) Four-storey (c) Two-storey MSB Braced Frames.

5.6 Conclusions

The severity of damage a building suffers depends on its vulnerability and the seismic hazard it is exposed to. Vulnerability is controlled by the overall capacity of the building, which could be a function of the inter-storey drift, plastic rotations, or member forces. Earthquake ground accelerations cause building response resulting in drifts and member forces, all of which can represent demands. If both the ground motion demand and the structure's capacity to resist this demand could be predicted with some certainty, then buildings could be designed with some level of confidence of performing as desired.

In this chapter, an understanding of the inelastic effects in modular steel building braced frames under earthquake ground motions has been developed. The influence of ground motion intensities and number of stories on maximum drift demands have been assessed. The heightwise distribution and record-to-record variability of maximum drift demands was also studied. The study has also predicted drift and ductility demands given any particular level of ground motion and has estimated the capacities at the collapse prevention level with a corresponding probability that this performance level may not be exceeded. The specific conclusions drawn from the results of this study are summarised below:

1. The selected MSB braced frames exhibited predominantly first-mode response (i.e. 94%, 81%, and 74% mass participation for 2-, 4-, and 6-storey frames respectively) but there was some sensitivity to higher modes (i.e. 5%, 15%, and 17% second mode mass participation for 2-, 4-, and 6-storey frames respectively).

2. At the design level ground motion intensity of all the selected MSB braced frames, the predicted drift demands based on the median ground motions gave satisfactory performance on the basis of the NBCC drift limits.
3. Within the entire range of structural response of the three MSB heights considered in the study, floor-to-floor inter-storey drifts can satisfactorily represent inter-storey drift demand without explicitly considering the effect of drift at the ceiling beam levels.
4. The distribution of inter-storey drift demand along the height of the frames varies from record to record in terms of amplitude but follows a very similar pattern. The upper storey levels generally experience maximum drift demands in the elastic range of response. In the inelastic range of response, there is a high concentration of inelasticity in mainly the 1^{st} storey level. This is due to inelastic behaviour of braces and the limited redistribution of internal forces from one storey level to the other.
5. The median capacities in terms of spectral acceleration, $S_a(T_1, 5\%)$, for the collapse prevention drift limit state are in the range of between 1.4 and 2.0 times the median capacities associated to the NBCC drift limit of 2.0%.
6. The median capacities in terms of maximum inter-storey drift based on collapse prevention levels are between 2.0 and 3.3 times the NBCC drift limit.
7. Both drift and ductility demands vary from record to record and with frame height.

8. All three MSB braced frames possess significant ductility capacity of between 1.8 and 2.8 based on the median capacities associated to the NBCC drift limit, and between 3.9 and 4.8 based on the median capacities associated to collapse prevention levels.

5.7 References

Annan, C.D., Youssef, M.A. and El-Naggar, M.H. [2005] "Analytical investigation of semi-rigid floor beams connection in modular steel structures," *33rd Annual general conference of the Canadian Society for Civil Engineering,* Toronto, Canada, GC-352.

Annan, C. D., Youssef, M. A. and El-Naggar, M. H. [2007] "Seismic performance of modular steel braced frames," *Proc. of the Ninth Canadian Conference on Earthquake Engineering*, Ottawa, Ontario, Canada.

Annan, C.D., Youssef, M.A. and El-Naggar, M.H. [2008a] "Effect of directly welded stringer-to-beam connections on the analysis and design of modular steel building floors," *Advances in Structural Engineering,* Accepted in October 2008.

Annan, C. D., Youssef, M. A. and El-Naggar, M. H. [2008b] "Assessment of overstrength and ductility of a four-storey modular steel building braced frames," *Proc. of the Second Canadian Conference on Effective Design of Structures*, Hamilton, Ontario, Canada.

Annan, C. D., Youssef, M. A. and El-Naggar, M. H. [2009] "Seismic overstrength in braced frames of Modular Steel Buildings," *Journal of Earthquake Engineering*, 13(1), 1-12.

CSA [2001] *Handbook of Steel Construction, 7th Edition*, Canadian Institute of Steel Construction, Willowdale, Ontario, Canada.

Dhakal, R. P., Mander, J. B. and Mashiko, N. [2006] "Identification of critical ground motions for seismic performance assessment of structures," *Earthquake Engineering and Structural Dynamics* 35, 989-1008.

FEMA [2000a] *Recommended seismic design criteria for new steel moment frame buildings*, FEMA-350, SAC Joint Venture, Federal Emergency Management Agency, Washington, DC.

FEMA [2000b] *Recommended seismic evaluation and upgrade criteria for existing welded steel moment frame buildings*, FEMA-351, SAC Joint Venture, Federal Emergency Management Agency, Washington, DC.

Hamburger, R. O., Foutch, D. A. and Cornell, A. C. [2003] "Translating research to practice: FEMA/SAC performance-based design procedures," *Earthquake Spectra, Special issue: Welded steel moment-frame structures – Post-Northridge* 19(2).

Jain, A.K. and Goel, S.C. [1978] *Hysteresis models for steel members subjected to cyclic buckling or cyclic end moments and buckling – User's guide for DRAIN-2D: EL9 and EL10*, Report UMEE 78R6, Department of Civil Eng., Univ. of Michigan, Ann Arbour, MI, USA.

Khatib, I.F., Mahin, S.A. and Pister, K.S. [1988] *Seismic behaviour of concentrically braced steel frames*, Report UCB/EERC-88/01, Earthquake Engineering Research Center, University of California, Berkeley, CA, USA.

Luco, N. and Cornell, C. A. [1998] "Effects of random connection fractures on the demands and reliability for a three-story pre-Northridge (SMRP) structure," *Proc. of the sixth U.S. National Conf. on Earthquake Eng.*, Earthquake Engineering Research Institute, Oakland, California.

Martinelli, L., Perotti, F. and Bozza, A. [2000] "Seismic design and response of a 14-story concentrically braced steel building," *Proc. STESSA 2000 Conf.*, Montreal, Canada, pp. 327-334.

NBCC [2005] *National Building Code of Canada*, Institute for Research in Construction, National Research Council of Canada, Ottawa, Ontario, Canada.

Newmark, N.M. [1959] "A method of computation for structural dynamics," Journal of the Engineering Mechanics Division, ASCE 85(EM3), 67-94.

Perotti, F. and Scalassara, P. [1991] "Concentrically braced frames under seismic actions: Nonlinear behaviour and design coefficients," *Earthquake Engineering and Structural Dynamics* 20, 409-427.

Redwood, R.G. and Channagiri, V.S. [1991] "Earthquake resistant design of concentrically braced frames," *Canadian Journal of Civil Engineering* 18(5), 839-850.

Remennikov, A. and Walpole, W. [1997] "Analytical prediction of seismic behaviour for concentrically-braced steel systems," *Earthquake Engineering and Structural Dynamics* 26, 859-874.

Reyes-Salazar, A. [2002] "Ductility and ductility reduction factor for MDOF systems," *Structural Engineering and Mechanics* 13(4), 369-385.

Sabelli, R. [2001] *Research on improving the design and analysis of earthquake-resistant steel-braced frames*, The 2000 NEHRP Professional Fellowship Report, Earthquake Engineering Research Institute, USA.

Sharpe, R. D. [1974] *The seismic response of inelastic structures*, Ph.D Thesis, Department of Civil Engineering, University of Cantebury.

Shome, N. and Cornell, C.A. [1999] *Probabilistic seismic demand analysis of nonlinear structures*, RMS Report-35, Reliability of Marine structures Group, Stanford University, Stanford.

Shome, N., Cornell, C.A., Bazzurro, P. and Carballo, J. [1998] "Earthquake, records, and nonlinear MDOF responses," *Earthquake Spectra* 14(3), 469-500.

Tremblay, R. and Robert, N. [2001] "Seismic performance of low- and medium-rise chevron braced steel frames," *Canadian Journal of Civil Engineering* 28(4), 699-714.

Tremblay, R. [2000] "Influence of brace slenderness on the seismic response of concentrically braced steel frames," *Proc. STESSA 2000 Conference*, Montreal, Canada, pp. 527-534.

Tremblay, R. [2002] "Inelastic seismic response of steel bracing members," *Journal of Constructional Steel Research* 58, 665–701.

Uriz, P. and Mahin, S. A. [2004] "Seismic Performance assessment of concentrically braced steel frames," *Proc. of the 13th World Conf. on Earthquake Eng.*, Vancouver, Canada, Paper No. 1639.

Vamvatsikos, D. and Cornell, C. A. [2002] "Incremental dynamic analysis," *Earthquake Engineering & Structural Dynamics* 31(3), 491-514.

Vamvatsikos, D. and Cornell, C. A. [2004] "Applied incremental dynamic analysis," *Earthquake Spectra* 20(2), 523-553.

Yun, S., Hamburger, R.O., Cornell, C.A. and Foutch, D.A. [2002] "Seismic performance evaluation for steel moment frames," *Journal of Structural Engineering* 128(4), 534-545.

CHAPTER SIX

CONCLUSIONS AND RECOMMENDATIONS

6.1 Review and Conclusions

This thesis work has involved both experimental and analytical investigations. The study has addressed a rapidly evolving steel building system composed of prefabricated units and referred to as Modular Steel Buildings. The primary aim was to provide an understanding of the behaviour of Modular Steel Buildings to improve on their design methodology. This thesis is the first technical documentation of detailed description of this unique building system and its detailing requirements, and has also introduced its first seismic investigation.

The behaviour of Modular Steel Buildings (MSBs) under both gravity and seismic loads was studied. In the former, the effect of the directly welded stringer-to-beam connections on the behaviour and design of MSBs floor system was investigated using finite element analysis. The analysis results revealed that consideration of the actual behaviour of the directly welded connections leads to distribution of forces and moments that are different from conventional steel buildings. In the latter, braced frames of a typical MSB were used to represent its lateral force resisting system. The nonlinear performance characteristics of these frames were studied using cyclic load testing, nonlinear static (pushover) analysis, and incremental dynamic analysis. This behaviour study typically involved the following:

(i) Experimental investigation of the seismic performance of MSB braced frame

(ii) Strength and ductility capacity design of braced frames of a typical MSB for specified gravity and seismic loading

(iii) Development of analytical models which account for the unique detailing requirements of MSBs and the hysteretic behaviour of the frame

(iv) Study of the effect of design philosophy on the nonlinear behaviour of MSB braced frames using pushover analysis

(v) Evaluation of structural overstrength and displacement ductility of the braced frames using pushover analysis,

(vi) Assessment of inelastic drift and ductility demands and capacities of the braced frames using incremental dynamic analysis.

From these studies, it is concluded that while the MSB frame configuration may not significantly affect certain design and behavioural characteristics, in some others, its unique detailing requirements need to be considered during their design to eliminate undesirable seismic response.

The following sub-sections briefly review main points developed and conclusions drawn in each of the four major chapters (i.e. Chapters Two, Three, Four, and Five).

6.1.1 Effect of Directly Welded Stringer-To-Beam Connections on the Analysis and Design of Modular Steel Building Floors

Chapter Two highlighted the uniqueness of the modular design and construction, and provides a detailed description of the detailing requirements of modular steel buildings, as observed by experience and practice in the modular steel industry. The chapter also studied the effect of direct welding between webs of the floor stringers and the floor beams on the analysis and design of floor beams, stringers, and the welded connections. The analysis revealed that this unique connection type significantly affects the design of the floor stringers and the welded connections, but have little effect on the floor beams design. A simplified analytical model was proposed which, in practice, can predict the actual forces and moments in the floor stringers and welded connections and, thus lead to an optimal design of modular steel building floors. A step-by-step design methodology was also proposed for ease of practical application.

6.1.2 Experimental Evaluation of the Seismic Performance of Modular Steel Braced Frames

Chapter Three assessed the hysteretic characteristics of braced frames of modular steel buildings under reverse cyclic loading. It also assessed the behaviour of regular concentrically braced frame with similar physical characteristics for comparison. This investigation allowed an assessment of the strength, stiffness, inelastic deformation and energy dissipation characteristics of the modular steel building braced frame. The lateral force distribution pattern was also studied and compared for the two braced systems.

While some similarities were observed in the behaviour and response characteristics of the two systems (e.g. normalized cumulative energy dissipation), some differences (e.g. lateral stiffness, and load transfer mechanism) suggested that for improved performance of MSB braced frames, the specific detailing requirements of the system need to be incorporated into their design. The experimental results were also used to validate a proposed analytical model to predict the seismic behaviour of MSBs. This analytical model was subsequently utlised in analytical investigations in Chapters Four and Five.

6.1.3 Seismic Overstrength in Braced Frames of Modular Steel Buildings

Chapter Four studied inelastic behaviour of typical braced frames of Modular Steel Buildings using nonlinear static pushover analyses. The analysis results revealed that in the design of frame columns in a multi-storey MSB, the use of direct summation accumulation approach for brace induced column actions would yield the desired response and must be preferred to the square root of the sum of squares approach. Structural overstrength resulting from redistribution of internal forces in the inelastic range, design assumptions, and strain hardening behaviour of steel and displacement ductility were evaluated. The results showed that the reserve strength of MSB braced systems is greater than that prescribed by the Canadian code for regular braced systems. It also appeared that ductility and overstrength depends on building height, contrary to what has been prescribed in many seismic design codes for regular braced frames.

6.1.4 Seismic Vulnerability Assessment of Modular Steel Buildings

Chapter Five developed an understanding of the inelastic seismic behaviour of braced frames of modular steel buildings and assessed their seismic demands and capacities. Nonlinear incremental dynamic analysis was utilised under an ensemble of 20 ground motions to study the dynamic behaviour. The maximum inter-storey drift and peak global roof drift were adopted as critical response parameters for the estimation of structural drift and ductility demands and capacities. The study revealed a significant global structural capacity and a satisfactory performance at design intensity levels. High concentration of inelasticity, however, was observed in the first storey level which is due to limited redistribution of internal forces from one storey level to the other.

6.2 Major Research Contributions

The following is an outline of significant research contributions:

1) The research has documented for the first time detailed description of the modular steel building system, highlighting its unique detailing requirements. This is expected to provide other researchers with an opportunity to study its critical elements.

2) A simplified analytical model was proposed to predict the more realistic forces and moments in the direct welded floor grid structure of modular steel buildings. Regression functions that describe this model were developed, and a step-by-step design methodology has been provided for easy application.

3) The research revealed that braced frames of modular steel buildings have comparable cumulative energy dissipation characteristics with braced frames of regular buildings up to large ductility demands. Lateral stiffness characteristics are also comparable between ductilities of 2 and 6. Outside this range, braced frames of regular buildings are superior.

4) An analytical model to predict seismic behaviour of braced frames of modular steel buildings was developed and validated.

5) The use of SRSS (square root of the sum of squares) accumulation approach, often used to determine brace induced column actions in capacity design of multi-storey regular braced frames, was found not to be conservative for modular steel buildings. The direct summation accumulation approach was therefore recommended for use in their design as it was found to yield the desired response.

6) Braced frames of modular steel buildings were found to possess significant and reliable overstrength. However, contrary to the prescription of many seismic design codes for regular buildings, this behaviour characteristic was found to depend on building height, increasing with a decrease in this height. It was therefore cautioned that the value prescribed by the current National Building Code of Canada may not be conservative for braced frames of modular steel buildings with more than six stories.

7) The research revealed that, in seismic analysis of braced frames of modular steel buildings, the use of median ground motions would yield satisfactory performance, in terms of drift demand, in any building category (i.e. post-disaster buildings, high importance buildings, or other buildings) in the current National Building Code of Canada . Thus, the NBCC drift limits for regular buildings provide conservative designs for modular steel buildings and are therefore recommended

8) The research revealed that, in the analysis of braced frames of modular steel buildings, floor-to-floor inter-storey drifts can satisfactorily represent inter-storey drift demand without explicitly considering the ceiling beam levels.

6.3 Recommendations for Further Studies

Modular Steel Buildings are fast evolving as an effective alternative to conventional on-site steel construction. This research has documented the development of the concept and application of this building system and has provided detailed description of its detailing requirements. This is expected to pave way for other researchers to study critical elements of this unique building system. Some aspects of the system have been addressed in the present study. The following recommendations are made for further investigations:

1. The interaction between ceiling framing and floor framing needs to be investigated for the configuration where the floor beams bear directly on the ceiling beams without mechanical connections except at column locations.

2. The behaviour of the horizontal connections of different modular units should be studied using three-dimensional analysis and component testing in order to ascertain their ability to transfer seismic forces within the floor to the lateral force resisting system.

3. A more extensive experimental investigation of full scale specimens, using more than one specimen, should be carried out to better understand the hysteretic and inelastic characteristics of the lateral force resisting frame and the distribution of lateral load into various members of the frame.

4. Studies should be conducted using other lateral load resisting systems such as moment frames in order to determine the most efficient configuration.

5. Investigations into the use of alternative components and detailing of vertical and horizontal connections of units of MSB should be carried out to improve upon the efficiency of the entire modular structural system.

6. Analytical studies should be conducted to study the application of the modular steel building technology to higher storey structures.

APPENDIX I: Sample SAP2000 Data File for Model of Modular Steel Floor Grid Structure

```
MODULAR STEEL SYSTEM

SYSTEM
  LENGTH=MM    FORCE=N

JOINTS                                  ; Define joints coodinates
   1 X=0  Y=0 Z=98.3
   2           Z=95.1
   12          Z=-95.1
  LGEN=2,12,1
   13 X=0  Y=0 Z=-98.3
   1561 X=0  Y=3600 Z=98.3
  LGEN=1,1561,13
  FGEN=1,1561,13,13,1
   1574 X=-66.5  Y=0 Z=98.3
   1582 X=66.5  Y=0 Z=98.3
   2654 X=-66.5  Y=3600 Z=98.3
  LGEN=1574,2654,9
  LGEN=1574,1582,1
  FGEN=1574,2654,9,1582,1
   2663 X=-66.5  Y=0 Z=-98.3
   2671 X=66.5  Y=0 Z=-98.3
   3743 X=-66.5  Y=3600 Z=-98.3
  LGEN=2663,2671,1
  LGEN=2663,3743,9
  FGEN=2663,3743,9,2671,1
   3752 X=1750  Y=0 Z=98.3
   3753          Z=95.1
   3763         Z=-95.1
  LGEN=3753,3763,1
   3764 X=1750  Y=0 Z=-98.3
   5312 X=1750  Y=3600 Z=98.3
  LGEN=3752,5312,13
  FGEN=3752,5312,13,3764,1
   5325 X=1683.5  Y=0 Z=98.3
   5333 X=1816.5  Y=0 Z=98.3
   6405 X=1683.5  Y=3600 Z=98.3
  LGEN=5325,6405,9
  LGEN=5325,5333,1
  FGEN=5325,6405,9,5333,1
   6414 X=1683.5  Y=0 Z=-98.3
   6422 X=1816.5  Y=0 Z=-98.3
   7494 X=1683.5  Y=3600 Z=-98.3
  LGEN=6414,6422,1
  LGEN=6414,7494,9
  FGEN=6414,7494,9,6422,1
   7503 X=3500  Y=0 Z=98.3
   7504          Z=95.1
   7514         Z=-95.1
  LGEN=7504,7514,1
   7515 X=3500  Y=0 Z=-98.3
   9063 X=3500  Y=3600 Z=98.3
  LGEN=7503,9063,13
  FGEN=7503,9063,13,7515,1
   9076 X=3433.5  Y=0 Z=98.3
   9084 X=3566.5  Y=0 Z=98.3
   10156 X=3433.5  Y=3600 Z=98.3
  LGEN=9076,10156,9
```

```
LGEN=9076,9084,1
FGEN=9076,10156,9,9084,1
 10165 X=3433.5  Y=0 Z=-98.3
 10173 X=3566.5  Y=0 Z=-98.3
 11245 X=3433.5  Y=3600 Z=-98.3
LGEN=10165,10173,1
LGEN=10165,11245,9
FGEN=10165,11245,9,10173,1
 11254 X=5250  Y=0 Z=98.3
 11255           Z=95.1
 11265          Z=-95.1
LGEN=11255,11265,1
 11266 X=5250  Y=0 Z=-98.3
 12814 X=5250  Y=3600 Z=98.3
LGEN=11254,12814,13
FGEN=11254,12814,13,11266,1
 12827 X=5183.5  Y=0 Z=98.3
 12835 X=5316.5  Y=0 Z=98.3
 13907 X=5183.5  Y=3600 Z=98.3
LGEN=12827,13907,9
LGEN=12827,12835,1
FGEN=12827,13907,9,12835,1
 13916 X=5183.5  Y=0 Z=-98.3
 13924 X=5316.5  Y=0 Z=-98.3
 14996 X=5183.5  Y=3600 Z=-98.3
LGEN=13916,13924,1
LGEN=13916,14996,9
FGEN=13916,14996,9,13924,1
 15005 X=7000  Y=0 Z=98.3
 15006           Z=95.1
 15016          Z=-95.1
LGEN=15006,15016,1
 15017 X=7000  Y=0 Z=-98.3
 16565 X=7000  Y=3600 Z=98.3
LGEN=15005,16565,13
FGEN=15005,16565,13,15017,1
 16578 X=6933.5  Y=0 Z=98.3
 16586 X=7066.5  Y=0 Z=98.3
 17658 X=6933.5  Y=3600 Z=98.3
LGEN=16578,17658,9
LGEN=16578,16586,1
FGEN=16578,17658,9,16586,1
 17667 X=6933.5  Y=0 Z=-98.3
 17675 X=7066.5  Y=0 Z=-98.3
 18747 X=6933.5  Y=3600 Z=-98.3
LGEN=17667,17675,1
LGEN=17667,18747,9
FGEN=17667,18747,9,17675,1
 18756 X=8250  Y=0 Z=98.3
 18757           Z=95.1
 18767          Z=-95.1
LGEN=18757,18767,1
 18768 X=8250  Y=0 Z=-98.3
 20316 X=8250  Y=3600 Z=98.3
LGEN=18756,20316,13
FGEN=18756,20316,13,18768,1
 20329 X=8183.5  Y=0 Z=98.3
 20337 X=8316.5  Y=0 Z=98.3
 21409 X=8183.5  Y=3600 Z=98.3
LGEN=20329,21409,9
LGEN=20329,20337,1
FGEN=20329,21409,9,20337,1
 21418 X=8183.5  Y=0 Z=-98.3
 21426 X=8316.5  Y=0 Z=-98.3
```

```
 22498 X=8183.5  Y=3600 Z=-98.3
LGEN=21418,21426,1
LGEN=21418,22498,9
FGEN=21418,22498,9,21426,1
 22507 X=9500  Y=0 Z=98.3
 22508          Z=95.1
 22518         Z=-95.1
LGEN=22508,22518,1
 22519 X=9500  Y=0 Z=-98.3
 24067 X=9500  Y=3600 Z=98.3
LGEN=22507,24067,13
FGEN=22507,24067,13,22519,1
 24080 X=9433.5  Y=0 Z=98.3
 24088 X=9566.5  Y=0 Z=98.3
 25160 X=9433.5  Y=3600 Z=98.3
LGEN=24080,25160,9
LGEN=24080,24088,1
FGEN=24080,25160,9,24088,1
 25169 X=9433.5  Y=0 Z=-98.3
 25177 X=9566.5  Y=0 Z=-98.3
 26249 X=9433.5  Y=3600 Z=-98.3
LGEN=25169,25177,1
LGEN=25169,26249,9
FGEN=25169,26249,9,25177,1
 26258 X=11250  Y=0 Z=98.3
 26259          Z=95.1
 26269         Z=-95.1
LGEN=26259,26269,1
 26270 X=11250  Y=0 Z=-98.3
 27818 X=11250  Y=3600 Z=98.3
LGEN=26258,27818,13
FGEN=26258,27818,13,26270,1
 27831 X=11183.5  Y=0 Z=98.3
 27839 X=11316.5  Y=0 Z=98.3
 28911 X=11183.5  Y=3600 Z=98.3
LGEN=27831,28911,9
LGEN=27831,27839,1
FGEN=27831,28911,9,27839,1
 28920 X=11183.5  Y=0 Z=-98.3
 28928 X=11316.5  Y=0 Z=-98.3
 30000 X=11183.5  Y=3600 Z=-98.3
LGEN=28920,28928,1
LGEN=28920,30000,9
FGEN=28920,30000,9,28928,1
 30009 X=13000  Y=0 Z=98.3
 30010           Z=95.1
 30020          Z=-95.1
LGEN=30010,30020,1
 30021 X=13000  Y=0 Z=-98.3
 31569 X=13000  Y=3600 Z=98.3
LGEN=30009,31569,13
FGEN=30009,31569,13,30021,1
 31582 X=12933.5  Y=0 Z=98.3
 31590 X=13066.5  Y=0 Z=98.3
 32662 X=12933.5  Y=3600 Z=98.3
LGEN=31582,32662,9
LGEN=31582,31590,1
FGEN=31582,32662,9,31590,1
 32671 X=12933.5  Y=0 Z=-98.3
 32679 X=13066.5  Y=0 Z=-98.3
 33751 X=12933.5  Y=3600 Z=-98.3
LGEN=32671,32679,1
LGEN=32671,33751,9
FGEN=32671,33751,9,32679,1
```

```
 33760 X=14750  Y=0 Z=98.3
 33761           Z=95.1
 33771          Z=-95.1
LGEN=33761,33771,1
 33772 X=14750  Y=0 Z=-98.3
 35320 X=14750  Y=3600 Z=98.3
LGEN=33760,35320,13
FGEN=33760,35320,13,33772,1
 35333 X=14683.5  Y=0 Z=98.3
 35341 X=14816.5  Y=0 Z=98.3
 36413 X=14683.5  Y=3600 Z=98.3
LGEN=35333,36413,9
LGEN=35333,35341,1
FGEN=35333,36413,9,35341,1
 36422 X=14683.5  Y=0 Z=-98.3
 36430 X=14816.5  Y=0 Z=-98.3
 37502 X=14683.5  Y=3600 Z=-98.3
LGEN=36422,36430,1
LGEN=36422,37502,9
FGEN=36422,37502,9,36430,1
 37511 X=16500  Y=0 Z=98.3
 37512           Z=95.1
 37522          Z=-95.1
LGEN=37512,37522,1
 37523 X=16500  Y=0 Z=-98.3
 39071 X=16500  Y=3600 Z=98.3
LGEN=37511,39071,13
FGEN=37511,39071,13,37523,1
 39084 X=16433.5  Y=0 Z=98.3
 39092 X=16566.5  Y=0 Z=98.3
 40164 X=16433.5  Y=3600 Z=98.3
LGEN=39084,40164,9
LGEN=39084,39092,1
FGEN=39084,40164,9,39092,1
 40173 X=16433.5  Y=0 Z=-98.3
 40181 X=16566.5  Y=0 Z=-98.3
 41253 X=16433.5  Y=3600 Z=-98.3
LGEN=40173,40181,1
LGEN=40173,41253,9
FGEN=40173,41253,9,40181,1
 41262 X=0 Y=3600 Z=120.65
 41263 X=0 Y=3600 Z=115.8
 41264 X=0 Y=3600 Z=98.3
 41265 X=0 Y=3600 Z=95.1
 41275 X=0 Y=3600 Z=-95.1
LGEN=41265,41275,1
 41276 X=0 Y=3600 Z=-98.3
 41280 X=0 Y=3600 Z=-174.8
LGEN=41276,41280,1
 41281 X=0 Y=3600 Z=-179.65
 47862 X=16500 Y=3600 Z=120.65
LGEN=41262,47862,20
FGEN=41262,47862,20,41281,1
 47882 X=0 Y=3682.5 Z=120.65
 47892 X=0 Y=3517.5 Z=120.65
 51512 X=16500 Y=3682.5 Z=120.65
LGEN=47882,47892,1
LGEN=47882,51512,11
FGEN=47882,51512,11,47892,1
 51523 X=0 Y=3682.5 Z=-179.65
 51533 X=0 Y=3517.5 Z=-179.65
 55153 X=16500 Y=3682.5 Z=-179.65
LGEN=51523,51533,1
LGEN=51523,55153,11
```

```
FGEN=51523,55153,11,51533,1
 55164 X=0 Y=0 Z=120.65
 55165 X=0 Y=0 Z=115.8
 55166 X=0 Y=0 Z=98.3
 55167 X=0 Y=0 Z=95.1
 55177 X=0 Y=0 Z=-95.1
LGEN=55167,55177,1
 55178 X=0 Y=0 Z=-98.3
 55182 X=0 Y=0 Z=-174.8
LGEN=55178,55182,1
 55183 X=0 Y=0 Z=-179.65
 61764 X=16500 Y=0 Z=120.65
LGEN=55164,61764,20
FGEN=55164,61764,20,55183,1
 61784 X=0 Y=82.5 Z=120.65
 61794 X=0 Y=-82.5 Z=120.65
 65414 X=16500 Y=82.5 Z=120.65
LGEN=61784,61794,1
LGEN=61784,65414,11
FGEN=61784,65414,11,61794,1
 65425 X=0 Y=82.5 Z=-179.65
 65435 X=0 Y=-82.5 Z=-179.65
 69055 X=16500 Y=82.5 Z=-179.65
LGEN=65425,65435,1
LGEN=65425,69055,11
FGEN=65425,69055,11,65435,1
 69066 X=-66.5 Y=0 Z=120.65
 69067 X=-66.5 Y=0 Z=115.8
 69068 X=-66.5 Y=0 Z=98.3
 69069 X=-66.5 Y=0 Z=95.1
 69079 X=-66.5 Y=0 Z=-95.1
LGEN=69069,69079,1
 69080 X=-66.5 Y=0 Z=-98.3
 69084 X=-66.5 Y=0 Z=-174.8
LGEN=69080,69084,1
 69085 X=-66.5 Y=0 Z=-179.65
 69086 X=-33.25 Y=0 Z=120.65
FGEN=69066,69085,1,69086,20
 69106 X=16533.25 Y=0 Z=120.65
 69107 X=16533.25 Y=0 Z=115.8
 69108                Z=98.3
 69109                Z=95.1
 69119                Z=-95.1
LGEN=69109,69119,1
 69120 X=16533.25 Y=0 Z=-98.3
 69124                Z=-174.8
LGEN=69120,69124,1
 69125 X=16533.25 Y=0 Z=-179.65
 69126 X=16566.5 Y=0 Z=120.65
FGEN=69106,69125,1,69126,20
 69146 X=-66.5 Y=82.5 Z=120.65
 69156 X=-66.5 Y=-82.5 Z=120.65
LGEN=69146,69156,1
 69157 X=-33.25 Y=82.5 Z=120.65
FGEN=69146,69156,1,69157,11
 69168 X=16533.25 Y=82.5 Z=120.65
 69178           Y=-82.5
LGEN=69168,69178,1
 69179 X=16566.5 Y=82.5 Z=120.65
FGEN=69168,69178,1,69179,11
 69190 X=-66.5 Y=82.5 Z=-179.65
 69200         Y=-82.5
LGEN=69190,69200,1
 69201 X=-33.25 Y=82.5 Z=-179.65
```

```
  FGEN=69190,69200,1,69201,11
   69212 X=16533.25 Y=82.5 Z=-179.65
   69222            Y=-82.5
  LGEN=69212,69222,1
   69223 X=16566.5 Y=82.5 Z=-179.65
  FGEN=69212,69222,1,69223,11
   69234 X=-66.5 Y=3600 Z=120.65
   69235 X=-66.5 Y=3600 Z=115.8
   69236 X=-66.5 Y=3600 Z=98.3
   69237 X=-66.5 Y=3600 Z=95.1
   69247 X=-66.5 Y=3600 Z=-95.1
  LGEN=69237,69247,1
   69248 X=-66.5 Y=3600 Z=-98.3
   69252 X=-66.5 Y=3600 Z=-174.8
  LGEN=69248,69252,1
   69253 X=-66.5 Y=3600 Z=-179.65
   69254 X=-33.25 Y=3600 Z=120.65
  FGEN=69234,69253,1,69254,20
   69274 X=16533.25 Y=3600 Z=120.65
   69275 X=16533.25 Y=3600 Z=115.8
   69276                   Z=98.3
   69277                   Z=95.1
   69287                   Z=-95.1
  LGEN=69277,69287,1
   69288 X=16533.25 Y=3600 Z=-98.3
   69292                   Z=-174.8
  LGEN=69288,69292,1
   69293 X=16533.25 Y=3600 Z=-179.65
   69294 X=16566.5 Y=3600 Z=120.65
  FGEN=69274,69293,1,69294,20
   69314 X=-66.5 Y=3682.5 Z=120.65
   69324 X=-66.5 Y=3517.5 Z=120.65
  LGEN=69314,69324,1
   69325 X=-33.25 Y=3682.5 Z=120.65
  FGEN=69314,69324,1,69325,11
   69336 X=16533.25 Y=3682.5 Z=120.65
   69346            Y=3517.5
  LGEN=69336,69346,1
   69347 X=16566.5 Y=3682.5 Z=120.65
  FGEN=69336,69346,1,69347,11
   69358 X=-66.5 Y=3682.5 Z=-179.65
   69368         Y=3517.5
  LGEN=69358,69368,1
   69369 X=-33.25 Y=3682.5 Z=-179.65
  FGEN=69358,69368,1,69369,11
   69380 X=16533.25 Y=3682.5 Z=-179.65
   69390            Y=3517.5
  LGEN=69380,69390,1
   69391 X=16566.5 Y=3682.5 Z=-179.65
  FGEN=69380,69390,1,69391,11

RESTRAINT
  ADD=2114,2122,1     DOF=UX
  REM=2118            DOF=UX
  ADD=5865,5873,1     DOF=UX
  REM=5869            DOF=UX
  ADD=9616,9624,1     DOF=UX
  REM=9620            DOF=UX
  ADD=13367,13375,1   DOF=UX
  REM=13371           DOF=UX
  ADD=17118,17126,1   DOF=UX
  REM=17122           DOF=UX
  ADD=20869,20877,1   DOF=UX
  REM=20873           DOF=UX
```

```
ADD=24620,24628,1   DOF=UX
REM=24624           DOF=UX
ADD=28371,28379,1   DOF=UX
REM=28375           DOF=UX
ADD=32122,32130,1   DOF=UX
REM=32126           DOF=UX
ADD=35873,35881,1   DOF=UX
REM=35877           DOF=UX
ADD=39624,39632,1   DOF=UX
REM=39628           DOF=UX
ADD=47882,47892,1   DOF=UY
REM=47887           DOF=UY
ADD=48267,48277,1   DOF=UY
REM=48272           DOF=UY
ADD=48652,48662,1   DOF=UY
REM=48657           DOF=UY
ADD=49037,49047,1   DOF=UY
REM=49042           DOF=UY
ADD=49422,49432,1   DOF=UY
REM=49427           DOF=UY
ADD=49697,49707,1   DOF=UY
REM=49702           DOF=UY
ADD=49972,49982,1   DOF=UY
REM=49977           DOF=UY
ADD=50357,50367,1   DOF=UY
REM=50362           DOF=UY
ADD=50742,50752,1   DOF=UY
REM=50747           DOF=UY
ADD=51127,51137,1   DOF=UY
REM=51132           DOF=UY
ADD=51512,51522,1   DOF=UY
REM=51517           DOF=UY
ADD=61784,61794,1   DOF=UY
REM=61789           DOF=UY
ADD=62169,62179,1   DOF=UY
REM=62174           DOF=UY
ADD=62554,62564,1   DOF=UY
REM=62559           DOF=UY
ADD=62939,62949,1   DOF=UY
REM=62944           DOF=UY
ADD=63324,63334,1   DOF=UY
REM=63329           DOF=UY
ADD=63599,63609,1   DOF=UY
REM=63604           DOF=UY
ADD=63874,63884,1   DOF=UY
REM=63879           DOF=UY
ADD=64259,64269,1   DOF=UY
REM=64264           DOF=UY
ADD=64644,64654,1   DOF=UY
REM=64649           DOF=UY
ADD=65029,65039,1   DOF=UY
REM=65034           DOF=UY
ADD=65414,65424,1   DOF=UY
REM=65419           DOF=UY
ADD=51523,51533,1       DOF=UY,UZ
REM=51528               DOF=UY,UZ
ADD=53063,53073,1       DOF=UX,UY,UZ
REM=53068               DOF=UX,UY,UZ
ADD=53613,53623,1       DOF=UY,UZ
REM=53618               DOF=UY,UZ
ADD=55153,55163,1       DOF=UY,UZ
REM=55158               DOF=UY,UZ
ADD=65425,65435,1       DOF=UY,UZ
REM=65430               DOF=UY,UZ
```

```
  ADD=66965,66975,1        DOF=UX,UY,UZ
  REM=66970                DOF=UX,UY,UZ
  ADD=67515,67525,1        DOF=UY,UZ
  REM=67520                DOF=UY,UZ
  ADD=69055,69065,1        DOF=UY,UZ
  REM=69060                DOF=UY,UZ

WELD                              ; All top and bottom flanges with webs
constraints and welds
 NAME=SB1T TOL=0.000001
  ADD=1,1561,13
  ADD=1578,2658,9
 NAME=SB1B TOL=0.000001
  ADD=13,1573,13
  ADD=2667,3747,9
 NAME=SB2T TOL=0.000001
  ADD=3752,5312,13
  ADD=5329,6409,9
 NAME=SB2B TOL=0.000001
  ADD=3764,5324,13
  ADD=6418,7498,9
 NAME=SB3T TOL=0.000001
  ADD=7503,9063,13
  ADD=9080,10160,9
 NAME=SB3B TOL=0.000001
  ADD=7515,9075,13
  ADD=10169,11249,9
 NAME=SB4T TOL=0.000001
  ADD=11254,12814,13
  ADD=12831,13911,9
 NAME=SB4B TOL=0.000001
  ADD=11266,12826,13
  ADD=13920,15000,9
 NAME=SB5T TOL=0.000001
  ADD=15005,16565,13
  ADD=16582,17662,9
 NAME=SB5B TOL=0.000001
  ADD=15017,16577,13
  ADD=17671,18751,9
 NAME=SB6T TOL=0.000001
  ADD=18756,20316,13
  ADD=20333,21413,9
 NAME=SB6B TOL=0.000001
  ADD=18768,20328,13
  ADD=21422,22502,9
 NAME=SB7T TOL=0.000001
  ADD=22507,24067,13
  ADD=24084,25164,9
 NAME=SB7B TOL=0.000001
  ADD=22519,24079,13
  ADD=25173,26253,9
 NAME=SB8T TOL=0.000001
  ADD=26258,27818,13
  ADD=27835,28915,9
 NAME=SB8B TOL=0.000001
  ADD=26270,27830,13
  ADD=28924,30004,9
 NAME=SB9T TOL=0.000001
  ADD=30009,31569,13
  ADD=31586,32666,9
 NAME=SB9B TOL=0.000001
  ADD=30021,31581,13
  ADD=32675,33755,9
 NAME=SB10T TOL=0.000001
```

```
 ADD=33760,35320,13
 ADD=35337,36417,9
NAME=SB10B TOL=0.000001
 ADD=33772,35332,13
 ADD=36426,37506,9
NAME=SB11T TOL=0.000001
 ADD=37511,39071,13
 ADD=39088,40168,9
NAME=SB11B TOL=0.000001
 ADD=37523,39083,13
 ADD=40177,41257,9
NAME=MB1T TOL=0.000001
 ADD=41262,47862,20
 ADD=47887,51517,11
NAME=MB1TCL TOL=0.000001
 ADD=69234,69254,20
 ADD=69319,69330,11
NAME=MB1TCR TOL=0.000001
 ADD=69274,69294,20
 ADD=69341,69352,11
NAME=MB1B TOL=0.000001
 ADD=41281,47881,20
 ADD=51528,55158,11
NAME=MB1BCL TOL=0.000001
 ADD=69253,69273,20
 ADD=69363,69374,11
NAME=MB1BCR TOL=0.000001
 ADD=69293,69313,20
 ADD=69385,69396,11
NAME=MB2T TOL=0.000001
 ADD=55164,61764,20
 ADD=61789,65419,11
NAME=MB2TCL TOL=0.000001
 ADD=69066,69086,20
 ADD=69151,69162,11
NAME=MB2TCR TOL=0.000001
 ADD=69106,69126,20
 ADD=69173,69184,11
NAME=MB2B TOL=0.000001
 ADD=55183,61783,20
 ADD=65430,69060,11
NAME=MB2BCL TOL=0.000001
 ADD=69085,69105,20
 ADD=69195,69206,11
NAME=MB2BCR TOL=0.000001
 ADD=69125,69145,20
 ADD=69217,69228,11
NAME=SB1LMB2
 ADD=3,11,1
 ADD=55168,55176,1
NAME=SB1RMB1
 ADD=1563,1571,1
 ADD=41266,41274,1
NAME=SB2LMB2
 ADD=3754,3762,1
 ADD=55868,55876,1
NAME=SB2RMB1
 ADD=5314,5322,1
 ADD=41966,41974,1
NAME=SB3LMB2
 ADD=7505,7513,1
 ADD=56568,56576,1
NAME=SB3RMB1
 ADD=9065,9073,1
```

```
 ADD=42666,42674,1
NAME=SB4LMB2
 ADD=11256,11264,1
 ADD=57268,57276,1
NAME=SB4RMB1
 ADD=12816,12824,1
 ADD=43366,43374,1
NAME=SB5LMB2
 ADD=15007,15015,1
 ADD=57968,57976,1
NAME=SB5RMB1
 ADD=16567,16575,1
 ADD=44066,44074,1
NAME=SB6LMB2
 ADD=18758,18766,1
 ADD=58468,58476,1
NAME=SB6RMB1
 ADD=20318,20326,1
 ADD=44566,44574,1
NAME=SB7LMB2
 ADD=22509,22517,1
 ADD=58968,58976,1
NAME=SB7RMB1
 ADD=24069,24077,1
 ADD=45066,45074,1
NAME=SB8LMB2
 ADD=26260,26268,1
 ADD=59668,59676,1
NAME=SB8RMB1
 ADD=27820,27828,1
 ADD=45766,45774,1
NAME=SB9LMB2
 ADD=30011,30019,1
 ADD=60368,60376,1
NAME=SB9RMB1
 ADD=31571,31579,1
 ADD=46466,46474,1
NAME=S10LMB2
 ADD=33762,33770,1
 ADD=61068,61076,1
NAME=S10RMB1
 ADD=35322,35330,1
 ADD=47166,47174,1
NAME=S11LMB2
 ADD=37513,37521,1
 ADD=61768,61776,1
NAME=S11RMB1
 ADD=39073,39081,1
 ADD=47866,47874,1

MATERIAL                        ; Material Properties used by the Shell
Elements
 NAME=STEEL  TYPE=ISO  IDES=S  M=7850E-09  W=77008E-09
  E=200000  U=0.3

SHELL SECTION
 NAME=SEC1  TYPE=SHELL, THIN  MAT=STEEL  TH=5.0
 NAME=SEC2  TYPE=SHELL, THIN  MAT=STEEL  TH=5.0
 NAME=SEC3  TYPE=SHELL, THIN  MAT=STEEL  TH=6.4
 NAME=SEC4  TYPE=SHELL, THIN  MAT=STEEL  TH=5.8
 NAME=SEC5  TYPE=SHELL, THIN  MAT=STEEL  TH=5.8
 NAME=SEC6  TYPE=SHELL, THIN  MAT=STEEL  TH=9.7
```

```
SHELL
 E00001  J=1,2,14,15  SEC=SEC1
 E01429  J=1548,1549,1561,1562
  GEN=E00001,E01429,12   JINC=13
 E00012  J=12,13,25,26
 E01440  J=1559,1560,1572,1573
  GEN=E00012,E01440,12   JINC=13
 E00002  J=2,3,15,16  SEC=SEC2
 E00011  J=11,12,24,25
 E01430  J=1549,1550,1562,1563
  GEN=E00002,E00011,1,E01430,12  JINC=1,13
 E01441  J=1574,1575,1583,1584  SEC=SEC3
 E01448  J=1581,1582,1590,1591
 E02393  J=2645,2646,2654,2655
  GEN=E01441,E01448,1,E02393,8  JINC=1,9
 E02401  J=2663,2664,2672,2673  SEC=SEC3
 E02408  J=2670,2671,2679,2680
 E03353  J=3734,3735,3743,3744
  GEN=E02401,E02408,1,E03353,8  JINC=1,9
 E03361  J=3752,3753,3765,3766  SEC=SEC1
 E04789  J=5299,5300,5312,5313
  GEN=E03361,E04789,12   JINC=13
 E03372  J=3763,3764,3776,3777
 E04800  J=5310,5311,5323,5324
  GEN=E03372,E04800,12   JINC=13
 E03362  J=3753,3754,3766,3767  SEC=SEC2
 E03371  J=3762,3763,3775,3776
 E04790  J=5300,5301,5313,5314
  GEN=E03362,E03371,1,E04790,12  JINC=1,13
 E04801  J=5325,5326,5334,5335  SEC=SEC3
 E04808  J=5332,5333,5341,5342
 E05753  J=6396,6397,6405,6406
  GEN=E04801,E04808,1,E05753,8  JINC=1,9
 E05761  J=6414,6415,6423,6424  SEC=SEC3
 E05768  J=6421,6422,6430,6431
 E06713  J=7485,7486,7494,7495
  GEN=E05761,E05768,1,E06713,8  JINC=1,9
 E06721  J=7503,7504,7516,7517  SEC=SEC1
 E08149  J=9050,9051,9063,9064
  GEN=E06721,E08149,12   JINC=13
 E06732  J=7514,7515,7527,7528
 E08160  J=9061,9062,9074,9075
  GEN=E06732,E08160,12   JINC=13
 E06722  J=7504,7505,7517,7518  SEC=SEC2
 E06731  J=7513,7514,7526,7527
 E08150  J=9051,9052,9064,9065
  GEN=E06722,E06731,1,E08150,12  JINC=1,13
 E08161  J=9076,9077,9085,9086  SEC=SEC3
 E08168  J=9083,9084,9092,9093
 E09113  J=10147,10148,10156,10157
  GEN=E08161,E08168,1,E09113,8  JINC=1,9
 E09121  J=10165,10166,10174,10175  SEC=SEC3
 E09128  J=10172,10173,10181,10182
 E10073  J=11236,11237,11245,11246
  GEN=E09121,E09128,1,E10073,8  JINC=1,9
 E10081  J=11254,11255,11267,11268  SEC=SEC1
 E11509  J=12801,12802,12814,12815
  GEN=E10081,E11509,12   JINC=13
 E10092  J=11265,11266,11278,11279
 E11520  J=12812,12813,12825,12826
  GEN=E10092,E11520,12   JINC=13
 E10082  J=11255,11256,11268,11269  SEC=SEC2
 E10091  J=11264,11265,11277,11278
 E11510  J=12802,12803,12815,12816
```

```
 GEN=E10082,E10091,1,E11510,12  JINC=1,13
E11521  J=12827,12828,12836,12837  SEC=SEC3
E11528  J=12834,12835,12843,12844
E12473  J=13898,13899,13907,13908
 GEN=E11521,E11528,1,E12473,8  JINC=1,9
E12481  J=13916,13917,13925,13926  SEC=SEC3
E12488  J=13923,13924,13932,13933
E13433  J=14987,14988,14996,14997
 GEN=E12481,E12488,1,E13433,8  JINC=1,9
E13441  J=15005,15006,15018,15019  SEC=SEC1
E14869  J=16552,16553,16565,16566
 GEN=E13441,E14869,12   JINC=13
E13452  J=15016,15017,15029,15030
E14880  J=16563,16564,16576,16577
 GEN=E13452,E14880,12   JINC=13
E13442  J=15006,15007,15019,15020  SEC=SEC2
E13451  J=15015,15016,15028,15029
E14870  J=16553,16554,16566,16567
 GEN=E13442,E13451,1,E14870,12  JINC=1,13
E14881  J=16578,16579,16587,16588  SEC=SEC3
E14888  J=16585,16586,16594,16595
E15833  J=17649,17650,17658,17659
 GEN=E14881,E14888,1,E15833,8  JINC=1,9
E15841  J=17667,17668,17676,17677  SEC=SEC3
E15848  J=17674,17675,17683,17684
E16793  J=18738,18739,18747,18748
 GEN=E15841,E15848,1,E16793,8  JINC=1,9
E16801  J=18756,18757,18769,18770  SEC=SEC1
E18229  J=20303,20304,20316,20317
 GEN=E16801,E18229,12   JINC=13
E16812  J=18767,18768,18780,18781
E18240  J=20314,20315,20327,20328
 GEN=E16812,E18240,12   JINC=13
E16802  J=18757,18758,18770,18771  SEC=SEC2
E16811  J=18766,18767,18779,18780
E18230  J=20304,20305,20317,20318
 GEN=E16802,E16811,1,E18230,12  JINC=1,13
E18241  J=20329,20330,20338,20339  SEC=SEC3
E18248  J=20336,20337,20345,20346
E19193  J=21400,21401,21409,21410
 GEN=E18241,E18248,1,E19193,8  JINC=1,9
E19201  J=21418,21419,21427,21428  SEC=SEC3
E19208  J=21425,21426,21434,21435
E20153  J=22489,22490,22498,22499
 GEN=E19201,E19208,1,E20153,8  JINC=1,9
E20161  J=22507,22508,22520,22521  SEC=SEC1
E21589  J=24054,24055,24067,24068
 GEN=E20161,E21589,12   JINC=13
E20172  J=22518,22519,22531,22532
E21600  J=24065,24066,24078,24079
 GEN=E20172,E21600,12   JINC=13
E20162  J=22508,22509,22521,22522  SEC=SEC2
E20171  J=22517,22518,22530,22531
E21590  J=24055,24056,24068,24069
 GEN=E20162,E20171,1,E21590,12  JINC=1,13
E21601  J=24080,24081,24089,24090  SEC=SEC3
E21608  J=24087,24088,24096,24097
E22553  J=25151,25152,25160,25161
 GEN=E21601,E21608,1,E22553,8  JINC=1,9
E22561  J=25169,25170,25178,25179  SEC=SEC3
E22568  J=25176,25177,25185,25186
E23513  J=26240,26241,26249,26250
 GEN=E22561,E22568,1,E23513,8  JINC=1,9
E23521  J=26258,26259,26271,26272  SEC=SEC1
```

```
E24949  J=27805,27806,27818,27819
 GEN=E23521,E24949,12   JINC=13
E23532  J=26269,26270,26282,26283
E24960  J=27816,27817,27829,27830
 GEN=E23532,E24960,12   JINC=13
E23522  J=26259,26260,26272,26273  SEC=SEC2
E23531  J=26268,26269,26281,26282
E24950  J=27806,27807,27819,27820
 GEN=E23522,E23531,1,E24950,12  JINC=1,13
E24961  J=27831,27832,27840,27841  SEC=SEC3
E24968  J=27838,27839,27847,27848
E25913  J=28902,28903,28911,28912
 GEN=E24961,E24968,1,E25913,8  JINC=1,9
E25921  J=28920,28921,28929,28930  SEC=SEC3
E25928  J=28927,28928,28936,28937
E26873  J=29991,29992,30000,30001
 GEN=E25921,E25928,1,E26873,8  JINC=1,9
E26881  J=30009,30010,30022,30023  SEC=SEC1
E28309  J=31556,31557,31569,31570
 GEN=E26881,E28309,12   JINC=13
E26892  J=30020,30021,30033,30034
E28320  J=31567,31568,31580,31581
 GEN=E26892,E28320,12   JINC=13
E26882  J=30010,30011,30023,30024  SEC=SEC2
E26891  J=30019,30020,30032,30033
E28310  J=31557,31558,31570,31571
 GEN=E26882,E26891,1,E28310,12  JINC=1,13
E28321  J=31582,31583,31591,31592  SEC=SEC3
E28328  J=31589,31590,31598,31599
E29273  J=32653,32654,32662,32663
 GEN=E28321,E28328,1,E29273,8  JINC=1,9
E29281  J=32671,32672,32680,32681  SEC=SEC3
E29288  J=32678,32679,32687,32688
E30233  J=33742,33743,33751,33752
 GEN=E29281,E29288,1,E30233,8  JINC=1,9
E30241  J=33760,33761,33773,33774  SEC=SEC1
E31669  J=35307,35308,35320,35321
 GEN=E30241,E31669,12   JINC=13
E30252  J=33771,33772,33784,33785
E31680  J=35318,35319,35331,35332
 GEN=E30252,E31680,12   JINC=13
E30242  J=33761,33762,33774,33775  SEC=SEC2
E30251  J=33770,33771,33783,33784
E31670  J=35308,35309,35321,35322
 GEN=E30242,E30251,1,E31670,12  JINC=1,13
E31681  J=35333,35334,35342,35343  SEC=SEC3
E31688  J=35340,35341,35349,35350
E32633  J=36404,36405,36413,36414
 GEN=E31681,E31688,1,E32633,8  JINC=1,9
E32641  J=36422,36423,36431,36432  SEC=SEC3
E32648  J=36429,36430,36438,36439
E33593  J=37493,37494,37502,37503
 GEN=E32641,E32648,1,E33593,8  JINC=1,9
E33601  J=37511,37512,37524,37525  SEC=SEC1
E35029  J=39058,39059,39071,39072
 GEN=E33601,E35029,12   JINC=13
E33612  J=37522,37523,37535,37536
E35040  J=39069,39070,39082,39083
 GEN=E33612,E35040,12   JINC=13
E33602  J=37512,37513,37525,37526  SEC=SEC2
E33611  J=37521,37522,37534,37535
E35030  J=39059,39060,39072,39073
 GEN=E33602,E33611,1,E35030,12  JINC=1,13
E35041  J=39084,39085,39093,39094  SEC=SEC3
```

```
E35048  J=39091,39092,39100,39101
E35993  J=40155,40156,40164,40165
 GEN=E35041,E35048,1,E35993,8  JINC=1,9
E36001  J=40173,40174,40182,40183  SEC=SEC3
E36008  J=40180,40181,40189,40190
E36953  J=41244,41245,41253,41254
 GEN=E36001,E36008,1,E36953,8  JINC=1,9
E36961  J=41262,41263,41282,41283  SEC=SEC4
E43212  J=47842,47843,47862,47863
 GEN=E36961,E43212,19   JINC=20
E49831  J=69234,69235,69254,69255
E49850  J=69254,69255,41262,41263
E49869  J=47862,47863,69274,69275
E49888  J=69274,69275,69294,69295
E36979  J=41280,41281,41300,41301  SEC=SEC4
E43230  J=47860,47861,47880,47881
 GEN=E36979,E43230,19   JINC=20
E49849  J=69252,69253,69272,69273
E49868  J=69272,69273,41280,41281
E49887  J=47880,47881,69292,69293
E49906  J=69292,69293,69312,69313
E36962  J=41263,41264,41283,41284  SEC=SEC5
E36978  J=41279,41280,41299,41300
E47863  J=47843,47844,47863,47864
 GEN=E36962,E36978,1,E43213,19  JINC=1,20
E49832  J=69235,69236,69255,69256
E49848  J=69251,69252,69271,69272
 GEN=E49832,E49848,1  JINC=1
E49851  J=69255,69256,41263,41264
E49867  J=69271,69272,41279,41280
 GEN=E49851,E49867,1  JINC=1
E49870  J=47863,47864,69275,69276
E49886  J=47879,47880,69291,69292
 GEN=E49870,E49886,1  JINC=1
E49889  J=69275,69276,69295,69296
E49905  J=69291,69292,69311,69312
 GEN=E49889,E49905,1  JINC=1
E43231  J=47882,47883,47893,47894  SEC=SEC6
E43240  J=47891,47892,47902,47903
E46521  J=51501,51502,51512,51513
 GEN=E43231,E43240,1,E46521,10  JINC=1,11
E49907  J=69314,69315,69325,69326
E49916  J=69323,69324,69334,69335
 GEN=E49907,E49916,1  JINC=1
E49917  J=69325,69326,47882,47883
E49926  J=69334,69335,47891,47892
 GEN=E49917,E49926,1  JINC=1
E49927  J=51512,51513,69336,69337
E49936  J=51521,51522,69345,69346
 GEN=E49927,E49936,1  JINC=1
E49937  J=69336,69337,69347,69348
E49946  J=69345,69346,69356,69357
 GEN=E49937,E49946,1  JINC=1
E46531  J=51523,51524,51534,51535  SEC=SEC6
E46540  J=51532,51533,51543,51544
E49821  J=55142,55143,55153,55154
 GEN=E46531,E46540,1,E49821,10  JINC=1,11
E49947  J=69358,69359,69369,69370
E49956  J=69367,69368,69378,69379
 GEN=E49947,E49956,1  JINC=1
E49957  J=69369,69370,51523,51524
E49966  J=69378,69379,51532,51533
 GEN=E49957,E49966,1  JINC=1
E49967  J=55153,55154,69380,69381
```

```
E49976  J=55162,55163,69389,69390
 GEN=E49967,E49976,1  JINC=1
E49977  J=69380,69381,69391,69392
E49986  J=69389,69390,69400,69401
 GEN=E49977,E49986,1  JINC=1
E49987  J=55164,55165,55184,55185  SEC=SEC4
E56238  J=61744,61745,61764,61765
 GEN=E49987,E56238,19   JINC=20
E62857  J=69066,69067,69086,69087
E62876  J=69086,69087,55164,55165
E62895  J=61764,61765,69106,69107
E62914  J=69106,69107,69126,69127
E50005  J=55182,55183,55202,55203  SEC=SEC4
E56256  J=61762,61763,61782,61783
 GEN=E50005,E56256,19   JINC=20
E62875  J=69084,69085,69104,69105
E62894  J=69104,69105,55182,55183
E62913  J=61782,61783,69124,69125
E62932  J=69124,69125,69144,69145
E49988  J=55165,55166,55185,55186  SEC=SEC5
E50004  J=55181,55182,55201,55202
E56239  J=61745,61746,61765,61766
 GEN=E49988,E50004,1,E56239,19  JINC=1,20
E62858  J=69067,69068,69087,69088
E62874  J=69083,69084,69103,69104
 GEN=E62858,E62874,1  JINC=1
E62877  J=69087,69088,55165,55166
E62893  J=69103,69104,55181,55182
 GEN=E62877,E62893,1  JINC=1
E62896  J=61765,61766,69107,69108
E62912  J=61781,61782,69123,69124
 GEN=E62896,E62912,1  JINC=1
E62915  J=69107,69108,69127,69128
E62931  J=69123,69124,69143,69144
 GEN=E62915,E62931,1  JINC=1
E56257  J=61784,61785,61795,61796  SEC=SEC6
E56266  J=61793,61794,61804,61805
E59547  J=65403,65404,65414,65415
 GEN=E56257,E56266,1,E59547,10  JINC=1,11
E62933  J=69146,69147,69157,69158
E62942  J=69155,69156,69166,69167
 GEN=E62933,E62942,1  JINC=1
E62943  J=69157,69158,61784,61785
E62952  J=69166,69167,61793,61794
 GEN=E62943,E62952,1  JINC=1
E62953  J=65414,65415,69168,69169
E62962  J=65423,65424,69177,69178
 GEN=E62953,E62962,1  JINC=1
E62963  J=69168,69169,69179,69180
E62972  J=69177,69178,69188,69189
 GEN=E62963,E62972,1  JINC=1
E59557  J=65425,65426,65436,65437  SEC=SEC6
E59566  J=65434,65435,65445,65446
E62847  J=69044,69045,69055,69056
 GEN=E59557,E59566,1,E62847,10  JINC=1,11
E62973  J=69190,69191,69201,69202
E62982  J=69199,69200,69210,69211
 GEN=E62973,E62982,1  JINC=1
E62983  J=69201,69202,65425,65426
E62992  J=69210,69211,65434,65435
 GEN=E62983,E62992,1  JINC=1
E62993  J=69055,69056,69212,69213
E63002  J=69064,69065,69221,69222
 GEN=E62993,E63002,1  JINC=1
```

```
 E63003  J=69212,69213,69223,69224
 E63012  J=69221,69222,69232,69233
  GEN=E63003,E63012,1  JINC=1

LOAD
 NAME=SELF        SW=1
 NAME=ESBDL
  TYPE=UNIF
  ADD=E01441,E01448,1,E02393,8     UZ=-78.11E-03
  ADD=E35041,E35048,1,E35993,8     UZ=-78.11E-03
 NAME=ESBLL
  TYPE=UNIF
  ADD=E01441,E01448,1,E02393,8     UZ=-23.684E-03
  ADD=E35041,E35048,1,E35993,8     UZ=-23.684E-03
 NAME=ISB1DL
  TYPE=UNIF
  ADD=E04801,E04808,1,E05753,8     UZ=-53.20E-03
  ADD=E08161,E08168,1,E09113,8     UZ=-53.20E-03
  ADD=E11521,E11528,1,E12473,8     UZ=-53.20E-03
  ADD=E24961,E24968,1,E25913,8     UZ=-53.20E-03
  ADD=E28321,E28328,1,E29273,8     UZ=-53.20E-03
  ADD=E31681,E31688,1,E32633,8     UZ=-53.20E-03
 NAME=ISB1LL
  TYPE=UNIF
  ADD=E04801,E04808,1,E05753,8     UZ=-47.37E-03
  ADD=E08161,E08168,1,E09113,8     UZ=-47.37E-03
  ADD=E11521,E11528,1,E12473,8     UZ=-47.37E-03
  ADD=E24961,E24968,1,E25913,8     UZ=-47.37E-03
  ADD=E28321,E28328,1,E29273,8     UZ=-47.37E-03
  ADD=E31681,E31688,1,E32633,8     UZ=-47.37E-03
 NAME=ISB2DL
  TYPE=UNIF
  ADD=E14881,E14888,1,E15833,8     UZ=-95.12E-03
  ADD=E21601,E21608,1,E22553,8     UZ=-95.12E-03
 NAME=ISB2LL
  TYPE=UNIF
  ADD=E14881,E14888,1,E15833,8     UZ=-46.24E-03
  ADD=E21601,E21608,1,E22553,8     UZ=-46.24E-03
 NAME=ISB3DL
  TYPE=UNIF
  ADD=E18241,E18248,1,E19193,8     UZ=-38.06E-03
 NAME=ISB3LL
  TYPE=UNIF
  ADD=E18241,E18248,1,E19193,8     UZ=-45.11E-03
 NAME=MBDL
  TYPE=UNIF
  ADD=E56257,E56266,1,E59547,10    UZ=-49.45E-03
  ADD=E62933,E62942,1,E62943,10    UZ=-49.45E-03
  ADD=E62953,E62962,1,E62963,10    UZ=-49.45E-03
  ADD=E43231,E43240,1,E46521,10    UZ=-49.45E-03
  ADD=E49907,E49916,1,E49917,10    UZ=-49.45E-03
  ADD=E49927,E49936,1,E49937,10    UZ=-49.45E-03

COMBO
 NAME=COMBOS  TYPE=ADD
  LOAD=SELF     SF=1
  LOAD=ESBDL    SF=1
  LOAD=ESBLL    SF=1
  LOAD=ISB1DL   SF=1
  LOAD=ISB1LL   SF=1
  LOAD=ISB2DL   SF=1
  LOAD=ISB2LL   SF=1
  LOAD=ISB3DL   SF=1
  LOAD=ISB3LL   SF=1
```

```
  LOAD=MBDL      SF=1
 NAME=COMBOF   TYPE=ADD
  LOAD=SELF      SF=1.25
  LOAD=ESBDL     SF=1.25
  LOAD=ESBLL     SF=1.5
  LOAD=ISB1DL    SF=1.25
  LOAD=ISB1LL    SF=1.5
  LOAD=ISB2DL    SF=1.25
  LOAD=ISB2LL    SF=1.5
  LOAD=ISB3DL    SF=1.25
  LOAD=ISB3LL    SF=1.5
  LOAD=MBDL      SF=1.25
 NAME=WORSE   TYPE=ENVE
  COMB=COMBOS    SF=1
  COMB=COMBOF    SF=1

END
```

APPENDIX II – Sample Data Used in Multiple Regression Analysis

L_s/d_s	L_w/d_s	t_{wb}/t_{ws}	d_b/d_s	B/t_{wb}
17.73	0.80	1.16	1.53	688.90
17.73	0.80	1.16	2.34	822.97
17.73	0.80	1.16	3.18	879.97
17.73	0.80	2.32	1.53	57.00
17.73	0.80	2.32	2.34	93.88
17.73	0.80	2.32	3.18	95.05
17.73	0.80	3.48	1.53	11.23
17.73	0.80	3.48	2.34	23.69
17.73	0.80	3.48	3.18	29.30
17.73	0.40	1.16	1.53	516.23
17.73	0.40	1.16	2.34	613.12
17.73	0.40	1.16	3.18	689.11
17.73	0.40	2.32	1.53	35.35
17.73	0.40	2.32	2.34	51.21
17.73	0.40	2.32	3.18	59.70
17.73	0.40	3.48	1.53	7.45
17.73	0.40	3.48	2.34	12.61
17.73	0.40	3.48	3.18	15.53
35.47	0.80	1.16	1.53	345.81
35.47	0.80	1.16	2.34	437.81
35.47	0.80	1.16	3.18	452.44
35.47	0.80	2.32	1.53	27.84
35.47	0.80	2.32	2.34	57.43
35.47	0.80	2.32	3.18	67.04
35.47	0.80	3.48	1.53	4.58
35.47	0.80	3.48	2.34	12.24
35.47	0.80	3.48	3.18	16.64
35.47	0.40	1.16	1.53	190.30
35.47	0.40	1.16	2.34	242.58
35.47	0.40	1.16	3.18	272.77
35.47	0.40	2.32	1.53	14.63
35.47	0.40	2.32	2.34	26.34
35.47	0.40	2.32	3.18	31.84
35.47	0.40	3.48	1.53	3.07
35.47	0.40	3.48	2.34	6.65
35.47	0.40	3.48	3.18	8.78
53.20	0.80	1.16	1.53	248.37
53.20	0.80	1.16	2.34	333.49
53.20	0.80	1.16	3.18	340.71
53.20	0.80	2.32	1.53	17.44
53.20	0.80	2.32	2.34	42.04
53.20	0.80	2.32	3.18	51.60
53.20	0.80	3.48	1.53	2.52
53.20	0.80	3.48	2.34	2.46
53.20	0.80	3.48	3.18	11.05
53.20	0.40	1.16	1.53	110.40
53.20	0.40	1.16	2.34	151.37
53.20	0.40	1.16	3.18	170.68
53.20	0.40	2.32	1.53	7.80
53.20	0.40	2.32	2.34	19.04
53.20	0.40	2.32	3.18	23.78
53.20	0.40	3.48	1.53	1.80
53.20	0.40	3.48	2.34	4.52
53.20	0.40	3.48	3.18	6.28

APPENDIX III – Stress-Strain Relationships from Standard Coupon Material Tests

Coupon Standard Dimensions: Width = 0.01 m ; Thickness = 0.003 m

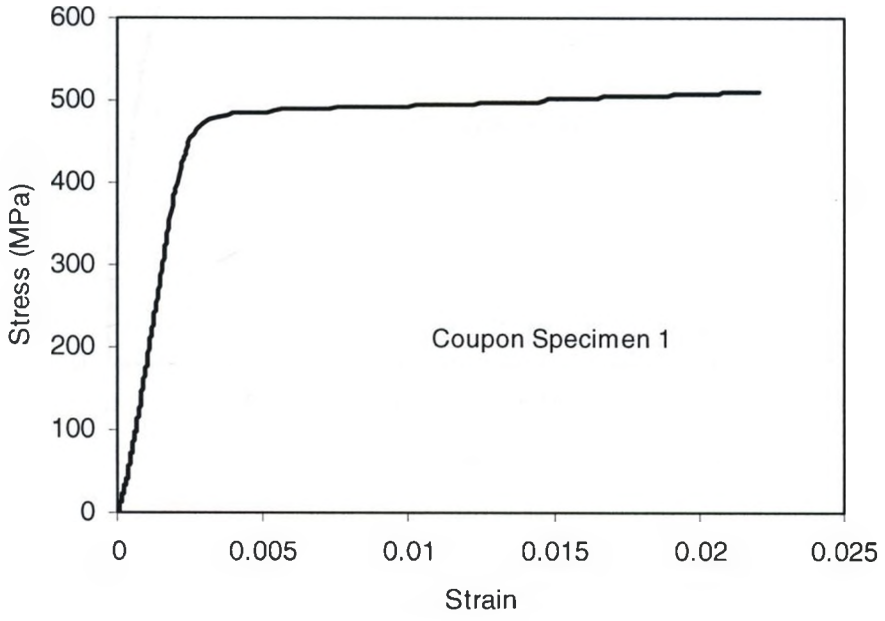

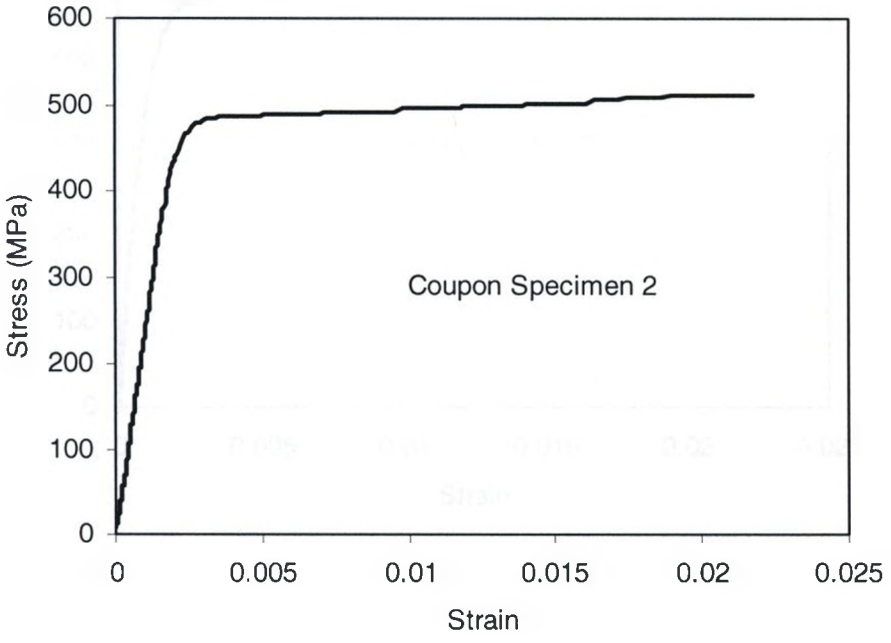

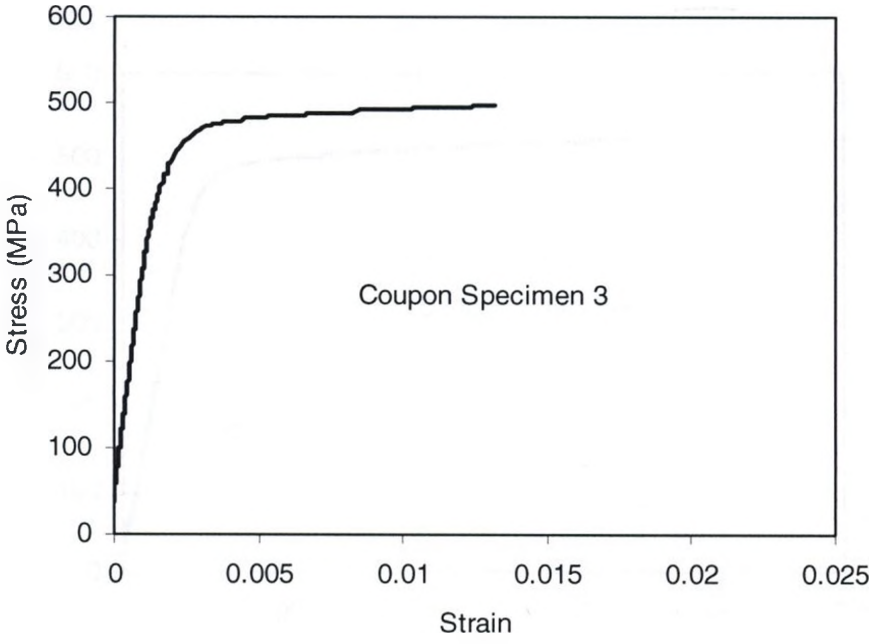
600
500
400
300
200
100
0
Stress (MPa)
Coupon Specimen 3
0
0.005
0.01
0.015
0.02
0.025
Strain

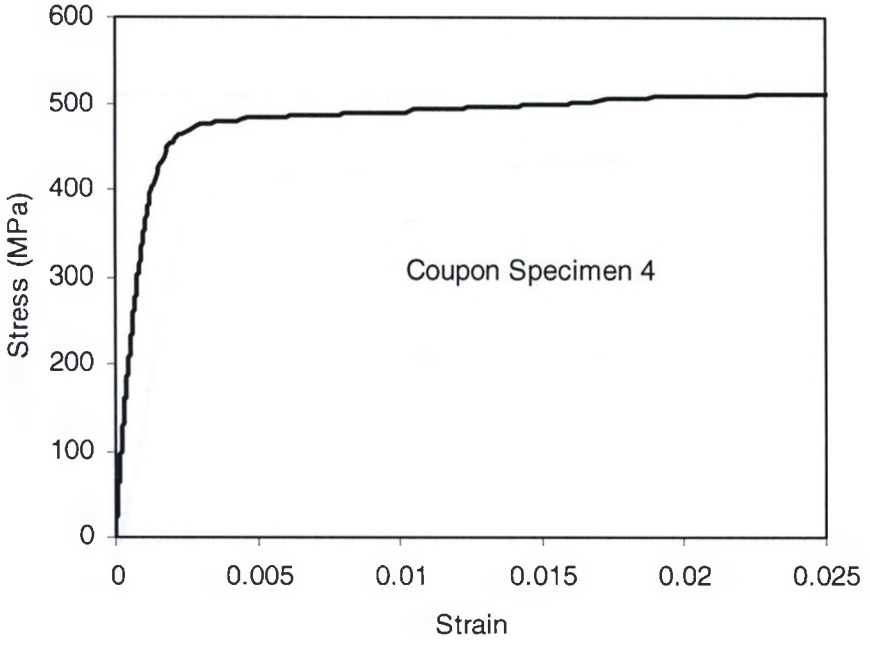
600
500
400
300
200
100
0
Stress (MPa)
Coupon Specimen 4
0
0.005
0.01
0.015
0.02
0.025
Strain

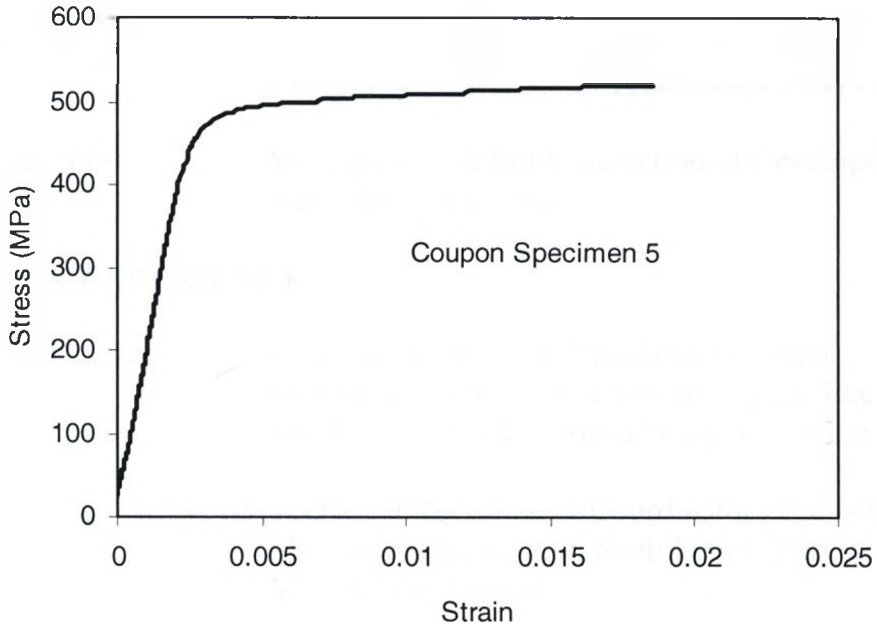
600
500
400
300
200
100
0
Stress (MPa)
Coupon Specimen 5
0
0.005
0.01
0.015
0.02
0.025
Strain

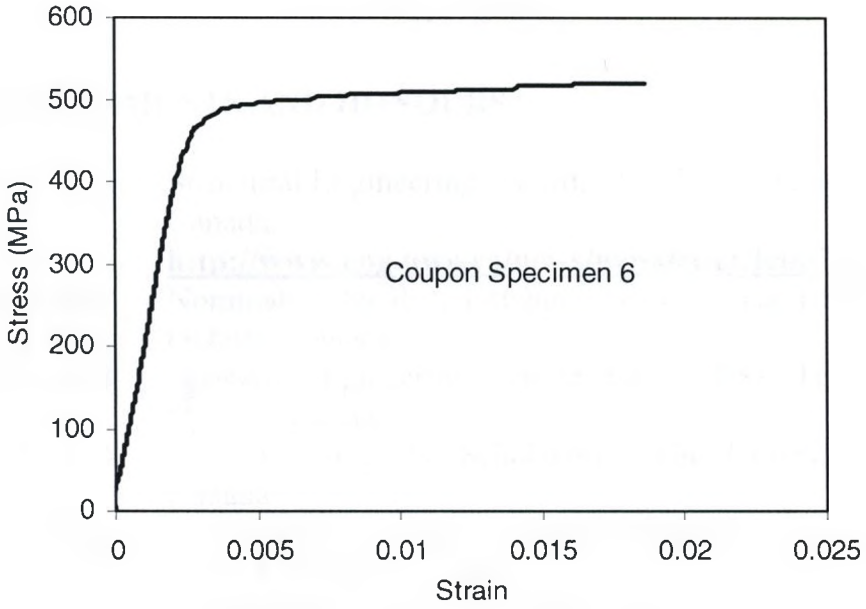
600
500
400
300
200
100
0
Stress (MPa)
Coupon Specimen 6
0
0.005
0.01
0.015
0.02
0.025
Strain